Does BRF1, a component of the transcription factor (TFIIIB), have a role in prostate carcinogenesis?

Dr. Sarah Jane Slater BSc, MMedSci, MbChB

Submitted in fulfilment of the requirement for the Degree of Doctor of Philosphy (PhD)

January 2016

Beatson Institute for Cancer Research

Institute of Cancer Sciences & Molecular Pathology

College of Medical, Veterinary and Life Sciences

University of Glasgow

Abstract

Prostate cancer is the commonest cancer diagnosed in UK men and the second commonest cause of cancer mortality. There is an urgent need to improve our ability to differentiate indolent from aggressive disease to achieve optimal evidence-based treatment choices. Tumourigenesis involves deranged cellular proliferation, which in turn necessitates gene translation to drive protein synthesis. The transcription products of RNA polymerase III (Pol III) play a critical role in protein synthesis. TFIIB-related factor 1 (BRF1) is a vital transcription factor and functions as part of the Pol III transcription apparatus to mediate transcription of transfer RNAs (tRNAs).

In this thesis, using a range of *in vitro*/ *in vivo* pre-clinical models and clinical resources, I have characterised the status of BRF1 in prostate cancer. Abnormal BRF1 expression has been previously suggested in small pilot studies in a number of tumour types. Our recent immunohistochemistry data showed evidence of upregulated BRF1 expression in clinical prostate tumours. I observed high levels of BRF1 expression in a comprehensive panel of human prostate cancer cell lines. To further examine the functional significance of BRF1 in prostate cancer, BRF1 expression was manipulated. Upon transient over-expression of BRF1, cell proliferation was upregulated in several prostate cancer cell lines. In contrast, when Brf1 expression was reduced, cell proliferation decreased, along with associated G2/M accumulation.

To test the *in vivo* function of BRF1 in prostate carcinogenesis, a genetically engineered mouse model (GEMM) was developed with enhanced Brf1 expression in the prostate, namely *Pten-Brf1*, while *Pten* was deleted to recapitulate commonly observed activation of PTEN/AKT pathway in clinical prostate cancer. The *Pten-Brf1* mice harboured enhanced growth of their prostate tumours, although they were histologically similar to prostate tumours driven by homozygous *Pten* deletion (or *Pten*-). Overall, *Pten-Brf1* mice survived significantly shorter period than the control *Pten*- mice.

In summary, my research conducted in this thesis highlights a potential role for BRF1 (as part of the Pol III transcriptional apparatus) in prostate carcinogenesis. Further research is therefore warranted to define its role as a cancer biomarker and as a novel target for therapy.

Table of Contents

List of Tables

List of Figures

Acknowledgement

First and foremost, I would like to thank my two supervisors Professor Hing Y. Leung and Dr. Kirsteen Campbell for their tremendous support, guidance, encouragement and patience. They really have understood when to push me and when to back off and I really appreciate that. I would also like to thank, Professor Robert J. White who helped me write my research grant proposal and taught me all I need to know and more about RNA polymerase III.

I will be eternally grateful for all the members of R21 (Professor White's Lab) for warmly welcoming back to science and helping me adapt to laboratory life and R8 (Professor Hing's Lab) for their encouragement, friendship and good humour. I especially want to thank Janis Fleming, Louise Mitchell, Rachana Patel, Jackie Stockley and Kirsteen Campbell for all their technical advice and always answering my questions with clarity and patience.

I would also like to thank many people at the Beatson Institute; my advisor Professor Mike Olson, for his advice and encouragement; Dr. Karen Blyth and Professor Owen Sansom for all their advice and expertise with setting up and managing the mouse models; Ann Hedley for help analysing the RNA sequencing data; Colin Nixon and the rest of the histology staff and Central Services.

Last but not least I would like to thank my family and friends and especially, my two wonderful children Isla and Sam, whose smiling faces have kept me sane and my often unappreciated partner Peter Appleby for being a great father to Isla and Sam and keeping the household in some kind of functional state.

This study was funded by the Medical Research Council UK.

Author’s Declaration

I hereby declare that this thesis is my own composition, that it is a record of the work completed by myself, and that it has not been presented in any previous application for a higher degree.

Definitions/Abbreviations

ADT	androgen deprivation therapy
APS	ammonium persulphate
AR	Androgen receptor
ARPPPo	acidic ribosomal phosphoprotein Po
ATP	Adenosine triphosphate
BDP1	B double prime 1
bp	base pairs
BPH	benign prostate hyperplasia
BRF1	TFII**B**-**r**elated **f**actor **1**
BRF2	TFII**B**-**r**elated **f**actor **2**
BSA	Bovine serum albumin
ChIP	chromatin immunoprecipitation
CRPC	Castration resistant prostate cancer
CTC	Circulating tumour cells
DAPI	4’6-diamidino-2-phenylindole
DEPC	Diethyl pyrocarbonate
DMEM	Dulbecco’s Modified Eagle Medium
DMSO	Dimethyl sulphoxide
DNA	Deoxyribonucleic acid
DRE	Digital rectal examination
DTC	Disseminated Tumour Cells
DTT	Dithiothreitol
EBV	Epstein-Barr virus
ECL	Enhanced chemiluminescence
EDTA	Ethylene diamine triacetic acid

EGF	Epidermal growth factor
EGFR	Epidermal growth factor receptor
ELISA	Enzyme-linked immunosorbent assay
ERK	Extracellular signal-related kinase
FBS	Foetal bovine serum
GEMM	Genetically modified mouse model
GFP	Green fluorescent protein
H&E	Hematoxylin and eosin
HA	Haemagglutinin
HCl	Hydrogen chloride
HeLa	Henrietta Lacks (cervical cancer cell line)
HEPES	4-2hydroxycthyl-1-pipcrazinccthancsulfonic acid
HGPIN	High grade prostatic intraepithelial neoplasia
HPRT	Hypoxanthine phosphoribosyltransferase 1
HPV	Human papilloma virus
IgG	Immunoglobulin G
IHC	Immunohistochemistry
ISH	In situ hybridisation
JNK	C-jun NH2-terminal kinase
Kb	kilobase
KD	Knock down
kDa	kilodalton
LHRH	Luteinizing hormone releasing hormone
MAPK	Mitogen activated protein kinase
MEK	MAPK/ ERK kinase
MgCl2	Magnesium chloride
mRNA	messenger RNA

MW	molecular weight
NaCl	Sodium chloride
NaF	Sodium fluoride
NaOH	Sodium hydroxide
NCI	National Cancer Institute
NGS	Next-generation sequencing
PAGE	Polyacrylamide gel electrophoresis
PBS	Phosphate buffered saline
PBST	Phosphate buffered saline with Tween
PC	Prostate cancer
PCA3	Prostate cancer antigen 3
PCR	Polymerase chain reaction
PFA	Paraformaldehyde
PI3K	Phosphatidylinositiol-3-kinase
PIN	Prostatic intraepithelial neoplasia
PMSF	Phenylmethane sulphonyl fluoride
Pol I	RNA Polymerase I
Pol II	RNA Polymerase II
Pol III	RNA Polymerase III
PSA	Prostate specific antigen
PTEN	Phosphatase and tensin homolog located on chromosome 10
PVDF	Polyvinylidene difluoride
pRb	Retinoblastoma protein
rRNA	ribosomal RNA
RNA	Ribonucleic acid
RNAse	Ribonuclease
RPM	Revolutions per minute

RPMI	Roswell Park Memorial Institute
RT	Reverse Transcriptase
SCNA	Somatic copy number alteration
SDS	Sodium dodecyl sulphate
SINE	Short interspersed repeat
siRNA	Short interfering RNA
TE	Tris-EDTA buffer
TNM	Tumour, Node and Metastasis stage
TBS	Tris buffered saline
TBST	Tris buffered saline with Tween
TEMED	N,N,N',N'- tetramethylethylenediamine
TFIIIB	Transcription factor IIIB
TFIIIC	Transcription factor IIIC
TMA	Tissue microarray
TOR	Target of rapamycin
Tris	2-amino-2-(hydroxymethyl)-1,3- propanediol
tRNA	transfer RNA
TRUS	Transrectal ultrasonography
TURP	Transurethral resection of the prostate
VEGF	Vascular endothelial growth factor
vRNA	Vault RNA

1 Introduction

1.1 Prostate Cancer

1.1.1 Natural history and Epidemiology of Prostate Cancer

Prostate cancer (PC) is the most common cancer and the second most common cause of cancer death in UK men. Lifetime risk for a UK male is 30% but only 8% will get clinically significant PC and 3% will die from PC (http:www.cancerresearchuk.org). This is because PC commonly has a slow natural history and is predominantly a cancer of elderly men. The peak age for diagnosis of PC in UK is 75-79 years old with 80% of men over the age of 80 having detectable PC but the majority of these men will die with PC rather than from it. However, more than 10,000 UK men die from PC each year, and disappointingly, PC mortality rates have remained static for the last 20 years (http://www.ncin.org.uk).

PC is a massive health problem in the western world mainly due to the morbidity associated with the disease itself but also the toxicity and side effects of its treatment. Its importance on health economics will rapidly increase with an aging population and increasing life expectancy. Population of men aged 65 or older is predicted to increase 4-fold between years 2000-2050 and by 2030 the over 65 population is likely to make up a fifth of the global population demographics (Lunenfeld, 2002). More worryingly, all established risk factors are not modifiable, such as Afro-Caribbean ethnicity and family history and therefore, there is no potential prevention strategy to reduce PC incidence.

Another huge challenge is that PC has enormous biological heterogeneity with patients having wide variations in the clinical behaviour and timeframe of their disease. For example, some patients will die of metastatic disease within 2 years of their diagnosis whilst others living up to 20 years with localised indolent prostate tumours. Even patients with similar histological patterns and pathological grading can vary substantially. It is estimated 30-50% of men with PC diagnosis could avoid radical treatments, such as surgery or radiotherapy and their side effects, because they have good prognosis relatively dormant tumours (Cooperberg et al, 2005). Before significant advances in risk stratification and personalised anti-cancer treatments can be achieved it is essential we fully understand the biology of PC especially the genetic

and molecular characteristics that distinguish between indolent and lethal PC is essential for improving patient outcomes.

1.1.2 Prostate Carcinogenesis

Prostate carcinogenesis proceeds through a series of defined stages, including precursor lesions called prostatic intraepithelial neoplasia (PIN), PC *in situ*, invasive and metastatic cancer. Over 90% of PCs are adenocarcinomas, most displaying acinar histological features. Other variants of adenocarcinomas include ductal, foamy, mucinous, atrophic, pseudo-hyperplastic, oncocytic and two types with poor clinical prognosis are lymphoepithelioma-like and signet ring cell PC. Squamous cell, small cell (neuroendocrine) and adeno-squamous PC are rare and behave more aggressively with a very poor prognosis. Some adenocarcinomas show focal neuroendocrine differentiation and furthermore, can transform into a neuroendocrine phenotype. Since neuroendocrine cells lack androgen receptors (AR) and secrete various neuroendocrine peptides that stimulate androgen-independent proliferation, it is thought this is a possible mechanism by which tumours can progress to castration refractory/resistant prostate cancer (CRPC) (Nouri et al, 2014; Terry et al, 2014).

A primary tumour is composed of a population of multiple competing subclones. This evolutionary competition results in the more aggressive or "survival" subclones forming metastases (Nowell et al, 1976; Greaves et al, 2012). Metastatic cancer is the cause of 90% of all cancer-related deaths (Gupta & Massague, 2006). The principles governing "when, how and where" cancer cells disseminate to distant organs are not understood. It is generally believed that each metastasis originates from a single tumour cell (Poste & Fidler, 1980; Fidler, 2003; Talmadge & Fidler, 2010). However, recent mouse model studies have highlighted the presence of polyclonal seeding from and inter-clonal co-operation between multiple subclones (McFadden et al, 2014; Cleary et al, 2014).

The multiple steps of prostate carcinogenesis and progression are a consequence of dysregulated signalling pathways caused by genetic alterations such as epigenetic events, changes in gene copy number and chromosomal rearrangements (Taylor et al, 2010; Berger et al; 2011; Grasso et al, 2012; Baca et al; 2013). All aspects of prostate

gland development and homeostasis and prostate carcinogenesis are critically dependent on androgens. Research to elucidate and characterise the complex relationship between molecular mechanisms that initiate and drive prostate carcinogenesis is essential as a means of identifying biomarkers for early risk stratification of patients and discovering potential therapeutic targets.

In this post-genomics era, there has been comprehensive profiling of human malignancies to increase our understanding of the complex biology of cancer with the ultimate goal to identify oncogenic driver events that can be regulated or manipulated to improve patient survival. Genomic profiling studies of primary and metastatic PC have identified a number of oncogenic events in PC, including loss of tumour suppressors *PTEN* and *TP53*, genomic arrangements of *ERG* and other *ETS* fusions and amplification of *MYC* and *AR* that all drive PC development and progression (Shen et al, 2010; Grasso et al, 2012; Taylor et al, 2010). Recent transcriptome and genomic studies have defined general PC signatures but no prognostic categorisation of PC subtypes has been identified, unlike breast cancer (Taylor et al, 2010, Berger et al; 2011; Grasso et al, 2012; Baca et al; 2013). With rapidly expanding technologies and falling costs for next generation sequencing-based analysis, new gene therapeutic targets will emerge and personalised medicine will have to focus on tumour heterogeneity and drug resistance.

1.1.3 Patient Pathway: Presentation and Diagnosis

Early or localised PC is typically asymptomatic or associated with symptoms similar to benign prostatic hyperplasia (BPH) or urinary tract infection such as urine frequency, hesitancy, poor urine flow, dysuria and urinary retention. The initial diagnostic tests for PC are the digital rectal examination (DRE) and serum prostate specific antigen (PSA) measurement. PSA is also used as a screening tool for asymptomatic patients considered at risk, for example, a family history of PC. If the DRE is abnormal and / or the PSA is raised (>2ng/ml for 40-49 year olds; > 3ng/ml for 50-59 year olds; > 4ng/ml for 60-69 year olds; >5ng/ml for over 70 year olds) a trans-rectal ultra-sound guided biopsy, TRUS, will be performed to confirm diagnosis

and histological staging and grading and MRI of pelvis to determine pathological staging.

Advanced or metastatic PC patients commonly present with bony pain, pathological fractures, lower limb weakness caused by spinal cord compression and general decline, weight loss and cachexia. PSA and /or biopsy would be required to confirm diagnosis and for treatment response monitoring. Computed tomography CT chest/abdomen/pelvis and radioisotope bone scan and/or MRI of spine would be required for clinical staging of the disease.

A family history of PC means a patient has a father or brother diagnosed with PC and this increases the patient's risk of PC 2-3 times or about 4 times if more than one first degree relative has PC greater than the general population risk. The younger the age of the relative diagnosed with PC increases the likelihood that an inherited faulty gene is the cause. Men also have a higher risk of PC if their mother or sister has had breast cancer, especially if the first degree female relative is a confirmed *BRCA2* mutation carrier. *BRCA2* mutation carriers have a 5-7 times higher risk of PC than the general population and recent studies suggest they have a worse prognosis than the general PC population (http//:www.cancerreseacrhuk.org; Castro et al, 2015; Risbridger et al, 2015).

1.1.4 Patient Pathway: Localised PC

Clinically localised PC should be categorised as National Comprehensive Cancer Network (NCCN) risk groups – low, intermediate- or high- risk which identifies patients with a 10%, 40% and 70% probability of biochemical progression (PSA levels increasing) at 5 years (D'Amico et al, 1998) (Table 1.1). Complete resection of localised disease with radical prostatectomy is the only curative option but there is significant potential risk of comorbidity with surgery including long term urine incontinence and erectile dysfunction. Similarly, radiation based primary radical therapy may also result in symptoms as a result of radiation to adjacent organs. Therefore, currently there is no agreed optimal management of localised disease due to the co-morbidities of the elderly PC population and the often slow natural history of

PC; possible treatments include PSA monitoring, (watchful waiting or active surveillance), surgery (open/laparoscopic/robot-assisted radical prostatectomy) and radiotherapy (external beam and brachytherapy). Crucially all patients with PC should have access to multidisciplinary team (MDT) expertise including oncologists, radiologists, pathologists, urologists and specialist nurse practitioners (and palliative doctors and nurses where appropriate). All patients must be adequately counselled about their treatment choices.

Men with low risk PC have a < 1% disease-specific mortality over 10 years with no survival benefit for active treatment (Dall'Era et al, 2012). Intermediate and high risk PC groups have approximately 10% cancer specific mortality at 10 years without radical treatment (Bill-Axelson et al, 2011), whereas locally advanced PC has a 23.9% 10 year cancer specific mortality rate (Widmark et al, 2009). In men with high risk or locally advanced disease, external beam radiotherapy plus androgen deprivation therapy (ADT) for 2 plus years or radical prostatectomy plus extended lymphadenectomy in highly selected patients is recommended (Horwich et al, 2013). Neoadjuvant Luteinising hormone-releasing hormone (LHRH) agonist therapy for 4-6 months in men having radical radiotherapy with high or intermediate risk disease followed by adjuvant hormone therapy for 2-3 years is advised (Horwich et al, 2013). After radical prostatectomy, adjuvant hormone therapy is not recommended but serum PSA levels should be monitored and if relapse with PSA failure and no metastatic spread confirmed, salvage RT should commence (Horwich et al, 2013).

1.1.5 Patient Pathway: Metastatic PC

Metastatic PC patients have a poor prognosis with average survival of 3.5 years from diagnosis and once CRPC has developed time to death is usually within 22 months (Demir et al, 2014). In 1941, Huggins and Hodges discovered castration was an effective therapy for metastatic PC; ADT is still the main palliative treatment for metastatic PC. Unfortunately, these tumours eventually become androgen independent or clinically termed CRPC. Interestingly, CRPC may remain driven by

AR signalling via *AR* amplification, gain-of-function *AR* mutations, splice variants and overexpression of AR or its co-activators.

ADT is first line treatment for metastatic PC, which includes LHRH agonist/ antagonist or bilateral orchidectomy. A new generation of AR-targeting agents have been shown to prolong survival by approximately four months, such as abiraterone acetate (which inhibits CYP17, a rate limiting enzyme involved in androgen biosynthesis) (de Bono et al, 2011) and enzalutamide (which inhibits AR-mediated signalling) (Scher et al, 2012) and so these are now preferred second line hormone therapies.

Once hormone therapies have failed, chemotherapy such as docetaxel may be offered for symptomatic, CRPC and gives a median survival of approximately 19 months (Tannock et al, 2004; Berthold et al, 2008). Cabazitaxel, a novel tubulin-binding cytotoxic drug, results in a 2.4 months survival advantage over mitoxanthrone and should be considered for second line chemotherapy (de Bono et al, 2010). For patients with bone metastases radium 223, zoledronic acid and denosumab have all been shown to delay first skeletal related event (Parker et al, 2013; Saad et al, 2002; Fizazi et al, 2011).

Improved treatments are being actively developed and evaluated in clinical studies. For example, Sipuleucel-T is the first new immunotherapeutic agent that has showed a survival advantage in metastatic CRPC of 4.1 months versus placebo. Another recent clinical trial testing Cabozantinib (XL184) a dual MET/VEGFR2 inhibitor, showed dramatic resolution of bone scan abnormalities in 86% of patients but soft tissue responses and serum PSA declines in only 25-30% (Kurzrock et al, 2011; Yakes et al, 2011). It is thought that the bone scan effect may be through inhibition of a target in the bone microenvironment, whereas the antitumor effect is due to *MET* amplification only being found in ~ 30% of metastatic human PC specimens (Wanjala et al, 2015).

1.1.6 Biomarkers of PC

Prostate Specific Antigen (PSA) is currently the most widely used cancer biomarker and its use aids in the diagnosis of PC and monitoring of disease response to anticancer therapies. However, its specificity as a diagnostic tool is limited as it is also produced by normal prostatic epithelium and its detection in serum is proportional to the prostate size. It can also be raised by inflammation, such as prostatitis, urinary tract infection and long distance cycling. Elevated PSA > 3 ng/ml with abnormal DRE gives a positive predictive value for PC of nearly 50% (Gosselaar et al, 2008). To improve the diagnostic accuracy of non-invasive tests, recent research has led to the development of a commercially available urine diagnostic test Prostate Cancer Antigen 3 (PCA3, a long non-coding RNA, Progensa™), while the *TMPRSS2-ERG* fusion gene represents another potential urine biomarker (Tomlins, 2014).

Majority of clinical PC are diagnosed by transrectal ultrasound (TRUS) guided prostatic biopsies. However, due to prostate adenocarcinomas being multifocal, a patient may be recalled for a second biopsy if clinical suspicion is high when the first set of biopsies is negative. More than 90% of PC can be detected by two successive biopsies (Roehl et al, 2002). The PC pathology report includes Gleason grading, tumour quantification (percentage of tumour in biopsies), presence or absence of peri-neural invasion and extra-prostatic extension. Unlike other cancers, such as breast cancer, there are currently no routine molecular markers used to help plan personalised treatment strategies for PC patients. Furthermore, studies have shown that prostatic core biopsies underestimate tumour grade in up to 45% of cases and overestimate it in up to 32% of cases (Fine et al, 2008). Therefore, there is a great urgency to discover sensitive and specific clinical biomarkers for early diagnosis of PC and more accurate stratification of cancer progression risk. Recent studies looking for potential molecular markers have shown that high levels of microRNA miR-96 were predictive of early biochemical relapse (Schaefer et al, 2010; Walter et al, 2013) while gain of c-MYC was predictive for tumour recurrence after radiotherapy (Ribeiro et al, 2007; Zafarana et al, 2012) and p27 loss correlated with aggressive disease (Thomas et al, 2000; Vis et al, 2002; Wolters et al, 2010).

Recent evidence shows that metastatic tumours are heterogeneous especially when the patient has been heavily treated with anticancer therapies. Not only are the metastases genetically dissimilar from their primary tumour but also from other metastases within the same organ (Gundem et al, 2015). There are safety and technical difficulties that limit the feasibility of taking multiple biopsies from patients. Circulating and disseminated tumour cells (CTC and DTC) in the blood present an opportunity for repeated testing over the course of the patient's disease (Dawson et al, 2013). CTCs and DTCs molecular profiling has been shown to predict risk of relapse and quantify treatment responses (Doyen et al, 2012; Panteleakou et al, 2009). Very recent technical advances are beginning to allow such method to become a plausible means of monitoring tumour evolution and heterogeneity. Genomic profilings of DTCs from patients with advanced PC show a large number of somatic copy number alterations (SCNAs), which largely correspond to tumour biopsy results (Holcomb et al, 2008; Weckermann et al, 2009). However, DTCs from men with localised PC generally have fewer SCNAs, which may not correspond well with primary tumour SCNAs (Schoenborn et al, 2013).

1.1.7 Castration Resistance Prostate Cancer (CRPC)

Prostate epithelium is composed of three cell types: luminal, basal and neuroendocrine cells. There are two main layers of prostate epithelium. The androgen dependent secretory luminal layer is composed of tall differentiated columnar cells that produce PSA, PAP (prostatic acid phosphatase) and kallikrein-2 for the seminal fluid. This layer rests on the basal layer of cuboidal epithelial cells which in turn are lined by a basement membrane. Basal cells are the androgen-independent proliferating early progenitor cells. Their progeny, the intermediate cells give rise to a heterogeneous subpopulation of cells as they differentiate in transit from the basal layer into the luminal layer (as reviewed by Long et al, 2005).

Currently it is unclear which epithelial cell is the origin of prostate carcinogenesis. Classically PC is characterised by luminal cell expansion with the absence of a basal cell layer (Parsons et al, 2001). To add support to luminal cells being the origin of

PC, Wang et al 2009, have shown that a subpopulation of luminal cells expressing Nkx3.1 homeobox gene in the androgen-deprived prostate epithelium display stem cell properties capable of prostate regeneration. Early events in prostate carcinogenesis include loss of chromosomal region 8p21, *NKX3.1* loss frequently found in PIN (Abate-Shen et al, 2008). However, benign human prostate tissue basal cells can initiate PC in immune-deficient mice (Goldstein et al, 2010). To add to the confusion, precursor lesions for PC have been shown to have an intermediate cell phenotype, supporting the theory for intermediate cells being the origin of PC (as reviewed by Long et al, 2005).

There is great research interest in the emergence of androgen independence at the cellular level. It is currently unknown whether androgen independence (or CRPC) is acquired via a single event or appears independently in multiple cells (Gundem et al, 2015). Historically, there have been two main overriding theories. Firstly, the adaptation model whereby androgen independence arises from molecular alterations that occur during carcinogenesis, in that androgen dependent tumour cells when treated with ADT develop molecular adaptations resulting in androgen independence. In advanced disease the cells are poorly differentiated and have a greater number of chromosomal abnormalities, mutations and altered methylation states (Feldman et al, 2001). AR is usually wild type during initial emergence of androgen independence but acquires mutations during ADT (Gelmann, 2002). Furthermore, CRPC tumours can produce androgens to activate AR (Mohler et al, 2004) and AR expression is generally increased (Chen et al, 2004).

The second theory for emergence of CRPC is a clonal selection mechanism, in that a subpopulation of pre-existing androgen independent cells within the primary tumour undergoes clonal selection during ADT. Prostate tumours contain a heterogeneous ratio of basal to luminal cells that varies depending on the aggressiveness of the tumours, with more advanced tumours expressing a more basal phenotype (Lui et al, 1999). Craft et al, 1999 proposed that androgen independence arises in two distinct stages, firstly an initial selection for pre-existing cells that can survive in the absence of androgens, and secondly their subsequent clonal expansion (Gao et al, 2006b). In support of this theory, the Prostate Cancer Prevention Study, investigating long term finasteride, a 5 α reductase inhibitor, showed that the finasteride-treated patient cohort

displayed a significant reduction in PC incidence but when they developed cancer had higher grade disease (Thompson et al, 2003). One explanation for this is finasteride may promote an androgen-independent state in some PCs, perhaps those with pre-existing mutations of *PTEN* or other genes that enable prostate cells to survive under conditions of androgen deprivation (Gao et al, 2006b).

Using whole-genome sequencing, Gundem et al (2015) characterised 51 PC metastases from 10 CRPC patients. They showed that commonly PC cells move from one metastatic site to another, either as monoclonal or polyclonal seeding. They observed clonal diversification is essential for development of ADT resistance (Gundem et al, 2015). Furthermore, in 5 patients multiple polyclonal seeding had occurred suggesting these metastatic subclones had a significant evolutionary survival advantage. Interestingly, these metastatic subclones carried AR signalling pathway genetic alterations (such as *FOXA1*) or alternative mechanisms of androgen independence such as *MYC* amplification and *CTNNB1* mutation. (Gundem et al, 2015). Notably, the multiple metastases in closest proximity were closer genetic relatives to each other than any of them to the primary prostate tumour. This raises further research questions about inter-clonal cooperativity, tissue-specific seeding factors and/or remodelling of metastatic host organs by colonising PC clones, making them more attractive for future colonisation (Sun et al, 2012).

1.1.8 Molecular biology of prostate carcinogenesis

1.1.8.1 Introduction

The advent of next generation sequencing techniques (NGS) has allowed for comprehensive profiling of primary and metastatic tumours. It has made it possible to determine the genetic signatures consisting of an army of genetic drivers leading to activation of oncogenic pathways and suppression of tumour suppressor pathways that determine individual tumour progression. However, this is a massive oversimplification as it is now apparent that multifocal PC consists of separate tumours with different genetic signatures and microenvironments that control their ability to progress and metastasise. Furthermore, metastatic lesions appear not to

show similar genetic signatures to their primary tumours, but harbour driver mutations heavily influenced by their host organ (Gundem et al, 2015). Lastly, NGS techniques have shown that tumours react and evolve to anti-cancer therapies with increasing genetic instability resulting in drug resistance and often a more aggressive mutation driver leading to more rapid progression (Grasso et al, 2012). NGS techniques have highlighted the need for researchers to focus on epigenetic events and cellular interactions between PC cells and organ microenvironment.

PC is characterised by huge genomic complexity encompassing somatic copy number alterations (SCNAs), point mutations and, most strikingly, chromosomal rearrangements (Table 1.2). Primary PC has an estimated mean mutation frequency of 0.9/megabase which is similar to breast cancer (Berger et al, 2011). The upstream cause of this genomic instability is thought partly to be an orchestra of epigenetic modifications including aberrant DNA methylation, histone remodelling and microRNA expression (Jeronimo et al, 2011). Whole-genome sequencing has shown that loss of tumour suppressor gene *TP53* usually occurs as a single early event (Gundem et al, 2015) and this would result in further genomic instability. P53 has been named the "guardian of the genome" as it has a crucial role in cellular resistance to malignant transformation (Brown et al, 2009).

In comparison to 26 other cancer types, PC has one of the highest SCNAs, averaging 46 per sample (Beroukhim et al, 2010). SCNAs are genetic gains or losses that arise during cancer development and are present in nearly 90% of primary prostate tumours, with deletions typically outnumbering amplifications (Schoenborn et al, 2013). In primary prostate tumours, SCNAs tend to be focal with only small areas of the genome affected (Beroukhim et al, 2010; Tylor et al, 2010) whereas, in CRPC, larger portions of the genome are affected which implies increased genomic instability with cancer progression (Schoenborn et al, 2013) (Table 1.2).

1.1.8.2 ETS family and TMPRSS2-ERG

Tomlins et al, 2005 identified gene fusions in PC between members of the *ETS* family of genes and the androgen-responsive transmembrane protease serine 2 (TMPRSS2), which turns out to be the single most prevalent molecular lesion in PC. Almost 50%

of primary and advanced human PCs have gene fusions of the transcriptional regulator growth promoting *ERG* with *TMPRSS2*, although other partner genes, such as *ETV1*, *ETV4* and *ETV5*, may be involved in translocations. *TMPRSS2-ERG* tumours have distinct expression signatures and are associated with deletions of 10q, 17p and 3p14, whereas tumours without *ERG* rearrangement tend to be enriched for 6q deletion, 7q gain and 16q deletion (Taylor et al, 2010).

The ETS family of transcription factors are thought to be involved in many important cellular events including angiogenesis, migration, proliferation, differentiation, oncogenic transformation and apoptosis (Clark et al, 2009). *ETV* genes, which are members of the *PEA3* subfamily of *ETS* genes, have been implicated in cancer invasion and metastasis in a variety of cancer types (as reviewed by Aytes et al, 2013). Sun et al, 2008 reported that knockdown of ERG expression in VCaP cells inhibited cell growth and induced obvious morphological changes in cell culture and in SCID mice *in vivo*. Interestingly, this was not observed in LNCaP cells which lack the *TMPRRS2-ERG* genomic rearrangement. Furthermore, the *c-MYC* oncogene has been identified as an ERG target in PC cells (Zhong et al, 2009) and androgen signalling induces co-localisation of *TMPRSS2* and *ERG* (Lin et al, 2009).

Chromosomal rearrangements are thought to be critical initiating early events in PC as evidenced by the high prevalence of androgen-responsive promoters being fused to ETS transcription factors (Berger et al, 2011; Hollenhorst et al, 2011). While *TMPRSS2-ERG* or *TMPRSS2-ETV1* fusions are not thought to be sufficient to initiate prostate carcinogenesis in isolation, they may sensitise prostate epithelial cell genomes for further oncogenic mutations (Linn et al, 2015). About 25% of human prostate tumours have both *PTEN* genomic deletion and *TMPRSS2-ERG* fusion when evaluated by fluorescence in situ hybridisation (FISH) (Yoshimoto et al, 2006) and cooperate to promote disease progression in mice (Carver et al, 2009). Furthermore, *ETV1* has been shown to translocate in PC and collaborate with *PTEN* in PC progression (Tomlins et al, 2007).

Interestingly, genomic studies characterising the pattern and location of chromosomal rearrangements in primary PC samples showed breakpoints located independently of *TMPRRS2-ERG* but in close proximity to multiple known genes including tumour

suppressor *TP53* and proto-oncogene *ABL1* (Berger et al, 2011). This suggests that multiple genes can be controlled in parallel by complex translocations to drive prostate tumorigenesis (Berger et al, 2011).

Some studies have found an association between *TMPRSS2-ERG* fusions in PC and more aggressive pathology and cancer related death whereas, other studies have not (reviewed by Chaux et al, 2011). Grazzo et al, 2012 reported deleterious mutations of *ETS2* in a third of their CRPC exome dataset. Furthermore, PC patients with *TMPRSS2-ERG* fusions caused by deletion, rather than insertion, may be more aggressive because the deleted region may have harboured tumour suppressors, including *ETS2*.

Aytes et al, (2013) recently developed a mouse model with combined P13K and Ras activation which developed metastatic PC with poor survival and further analysis identified *Etv4* being significantly upregulated in these tumours and metastases. Analysing a human PC dataset (Taylor et al, 2010), they found *ETV4* expression significantly correlated with PI3-kinase and Ras signalling co-activation in human prostate tumours (Aytes et al, 2013). Furthermore, shRNA-mediated knock down of *ETV4* expression in a metastatic cell line derived from their PI3K and Ras driven PC model severely impaired its ability to form metastases when injected as subcutaneous xenografts in nude mice (Aytes et al, 2013). In addition, *ETV4* expression is upregulated in human PC3 cells and suppression of ETV4 expression impaired anchorage-independent growth (Hollenhorst et al, 2011). Interestingly, *KRAS* mutations are infrequent in PC (Carter et al, 1990; Prior et al, 2012) as are chromosomal rearrangements involving *KRAS* activation (Baca et al, 2013).

1.1.8.3 PTEN loss

Three key signalling pathways deregulated in PC are PI3-kinase/AKT, Ras/RAF and pRb which are altered in 34-43% of primary tumours and 74-100% of metastatic tumours (Taylor et al, 2010). PI3-kinase pathway is activated by *PTEN* loss (Shen et al, 2010) but it can also be activated by oncogenic activation or amplification of *PIK3CA, AKT1* and *MTOR* (Robbins et al, 2011). Amplification of *PIK3CA* has been detected in 13% to 39% of primary tumours and up to 50% of CRPCs (Edwards et al,

2003; Sun et al, 2009). Phosphoinositide -3 kinase (PI3K) signalling pathway regulates cell proliferation and growth in reaction to nutrient availability and growth factors (Manning and Cantley, 2007), thus playing an important role in protein synthesis regulation. More specifically, PI3K pathway may regulate initiation factor eIF4E release, an essential step for initiation of translation. Interestingly, when eIF4E is activated by phosphorylation on serine 209 or overexpressed it can behave like an oncogene (Wendel et al, 2007).

Phosphatase and tensin homolog chromosome 10 (*PTEN)* is a frequently deleted or mutated gene in human cancer and maps to chromosomal region, 10q23. Germline mutations in *PTEN* are prevalent in Cowden syndrome and related diseases manifesting as hyperplastic lesions with increased malignant transformation in multiple organs (Dahia, 2000). Loss of *PTEN* expression is associated with increasing Gleason score and advanced histopathological changes in PC (McMenamin et al, 1999). *PTEN* deletions and/or mutations are present in 30% of primary PC (Dahia, 2000) and 63% of metastatic PC samples (Suzuki et al, 1998). *PTEN* inactivating mutations have been found in 4% of primary prostate tumours and 42% of metastatic prostate tumours but deregulation of PI3K pathway in 42% of primary prostate tumours and 100% of all metastatic prostate tumours (Taylor et al, 2010).

PTEN encodes a lipid phosphatase that functions as a tumour suppressor through its ability to negatively regulate phosphatidylinositol 3'-kinase (PI3K) signalling cascade. Consequently, inactivation or loss of *PTEN* results in activation of the AKT serine/threonine kinase. AKT functions by phosphorylating key intermediate signalling molecules such as glycogen synthase kinase-3 (GSK3), BAD, caspase 9 and I*k*B which are linked to increased cell metabolism, growth and survival (Hanahan & Weinberg et al, 2000). Mice models with *Pten* deletion have shown that their prostate tumour growth is dependent on mTOR (Blando et al, 2009).

1.1.8.4 AKT/mTOR signalling

Mammalian Target-of-Rapamycin complex 1 (TORC1 or more generally mTOR) is a conserved serine/threonine kinase that is an important regulator of cell proliferation, metabolism and growth (Wullschleger et al, 2006). TORC1 can be activated by

nutrients and growth factors via the PI3kinase/PTEN/AKT kinase pathway and over activated in cancer by either loss of PTEN or oncogenic mutation in *P13K*. Furthermore, PTEN/PI3K-dependent transformation and tumours are sensitive to genetic and pharmacological inhibition of TORC1 signalling (Podsypanina et al, 2001; Hsieh et al, 2010).

Recent evidence has shown that activation of AKT/mTOR signalling is strongly and causally associated with advanced PC, including CRPC (as reviewed by Floc'h et al, 2012). Floc'h et al, 2012 showed that dual inhibition of AKT by MK-2206 and mTOR by ridaforolimus (MK-8669) was effective in inhibiting CRPC growth in a mouse model and human PC cell lines, whereas single agent inhibition had only limited efficacy. Further analysis suggested that the dual effect of AKT/mTOR inhibition was mediated by inhibition of cellular proliferation via the retinoblastoma (pRb) pathway (Floc'h et al, 2012). pRb pathway is known to be a key pathway affected in CRPC (Taylor et al, 2010; Sharma et al, 2010).

Wyatt et al, 2014 performed deep transcriptome sequencing on 25 high risk primary prostate tumours and showed enrichment of the translational control pathway 'EIF2' in 4 tumours, with 3 overexpressing mTOR signalling genes and upregulation of ribosomal biogenesis genes. These tumours also overexpressed genes involved with mitochondrial dysfunction. Interestingly, the patients in this translation/metabolism group had the worst biochemical recurrence-free survival (Wyatt et al, 2014).

1.1.8.5 AR (Androgen Receptor) and cofactors

The presence of AR alterations through mutation, gene amplification and/or overexpression was observed in 58% of metastatic PC samples (Schoenborn et al, 2013). Based on an integrative genomic profiling approach, virtually in all advanced PC, the AR is implicated directly or indirectly, including amplification or mutation of *AR* gene, and abnormalities of other AR pathway signalling components (Taylor et al, 2010). AR pathway analysis showed alteration in 56% of primary tumours and 100% of metastases (Taylor et al, 2010). Furthermore, they showed AR amplification is largely restricted to CRPC, suggesting a drug resistance mechanism rather than a

natural step in tumour progression (Taylor et al, 2010). Based on data from whole-genome sequencing, all analysed PC tumours harboured one or more alterations directly affecting the *AR* locus or its signalling pathway with huge heterogeneity and convergent evolution seen across multiple metastatic sites within the same patient (Gundem et al, 2015). Interestingly, aberrations in AR signalling commonly precede metastatic spread (Gundem et al, 2015).

Nuclear receptor co-activator (*NCOA2)* on 8q13.3 was identified as a potential oncogene in ~ 11% of primary prostate tumours (Taylor et al, 2010) and amplified in 24% of metastases (Schoenborn et al, 2013) and thought to act as a driver of AR signalling. Overexpression of NCOA2 primes AR to respond to reduced androgen levels and boosts the total magnitude of AR transcriptional response (Schoenborn et al, 2013). Oncogenic H874Y *AR* mutation increases the binding affinity of AR for testosterone (Askew et al, 2007). Furthermore, *AR* mutation, F876L, confers resistance to the potent AR antagonist, MDV3100, as evidence of the plasticity of the PC genome in responding to selective therapeutic pressures (Balbas et al, 2013).

Grasso et al, 2012 sequenced the exomes of 50 lethal heavily-pretreated metastatic CRPC tumours. Proteins that can bind to AR, such as *ERG* gene fusion products, FOXA1 and MLL complex proteins were found to be mutated in CRPC. MLL complex proteins are involved in chromatin/histone modification. When MLL is inhibited AR signalling is reduced, whereas, mutated FOXA1 inhibits androgen signalling and increases tumour growth (Grasso et al, 2012). Forkhead box protein A (FOXA) and O (FOXO) members are transcription factors that bind to AR and regulate its association with androgen response elements (Grasso et al, 2012).

Increased expression of FOXA1 correlates with Gleason score and is associated with poor prognosis (Imamura et al, 2012) and *in vitro* studies FOXA1 activity is oncogenic (Grasso et al, 2012). In contrast, *FOXO1* acts as a tumour suppressor gene and its deletion on 13q14 is found in about a third of all primary prostate tumours (Dong et al, 2006). Loss of *FOXO1* increases the basal activity of AR and sensitises it to lower androgen levels (Liu et al, 2008). FOXO1 is a direct downstream target of AKT. AKT can directly phosphorylate and inactivate FOXO1 by causing FOXO1 to move from the nucleus to the cytoplasm (Palian et al, 2014). It is worth noting that

FOXO1 has been recently reported to positively regulate MAF1, which in turn functions as a negative regulator of RNA Polymerase III (Palian et al, 2014). In other words, enhanced AKT function may result in upregulated RNA polymerase III (Pol III) function.

Approximately 20% of prostate tumours have mutations in the E3 ubiquitin ligase adapter *SPOP* and/or disruption to chromodomain helicase DNA-binding genes, for example (CHD1), a chromatin remodelling factor (Barbieri et al, 2012; Grasso et al, 2012; Baca et al, 2013). Tumours with *SPOP* mutations have been proposed to define a molecular subtype of PC with a more aggressive phenotype and are enriched with somatic deletions of *CHD1*, tumour suppressor *PRDM1* and transcription factor *FOXO3* in the absence of *ETS* rearrangements or mutations in *TP53, PTEN* and *PI3KA* (Grasso et al, 2012; Barbieri et al, 2012).

To identify shared molecular events, Wanjala et al (2015) studied four well established cancer mouse models for integrative mouse-human tumour PC genomic profiling. The four mouse models were: PB*Myc (Myc* overexpression under control of prostate specific probasin cre promotor) develop high grade PIN (HGPIN) at 2 months old and invasive adenocarcinoma by 12 months (Ellwood-Yen et al, 2003); *Pten*$^{lox/lox}$PB-*Cre (Pten* prostate conditional null mice develop HGPIN by 2 months and intraductal carcinoma by 6 months) (Trotman et al, 2003)*; Pten*$^{lox/lox}$ *p53*$^{lox/lox}$ PB-*Cre* (prostate conditional loss of *Pten* and T*p53* which is an aggressive phenotype of invasive carcinoma at 2 months and lethal at 6 months) (Chen et al, 2005)*;* Rosa-26$^{lox\text{-}stop\text{-}lox}$ *Erg-Pten*$^{lox/lox}$ PB-*Cre (*prostate conditional loss of *Pten* and overexpression of *Erg* with HGPIN by 2 months and invasive adenocarcinoma by 6 months*)* (Chen et al, 2013). *Met* receptor tyrosine kinase was amplified in 67% of *Pten/p53* conditional null driven PC. In contrast, amplification of *MET* was observed rarely in primary human PC and in ~ 30% of metastatic human PC when it is often associated with *PTEN* and *TP53* loss (Wanjala et al, 2015). Furthermore, MET overexpression in non-*MET*- amplified PC cells activated PI3K and MAPK signalling and increased tumour growth. Interestingly, inhibition of the MET kinase selectively inhibited MET amplified tumour growth but the efficacy of MET inhibitor therapy was limited by non-*Met* amplified cell proliferation within *Met*- amplified tumours (Wanjala et al, 2015).

1.2 Protein synthesis and cancer

In 1970 Francis Crick first explained the central dogma of molecular biology (Crick, 1970). He described that hereditary genetic code within a cell's DNA is recognised by RNA polymerases and transcribed into complementary RNA. Transcription is the fundamental process by which a genetic code in a strand of DNA is copied into a new messenger RNA (mRNA). Transcription is carried out by nuclear enzymes called RNA polymerases and a number of accessory proteins called transcription factors. These mRNA molecules are then translated by the ribosome utilising transfer RNAs (tRNAs) to produce proteins. tRNAs have a central role in translation acting as an adapter molecule translating codon triplet sequences into amino acids.

Protein makes up approximately 85% of dry cellular weight. Cell growth and proliferation rate is essentially dictated by rate of protein generation. It has been shown that a 50% reduction in translation can result in fibroblasts exiting the cell cycle and dying (Brooks, 1977). Furthermore, RNA content of cells, composed of 95% rRNA and tRNA, correlates strongly with rates of protein synthesis (Zetterberg & Killander, 1965). Analysis of the cancer transcriptome has shown characteristic changes in mRNA expression patterns that are associated with specific tumour-types or tumour signalling pathways (Tinker et al, 2006; Prat et al, 2012). However, changes in the transcriptome do not always equate to corresponding changes at the level of cellular protein expression. This implies a complicated network of post-transcriptional control and in particular, multiple layers of mRNA translational control (Grewal, 2014). Furthermore, cancer cell transcriptome analysis often excludes ribosomal RNAs (rRNA) and transfer RNAs (tRNA).

Transcription machinery components are known to be deregulated in cancers and there is growing evidence for the oncogenicity of these events (Bjornsti and Houghton, 2004; Mamane et al, 2004; Pandolfi, 2004; Johnson et al, 2008). Conceptually, it is logical that cells should be able to regulate protein synthesis so they can adapt rapidly to changing conditions. This occurs during embryogenesis, allowing production of superabundant proteins required for rapid growth and fuelled by aerobic glycolysis rather than oxidative phosphorylation for energy metabolism. It

is now known that cancer cells hijack this strategy to foster tumour growth (Christofk et al, 2008).

In 2000, Hanahan and Weinberg published their seminal Cell paper titled The Hallmarks of Cancer in which they described six traits (or hallmarks) that are acquired to transform normal cells into cancer cells. These traits are: i) Self sufficiency in growth signals; ii) Insensitivity to anti-growth signals; iii) Evading apoptosis; iv) Limitless replicative potential; v) Sustained angiogenesis; vi) Tissue invasion and metastasis (Hanahan & Weinberg, 2000). In 2011, Hanahan and Weinberg proposed two new hallmarks of cancer: vii) evading the immune system and viii) abnormal cell metabolic pathways. The discovery that cancer cells even in the presence of adequate oxygen preferentially metabolise glucose by glycolysis in the cytosol instead of the more energy efficient oxidative phosphorylation in the mitochondrial respiratory chain was first made by Otto Warburg and has since been named the Warburg Effect (Warburg, 1956).

The key components of the Warburg effect are increased glucose consumption and lactate production, increased intracellular glucose transport and expression of glycolyic enzymes, reduced pyruvate oxidation and inhibition of mitochondrial metabolism (Pedersen, 2007). Recent research has shown that cancer cell metabolic changes also include increased gluconeogenesis, increased glutaminolytic activity, reduced fatty oxidation, increased de novo fatty acid synthesis, increased glycerol turnover, modified amino acid metabolism and increased pentose phosphate pathway activity (as reviewed by Dakubo, 2010). Therefore, glycolysis is advantageous to cancer cells because not only does it permit cancer cells to survive in hypoxic conditions, it also provides most of the building blocks for cell proliferation and therefore, enables rapid tumour growth, progression, invasion and subsequent distant metastases (Lopez-Lazaro, 2008).

There is increasing evidence that aerobic glycolysis is an adaptive mechanism involving several coordinated metabolic and oncogenic pathways. For example, MYC activation results in increased expression of glycolytic genes, such as, hexokinase II, enolase, lactate dehydrogenase and phosphofructokinase (Shim et al, 2009; Osthus et al, 2000; Dang et al, 2008). PTEN loss and activation of PI3K/AKT

result in increased expression of glucose transporters, increased expression and activity of hexokinase II and phosphofructokinase (Elstrom et al, 2004; Robey & Hay, 2009). P53 has also been shown to be an important regulator of mitochondrial respiration and glycolsis (Bensaad et al, 2006; Matoba et al, 2006; Vousden & Ryan, 2009). Therefore, the known key molecular events in prostate carcinogenesis are all drivers of the biosynthetic cancer cell metabolism.

1.3 RNA polymerases

In prokaryotes, transcription only involves a single RNA polymerase whereas in eukaryotes three major RNA polymerases share this function and each one produces their own specific transcriptional products. In eukaryotes, there are three main types of RNA polymerases, RNA polymerase I, II and III (Pol I, II and III) (Roeder and Rutter, 1969). They are each devoted to the transcription of specific genes. It is thought Pol I contributes up to 70% and Pol II 20% of all nuclear transcription in actively growing cells. Pol III is the largest RNA polymerase with 17 subunits and responsible for 10% of all nuclear transcripts.

Pol I has 14 subunits and exclusively transcribes ribosomal RNA (rRNA) genes, of which there are approximately 400 copies in humans (reviewed in McStay and Grummt, 2008; Russell and Zomerdijk, 2006). rRNA is a major component of the ribosome and thus, the rate of Pol I transcription controls cellular proliferation and growth (Ruggero et al, 2003). In cancer cells Pol I transcription is deregulated and hyper-activated resulting in the boundless production of rRNA and ribosomes (Ruggero et al, 2003; Drygin et al, 2010; White et al, 2005). Furthermore, partially inhibiting rRNA synthesis with Pol I siRNA results in cancer cell death (Bywater et al, 2010).

Pol II has 12 subunits and transcribes protein- encoding genes, messenger RNA (mRNAs) and small non-coding nuclear RNAs (snRNAs), small nucleolar RNAs (snoRNAs) and micro RNAs (miRNAs) (as reviewed in Baumann et al, 2010). snoRNAs are protein noncoding molecules that associate with specific sets of proteins

to maintain proper ribosomal maturation in the nucleolus. Recent research has shown snoRNAs have tissue specific expression and may be useful as novel cancer biomarkers (as reviewed by Martens-Uzunova et al, 2015). For example, H/ACA-box snoRNA *SNORA42* is overexpressed in non-small cell lung cancer (NSCLC) and its expression is significantly inversely correlated with survival (Goeze et al, 2002; Mei et al, 2012).

snoRNAs are further processed to 20-24nt length small nucleolar RNA-derived RNAs (sdRNAs) (Martens-Uzunova et al, 2013). In 2015, Martens-Uzunova et al published deep sequencing data of patient derived samples from normal prostate and PC in different stages of diseases. This showed that at least 78 of the detected sdRNAs demonstrate strong differential expression in PC and some specific sdRNA expression have a prognostic implication. For example, *SNORD78* and its sdRNA were significantly higher in a subset of patients that developed metastatic PC (Martens-Uzunova et a, 2015).

RNA polymerases are recruited to specific transcription sites via interaction with transcription factors binding to specific DNA sequences called enhancer and promoter sequences. The RNA polymerases are commonly regarded as transcribing non-overlapping subsets of genes. However, recent evidence has shown that Pol III can accurately initiate transcription at some Pol II promoters *in vitro* and this suggests that polymerase specificity is not fixed, but rather depends on the properties of the promoter and transcription conditions (Duttke, 2014). Furthermore, chromatin immunoprecipitation (ChIP) –sequencing analysis found mapping of Pol II and Pol III localisation in human cell lines showed Pol II was closely associated with Pol III genes throughout the genome (Raha et al, 2010).

Strikingly, there are no recorded “gain of function” mutations in Pol I, II and III apparatus (Bywater et al, 2013). Therefore, upregulation of Pol I, II and III to ensure increased protein synthesis in cancer cells must be the result of activation of oncogenic signalling or release from tumour suppressor pathways (Quin et al, 2014).

1.3.1 The Nucleolus and Pol I transcription

The advent of light microscopy demonstrated the most prominent structure in the nucleus, the nucleolus. Nucleolus is a non-membrane bound structure and the site of rDNA transcription, rRNA processing and modification and ribosomal subunit assembly (Olson et al, 2005). It is a dynamic organelle with many of its constituents shuttling between the nucleolus and nucleoplasm. Almost all cancer types display enlarged and/or increased number of nucleoli (Pianese et al, 1896; MacCarty, 1936; Derenzini et al, 1986). The nucleolus disassembles at the onset of mitosis and reassembles during telophase, mirroring the inhibition of rRNA synthesis during prophase and its activation during telophase (Dundr et al, 2000). Ribosome biogenesis is an incredibly energy intensive cellular processes constantly being fine-tuned in response to growth conditions, such as cellular stress and cell cycle (Olson et al, 2005). It is a highly coordinated multi-stage process, with transcription of rDNA by Pol I being rate limiting (Chedin S et al, 2007).

Cancer cells have enlarged nucleoli meaning accelerated rates of transcription of ribosomal RNA genes (rDNA) transcription (by RNA polymerase I), 5S rRNA (by RNA polymerase III) and ribosomal protein (by RNA Polymerase II). Pol I transcription of rDNA leads to production of 47S rRNA precursor which is processed into 28s, 18s and 5.8S rRNAs. These rRNAs, together with Pol III transcription product 5S rRNA and Pol II transcription products ribosomal proteins (RP) are all essential components of the ribosome (reviewed by Leary et al, 2001). The rate of ribosome biogenesis controls cellular growth and proliferation (Ruggero et al, 2003). Therefore, in mammalian cells ribosome biogenesis is precisely regulated and responsive to extracellular stimuli, such as nutrient availability and stress. In cancer cells, the normal brakes on ribosome biogenesis are released and unbridled protein synthesis and tumour growth result (Drygin et al, 2011).

Pol I transcription is tightly controlled in healthy cells but is known to be elevated in various cancers and has been associated with a poor prognosis (Drygin et al, 2010; Williamson et al, 2006). During development, long term epigenetic mechanisms that regulate the balance of active to silent copies of rRNA genes control Pol I transcription. For example, hypo-methylation of rDNA promoters leading to

increased rRNA synthesis has been found in several tumour types (Drygin et al, 2014). Multiple proteins, including DNA methyltransferases and histone deacetylases, repress Pol I transcription, whereas histone acetyltransferases activate rRNA synthesis (Murayama et al, 2008). In response to acute cellular signalling and stress Pol I transcription is regulated by reversible modification of Pol I transcription factors and Pol I complex itself (Grummt et al, 2010; Goodfellow et al, 2012; Moss et al, 2007). rDNA transcription initiation needs assembly of 3 transcription factors SL1 (selectivity ligand 1) and a dimer of UBF (upstream binding factor) on the promoter and RRN3. Post-translational modifications such as UBF phosphorylation by cyclin-dependent kinases (CDK4/cyclin D) has been shown to increase rate of rDNA transcription while phosphorylation of SL1 by CDK1/cyclin B during mitosis stops Pol I transcription (Grummt et al, 2010).

Pol I transcription is regulated by oncogenes and tumour suppressors. MYC has been shown to enrich SL1 on rDNA promoter (Poortinga et al, 2011). AKT, mTOR and ERK can all phosphorylate UBF and other Pol I components to increase Pol I initiation and elongation (Hannan et al, 2003; Stefanovsky et al, 2006; Chan et al, 2011). ERBB2 (HER2) directly interacts with rDNA and Pol I to stimulate Pol I transcription in a PI3K and MEK/ERK-independent manner (Li et al, 2011). Two prominent tumour suppressors have been shown to inhibit Pol I transcription by disrupting UBF/SL1 interaction, namely pRb (Hannan et al, 2000) and p53 (Zhai et al, 2000).

Interestingly, proteomic analysis of the nucleolus has highlighted its functional diversity with less than half of 4500 proteins reported in the nucleolar protein database (NOPdb) having functional roles in ribosome biogenesis (http://lamondlab.com/NOPdb3.0). The nucleolus has been shown to be involved in modulation of the cellular stress response, regulation of senescence and cell cycle progression, RNA and ribonucleoprotein biogenesis and organisation of epigenome (Andersen et al, 2002; Scherl et al, 2002; Leung et al, 2006; Ahmad et al, 2009). Furthermore, the nucleolus is now thought to be a central stress sensor hub of the cell, oncogenic stress causes increased expression of tumour suppressor Alternate Reading Frame (ARF) which associates with E3 ubiquitin ligase Mouse double minute 2 homolog (MDM2) sequestering it in the nucleolus, resulting in activation of p53.

1.3.2 RNA Pol III transcription products

Pol III transcription factors and their products are overexpressed in some cancers (White et al, 2004; Daly et al, 2005). Breast cancer cells have significantly higher levels of nuclear-encoded and mitochondrial tRNAs than normal breast tissues (Pavon-Eternod et al, 2009; Zhou et al 2009). Pol III transcripts seem to localise in peri-nucleolar compartments (PNC) (Wang et al, 2003a) and increased histological detection of PNC has been correlated with tumour progression and poor prognosis (Norton et al, 2008). Scleroderma patients with auto-antibodies against Pol III are at a higher risk of a cancer diagnosis than patients who do not express these antibodies at high levels (Shah et al, 2010). Supporting evidence for the theory that Pol III activity is limiting to tumorigenesis, is an observed reduction of Pol III activity inhibiting tumour formation in a mouse xenograft model (Johnson et al, 2008). However, absence of recurrent mutations in Pol III subunits or associated transcription factors in tumours has led some to exclude Pol III as an important oncogenic driver.

Genes transcribed by Pol III are small untranslated RNAs, which are usually shorter than 300bp in length (White, 2002). Pol III transcribed RNAs are essential for protein translation and synthesis, including tRNAs and the 5S rRNA component of the ribosome, and mRNA processing, including U6 RNA and 7SK RNA which regulates Pol II activity (Schramm et al, 2002). Processing of RNA transcripts is performed by U6 snRNA, H1 RNA and MRP RNA, which are responsible for further editing the mRNA, tRNA and rRNA respectively. Pol III also transcribes short RNA sequences from viral genomes, such as adenovirus VA1 and VA2 RNA (Table 1.3). Genes transcribed by Pol III are called class III genes. Most promoters of class III genes are internal, that is they are located within the transcribed sequence. The promoters are commonly classified by their structure into 3 types (Table 1.4).

Interestingly, Pol III transcribed 5S rDNA genes can induce association of the genomic region in which they are integrated with the nucleoli (Fedoriw et al, 2013). It has been proposed that nucleolar association can result in repression of linked genes, demonstrating the association between rRNA transcription, nucleolar localisation and regulation of gene expression (Fedoriw et al, 2013). As non-coding repetitive elements derived from Pol III transcripts make up a large portion of the genome, these

could make a significant contribution to nucleolar association and therefore epigenetic regulation of the genome (Quin et al, 2014).

Mature transfer RNAs (tRNAs) are 70-90nt long adapter molecules, which facilitate the translation of mRNA molecules. Each tRNA recognises a specific three nucleotide codon on the mRNA and translates that codon to one of the twenty specific amino acids (Crick, 1968). tRNAs are essential for translation and until recently it has been assumed that tRNA levels are kept in excess in cells so as not to be a limiting step in translation and gene expression. However, increasing evidence has shown that oncogenes and tumour suppressor pathways can control tRNA synthesis and by regulating cellular tRNA levels, they can have significant effects on mRNA translation and hence, cell growth (Grewal et al, 2014).

tRNAs are among the most abundant molecules in a cell. For example, in yeast approximately 20% of all cellular transcription is devoted to making new tRNAs resulting in approximately 3 million new tRNAs being synthesised during each cell cycle (Grewal et al, 2014). The eukaryote genome has multiple copies for most of the tRNA genes and their transcription relies exclusively on RNA Pol III transcription machinery. The human nuclear genome encodes more than 500 tRNA genes (Chan et al, 2009) and countless genes of tRNA-"look-a-likes" similar to nuclear and mitochondrial tRNAs (Telonis et al, 2014). In yeasts, virtually all tRNAs are occupied by Pol III, whereas in humans approximately half of tRNA genes were considered unbound by Pol III in HeLa cells despite shared core promoter sequences (Oler et al, 2010). This suggests that additional controls influence promoter access in human cells (White, 2011). Interestingly, fewer Pol III transcribed genes were occupied in untransformed fibroblasts than in three transformed cell lines (Oler et al, 2010). Furthermore, gene expression microarrays have revealed that the relative proportion of individual tRNAs vary widely between different human tissues (Dittmar et al, 2006). ChIP-seq analysis suggests that differential promoter usage can explain most of this cell type specificity (Barski et al, 2010).

1.3.3 Is tRNA synthesis a limiting step for protein synthesis?

It has been generally assumed that tRNAs are abundant in cells, and as such the control of tRNA synthesis has not been considered a limiting step for protein synthesis. Most models propose signalling pathways regulate protein synthesis by changes in the activity or levels of eukaryotic initiation factors (eIFs). However, there is increasing evidence that stimulation of tRNA synthesis may be an additional control point in mRNA translation and therefore protein synthesis and growth (as reviewed by Grewal et al, 2014). It is thought that, by increasing total tRNA levels, mRNA translation would in turn be increased because more tRNAs would be available for incorporation into translating ribosomes A-site. As the initiator methionine tRNA ($tRNA_i^{Met}$) is required for ternary complex eIF2-GTP-$tRNA_i^{Met}$ formation, it is conceivable that specific increases in $tRNA_i^{Met}$ would increase rates of translation initiation (Grewal et al, 2014).

There is evidence that manipulation of tRNA levels can influence growth at the organism level. In *Drosophila* knockdown of Maf1, a repressor of Pol III leads to increased tRNA levels, accelerated larval development and increased growth (Rideout et al, 2012). Transgenic flies with extra copy of $tRNA_i^{Met}$ have the same phenotype as the *Maf1* knockdown flies (Rideout et al, 2012). Further analysis showed that increased mRNA translation was responsible for these growth effects as these *Maf1* knockdown and $tRNA_i^{Met}$ transgenic flies showed increased polysome content and the body size increases could be reduced in flies with genetically lowered ribosome levels (Rideout et al, 2012). Furthermore, elevated $tRNA_i^{Met}$ promoted increased cell proliferation in cultured mammary epithelial cells (Pavon-Eternod et al, 2013). Grewal et al, 2014 suggested oncogene and tumour suppressor pathways that increase tRNA levels may drive changes in mRNA translation and consequently tumour growth.

There is also some emerging evidence that cells can change the relative levels of specific amino acid tRNAs within their total pools depending on the proliferative status of the cells (Gingold et al, 2014). For example, cancer cells were seen to have increased mRNA levels of proliferation-associated genes and subsequent changes in relative tRNA expression levels to match codon usage in the proliferation gene

mRNAs in comparison to normal cells (Gingold et al, 2014). Furthermore, genome-wide Pol III ChIP/DNA sequencing studies suggest changes in surrounding chromatin and Pol II regulated genes may control tRNA gene expression (Barski et al, 2010; Oler et al, 2010). ChIP-seq analysis has shown epigenetic modifications, such as histone methylation and acetylation correlates with Pol III transcription in a broadly similar pattern as Pol II epigenetic modifications (Barski et al, 2010). White (2011) proposed that the SANT domain of BDP1 may allow TFIIIB to respond to histone modifications and these in turn may dictate which genes become active.

A further layer of possible control of mRNA translation is post-transcriptional tRNA modifications, such as splicing, cleaving, cytoplasmic-nuclear trafficking and numerous nucleotide modifications including methylation and thiolation. For example, for tRNAs to function in protein synthesis they have to undergo aminoacylation which involves joining the appropriate amino acid to correct isoacceptor tRNA catalysed by aminoacyl tRNA synthetases (aaRS). Interestingly, mRNA levels of aaRS genes are increased by MYC, TORC1 and PI3K in *Drosophila* (Lin et al, 2008; Teleman et al, 2008).

Hah et al, 2014 used global nuclear run-on coupled with massively parallel sequencing (GRO-seq) signalling pathways to explore estrogen responses in MCF-7 breast cancer cells. They showed that estrogen can control an impressively large fraction (26%) of the breast cancer transcriptome in a fast and hardy manner including upregulating the transcription of rRNAs (Pol I) and tRNAs (Pol III). In fact, short estrogen treatments can upregulate a third of the 500 tRNA genes in humans and this rises over time (Hah et al, 2011). The immediate effects of estrogen signalling are upregulation of mRNAs coding for transcription and nucleic acid metabolism whereas, the longer term effects focus on protein biosynthetic machinery (Hah et al, 2014).

1.3.4 tRNA fragments and cancer

Recent studies have suggested cellular stress results in some mature tRNAs being cleaved to smaller tRNA fragments and it is thought this may be a means of controlling mRNA translation (Thompson et al, 2009). Furthermore, tRNA fragments

(tRFs) are often overexpressed in tumour cells (Lee et al, 2009). Using deep sequencing of PC cell lines, LNCaP and C4-2, tRFs were discovered from precise processing at the 5'-3' end of mature or precursor tRNAs (Lee et al, 2009). Intriguingly, each tRF exhibited a characteristic expression pattern across a cell line panel, arguing against tRFs being random by-products from nonspecific degradation of tRNA (Lee et al, 2009). siRNA dependent knockdown of a particular tRF-1001 caused a decrease in cell proliferation with G2 arrest (Lee et al, 2009). Furthermore, tRNA halves have been found circulating as macromolecular complexes in serum (Dhahbi et al, 2013) and the abundance of specific circulating tRNA halves can change in the serum of breast cancer patients (Dhahbi et al, 2014).

It has been proposed that tRNA-derived small RNAs should be divided into two groups: i) tRNA-derived fragments (tRFs) 13-26nt in length and are products of precise processing at the 5' or 3' end of mature or precursor tRNAs (Sobala et al, 2011); ii) tRNA halves are 30-40nt derived from 5'-(5'-tRNA half) or 3'-part (3'-tRNA half) of mature tRNAs cleaved by stress activated ribonuclease angiogenin (Saikai et al, 2015). They are sometimes called tRNA-derived-stress-induced RNAs (tiRNAs) (Yamasaki et al, 2009) because their expression is increased by stresses, for example oxidative stress and UV irradiation (Thompson et al, 2009). Importantly, 5'-tiRNAs, but not 3'-tiRNAs, are functional molecules in that they promote formation of stress granules (Emara et al, 2010) and inhibit protein synthesis by displacing translational initiation factor complexes from mRNAs (Yamasaki et al, 2009; Ivanov et al, 2011). Furthermore, during hyperosmotic stress angiogenin-induced tiRNAs bind cytochrome c and inhibit binding of cytochrome c to apoptotic protease activating factor 1 (APAF1) protein, thus protecting cells from apoptosis (Saikia et al, 2014).

Honda et al, 2015 has recently discovered a new functional tRNA-derived small RNA that are predominantly expressed in estrogen receptor positive (ER+) breast cancer and androgen receptor (AR+) PC cell lines, termed Sex HOrmone-dependent tRNA-derived RNAs (SHOT-RNAs). They are produced by angiogenin (ANG)-induced anti-codon cleavage of amino-acylated mature tRNAs. In breast cancer human tumour samples, ER+ patient tissue showed an abundant expression level of SHOT-RNAs in contrast to ER-negative patient or normal breast tissues that did not. AR+

LNCaP-FGC cells expressed more of these SHOT-RNAs than AR-negative PC3 and DU145. siRNA knockdown studies of AR and hormone-free medium studies in LNCaP-FGC cells reduced amounts of SHOT-RNAs. Furthermore, siRNA-mediated depletion of 5'SHOT-RNAs, such as 5'SHOT-RNA^{AspGUC}, 5'SHOT-RNA^{HisGUG} and 5'SHOT-RNA^{LysCUU}, reduced cell proliferation in LNCaP-FGC cells by 50 % (Honda et al, 2015). Honda et al, 2015 proposed a model of sex hormone-signalling pathways stimulating ANG cleavage of aminoacylated mature tRNAs leading to production of SHOT-RNAs which enhances cell proliferation and therefore, may nurture tumour growth.

1.3.5 Pol III transcription machinery

RNA Pol III requires the assistance of two associated transcription factor complexes for transcription. These are called Transcription Factor IIIB (TFIIIB) and TFIIIC. TFIIIC recognises tRNA genes and binds to DNA at the internal tRNA gene promoters. TFIIIB can bind to DNA, TFIIIC and Pol III, and its recruitment of Pol III to specific genetic template is thought to be the main control point for tRNA synthesis as TFIIIC is present at both active and inactive tRNA genes (Kassavetis et al, 2006) (Figure 1.1).

TFIIIB is composed of three essential subunits, TATA-binding protein (TBP), BDP1, and either the TFIIB-related factors (BRF1) or the related subunit BRF2 (Geiduschek and Kassavetis, 2006; Schramm et al, 2002). The TFIIIB complex, used by gene internal Pol III promoters tRNA and 5S rRNA, consists of TBP, BDP1 and BRF1, whereas the upstream of initiation site external promoters of the U6 snRNA gene uses BRF2 (Schramm et al, 2002). The BDP1 subunit of TFIIIB contains a SANT domain, which is a motif of approximately 50 amino acid residues, and is thought to have a potential role in chromatin remodelling (Boyer et al, 2004). Interestingly, the chromatin environment seems to be important in dictating which Pol III templates are transcribed in human cells (White, 2011).

1.4 BRF1 (TFIIB-related factor 1)

BRF1 is a 90 kDa transcription factor TFIIIB subunit that binds to Pol III and specifically regulates Pol III transcription (Schramm et al, 2002). Repressing BRF1 decreases Pol III gene transcription (Zhang et al, 2013; Zhang et al, 2011; Zhong et al, 2013). BRF1 protein belongs to TFIIB-related transcription factor family, which all characteristically have a zinc ribbon domain and two internal cyclin repeats (Schramm et al, 2002). ChIP-seq data analysis showed BRF1 was 15 times more abundant than BRF2 at Pol III transcribed genes and that BRF1 co-localises with TFIIIC while BRF2 does not (Oler et al, 2010).

BRF1 expression can be induced in HPV-infected cervical cancer cells (Daly et al, 2005) and cardiomyocytes undergoing hypertrophy (Goodfellow et al, 2006 & 2007). Studies in cardiomyocytes showed BRF1 overexpression enhances Pol III transcription and this is required for inducing hypertrophic growth (Goodfellow et al, 2006). Zhong et al, 2014 recently found BRF1 is overexpressed in human breast cancer tissues. Furthermore, estrogen receptor positive (ER+) human breast cancer biopsies had higher BRF1 expression than estrogen receptor negative (ER-) breast cancer cases (Julka et al, 2008).

BRF2 (TFIIB-related factor 2, 50 kDa TFIIIB subunit) is structurally similar to BRF1, in that, they all have N-terminal zinc ribbon domains and core domains containing imperfect repeats. The structural difference between BRF1 and BRF2 is in their C-terminal extensions. BRF2 C-terminus is essential for association with TBP and SNAPc (small nuclear activating protein complex) on U6 promoter (Saxena et al, 2005). Overexpression of BRF2 has been seen in breast cancer (Melchor et al, 2007; Garcia et al, 2005), bladder cancer and lung squamous cell carcinoma (Lockwood et al, 2010). BRF2 overexpression was found to significantly correlate with cancer risk of metastases in a breast cancer (Cabarcas et al, 2011).

1.4.1 Regulation of Pol III transcription

Gene transcription is tightly regulated thus allowing cells to constantly adjust their RNA and protein content in response to environmental changes and metabolic requirements (White, 2001). Studies in yeast first showed that Pol III was regulated by growth cues, such as nutrient availability. Furthermore, in yeast, inhibition of Pol III transcription can stimulate stress-response pathways and indirectly disturb communication between Pol III and Pol II transcriptome (Conesa et al, 2005). Recent mammalian cell studies have described how oncogenes, tumour suppressors and cell cycle proteins can limit or amplify recruitment of Pol III to its target gene promoters (Sutcliffe et al, 2000; Felton-Edkins et al, 2003b; Stein et al, 2002; Gomez-Roman et al, 2003; White et al, 2004; White et al, 2005). The mechanisms of this control may involve gene upregulation of Pol III transcription factors, modified protein-protein interactions between the transcription factors or a direct effect on Pol III (White et al, 2004; White et al, 2005).

TFIIIB activity is suppressed by tumour suppressors in normal cells. pRb and p53 both bind to and inhibit TFIIIB in untransformed cells (Felton-Edkins et al, 2003b) and furthermore, loss of this repression results in Pol III transcription increase *in vivo* (Felton-Edkins et al, 2003b). pRb directly associates with and represses BRF1 (Larminie et al, 1997; Hirsch et al, 2004; Sutcliffe et al, 2000) whereas p53 interacts with TBP (Crighton et al, 2003) causing a defective TFIIIB complex that can no longer associate with TFIIIC or RNA Pol III. PTEN indirectly targets TFIIIB, perhaps by phosphorylation of BRF1, which induces disassociation of BRF1 and TBP and thus, also prevents functional TFIIIB complex formation (Woiwode et al, 2008). Another mechanism is through MAF1 repression of TFIIIB and this is switched off by mTOR phosphorylation, which in turn is antagonised by PTEN (Kantidakis et al, 2010).

It has been shown that some growth stimulatory pathways and oncogenes can stimulate Pol III mediated transcription; examples include Ras (Wang et al, 1997), c-MYC (Gomez-Roman et al, 2003) and activated PI3K (Wolwode et al, 2008). MAPK ERK2 can directly phosphorylate BRF1 and this seems not to disrupt association between BRF1 and BDP1, but instead enhances TFIIIB-TFIIIC and TFIIIB-RNA Pol

III interactions (Felton-Edkins et al, 2003a). Both BRF1 and BDP1 are phosphorylated at multiple sites (Woiwode et al, 2008; Felton-Edkins et al, 2003a; Fairley et al, 2003; Gottesfeld et al, 1994). Therefore, it is possible that changes in phosphorylation and/or other modifications may selectively enhance their function. Alternatively, recent studies support the idea that certain co-activators of Pol II transcription may be used to drive transcription of Pol III genes (Kenneth et al, 2008). Selective enhancement of function of these co-activators *in vivo* could potentially be used to drive increased Pol III transcription.

TBP is used by all three nuclear RNA polymerases, whereas BRF1 is Pol III specific. Johnson et al, 2008 showed that increased expression of TBP is sufficient to induce transformation and noted increased Pol III activity in these cells as well as in *c-MYC* transformed cells. However, modulating Pol III transcription alone did not alter proliferation rates or transforming properties of Rat1a cells. Overexpression and activated phosphorylation of BRF1 led to modest induction of Pol III transcription with subsequent increases in $tRNA_i^{Met}$ leading to more robust increase in transcription but both failed to promote cellular transformation (Johnson et al, 2008). Furthermore, RNA Pol II-defective TBP mutants which can still function in Pol I and III transcription, prevented TBP-mediated cellular transformation (Johnson et al, 2003). Johnson et al, 2003 concluded from these two studies that increased Pol III transcription is needed but not sufficient for cellular transformation (Johnson et al, 2008).

However, expression of mutant TBP proteins did not induce Pol III transcription nor anchorage-independent growth in Rat1a fibroblasts *in vitro,* but when these cells were subcutaneously injected into athymic mice there was stimulation of Pol III transcription and tumour formation (Johnson et al, 2008). The difference between these *in vitro* and *in vivo* results is most likely related to the *in vivo* environment and specifically the extracellular matrix components altering cellular signalling pathways and impinging on TBP-mediated changes in Pol II-dependent transcription and ultimately influencing Pol III-dependent transcription (Johnson et al, 2008).

1.4.2 Pol III is deregulated in cancer

1.4.2.1 Introduction

A hallmark trait of cancer is uncontrolled cell growth and proliferation (Hanahan & Weinberg, 2011). Therefore, unsurprisingly, deregulation of Pol III transcription has been seen in a variety of human cancers and altered levels of Pol III specific transcription factors are a common feature of mouse and human tumours (reviewed (reviewed by White, 2004; White et al, 2005). For example, in ovarian carcinomas, high levels of TFIIIC2 and tRNAs were consistently found (Winter et al, 2000). TBP overexpression has been observed in human colon cancer (Johnson et al, 2003). In breast cancer cells, tRNA levels have been reported as 10-fold higher than normal breast cells (Pavon-Eternod et al, 2009). Furthermore, increased Pol III products have been described in many different cells, when transformed by DNA tumour viruses including simian virus 40 (Larminie et al, 1999; White et al, 1990), polyomavirus and papovavirus (Felton-Edkins et al, 2002) and other viral products such as hepatitis B virus X protein (Wang et al, 1995) and human T-cell leukaemia virus type 1 Tax protein (Gottesfeld et al, 1996).

Pol III transcription is carefully controlled in normal cells by tumour suppressors but this regulation is overcome in cancer cells. Despite much evidence that Pol III transcription is enhanced in cancer, minimal is known about the underlying molecular mechanisms (Figures 1.2 & 1.3). In broad terms, Pol III activity can be increased not only by direct interaction with Pol III machinery and oncogenes and/or loss of interaction with tumour suppressors, but also through altered levels of Pol III itself and Pol III transcription factors such as BRF1.

1.4.2.2 Pol III and mTOR

The TOR kinase pathway is a key regulator of tissue growth. Extracellular growth factors and nutrients stimulate TOR activity (Wang and Proud, 2009) to control cell, tissue and organismal growth. Marshall et al, 2012 showed that Pol III-dependent transcription is a critical regulation target of TOR in Drosophila. It has been well studied that TORC1 can control mRNA translation initiation through the regulation of eukaryotic initiation factor (eIF) activity (Ma et al, 2009; Roux et al, 2012). However,

accumulating evidence shows TORC1 signalling can influence Pol III transcription by direct or indirect phosphorylation of components of Pol III machinery. For example, when TORC1 is inhibited, dephosphorylated MAF1 is localised within the nucleus and directly binds to Pol III or BRF1, therefore disrupting the Pol III transcription complex and preventing Pol III recruitment to tRNA genes. In contrast, TORC1 activation leads to direct MAF1 phosphorylation and Pol III transcription is no longer repressed (Kantidakis et al, 2010; Shor et al, 2010).

Another potential mechanism of TORC1 activation of Pol III transcription is through PTEN loss and subsequent activation of PI3K/AKT signalling leading to phosphorylation of BRF1 and stimulation of Pol III in a rapamycin sensitive manner (Woiwode et al, 2008). ChIP studies have shown TORC1 localisation at Pol III target genes (Kantidakis et al, 2010; Tsang et al, 2010) and genome wide analysis shows mTOR has 76% overlap with Pol III at tRNA genes (Chaveroux et al, 2013). Furthermore, *Drosophila* studies have shown larvae growth caused by Torc1 activation is blocked in cells mutant for Brf1 (Marshall et al, 2012). Interestingly, AKT activation is known to enhance rRNA synthesis and promotes tumour growth (Levy et al, 2009; Nguyen et al, 2013).

Recently, MAF1 was proposed as a tumour suppressor downstream of PTEN. PTEN-mediated changes in MAF1 expression involved PTEN-induced changes in PI3K/AKT/FOXO1 signalling (Palian et al, 2014). MAF1 is a negative controller of Pol III and some Pol II-dependent genes (Johnson et al, 2007). *Pten*-null mice prostates and livers have decreased Maf1 expression, whereas PTEN re-expression in human glioblastoma U87 deficient cells increases MAF1 expression (Palian et al, 2014). In mouse embryo fibroblasts (MEFs), *Pten* loss led to marked reduction in Maf1 protein levels (Palian et al, 2014). Furthermore, human PC samples with PTEN loss had significantly reduced MAF1 expression than normal healthy prostate epithelium without PTEN loss (Palian et al, 2014). Enhanced MAF1 expression in stable hepatoma Huh-7 cells reduced anchorage independent growth and tumour formation in mice (Palian et al, 2014). They concluded that MAF1 is an essential downstream effector of PTEN/PI3K/AKT/FOXO1 signalling and a central target to co-repress genes involved in proliferative, biosynthetic and metabolic processes (Palian et al, 2014).

1.4.2.3 Pol III and MYC

MYC is a transcription factor that binds to DNA as a dimer with its partner MAX to regulate genes involved in cell growth, proliferation and apoptosis (Grandori et al, 2000). More specifically, MYC acts as a master controller of ribosome biogenesis and protein synthesis (Gomez-Roman et al, 2006). It is one of the most frequently activated oncoproteins, being overexpressed in ~ 50% of all cancers (Nesbit et al, 1999; Dang, 2012). Overexpression of MYC drives ribosome biogenesis and mRNA translation, while MYC deficient cells are defective in these processes (Grewal et al, 2005; van Riggelen et al, 2010). This is consistent with earlier observations: Myc deficient mouse cells are defective in Pol III transcription, whereas overexpression of Myc can increase Pol III transcription and tRNA expression (Aaronson et al, 1991). *Drosophila* studies have shown Myc overexpression upregulates Brf1 and other Pol III factors to promote body growth (Grewal et al, 2005). Furthermore, Myc transforms Rat1a fibroblasts and promotes soft agar growth and xenograft tumour formation in mice in a Pol III/Brf1 dependent manner (Johnson et al, 2008).

Brf1 expression increases in a Myc- dependent manner in mice (Sansom et al, 2007), and the *Brf1* promoter region contains Myc/Max binding sites. However, it is unclear whether MYC directly or indirectly regulates BRF1 expression. Interestingly, ChIP-seq data found MYC at 74% of cellular loci occupied by Pol III. However, the presence of TFIIIB does not ensure MYC occupancy (Raha et al, 2010). Co-Immunoprecipitation studies have identified c-MYC binds stably to the TFIIIB complex, specifically to BRF1 (Gomez-Roman et al, 2003). In cycling fibroblasts, B cells and epithelial cells, endogenous c-MYC is located at the $tRNA^{Leu}$, $tRNA^{Tyr}$ and *5SrRNA* genes (Gomez-Roman et al, 2003). Taken together, these results show MYC can directly localise at tRNA genes due to an association between MYC and BRF1 (Gomez- Roman et al, 2003).

The *BRF1* promoter has binding sites for nuclear respiratory factor 1 (NRF1) (Huo et al, 2001), Zic2 (Ishiguro et al, 2008) and immediate early growth response (EGR1) (Adamson et al, 2002). It also has multiple binding sites for tumour suppressor ZF9 (also known as KLF6; Muhlbauer at al, 2003), KLF3 (Lomberk et al, 2005) and two ZF5 cis-regulatory elements, which are known negative regulators of the *c-MYC*

promoter (Numoto et al, 1995). These could all have a role in negative regulation of the *BRF1* promoter. ChIP-seq studies also discovered several factors co-localising with Pol III, including FOS, JUN and ETS1 (Oler et al, 2010; Raha et al, 2010), that may directly influence Pol III transcription (White, 2011).

Intriguingly, Pol II has been found to co-localise upstream of Pol III genes, including *tRNA*, *5S rRNA* and *U6 snRNA* genes (Barski et al, 2010; Oler et al, 2010; Raha et al. 2010). Pol II recruitment may result from presence of regulatory factors (such as MYC) at Pol III promoters, which are able to attract more than one RNA polymerase, or due to the establishment of more accessible chromatin environments. Previous studies have suggested that Pol II transcribed MYC target genes are involved in metabolism and translation (Coller et al, 2000; Boon et al, 2001). White (2011) proposed Pol III occupancy and upstream Pol II co-localisation is highly suggestive of a regulatory interaction and cancers may use Pol II recruitment to raise expression of key Pol III products during tumorigenesis. Furthermore, the capacity of MYC to positively regulate Pol II and Pol III-transcription may enable MYC to coordinate induction of protein synthesis in a synergistic manner (Gomez-Roman et al, 2003).

The Ras family of G proteins are involved in cell proliferation, growth, survival and differentiation. Overexpression of Ras in mouse models is sufficient to drive tumorigenesis (Pylayeva-Gupta et al, 2011). Ras activation leads to a cascade of kinase activation – RAF, MEK and ERK, all part of the Extracellular signal regulated kinase (ERK) pathway. Activation of ERK pathway can upregulate MYC protein levels (Sears et al, 1999) and has been shown to crosstalk with TORC1 (Roux et al, 2012). Furthermore, ERK can directly associate with and phosphorylate BRF1 leading to enhanced Pol III dependent tRNA synthesis in cultured fibroblasts (Felton-Edkins et al, 2003a) and Ras/ERK signalling can increase expression of TBP and BRF1 (Goodfellow et al, 2006; Zhong et al, 2004).

1.4.2.4 Pol III and JNK

JNK1 positively mediates Pol III gene transcription and c-Jun is a downstream target of JNK (Zhong et al, 2009). Alcohol induced increases in c-Jun activity increases estrogen receptor alpha (ERα) expression and ERα occupancy in the *BRF1* promoter

resulting in increased BRF1 expression (Zhong et al, 2014). In contrast, tamoxifen (a small molecule anti-estrogen agent) was shown to inhibit BRF1 expression and Pol III gene transcription via the c-Jun and ERα pathway to repress cell proliferation (Zhong et al, 2014). Tamoxifen treatment of breast cancer and non-tumour cells decreases cellular BRF1 mRNA and protein and reduces the occupancy of BRF1 in the promoters of *tRNA*^{Leu} and *5S rRNA* (Zhong et al, 2014).

1.4.2.5 Pol III and P53

p53 inactivation is a vital step in carcinogenesis (Vousden et al, 2007; Mills, 2012). Impairing ribosome biogenesis leads to activation of a nucleolar stress/ surveillance mechanism that can result in accumulation of p53 (Zhang et al, 2009; Deisenroth et al, 2010). Furthermore, p53 is activated in response to impairment of ribosome biogenesis and suppressed by increased ribosome biogenesis driven by proto-oncogenic growth and survival signals (Donati et al, 2011). P53 is a general repressor of Pol III genes including tRNAs and directly binds to TBP to prevent Pol III recruitment to its genetic template (Cairns et al, 1998; Crighton et a, 2003). Overexpression of p53 inhibits tRNA synthesis, whereas p53$^{-/-}$ mice fibroblasts have elevated Pol III transcription and tRNA levels (Cairns et al, 1998).

p53 is also a repressor of Pol I transcription and does this by disrupting pre-initiation complex formation, while Pol I transcription reciprocally inhibits p53 activation through ribosomal protein sequestration in the nucleolus (Budde et al, 1999; Zhai et al, 2000). Furthermore, inhibiting Pol I activity triggers “nucleolar stress” leading to ribosomal proteins translocating from nucleolus to nucleoplasm, leading to dissociation of MDM2 from p53, p53 stabilisation and p53–dependent apoptosis (Deisenroth et al, 2010). Therefore, by maintaining enhanced Pol I activity, cancer cells promote suppression of p53 and maintain nucleolar integrity (Haddach et al, 2012).

1.4.2.6 Pol III and RB

pRb is a 110 kDa protein which is phosphorylated in rapidly dividing cells and dephosphorylated in growth arrested cells (Buchkovich et al, 1989; Chen et al, 1989; DeCaprio et al, 1989; Ludlow et al, 1990). The tumour suppressor pRb controls cell

growth by restricting cell cycle entry by binding and inhibiting E2F, a transcription factor essential for cell cycle gene transcription (Dyson, 1998). Dysregulation of cell cycle control and specifically the CDK-cyclinD/INK4/pRb/E2F pathway regulating G1/S transition is a common feature of most cancers (Canavese et al, 2012). Furthermore, inactivating mutations of *RB1* are associated with a variety of human cancers (Burkhart et al, 2008).

Pol III transcription is under tight control during development and throughout the cell cycle. Pol III activity is maximal in late G1, S and G2 phases with lowest activity in early G1 and M phases (Johnson et al, 1974; Gottesfeld et al, 1994; White et al, 1995; Hu et al, 2004). Reduced Pol III activity in early G1 phase correlates with increased pRb activity at the same time in cell cycle (White et al, 1995). pRb represses Pol III activity *in vitro* and *in vivo* (White et al, 1996). *pRb*-deficient MEFs support elevated Pol III transcription, whereas matched wildtype MEFs did not (White et al, 1996). Co-immunoprecipitation assays have shown that pRb can co-purify with BRF1 and disrupt binding between BRF1 and TFIIIC2 (Larminie et al, 1997; Chu et al, 1997). Furthermore, pRb obstructed BRF1 association with TFIIIC and Pol III, but not with TBP (Sutcliffe et al, 2000). Genome-wide ChIP studies have shown that pRb can localise at Pol III genes, including tRNAs (Gjidodal et al, 2013). Overexpression of pRb inhibits Pol III transcription, whereas, $Rb^{-/-}$ cells have higher levels of tRNAs (White et al, 1996). Interestingly, ChIP-Seq experiments on human IMR90 fibroblasts showed increased pRb association with all Pol III genes during senescence (Chicas et al, 2010). As senescence induction represents an important mechanism for tumour suppression by pRb, this supports the notion that Pol III repression has a role in key cancer prevention networks (Gjidoda et al, 2009).

1.4.2.7 Pol III and BRCA1

BRCA1 (breast cancer susceptibility gene 1) carriers have an elevated risk of developing breast, ovarian, pancreatic, uterine, cervical and prostate cancers (Rosen et al, 2006). BRCA1's functions include cell cycle regulation, DNA repair, genome integrity, apoptosis and ubiquitination (Billack et al, 2005; Deng et al, 2006). BRCA1 has been identified as a general repressor of Pol III transcription (Veras et al, 2009). Veras et al, 2009 showed that BRCA1 inhibits Pol III transcription and that BRF1

overexpression relieves BRCA1-mediated inhibition of Pol III transcription (Veras et al, 2009).

1.5 Brf1 expression and Prostate Cancer

Interestingly, a PhD student (Noor Nam) working with both Professor White and Professor Leung's labs has previously analysed BRF1 protein expression in human prostate tumour samples and showed that BRF1 is overexpressed in Prostate Cancer in comparison to BPH. Analysing BRF1 expression at protein level was performed using an optimised immunohistochemistry (IHC) protocol (Unpublished, Nam 2013). Collectively, two independent tissue microarrays (TMAs) were employed. Firstly, a TMA from Glasgow, consisting of samples from 149 cases of untreated prostate cancer (PC) along with prostate tissue from 21 cases of benign prostatic hyperplasia (BPH) showed BRF1 immunoreactivity analysis on the Glasgow TMA cohort showed that PC samples had higher BRF1 protein expression than the BPH cohort (Figure 1.4A). This was confirmed with a larger TMA from Newcastle combined with the Glasgow TMA analysis showing BRF1 expression was upregulated in PC (n=518) relative to BPH (n = 134) (p=0.0034) (Figure 1.4B) (Unpublished, Nam 2013).

Further statistical analysis was performed to see whether BRF1 is associated with any prognostic markers of PC. While BRF1 expression was not found to be associated with clinical pathologic parameters such as Gleason sum score (p = 0.653) and serum PSA levels (p=0.381), it was significantly associated with Ki67 expression (p=0.034), signifying potential association with enhanced tumour proliferation (Unpublished Nam, 2013). Importantly, elevated BRF1 expression was significantly associated with unfavourable patient survival outcome in univariate analysis (Kaplan Meier analysis disease specific survival $p < 0.001$ and overall survival $p < 0.003$) (Figure 1.5) (Unpublished, Nam 2013).

This exciting clinical data led to another joint research venture between Professor White's Pol III research group and Professor's Leung Prostate Cancer research group; a successful MRC research grant application to further explore BRF1's role in Prostate Carcinogenesis. The results of this reseach will be presented and discussed in the following chapters.

1.6 Summary

Inflated protein synthesis is strongly linked to cancer, as may be expected to meet the demands for increased cell growth and division. Pol III transcription factors and their products are overexpressed in some cancers (White et al, 2004; Daly et al, 2005). BRF1 has no known role outside of Pol III transcription but is a molecular target of control by numerous tumour suppressors, including p53 (Felton-Edkins et al, 2003b), PTEN (Woiwode et al, 2008), ARF (Morton et al, 2007), pRb (Felton-Edkins et al, 2003b) and oncogene activation by c-MYC and MAPK/ERK (Felton-Edkins et al, 2003a, White, 2004) (Figures 1.2 and 1.3). The fact that BRF1 is a target of key tumour suppressors and needs to be kept under restraint in healthy cells suggests BRF1 has the potential for being a driver of carcinogenesis.

Risk	Tumour Stage	Gleason Score	PSA ng/ml	Biochemical progression at 5 yrs
Low	T1- T2a	and ≤6	and <10	10%
Intermediate	T2b	or 7	or 10-20	40%
High	≥T2c	or 8-10	or >20	70%

Table 1-1 Localised PC risk groups

(Adapted from D'Amico et al, 1998)

LOSS	GAIN
8p23-p11 (NKX3.1) (Primary 53-67%; CRPC 67-74%)	**1q32.1-q32.3 (ELK4)**
10q23 (*PTEN*) (Primary 12-30%, Advanced 36-80%)	**3q26.1 (PIK3CA)** (Primary 13-39%)
12p13 CDKN1B, *ETV6, DUSP16* (Primary 30%; Advanced 30-50%)	**8p12-q24.3 (*MYC*, *MAF*)** (Primary 20-30%; CRPC 64-82%)
13q12.3- q14.2 (*RB1, BRCA2, FOXO1*) (Primary 11-40%; CRPC 35-95%)	**Xp11.22-q13.1 (AR)** (CRPC 50 - 58%)
17p13.1 (*p53*) (Primary 20-30%)	
17q21.31 *ETV4* (Primary 20%)	
21q22.3 (*TMPRSS2-ERG)* **(**Primary 33-50%; Advanced 33%)	

Table 1-2 Most commonly altered chromosome locations and well characterised genes in human PC. The genes highlighted in red are known regulators of BRF1.

(Adapted from Schoenborn et al, 2013)

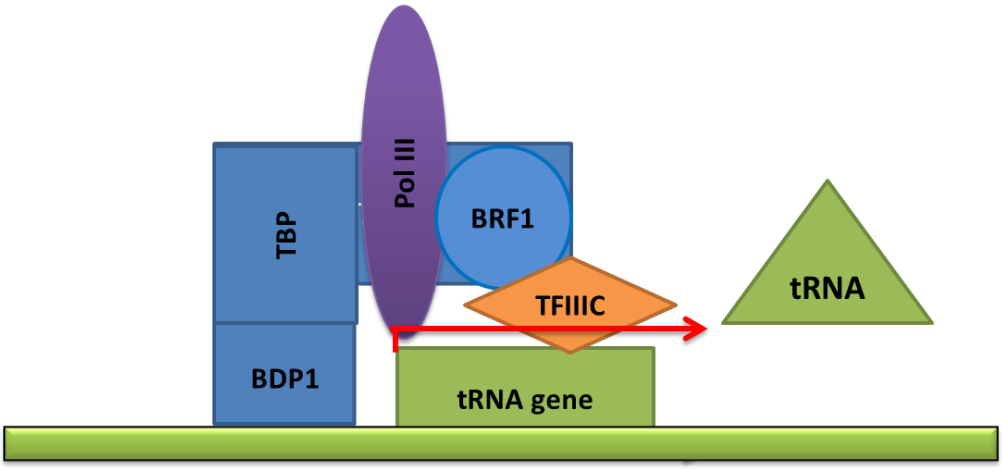

Figure 1-1 Pol III transcription machinery
TFIIIC binds to promoter DNA sequences within the transcribed region of a tRNA region of a tRNA gene. TFIIIC recruits TFIIIB by protein-protein interactions and positions it adjacent to the start of a tRNA gene. TFIIIB recruits Pol III to the transcription start site. TFIIIB is composed of three subunits TBP, BDP1 and BRF1 (colour coded blue).

RNA Pol III PRODUCT	FUNCTION
tRNA	Translation of mRNAs.
5S rRNA	Protein synthesis.
7SL RNA	Part of signal recognition particle (SRP) complex, responsible for intracellular protein transport. Acts as scaffold within SRP, which inserts nascent polypeptides into membranes.
7SK RNA	Binds to elongation factor p-TEFb and suppresses Pol II elongation. Regulates Pol II transcription elongation factor P-TEFb (Nguyen et al, 2001; Yang et al, 2001).
MRP RNA	Mitochondrial replication; Pre-rRNA processing; Processing of large rRNA (Clayton, 2001).
U6 snRNA	RNA processing and splicing precursor mRNAs.
H1 RNA	RNA component of RNase P, which processes the 5' end of tRNAs.
SINEs	Short interspersed nuclear elements. Unknown function.
Alu RNA	Inhibit Pol II transcription after heat shock in humans.
B2 RNA	Inhibit Pol II transcription after heat shock in mice.
Vault vRNA	Essential component of vault ribonucleoprotein (RNP) complex associated with development of multidrug resistance in human tumours (Dieci et al, 2007).
VA1 and VA2 RNA	Drive translation machinery in adenovirus infected cells to produce additional viral proteins.

Table 1-3 RNA Pol III transcription products

Promoter Type	RNA product
Type 1 (internal)	5S rRNA, SINE3-RNAs
Type 2 (internal)	tRNAs, 7SL RNA, vault RNA, Alu RNAs, B1 & B2 RNAs, adenoviral VA RNAs
Type 3 (external)	U6 snRNA, 7SK RNA, Y RNAs, H1 RNA, RNA component of RNase MRP

Table 1-4 RNA products of class III genes with different promoters
(Adapted from Nikitina et al, 2011)

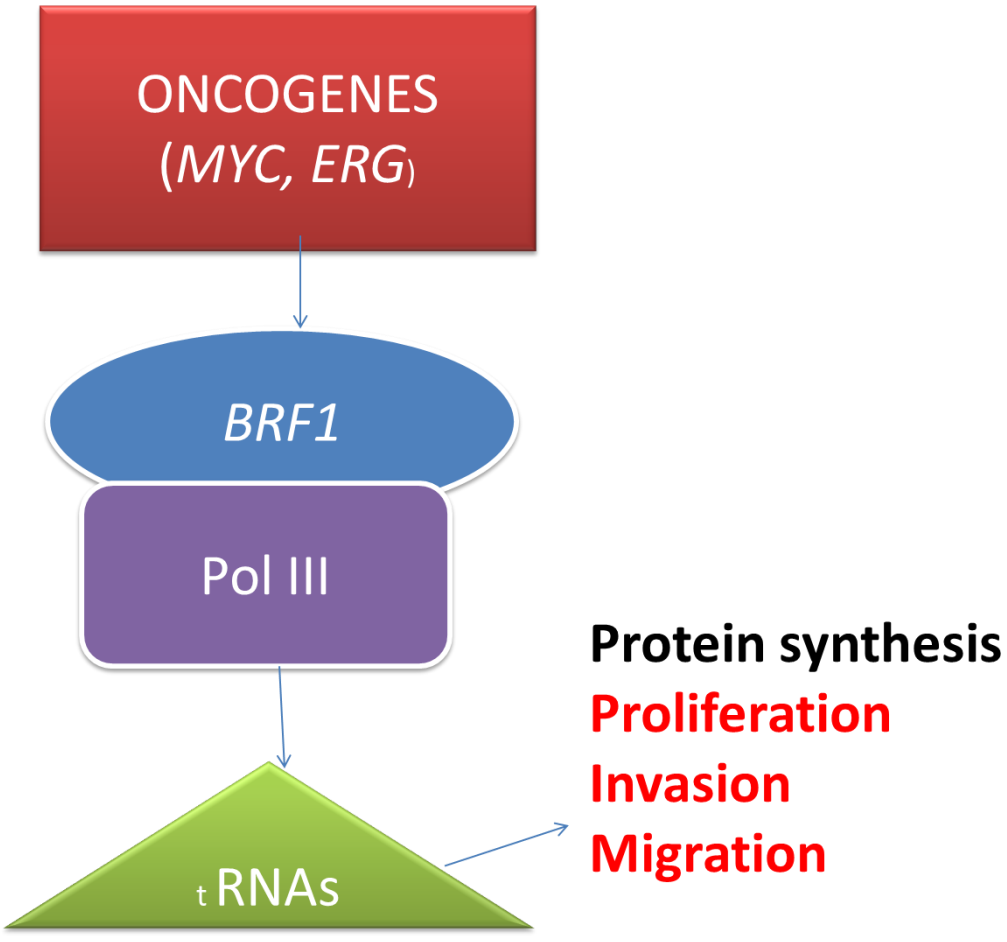

Figure 1-2 Proposed model of Pol III oncogenic pathway
Oncogenes bind to *BRF1* promoter causing activation of Pol III transcription complex and subsequent increase in Pol III products, such as tRNAs that can transform cell into a cancer phenotype with uncontrolled proliferation and growth.

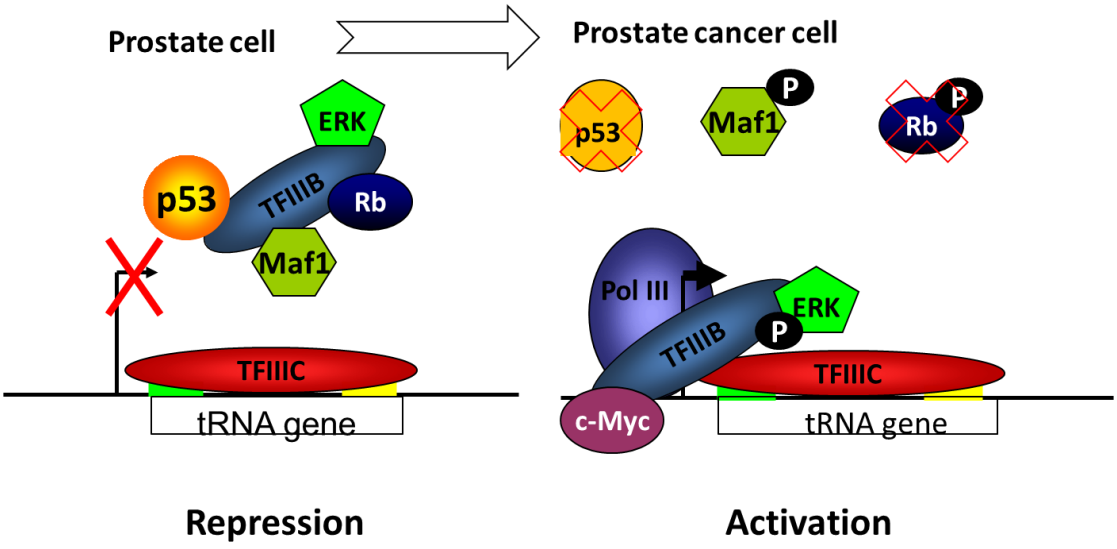

Figure 1-3 Proposed model of Pol III activation in prostate cancer.
TFIIIB, and more specifically BRF1, is a molecular target of regulation by many tumour suppressors, including p53, PTEN, pRb and oncogene c-MYC and mitogen activated protein kinase ERK (Felton-Edkins et al, 2003a&b, White, 2004; reviewed by Cabarcas et al, 2008).

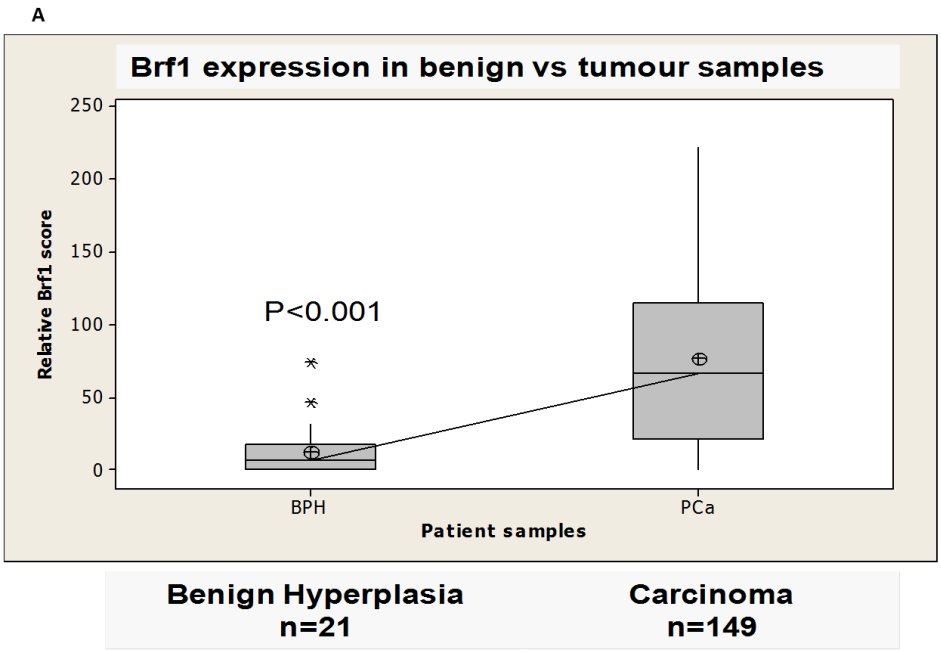

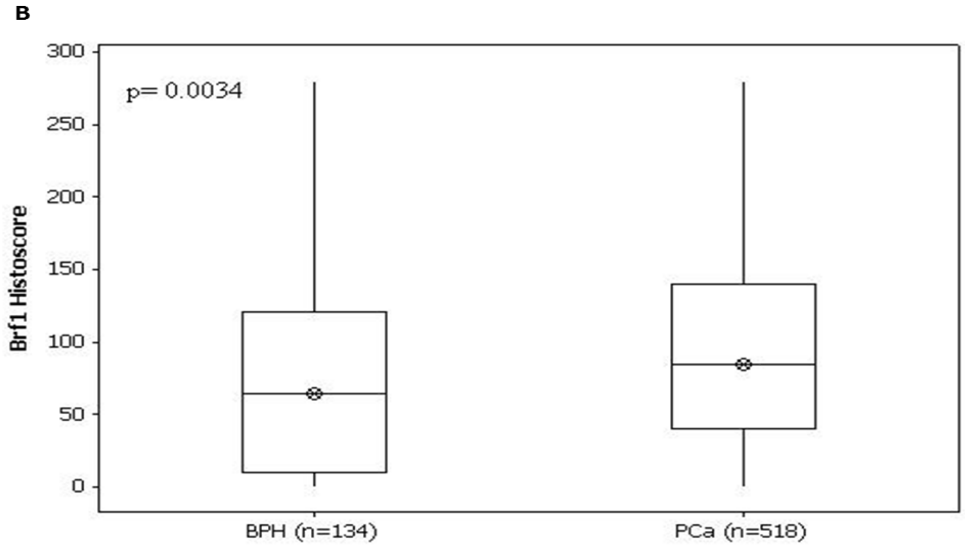

Figure 1-4 Box-plots showing BRF1 expression in benign prostatic hyperplasia (BPH) and prostate cancer patient TMAs.
A) Glasgow cohort.
B) Glasgow and Newcastle combined cohort.

BRF1 protein expression in prostate epithelium as determined by IHC was significantly elevated in prostate cancer in comparison to BPH in both the Glasgow cohort and combined Glasgow and Newcastle cohort. (Data provided by Nam, 2013, Unpublished)

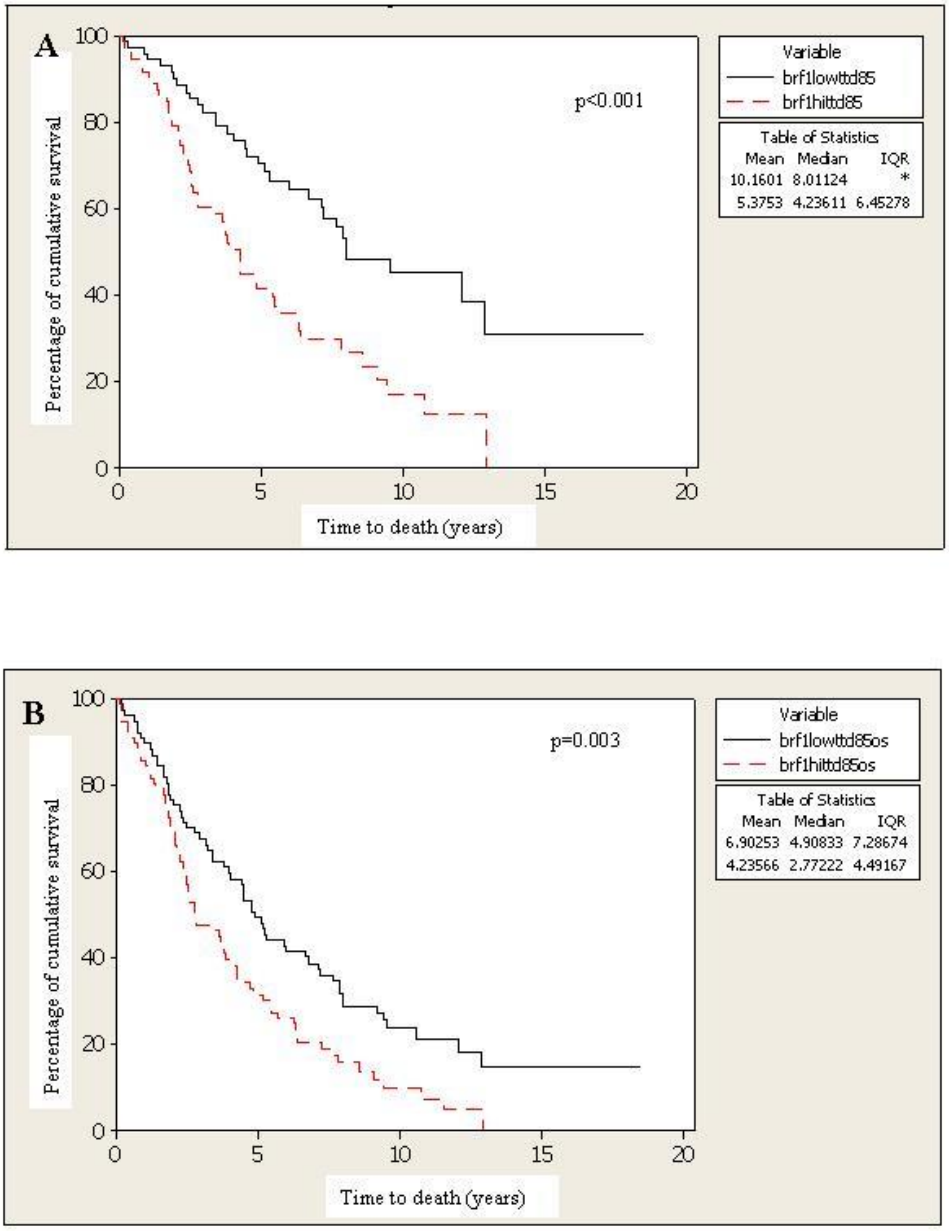

Figure 1-5 Kaplan-Meier (KM) survival curve analysis on combined Glasgow and Newcastle cohort

This KM curve shows significant correlation of the high BRF1 expression (red line) with poor patient outcome in both A) Disease specific (Log rank, $p < 0.001$).
B) Overall survival (log rank, $p < 0.003$). (Data provided by Nam, 2013, Unpublished).

Aims of study

To determine the functional importance of BRF1 for prostate carcinogenesis by measuring and manipulating levels of BRF1 expression in PC cell lines and mice models. The importance of this work is to provide evidence to support or refute Pol III machinery and BRF1 specifically as a potential driver and therapeutic target in PC.

The hypotheses of this study are two-fold:

1) Overexpression of BRF1 is an important step in prostate carcinogenesis.

2) Manipulation of BRF1 influences PC development.

2 Materials and Methods

2.1 Cell Culture

Human PC cell lines were purchased from ATCC and authenticated by LCG standards. All cell culture work was performed in a Class II tissue culture (TC) hood unless otherwise stated. Aseptic techniques with sterile equipment and reagents (cell culture grade) were adopted. All cell types were grown sub-confluent in humidified conditions containing 5% CO_2 at 37°C in a TC incubator.

DU145, LNCaP, PC3, PC3M and CWR-22 cells were grown in RPMI-1640 medium, 10% FBS and 2mM L-Glutamine. LNCaP-AI (a cell line derived from LNCaP cells following chronic androgen deprivation therapy with culture in charcoal stripped medium) were grown in RPMI-1640 medium, 10% charcoal stripped serum and 2mM L-Glutamine. RWPE-1 cells were grown in keratinocyte growth media with growth supplements. VCaP cells were grown in DMEM, 10% FBS and 2mM L-Glutamine. 22RV1 cells were grown in RPMI with no phenol, charcoal stripped serum and 2mM L-Glutamine. VCaP and 22Rv1 cells were grown in category 2 TC hoods and incubators. (All the reagents and their suppliers used in this study are listed in Table 2.1).

Cells were passaged approximately every 3 to 4 days at 70-85% confluency depending on cell type. Medium was aspirated and cells washed with Phosphate Buffered Solution (PBS) followed by incubation with buffered trypsin-EDTA (0.05% trypsin (Invitrogen), 0.02% EDTA (Sigma) for approximately 2 minutes. Fresh medium was then added to the non-adhered cells in order to neutralise the trypsin. Cells were counted using a CASY counter™ (Innovatis) and seeded as required, and cell suspensions were transferred to new flasks/ plates.

Cryo-freezing was used for storage of all cell lines. Cells were trypsinised using buffered trypsin-EDTA as already described, pelleted by centrifugation at 1,200 RPM (rev per min) and resuspended in 50% media (40% FBS and 10% (v/v) dimethyl sulphoxide (DMSO, Sigma). 1ml aliquots of cell suspension were transferred to cryotubes (Nunc) and immediately placed on dry ice and then frozen overnight wrapped in cotton wool in -80°C freezer. The frozen aliquots of cells were transferred on dry ice to liquid nitrogen for permanent storage.

Recovery of cells was performed by transferring the cryotubes from dry ice to 37°C water bath. Immediately after thawing, the cells were then diluted in fresh media, centrifuged at 1,200 RPM and the supernatants were aspirated off to completely remove the media containing DMSO. Cell pellets were resuspended in pre-warmed fresh media filled 25 cm^2 flasks and placed in the TC incubator.

2.2 Protein expression analysis

Bio-RAD® western blot equipment was used for sodium-dodecyl sulphate (SDS) polyacrylamide gel electrophoresis. Proteins were resolved using denaturing SDS-PAGE polyacrylamide gels. Lower SDS-PAGE gel components were added to a universal tube, mixed and then immediately poured in between gel plates. For example, 7.8% gels were made to assess for BRF1 protein expression. A lower gel was composed of 4.8ml of dH_20, 2.5ml lower gel buffer (1.5M Tris Base and 0.4% SDS pH 8.8), 2.6ml 30% acrylamide, 60µl 20% ammonium persulphate (APS) and 22µl tetramethylethylenediamine (TEMED). Once the lower gel was set the upper gel components (3ml dH_20, 1.25ml upper gel buffer (0.5M Tris and 0.4% SDS pH 6.8) 0.7ml 30% acrylamide, 30µl 20% APS and 11µL TEMED) were then added to the universal and immediately poured over the top of the lower gel between two gel plates. Gel forks were placed in the upper gel and removed once the gel was set and forked surface of set gel was washed out with distilled water.

Western blot cell lysates were prepared directly from 70-85% confluent cells grown in 6 or 10cm plates. Cell media was aspirated off and cells were washed in ice cold PBS twice. The preparation of cell lysates was performed on ice rapidly to avoid protein degradation. 100µL of cell lysis buffer (Table 2.2) was pipetted directly onto the cell plates and cells were scraped off with cell scrappers. Cell lysates were pipetted into labelled eppendorfs and left on ice for 15 minutes. They were then centrifuged for 15 minutes at 13,200 RPM at 4°C. The supernatants were then collected and protein concentration was measured using Bradford's reagent diluted 1:5 with dH_20 at 595 nm in a spectrophotometer. (For preparation of extracts from mouse prostate tissue please see section 2.22). All the protein samples were adjusted to be at equal concentration

(1µg/µl in 25µl total volume) with 4 x loading buffer (62.5mM Tris pH6.8, 0.5% SDS, 5% β-mercaptoethanol, 10% glycerol, 0.125% bromophenol blue) and distilled water. These adjusted protein samples were then heated at 100°C for 5 minutes in a heat block.

25µg protein samples were loaded onto the SDS-PAGE gel with a protein ladder marker (Spectra™ Multicolour Broad Range Protein Ladder, ThermoFisher #26623) and electrophoresed in Bio-RAD tanks at 180V in 1x SDS running buffer (0.1% SDS, 76.8mM glycine, 10mM Tris, pH8.3).

After separation by SDS-PAGE, the resolved proteins were transferred to a polyvinylidene difluoride (PVDF) membrane (Millipore Immobilon®-P Transfer Membrane) using a Bio-RAD Mini Trans-Blot Electrophoretic Transfer Cell system. The transfer buffer consisted of 20% methanol, 76.8mM glycine, 10mM Tris pH8.3 and distilled water. Each gel was transferred at 90V for 2 hours with ice packs at 4°C. Subsequently, the membranes were incubated in a blocking buffer (5% Marvel milk /TBST) (Table 2.2) for 1 hour and then washed in TBST three times for 5 minutes. They were then incubated in a primary antibody diluted in blocking buffer overnight at 4°C. The primary antibody was removed and membranes washed with TBST three times for 5 minutes. The secondary antibody was then added (diluted in blocking buffer) for 1 hour at room temperature. The membranes were washed with TBST three times for 5 minutes. The bound antibodies were then detected on the membrane with an enhanced chemiluminescense (ECL detection kit, GE Healthcare) in the dark room. All the antibodies used in this study are listed in Table 2.3.

2.3 Chromatin Immunoprecipitation (ChIP)

ChIP is a multistep 3 day protocol that was optimised in terms of the primers, antibodies, sonication times and beads used (data not shown). Cells at 80% confluency culture in a 10cm plate were used for individual immunoprecipitation (IP) experiment. Cells in their normal media were incubated for 7 minutes at room temperature under a TC hood in final concentration of 1% formaldehyde to cross-link

the protein-DNA complexes. The cross-linking was quenched by addition of final concentration of 0.125M Glycine for 5 minutes incubation at room temperature. This solution was aspirated and safely discarded. Cell plates were transferred to ice and 5ml of ice cold PBS was added to these plates and cells were scraped off into a 50ml Falcon tube (with total of ice cold 40ml PBS). These falcon tubes were centrifuged at 1,500 RPM at 4°C for 5 minutes. The supernatants were aspirated off, and cell pellets were washed two more times in ice cold PBS. At this point cells could be frozen at -80°C.

For nuclear extraction 1ml of NEBA (Nuclear extract buffer A) (Table 2.2) was added to frozen cells and transferred to eppendorf tubes. Cells were pelleted with their supernatant discarded. 2.5ml NEBA, 25µl igepal, 25µl protease inhibitor cocktail (PIC), 2.5µl dithiothreitol (DTT) were mixed together and 1ml of this was used to resuspend cell pellets with 5 minutes incubation on ice with light shaking regularly. Cells were then pelleted and resuspended in 2ml FA lysis buffer (Table 2.2) (with 20µl PIC added to FA lysis buffer) and passed through a 26G needle three times. Cell suspensions were sonicated for 30 minutes in a cold room with ice being changed every 10 minutes. Sonication was performed by a water bath sonicator, Biorupter™ Diagenode, and is used to shear the chromatin into fragments smaller than 0.5 kb. Cell debris was pelleted by centrifugation for 2 minutes at 4°C at 13,000 RPM. 10% of the supernatant was labelled in eppendorf as Input (30µl). The remaining supernatant was aliquoted equally into eppendorfs labelled with antibody names. 20µl (per antibody sample) of Protein A and G Dynabeads® (ThermoFisher) were washed three times in RIPA buffer and then beads were blocked with 800µl radio immunoprecipitation assay (RIPA) buffer (Table 2.2), 100µl bovine serum albumin (BSA) (1mg/ml) 100µl salmon sperm (SS) (1mg/ml) and left on rotation at room temperature for 30 minutes. Magnetic tube holders were used to remove RIPA/BSA/SS solution. Dynabeads® were resuspended in RIPA. For immunoprecipitation, the antibodies were added to appropriately labelled eppendorfs and 20µl beads added to each antibody labelled eppendorf (not Input) and left on rotation overnight in cold room. Taf1-48 (a component of the basal transcription apparatus for RNA polymerase I) was used as a negative control antibody (Antibodies used on Table 2.3).

To wash the Dynabeads®, a magnetic eppendorf holder was used and samples were washed twice with ice cold RIPA, twice with ice cold LiCl buffer (Table 2.2) and twice with ice cold Tris-EDTA (TE). For DNA elution, 400µl TE/1% SDS was added and incubated for 5 minutes at room temperature. The eluted material was transferred into new labelled eppendorfs and beads were discarded. To remove any contaminating RNA, 2µl RNAse (0.5 mg/ml) was added to all eppendorfs including Input and incubated in 37°C water bath for 1 hour. To reverse crosslinks and degrade protein, 5µl proteinase K (10mg/ml) was then added to digest each sample and left in 37°C water bath for 1 hour and then moved to 65°C heat block overnight. Qiagen PCR purification kit was used, as per manufacturer's instructions, for DNA purification. The ChIP DNA was then analysed by PCR.

2.4 RNA analysis

RNA extraction was achieved using the Qiagen RNeasy mini kit for all long coding RNA, including BRF1 mRNA. Qiagen kit was used for complete reverse transcription (RT) protocol using gDNA wipeout buffer, quantiscript RT buffer, RT primer mix, oligoDT and quantiscript RT as per manufacturer's instructions. The Applied Biosystem Kit was used for cDNA preparation and manufacturer protocols were followed. RNA extraction with TRIZOL reagent was used to analyse tRNAs and other small Pol III products which would have been lost using the Qiagen RNeasy mini kit.

10 cm cell plates that had reached 70-80% confluency were first washed twice with PBS at room temperature. 1ml of TRIZOL reagent was then added to the plates, and cells were scraped and pipetted up and down to resuspend properly in the TRIZOL reagent, and were then placed in labelled eppendorfs. 200ml chloroform was then added, and the eppendorfs were vortexed for 15 seconds and followed by centrifugation at 13,000 RPM for 15 minutes at 4°C. The top clear layers were then removed and placed into new labelled eppendorfs. Middle and bottom layers were discarded safely into phenol waste in fume hood. 500µl of isoproponal was added to all the eppendorfs, followed by further vortexed, and centrifugation at 13,000 RIPM for 10 minutes at 4°C. The supernatants were removed with double pipette tip and

discarded. The RNA pellets were washed with 1ml 70% ethanol/DEPC (Diethylpyrocarbonate) treated dH_20. These were vortexed and centrifuged at 13,000 RPM for 5 minutes at 4°C. The supernatants were removed with double pipette tip and discarded. The RNA pellets were left to air dry at room temperature with care taken not to let them completely dry out. The RNA was then resuspended with 25–50 µl of DEPC dH_20 depending on size of RNA pellet on a shaker for 15 minutes at 55°C. A mixture of DNAse 1 (10µl) and RDD buffer (70µl) per RNA sample (RNAse-free DNase set, Qiagen) was added to each RNA sample and incubated for 15 minutes at room temperature to remove all the DNAs. The TRIZOL protocol must then be repeated to remove DNAse 1. The resulting resuspended RNA pellet in DEPC dH_20 was quantified using a spectrophotometer (A_{260}/A_{280}) with nuclease free dH_20 as blank. At this point RNA samples could be frozen on dry ice and stored -80°C freezer.

2.5 Polymerase Chain Reaction (PCR)

Quantitative PCR (qPCR) for ChIP analysis was performed using the C1000™ Thermal Cycler (BIO-RAD). The qPCR reaction is carried out in a total volume of 10µl with 1µl of template DNA (from 50µl total of DNA elution volume). The following master mix for the DNA inputs is used, containing PerfeCTa™ SYBR® Green FastMix™ (5µl SYBR® green), 0.5µl forward primer (5mM working stock), 0.5µl reverse primer (5mM working stock) and 3µl dH_20 for each reaction (Table 2.5 for PCR primer sequences).

The design of highly specific primers is essential for successful (real-time) PCR. BRF1 primers were designed and purchased from Invitrogen. Gene Desert primer was used as a negative control primer. An appropriate standard curve encompassing the DNA inputs within a linear range was constructed for each qPCR. To avoid pipetting errors each sample was loaded in duplicate. The expression levels in qPCR were obtained using the average of duplicate samples and the average of the loading control, acidic ribosomal phosphoprotein P0 (ARPP P0). The ChIP signal was quantified with the formula (Ave. IP/ Ave. Input) – (Ave Neg. IP/ Ave. Input).

Experiments were performed in triplicate and overall means and standard deviations were calculated.

Taqman was used for qPCR for BRF1 mRNA quantification of PC3 and PC3M cells using Applied Biosystems 7500 Fast Real-Time PCR systems (ThermoFisher). Cascade 3 primers and probe (UPL) 84 were used for control with standard curve dilutions at 1:2, 1:4, 1:16, 1:32. BRF1 primer 2 used probe 62. BRF1 standard curve dilutions were at 1:5, 1:25, 1:125, 1:625, 1:3125. For final analysis comparing triplicate PC3 and PC3M (3 different cell passages) RNA levels of BRF1 at 1:25 dilution used.

We also wanted to quantify the mRNA levels of tRNAs in the stable PC3-BRF1 versus BRF1-empty cells. However, due to the small and repetitive nature of tRNA sequences we were not able to design Taqman suitable tRNA primers and PerfeCTa™ SYBR® Green Fast was therefore used for tRNA qPCR. This showed that tRNAs were present in abundance but no successful quantification could be achieved.

2.6 siRNA transfection using HiPerFect (Qiagen)

1 million PC3M cells were seeded on 10cm plates in the morning. Once the cells were settled on the plate, bijous were labelled mock (no siRNA), control (scrambled siRNA) 10µM, Pol III 5µM (Pol III 45), Pol III 10µM (Pol III 45), TFIIIC 10µM and 20µM and each bijoux had 1.5ml of serum free media (SFM) + L-Glutamine 2mM added and then the appropriate siRNAs added as per label 5-20µl depending on desired molarity. To each sample, 22.5µl of HiPerFect (Qiagen) were then added. The bijous were gently mixed and incubated at room temperature for 10 minutes. Media were then aspirated and replaced with 8.5ml of the normal culture media. The siRNA mix from each bijoux was added onto labelled cell plates in a drop wise manner, and plates were gently rocked to mix in siRNA solutions. The cell plates were harvested 48 hours later for western blot analysis.

2.7 siRNA transfection using Amaxa system (Electroporation)

PC3M cells were optimised for transfection with the Amaxa system, using Kit V and the Amaxa machine was set at T-13. Labelled eppendorfs with 10µl of each 10mM siRNA was prepared in a sterile TC hood. 1 million cells per 100µl Nucleofector solution reaction was used in accordance with the manufacturer's instruction. Cells, Nucleofector solution and siRNAs were placed in labelled cuvettes and electroporated in Amaxa machine. 9ml of normal cell media was placed in labelled universals and cuvette samples were quickly transferred into the appropriately labelled universal containers, and were then plated onto labelled 10cm petri cell dishes. Cells were harvested after culture for 48 hours for Western blot and BrdU analyses.

2.8 siRNA transfection using RNAimax

Cells were plated on the day before transfection, with 500,000 cells for each 10cm plate. On the following day, solution A was prepared, consisting of 10µl RNAimax and 500µl Optimem, for each transfection, which was multiplied by number of experimental plates (x 6 = Mock, NTsiRNA2 Dharmacon, NTsiRNA3 Allstars, BRF1 siRNA1, BRF1 siRNA 2, BRF1 siRNA3). All BRF1 siRNAs were designed through Ensembl BLAST and Roche UPL (Universal Probe Library) primer design programs and ordered through Ambion® by Life Technologies™ (Table 2.4 for siRNA sequences). Solution B was composed of 500µl Optimem and 4µl siRNA for each siRNA transfection dish. 1ml of solution A was added to solution B in labelled universals and incubated for 5 minutes at room temperature. 9ml of normal media were added to labelled universals. Media was removed from the labelled cell plates and replaced with media plus solution A and B universal mixture. These cell plates were then placed back in the TC incubators for 48 hours and then prepared for Western blot or BrdU/FACS analysis. BRF1 and Pol III siRNAs were purchased from Ambion. NT siRNA2 and NT siRNA3 were purchased from Dharmacon and Qiagen, respectively.

For WST1 analysis, siRNA transfection was performed using RNAimax and solution A and B were scaled down for 96 well plates. Cells were plated the day before with 10,000 cells per well in 150µl of (normal) culture media. Solution A was prepared for 6 wells in 96 well dish (consisting of 50µl Optimem and RNAimax 3µl for each well) to prepare mastermix (i.e. 300µl Optimem and 18µl RNAimax). Solution B was prepared 50µl Optimem and 3µl siRNA (10mM) in labelled eppendorfs for each siRNA. 53µl of solution A was added to all solution B samples, and incubated for 5 minutes at room temperature. 360µl of normal media was added to all samples. 100µl of normal media from the cell dishes was aspirated off, followed by the addition of 50µl of solution A+B to appropriately labelled-well. The 96 well plates were then incubated for 48 hours in a TC incubator. 10µl of WST1 assay reagent (Roche) was added to each well and after 120 minutes samples were analysed in the microplate reader at 450 and 650nm wavelengths.

2.9 Transformation

20µl DH5α cells (Invitrogen) were placed in a labelled eppendorf and 10ng DNA was added (pcHA-Brf1; pcHA-empty; EGFP-Brf1; EGFP-empty). pEGFP-C1 (CLONTECH) was used as the EGFP plasmid. This was left on ice for 30 minutes, heat shocked for 45 seconds in 42°C water bath, and then returned to ice for another 2 minutes. 200µl Lysogeny Broth (LB) was added and cells incubated with shaking at 225 RPM at 37°C for 1 hour. Cells were then plated on LB agar plates containing relevant antibiotics to select for growth of transformed *E.coli* (Ampicillin plates for HA-plasmid cells and Kanomycin plates for EGFP-plasmid cells) and plates incubated overnight at 37°C. One colony was selected from each plate and placed in 10ml LB with appropriate antibiotic in flask and incubated with shaking at 37°C at 225 RPM for 6-8 hours. This solution was then added to 150ml of LB and appropriate antibiotic and cultured in a shaker incubator at 37°C overnight. This was then centrifuged in large sealed plastic containers at 3,000 RPM at 20°C for 30 minutes. The cell pellets were then stored in freezer at -20°C. The maxi prep from these cell pellets were carried out by core service within the Beatson Institute.

2.10 Transient BRF1 plasmid transfection

Transient protein overexpression was performed in PC3, PC3M, DU145 and LNCaP cells in 96 well dishes for WST1 assay. A master mix for each plasmid was prepared in an eppendorf to make up solution for 5 wells (per well, 20µl Opti-MEM® reduced serum media (Invitrogen), 0.1µg DNA plasmid and 0.5µl Lipofectamine2000® (LTX) (Invitrogen)) and labelled with each plasmid name; EGFP-Empty, EGFP-Brf1, HA-empty and HA-Brf1. 1.2ml of cells with media was then added to give 10,000 cells/well to each labelled bijoux. 200µl was added to each of the wells and placed in a TC incubator. Samples were tested with WST1 assay 48 hours later as a surrogate for cell proliferation. The transfection experiment was scaled up to a 6 well dish so that protein expression could be checked by a western blot. For a 6 well dish, 500µl Opti-MEM®, 2µg DNA plasmid and 6.25µl LTX with 200,000 cells per well were required. Plates were placed in a TC incubator for 48 hours at 37°C and 5% CO2. Western blot lysates for protein expression were prepared 48 hours later.

2.11 Generation of stable cell clones with manipulated levels of BRF1 expression

Two techniques were tried and both were successful in generating stable cell lines with upregulated BRF1 expression. In this study, the use of lipofectamine technique had a higher yield of transfected cells and therefore quicker to get the cell populations selected and growing than the Amaxa electroporation method.

For transfection using the Amaxa system, 5µg of the one of the following plasmids were added to an appropriately labelled eppendorf: EGFP-Empty; EGFP-Brf1; HA-Empty; HA-Brf1. To achieve 1x 10^6 cells per Amaxa reaction, 4.5 x 10^6 cells were resuspended in 450µl Nucleofector™ solution (Kit V for PC3 and kit R for LNCaP, respectively per manufacturer recommendation). 100µl of this mix was then added to each plasmid labelled eppendorf, gently mixed and added to plasmid labelled cuvettes. Optimised Amaxa™ programs were used: T-013 for PC3 and T-009 LNCaP cells, respectively. These cuvette solutions was then transferred to plasmid labelled

universals of 9ml normal media and plated on 6cm labelled dishes and incubated for 48-72 hours, depending on cell confluency.

For transfection using the lipofectamine system, 10µg of plasmid DNA was diluted in 1.3ml of Opti-MEM® Plus:Reagent Mix Plus at 1:1 ratio. This was mixed gently and left to incubate for 10 minutes at room temperature. 17µl of lipofectamine-LTX reagent was then added and mixed gently, followed by incubation for 25 minutes at room temperature. Media was aspirated off labelled 6cm plates with 60-70% cell confluency and replaced with 5ml of growth media to dish. 1.3ml of DNA-lipofectamine LTX complex was then added directly to each dish with cells, and mixed gently by rocking the plates back and forth. The cells were incubated at 37°C in TC incubator for 48 hours, with an appropriate selecting agent added to media at 48 hours post-transfection.

Selection process for cells containing plasmids used a 300µg/ml G418S sulphate solution (FORMEDIUM ™) in normal media for PC3 cells. Once cells were growing well, cells were harvested and analysed by Western blotting to confirm the presence of a transfected expression construct and the level of transgene expression. EGFP adds 27 kDa above normal BRF1 size (90 kDa). HA adds 1 kDa above normal BRF1 size. The stable cell clones could then be frozen down and stored at -80°C.

2.12 Cell number analysis (CASY counter™ (Innovatis))

1 million PC3 BRF1- and empty- plasmid stable cells were seeded into 25cm^3 flasks with a total volume of 15ml normal media. The cell number was counted after every 72 hours of culture. This was repeated six times in duplicate to calculate the mean cell doubling time.

2.13 Cell proliferation reagent (WST1) Assay

After various transfections and treatments for 48-72 hours at 37°C and 5% $C0_2$ condition, 10µl of cell proliferation reagent Water soluble tetrazolium salt-1 (WST-1, Roche) was added and incubated for 120 minutes. WST-1 reagent is a non-radioactive, spectrophotometric quantification of cell proliferation, growth, viability and chemo-sensitivity for 96-well-plate experiments. The absorbance of the samples using a microplate reader was used against a background control. The wavelength for measuring the absorbance was 450nm and the reference wavelength was set at 650nm.

2.14 BrdU FACS Cell Cycle Analysis

10µl of BrdU (Cell labelling reagent, VWR) was added to 10cm plates (1:1000) and after gentle mixing, these plates were placed into a TC incubator for 1 hour. Then all the media was removed and placed in 15ml labelled falcon tubes (so that all the dead cells are included in FACS analysis). 2ml of PBS was added to the plates and the cells were scraped off into labelled Falcon tubes. Cell pellets were generated by centrifugation at 1,000 RPM for 5 minutes, with all subsequent washes followed by centrifuging at 1,000 RPM for 5 minutes to pellet the cells. The cell pellets were then washed twice in 3 ml PBS. Cells were resuspended in 300µl PBS and 700µl of pure ethanol added drop by drop with mixing to avoid cells clumping. Cells were fixed in 70% ethanol at -20°C for at least 1 hour.

Cells were then pelleted and ethanol aspirated off. Cells were washed in PBS and resuspended in 100µl PBS and 100µl 4N hydrochloric acid and incubated for 15 minutes at room temperature. 1ml PBS wash was followed by 1ml PBT wash (18ml PBS + 2ml PBS/5%BSA+ 20µl Tween). 100µl anti-BrdU antibody mix (BD Biosciences) (1:40 PBT dilution) was then added to the resuspended cell pellets, and incubated at room temperature for 30 minutes. 1ml PBT wash was repeated and the supernatant removed. A secondary antibody anti-mouse Alexa Fluor 488 (1:40 PBT dilution) was added and incubated for 30 minutes at room temperature in the dark.

This was then removed and 1ml PBT wash was followed by 1ml PBS wash. The cell pellets were finally resuspended in 300µl PBS containing 10 µg/ml Propidium Iodide (PI, stock 1mg/ml in PBS) for 30 minutes at room temperature and then analysed on a FACS Calibur machine.

2.15 Propidium Iodide (PI) staining for FACS Cell Cycle Analysis

PI is a fluorescent dye which binds to DNA and can be used to quantify the DNA content of the cells, thus determining the stage in the cell cycle (e.g. G2/M cells have doubled the DNA content of cells in G1 phase). The cytometer is able to exclude cell doublets as a true G2 cell will have a smaller width than two G1 cells passing through the beam together consecutively. PI staining was used for cell cycle analysis instead of BrdU for stable cell lines containing EGFP, as EGFP expression generates light of a similar wavelength to that emitted by the BrdU/Alexa Fluor 488 antibody complex.

Cells were harvested including floating and loosely adherent cells. Cells were washed in PBS and pelleted. Cells were resuspended in 1ml 2% FBS + PBS. 250µl of PI/Triton stock (250µl PI stock 1mg/ml/ 750µl 5% Triton in dH20) and 100µl of RNAse was then added. The samples were incubated for 10 minutes at room temperature in the dark or wrapped in tin foil, and then analysed in FACS Calibur machine.

2.16 Colony Forming Assay (Anchorage independent growth)

Soft agar assay was used to test the colony forming potential of the PC3 BRF1-plasmid and empty-plasmid control stable cell lines. 2% agarose (Sigma 15517-022) was made in dH_20 and autoclaved. 2X RPMI solution was made, comprising of 10ml of 10X RPMI (1640-medium , Sigma 037k2364-R1145), 1ml 100x L-Glutamine ; 2.7ml 7.5% sterile filtered sodium bicarbonate Sigma S8761; 10µl 1mg/ml folic acid

Sigma F8758 dissolved in 1M NaOH; 10ml FBS and 26.3ml sterile dH_20. The base layer consisted of mixing 2% agarose and 2X RPMI at 1:1 ratio in a sterile universal. 1.5ml of this mixed solution was added into each well of a 6-well plate and allowed to set at 4°C for 30 minutes. The stable cell lines were tested in triplicates. Cells were harvested and passed through a 40µM nylon BD Falcon cell strainer and then added to 1.5ml top layer solution of (3ml 2XRPMI + 2ml sterile H_20 + 1ml 2% agarose) at 30,000 cells per well in volume of 0.3ml media. The top layer was allowed to set at room temperature under the TC hood for 1 hour. Cell plates were moved to TC incubator for 14 days, following which colonies were counted using the immunofluorescence microscope.

2.17 Immunofluorescence

Cells were plated on glass bottom plates with 2ml of normal media. Once the cells reached 70-80% confluency, they were washed with 1ml PBS. Cells were fixed with 200µl 4% paraformaldehyde in PBS, for 15 minutes. Then, the cells were washed with 1ml of PBS. To permeabilise the cells, 200µl ice cold 100% methanol for 10 minutes at -20°C was added to cells. Cells were then washed with PBS. Blocking of non-specfic signals was carried out for 1 hour with 200µl of 10% FBS + 0.5% BSA + 0.3% Triton x100 in PBS pipetted over fixed cells. Blocking solution was removed and a primary antibody solution was prepared (1% BSA + PBS + 0.3% Triton X100) with an appropriate antibody dilution (BRF1 Bethyl Laboratories 1:100 and HA-Tag (6E2) mouse mAb 1:100 Cell signalling Technology®). 100µl primary antibody solution was pipetted and left on cells overnight at 4°C. Cells were washed with PBS and 100µl secondary antibody solution (1% BSA + PBS + 0.3% Triton X100) at 1:250 dilution of antibody (mouse and rabbit monoclonal antibody Alexa 555) was added for 1 hour at room temperature in dark. Then the glass bottom plates were rinsed with PBS and one droplet of DAPI mounting medium for fluorescence was added and left in dark at 4°C. Cells were analysed with the Nikon A1R immunofluorescence laser microscope.

2.18 Scratch wound healing assay (IncuCyte, Essen Bioscience)

15,000 cells/ well were plated on Essen Bioscience 96 well ImageLock Microplates (4379), and incubated for 72 hours in a TC incubator. Once the cells had reached 100% confluence, they were washed with PBS and then scratched with the WoundMaker^{TM} to make homogenous 700-800 micron wide scratch wounds. They were then washed twice more with PBS to wash away any cell debris and then 100µl of media was replaced. Cells were then placed in the IncuCyte incubator for 2 hourly images to be recorded for 24-48 hours. Analysis was performed to calculate wound density/ time with the IncuCyte computer program.

2.19 Docetaxel siRNA experiments

Reverse transfection protocol was adopted to assess whether transient inhibition of BRF1 by RNAimax and docetaxel treatment co-operated to inhibit PC3M and DU145 cells growth. For these experiments we used 10,000 cells/ well for 96 plate dish. A master mix was made up in a sterile eppendorf in TC hood per well of 10µl OptiMEM, 3pmol/µL siRNA and 0.3µl RNAimax and scaled up according to the number of wells required for each treatment. siRNA master mix was briefly vortexed and 10µl of the mixture was put in each well and incubated in a TC hood at room temperature for 30 minutes. 90µl of cells was then added to each well and incubated overnight at 37C and 5% CO_2. The next day, 100µl of either 2nM (GI_{10}) or 4nM (GI_{20}) docetaxel or 0.1% DMSO vehicle control or normal media was added to the cells with siRNA master mix as per labelled plate design. The cells were then incubated for 48 hours in a TC incubator and then the WST1 assay was performed as a marker of cell proliferation analysis.

2.20 Mouse models

Prior to starting animal work, Home Office Licenses were obtained (project license 60/3947, personal license 60/13374). The mice were housed in individually ventilated cages on autoclaved sawdust bedding. The room conditions were maintained at 20-22°C, humidity 60-70% and light/dark 14/10 hours. Mice were fed with a commercial rodent pelleted food and autoclaved water. All procedures were in compliance with Home Office License. Mice were ear-notched for identification purposes at weaning and ear clippings sent to Transnetyx^{TM} (Cordova, Tennessee USA) for genotyping by PCR.

Mice were euthanised at various ages by carbon dioxide asphyxiation and immediately weighed prior to post-mortem. At post-mortem prostate, enlarged lymph nodes, liver, kidney and lung were dissected out. Prostate tissues were harvested and equally divided for snap-freezing in dry ice and stored at -80^{o}C for protein and nucleotide analysis and fixing in 10% neutral buffered formalin and then paraffin embedded for histopathological and immunohistological analysis. Other dissected organs were sent for histological analysis in formalin.

Three novel genetically modified mouse models (GEMMs) were developed in this study. Firstly, a GEMM with prostate specific *Brf1* overexpression to assess whether this could drive prostate carcinogenesis and secondly, an inducible prostate specific *Brf1* knock down GEMM to see whether this could affect prostate homeostasis and morphology. Transgenic mice were specifically designed carrying the human *BRF1* transgene *(hBRF1Tg*) and these were crossed firstly with Probasin-cre (*Pb-Cre*) mice to see whether *Brf1* could be a sole driver of prostate carcinogenesis and secondly with a known PC GEMM that has homozygote *Pten* loss in prostate epithelial cells (Wang et al, 2003) to see whether *Brf1* overexpression resulted in a more aggressive PC phenotype. *Brf1* knockdown in prostate epithelial was achieved using the inducible *Nkx3.1-Cre^{ERT2}* GEMM (Wang et al, 2009). These three GEMMs are fully explained in Chapter 5.

PB-Cre positive males, but not females, were used for breeding, because the probasin promoter is active in the oocytes of *PB-Cre* females resulting in the recombination of *loxP* – flanked alleles in a number of tissues in the offspring. Both male and female *Nkx3.1* mice were used for mating and therefore, these cohorts were quicker to set up.

2.21 Immunohistochemistry (IHC)

Mouse tissues for histological analysis were formalin fixed paraffin-embedded and stained with H&E (hematoxylin and eosin) and evaluated for precursor lesions, such as hyperplasia, low and high grade PIN and adenocarcinoma (as defined by Shappell et al, 2004). The tissue sections were prepared and stained in the Beatson Institute histology laboratories with optimised protocols. Intensity of IHC staining was graded on a scale of: no apparent staining, weak staining, moderate staining and strong staining. Antibodies used for IHC are listed in Table 2.3.

2.22 Preparing protein lysate from mouse prostate samples

1.5ml T-PER reagent (ThermoFisher Scientific), 15µl protease inhibitor cocktail (PIC) 10µl phenylmethylsulfonyl fluoride (PMSF) and 1.5µl 1M dithiothreitol (DTT) were added and mixed in a bijoux. 300µl of this cell lysing solution was added to the fine grounded tissue samples from individual mouse prostates in Precellys lysing tube containing ceramic beads on ice. A Precellys 27 lysing and homogenising machine was used following manufacturer's protocol. Precellys tubes were centrifuged at 1,000 RPM for 5 minutes at 4°C to pellet ceramic beads. Homogenised and lysed samples were transferred to labelled eppendorfs and 13,000 RPM centrifuged for 15 minutes at 4°C. The supernatants were kept and protein samples were used for western blotting.

2.23 RNA microarray preparation for mouse samples

The Qiagen RNA extraction and cDNA preparation protocol were used for RNA microarray preparation of mouse prostate samples. Quality of RNA extraction was

calculated on the Bioanalyser A260/A280 and RNA electrophoresis was performed to calculate RIN and rRNA ratio 28s:18s (© 2003-2009 Agilent Technologies Inc.). Illumina® (Ambion/ Life Technologies) TotalPrep™ RNA Amplification kit and protocol were used and manufacturer's instructions were followed.

2.24 Statistical Analysis

Statistical analysis was performed using Prism 5 and Microsoft Excel 2010 software. Prism 5 was used to generate the KM survival curves and calculate Log rank P values. All other statistics and figures were analysed and generated in Excel and Powerpoint. All experiments were repeated in triplicate unless stated otherwise and the mean of these experiments was calculated. The error bars were calculated and represented in terms of mean ± standard deviation.

For all WST1 assay experiments 2-tailed 2-sample equal variance student T tests were performed, to see whether there was a significant difference between the control samples (for example empty plasmid or NTsiRNA control) and the Brf1 manipulated samples.

For all FACS cell cycle experiments 2-tailed 2-sample equal variance student T tests were performed, to calculate whether there was a significant difference between the control (NTsiRNA2) and the Brf1 manipulated samples.

For RTqPCR and ChIP experiments 2-tailed 2-sample equal variance student T test were performed to see whether there was a significant difference between the PC3 and PC3M mRNA BRF1 levels (RTqPCR) and the Brf1 promoter binding of oncogenes and control Gene Desert binding of oncogenes (ChIP).

Reagent	Supplier
BSA (Bovine Serum Albumin)	Sigma (Missouri, USA)
DAPI (4'6-diamidino-2-phenylindole)	Vector (California, USA)
DMEM (Dulbecco's Modified Eagle's Medium)	GIBCO (California, USA)
DMSO (dimethyl sulfoxide)	ThermoFisher (Massachusetts, USA)
ECL (enhanced chemiluminescence)	GE Healthcare (Buckinghamshire, UK)
Ethanol	Sigma
FBS (fetal bovine serum)	PAA (Pasching, Austria)
L-glutamine	GIBCO
Lipofectamine 2000	Invitrogen (California, USA)
Methanol	Sigma
MOPS SDS running buffer	Invitrogen
NaCl	Sigma
PFA (paraformaldehyde)	Science Services (Munich, Germany)
Phosphatase inhibitors cocktail	ThermoFisher
Protease inhibitors cocktail	ThermoFisher
PVDF membranes (Polyvinylidene fluoride)	GE Healthcare
RNA Imax	Invitrogen
RPMI-1640 (Roswell Park Memorial Institute)	GIBCO
Tris-HCL	Sigma
Triton X-100	Sigma
Trypsin	GIBCO
Tween-20	Sigma
β-Mercaptoethanol	Sigma
WST-1 Cell Proliferation Reagent	Roche (Risch-Rotkreuz, Switzerland)

Table 2-1 List of Reagents

Solution	Composition
Phosphate Buffered Saline (PBS)	170mM NaCl 3.3mM KCl 1.8mM Na2HPO4 10.6mM KH2PO4 pH 7.4
Tris-Buffered Saline-Tween (TBST)	25mM Tris-HCl pH 7.4 137mM NaCl 5mM KCl 0.1% Tween-20
Immunoblotting cell lysis buffer	50mM Tris pH7.6 150mM NaCl 1% Triton x100 0.5% Deoxycholate 0.5% SDS 1mM Na ortho-vanadate 1Mm NaF 1X protease inhibitor cocktail mix 10.05mM PMSF 1X phosSTOP (Roche) dH20
Fixing solution	4% PFA 96% PBS
Immunoblotting blocking buffer	5% milk powder in TBST
Immunofluorescence blocking buffer	10% FBS 1% BSA 90% PBS
Tris-EDTA	10mM Tris-HCl pH 8.0 1mM EDTA
Tris-buffered Saline (TBS)	25mM Tris – HCl pH 7.4 137mM NaCl 5mM KCl
Nuclear extract buffer A (NEBA)	10mM Hepes pH 7.9 1.5mM $MgCl_2$ 10mM KCl 1mM DTT 0.1mM PMSF
FA lysis buffer	50mM HEPES-KOH pH 7.5 (1.2g HEPES) 140mM NaCl (2.8ml 5M stock) 1mM EDTA pH 8 1 % Triton x-100 0.1% Sodium Deoxycholate 0.1% SDS
RIPA buffer	50mM Tris-Cl pH 8.0 150mM NaCl 0.1% SDS 0.5% deoxycholate 1% NP-40

LiCl buffer	10mM Tris-Cl, pH 8.0 250Mm LiCl 0.5% deoxycholate 0.5% NP-40 1mM EDTA

Table 2-2 List of buffers and their composition

Antigen	Supplier	Cat/I.D. No.	Application/ Dilution
Actin (C-11)	Santa Cruz (Texas, USA)	sc-1615	WB/ 1:1000
AR	Santa Cruz	sc-816	WB/ 1:1000
BrdU	BD Biosciences (California, USA)	347580	FACS/ 1:40
BRF1	Bethyl (Texas, USA)	A301-228A	WB (1:5000), IHC (1:1000), IP (3µg/mg lysate), IF (1:500)
BRF2	Abcam (Cambridge, UK)	ab154658	WB/ 1:1000
ELK-1 (H-160)	Santa Cruz	sc-22804	WB (1:1000), IP
ERG (C-20)	Santa Cruz	sc-354	WB (1:1000), IHC, IP
ERG	Epitomics (California, USA)	5115-1	WB/ 1:5000
HNF-4α	Santa Cruz	sc- 8987	WB / 1:1000
HSP-70	Abcam	Ab3148-500	WB/ 1:5000
c-MYC N262	Santa Cruz	sc-764	IP, WB/ 1:1000
Pol II	Abcam	Ab-5408	IP
Pol III	In house	RPC 155	WB/ 1:1000
Taf I-48	Santa Cruz	sc-6571	IP
TFIIIC 110	Santa Cruz	81406	WB/ 1:1000
TFIIIC 220	Abcam	Ab-67	WB/ 1:5000
α-Tubulin	Sigma	T6557	WB/ 1:2000
Anti-rabbit IgG, HRP-linked	Cell Signalling (Massachussetts, USA)	7074	WB/ 1:5000
Anti-mouse IgG, HRP-linked	Cell Signalling	7076	WB/ 1:5000

Table 2-3 List of antibodies

Oligo pair name	5’ to 3’ sequence
BRF1 siRNA2 (s223824) Ambion California, USA	Sense GCCAGAAUGCAUGACUUCATT Anti UGAAGUCAUGCAUUCUGGCTG
BRF1 siRNA3 (s194479)	Sense CACCAGUCAGUUGACCAUUTT Anti AAUGGUCAACUGACUGGUGGG
BRF1 siRNA1 (s6323)	Sense GGCUCACGGAAUUUGAAGATT Anti UCUUCAAAUUCCGUGAGCCTC
NTsiRNA2 Dharmacon, Colorado, USA	Not disclosed
NTsiRNA3 Qiagen All Stars, Hilden Germany	Not disclosed
Pol III (45) Ambion	CAAGUAUGGUGACAUCGU, Ambion pre-designed s21945:, si 2 UCUAACCGUGGUUUCUCAAUUGGGA, Invitrogen custom Stealth RNA),
TFIIIC (27) Ambion	CAGUGAACGGAGAACGAU, Ambion pre-designed s6327

Table 2-4 List of siRNA sequences

Table 2.5 PCR primer sequences	
Locus name (Species)	Primer Sequence 5’-3’
BRF1 B taq	F CCA GCC GTC TGT TTC CAT A
	R ACA CCT CGT GGT TCT TCT CC
BRF1 Mouse	F ATG TGA GTC CAC ACT ACG GAA G
	R GAG CTG ACT GGT TGG AGT GTC
ChIP BRF1 0.6 upstream	L ACC GGG GAC TAG AGC TAA GG
	R GAG ACC GCG CTC ACT ATC C
ChIP ARPPP0 (220)	L GCA CTG GAA GTC CAA CTA CTTC
	R TGA GGT CCT CCT TGG TGA ACAC
Gene Desert	Not disclosed

Table 2-5 List of PCR primer sequences

3 BRF1 expression and transient manipulation of BRF1 in human prostate cancer cells

3.1 BRF1 expression in prostate cancer

3.1.1 Introduction

Pol III transcription products have been seen to be overexpressed in transformed and tumour cells (Scott et al, 1983; Chen et al, 1997; Winter et al, 2000; Felton-Edkins & White, 2002; Gomez-Roman et al, 2003). Pol III transcription is tightly regulated in normal cells by tumour suppressors but this regulation is lost in cancer cells. Most studies of Pol III regulation have proposed that control is mediated through TFIIIB (Marshall and White, 2008). TFIIIB can bind to DNA, TFIIIC and Pol III, and its recruitment of Pol III to its specific genetic template is seen as the main control point for tRNA synthesis. TFIIIB, and more specifically BRF1, is a molecular target of regulation by a wide variety of tumour suppressors, including p53 (Felton-Edkins et al, 2003b), PTEN (Woiwode et al, 2008), ARF (Morton et al, 2007), pRb (Felton-Edkins et al, 2003) and oncogene activation by c-MYC and mitogen activated protein kinase ERK (Felton-Edkins et al, 2003a, White, 2004). TORC1, MYC, Ras, p53 and pRb have all been shown to be deregulated pathways in PC and all can influence Pol III transcription.

In this chapter, I present data investigating BRF1 expression in PC cell lines to define a possible role for BRF1 in this disease. Relevant human PC cell lines will be identified to study the impact of altered BRF1 levels on cellular activity *in vitro* to help determine role of BRF1 in PC. Tissue microarray (TMA) work is an invaluable tool merging the disciplines of pathology and molecular biology and is becoming essential for finding potential key gene targets in carcinogenesis. Further samples will be investigated through oncomine (www.oncomine.org), a web based DNA microarray database and analysis program. It identifies five independent studies of PC in which BRF1 mRNA is expressed at elevated levels. For example, data collected by Magee et al, 2001 suggests significant upregulation of BRF1 mRNA expression in clinical prostate carcinoma relative to control benign prostate tissue. In addition, BRF1 transcript levels were elevated further in PC metastases when compared to the primary tumours (Grasso et al, 2012; Varambally et al, 2005) and PC of higher Gleason score (Luo et al, 2002) (Figure 3.1). Another Oncomine study developed primary cell cultures from thirty human PC prostatectomy tumours and

showed that BRF1 expression was significantly higher in the patients whose cancers recurred at one year versus those that did not (P = 0.018) (Nanni et al, 2006).

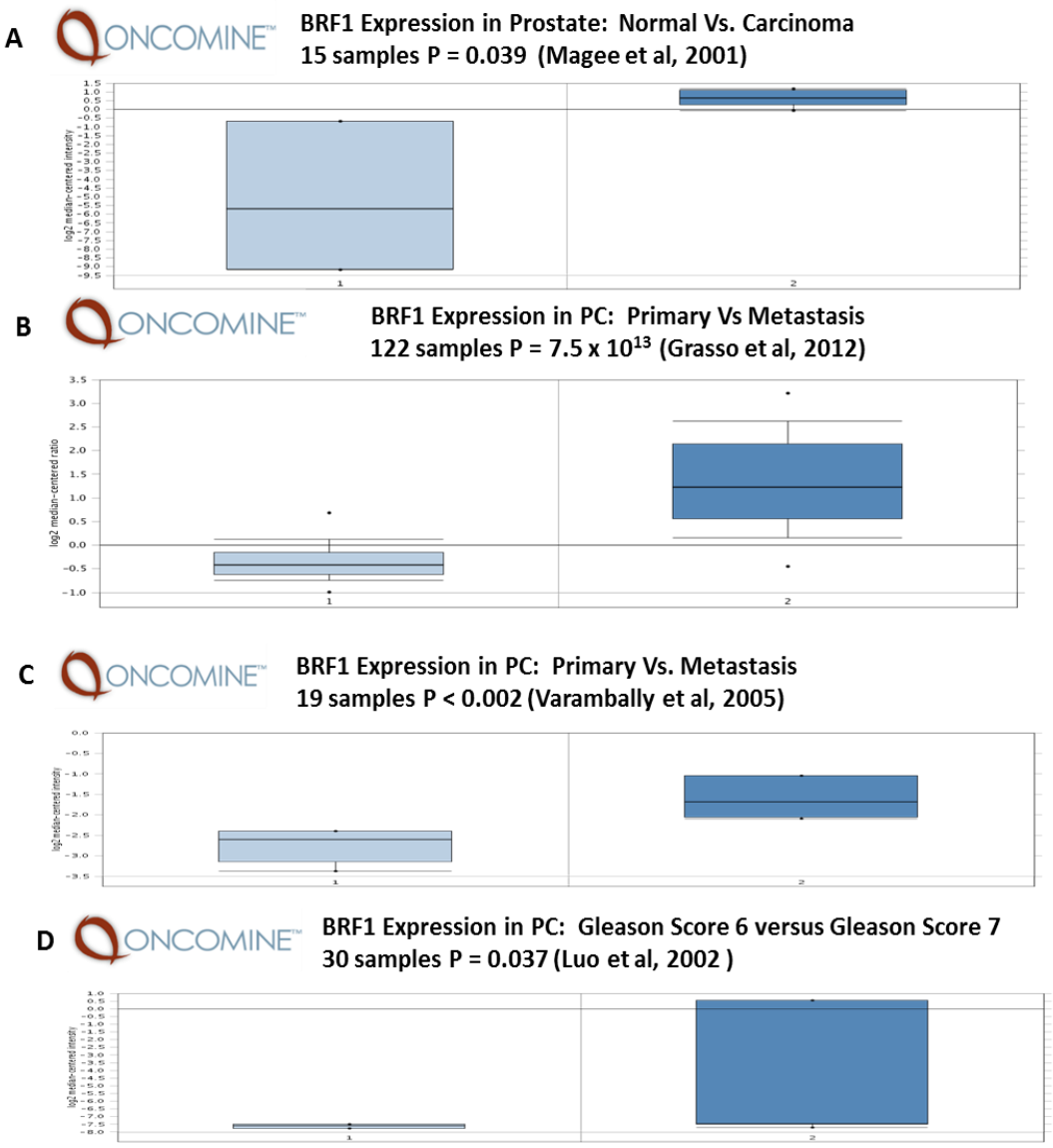

Figure 3-1 Oncomine RNA microarray database analysis of BRF1 overexpression in PC human tumour samples

Four studies showing increased BRF1 expression on transcriptomic analysis in PC human clinical samples. A) Magee et al, 2001 data shows BRF1 expression significantly elevated in PC in comparison to normal prostate samples (p =0.039). B) Grasso et al, 2012 data shows BRF1 expression significantly higher in metastatic PC samples in comparison to primary PC ($P = 7.5 \times 10^{13}$). C) Varambally et al, 2005 data also shows BRF1 expression significantly higher in metastatic PC samples in comparison to primary PC ($P < 0.002$). D) Luo et al, 2002 data showing BRF1 expression significantly higher in PC samples with higher Gleason Score 7 versus Gleason Score 6 ($p = 0.037$).

3.1.2 Results

3.1.2.1 BRF1 expression in clinical prostate cancer

Analysis of The Cancer Genome Atlas data through the cBioportal database (www.cbioportal.org) shows BRF1 expression is altered in 17% of all PC samples, with 12% being overexpressed and 5% of samples showing under expression. In the metastatic dataset BRF1 expression is altered in 27% of samples with 22% being over expressed and 5% samples having BRF1 low expression. BRF1 is upregulated more frequently than BRF2 and BDP1 for all PC and metastatic PC database. BRF1 expression is higher in the metastatic PC database than the all PC database. AR and MYC are also more highly expressed in the metastatic database with PTEN under expression being greater in the metastatic database. Interestingly, the status of altered AR and BRF1 expression was found to be significantly mutually exclusive (Fisher exact test, $p<0.001$). The samples with the highest MYC expression do not correlate closely with high BRF1 expression (Figure 3.2).

3.1.2.2 BRF1 expression *in vitro* in human prostate cancer cell models

Building on the evidence of upregulated BRF1 expression in clinical PC and its potential association with aggressive disease (Figures 1.4 & 1.5) I sought to characterise the status of BRF1 expression in a panel of human PC cell model as a tool for future studies on its functional significance in PC.

Using Western blotting, BRF1 expression was detectable but at varying levels in a panel of PC cells and in the normal human prostate epithelial RWPE1 cell line (Figure 3.3). DU145 cells appeared to have the lowest levels of BRF1 expression while CWR22 cells expressed BRF1 at the highest level. It is worth noting that all of the androgen receptor positive cells, namely CWR22, VCaP, LNCaP, expressed BRF1 at significant levels. Also of note, following prolonged (4 hours) exposures, a second lower molecular weight band appears on the western blot for BRF1 expression. Importantly, analysing the PC3 cell line and its isogenic metastatic derived PC3M cells, I observed that PC3 expressed BRF1 protein at lower level than the more

aggressive PC3M cells, whereas LNCaP and CWR22 cells expressed higher BRF1 expression than LNCaP-AI and 22RV1 cells, their respective androgen independent derivatives. Intriguingly, to validate the data on this isogenic cell pair from Western blot analysis, quantitative RT-PCR (qRT-PCR) was performed to study BRF1 mRNA levels. It is interesting to note that, despite enhanced BRF1 protein expression, PC3M cells demonstrated significantly lower levels of BRF1 transcript when compared to the parental PC3 cells (Figure 3.4), suggesting that BRF1 expression is, at least in part, controlled at the post-transcriptional level.

In an attempt to characterise BRF2 expression in the context of data from BRF1 expression, I performed Western blotting to probe for BRF2 in the same human prostate cell panel. Due to a combination of poor performance of the available Brf2-targeting antibody and possibly the low levels of BRF2 expression, I was not able to convincingly demonstrate its expression by Western blot analysis (data not shown). This is consistent with data from the literature: (i) cBio portal data (Taylor et al 2010), suggesting that BRF1 expression to be higher than BRF2 in clinical PC samples, and (ii) Cabarcas et al, 2008 demonstrated very low levels of BRF2 expression in DU145 cells.

Transcription factor IIIC (TFIIIC) is an essential part of the RNA pol III transcription complex. I further studied the expression of TFIIIC (subunit 110 kDa) in parallel to BRF1 expression in the selected cell panel. Similar to BRF1 expression, TFIIIC expression varied significantly across different cell lines studied. The androgen receptor expressing (CWR22, LNCaP and VCaP) cells expressed moderate levels of TFIIIC, while the AR-negative DU145 and PC3 cells tended to express TFIIIC at lower levels. Consistent with the differential BRF1 expression observed in PC3 and PC3M cells, TFIIIC was expressed at higher levels in PC3M cells when compared to the parental PC3 cells (Figure 3.5).

To gain a better understanding of the BRF1-related pathway, I analysed the expression status of relevant oncogenic regulators of BRF1 transcription. The expression level of cMYC, a key transcriptional factor for BRF1 and a very important oncogene in multiple tumour types, was studied by Western blot. Figure 3.6 shows that, apart from VCaP and RWPE1 cells, cMYC expression was surprising similar across the rest

of the cell lines studied. This contrasts with the pattern of BRF1 expression in the same PC cell panel, suggesting that other factors are involved in the regulation of BRF1 expression in prostate cancer. Furthermore, in the cBioportal database, there is some co-occurrence between MYC and BRF1 mRNA overexpression but the areas of highest MYC overexpression do not appear to have high levels of BRF1 mRNA (Figure 3.2).

c-MYC and ELK of the ETS family of transcription factors are known regulators of BRF1 expression (Gomez-Roman et al, 2003; Sansom et al, 2007; Raha et al, 2010; Oler et al, 2010) and therefore, potentially responsible for the upregulated BRF1 described above. There is also the possibility that ERG may regulate BRF1 expression, as ERG shares DNA binding specificity with ELK-1 (Wei et al, 2010) and ELK-1 has been found to bind to the BRF1 promoter (Zhong et al, 2009).

Approximately 50% of human prostate cancers have ERG-TMPRSS2, a recently identified gene fusion and possible oncogene (Hollenhorst et al, 2011). VCaP cell model closely resembles prostate tumours that harbour TMPRSS2-ERG fusions and express prostate epithelial markers (Sun et al, 2008). However, VCaP is the only cell line available to us that expresses the ERG-TMPRSS2 protein. Our western blot using an ERG antibody (ERG 1/2/3 C-20 sc-353) also shows that VCaP is the only cell line to express ERG at appreciable levels (Figure 3.6). Another antibody specific for ERG-TMPRSS2 showed the same result (not shown). ELK-1 was detectable in all the PC cell lines. Two different antibodies were tried for ELK-1 (Santa Cruz: ELK-1 sc-355 and ELK-1 sc-22804), with both producing multiple bands on western blots. ELK-1 (sc-22804) seemed to produce the most consistent results and the data is shown in Figure 3.6, showing a dominant band at the expected molecular weight of 62 kDa. However, it is difficult to compare ELK-1 levels among different cell lines due to the multiple bands at higher exposure times.

ChIP (Chromatin immunoprecipitation) was used to investigate whether MYC, ERG, and ELK-1 are bound to the *BRF1* promoter in PC3, LNCaP and VCaP (Figure 3.7). RNA Pol II antibody was used as a positive control as it transcribes BRF1. Taf 1-48 antibody, a Pol I transcription factor subunit, was used as a negative control. *BRF1* primers were designed using the UCSC human genome sequence database website.

Gene Desert primers mapping to a chromosomal region devoid of genes were used as a negative control. PCR values (SQ or starting quantity) were normalised to inputs and subtracted from the negative control SQ values, Taf 1-48 (Figures 3.8 - 3.11).

Pol II does occupy the *BRF1* promoter in all PC cancer cells (Figure 3.8), reaching statistical significance in the LNCaP cells versus Gene Desert primer binding (t test, $p< 0.05$). The high variability in the PCR values is likely due to the technical challenge of the ChIP protocol rather than a biological variation within the PC cells. VCaP has the highest ERG occupancy of the *BRF1* promoter (Figure 3.10), which correlates well with ERG protein expression levels. However, due to high variability in PCR values, this result did not reach statistical significance. c-MYC had low levels of binding to *BRF1* promoter which reached statistical significance in the LNCaP cells (t test, p value <0.05) (Figure 3.9). ELK-1 had negligible binding to the *BRF1* promoter in this ChIP experiment (Figure 3.11). Overall, due to experimental variabilities, ChIP results on the regulation of the *BRF1* promoter were inconclusive.

Taken together, transcriptional control of *BRF1* gene may not be the only mechanism that controls the overall level of BRF1 protein expression. Hence, I carried out a series of serum starvation experiments on PC3M cells, which express high levels of BRF1 protein. Following serum starvation in PC3M cells, BRF1 expression at protein level drops by 24 hours but is then maintained at a constant level for up to 72 hours, following which BRF1 levels drastically diminished at 96 hours (Figure 3.12). Therefore, in the absence of growth stimulatory signals, BRF1 protein can be maintained, perhaps through basal levels of transcription/translation. In addition, BRF1 may be a stable protein with prolonged half-life. Treatment of cells with cyclohexamide to block translation can be used to investigate the protein half-life. In the case of BRF1, protein levels were maintained to 72 hours, at time point at which we found significant cyclohexamide mediated toxicity (data not shown), hindering further study.

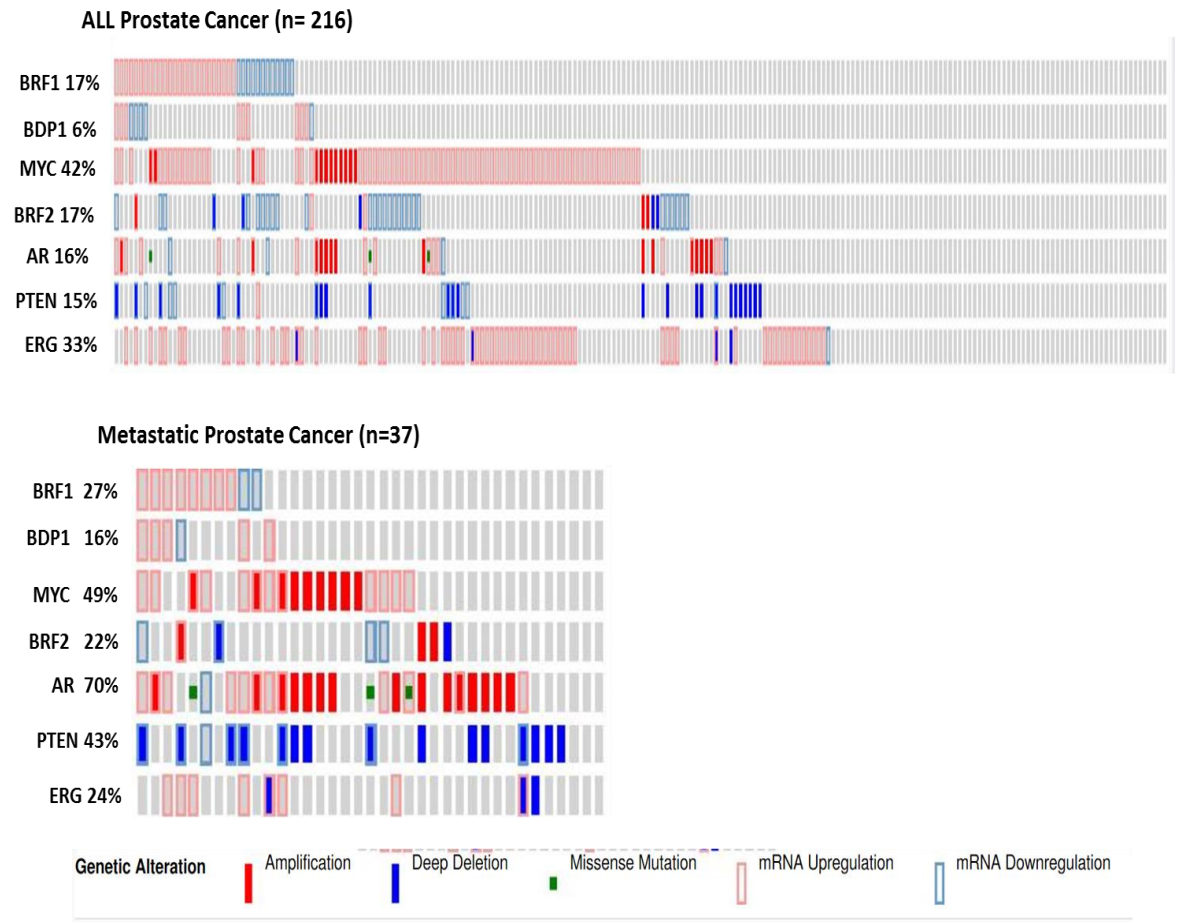

Figure 3-2 cBioportal analysis of PC samples

Red shading means over expression and blue shading means under expression with mRNA expression analysed as a Z score = 2.0 compared to normal samples. Data analysis was performed using TCGA dataset (All PC n=216; Metastatic PC n=37). BRF1 expression is altered in 17% of all PC samples, with 12% being overexpressed and 5% of samples showing under expression. In the metastatic dataset BRF1 expression is altered in 27% of samples with 22% being over expressed and 5% samples having BRF1 low expression.

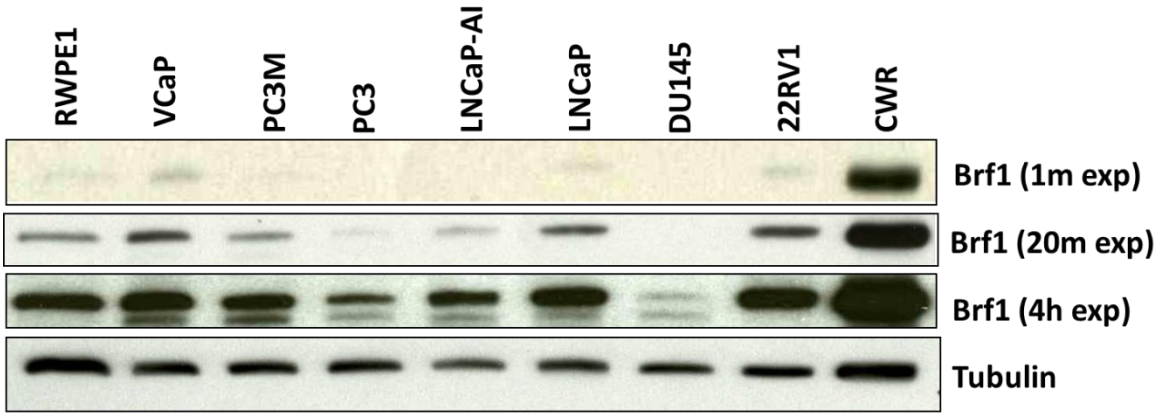

Figure 3-3 BRF1 expression in human PC cell lines
Western blot in a panel of PC cell lines (VCaP, PC3M, PC3, LNCaP,-AI, LNCaP , DU145 cells, 22RV1, CWR22) and the benign RWPE1 cells (m = minute, h = hour, exp = exposure).

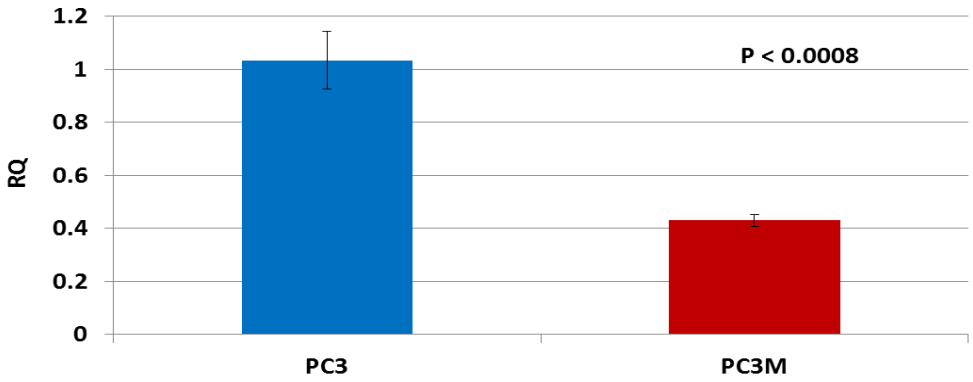

Figure 3-4 RT-qPCR of BRF1 RNA levels in PC3 and PC3M cells
RT-qPCR analysis was performed on total RNA extracted from PC3 or PC3M cells and normalised relative to the expression of a house keeping gene (Cascade 3). Data represents mean of triplicate samples tested with error bars showing mean ± SD, n=3. PC3 cells have higher BRF1 RNA expression than PC3M cells (student t test 2 tailed 2 sample equal variance analysis, $p < 0.0008$). This is in contrast to BRF1 protein expression levels, where PC3M cells have more BRF1 than PC3 cells.

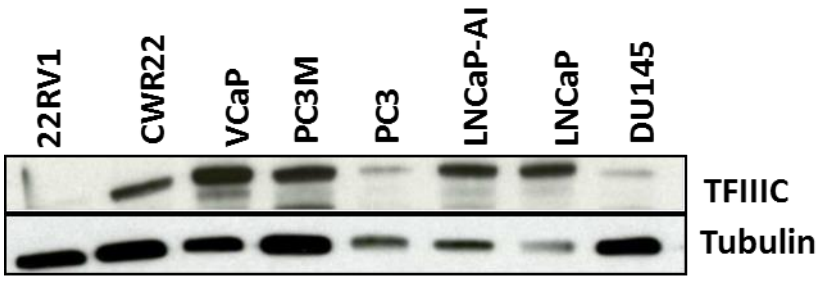

Figure 3-5 WB of TFIIIC expression in a panel of PC cell lines
PC3 and DU145 cells (androgen independent) expressed the lowest levels of TFIIIC (110 kDa), similar to the BRF1 expression in Figure 3.3. The cells with the highest TFIIIC expression are VCaP and LNCaP, which are androgen sensitive and also have high levels of BRF1 (Figure 3.3).

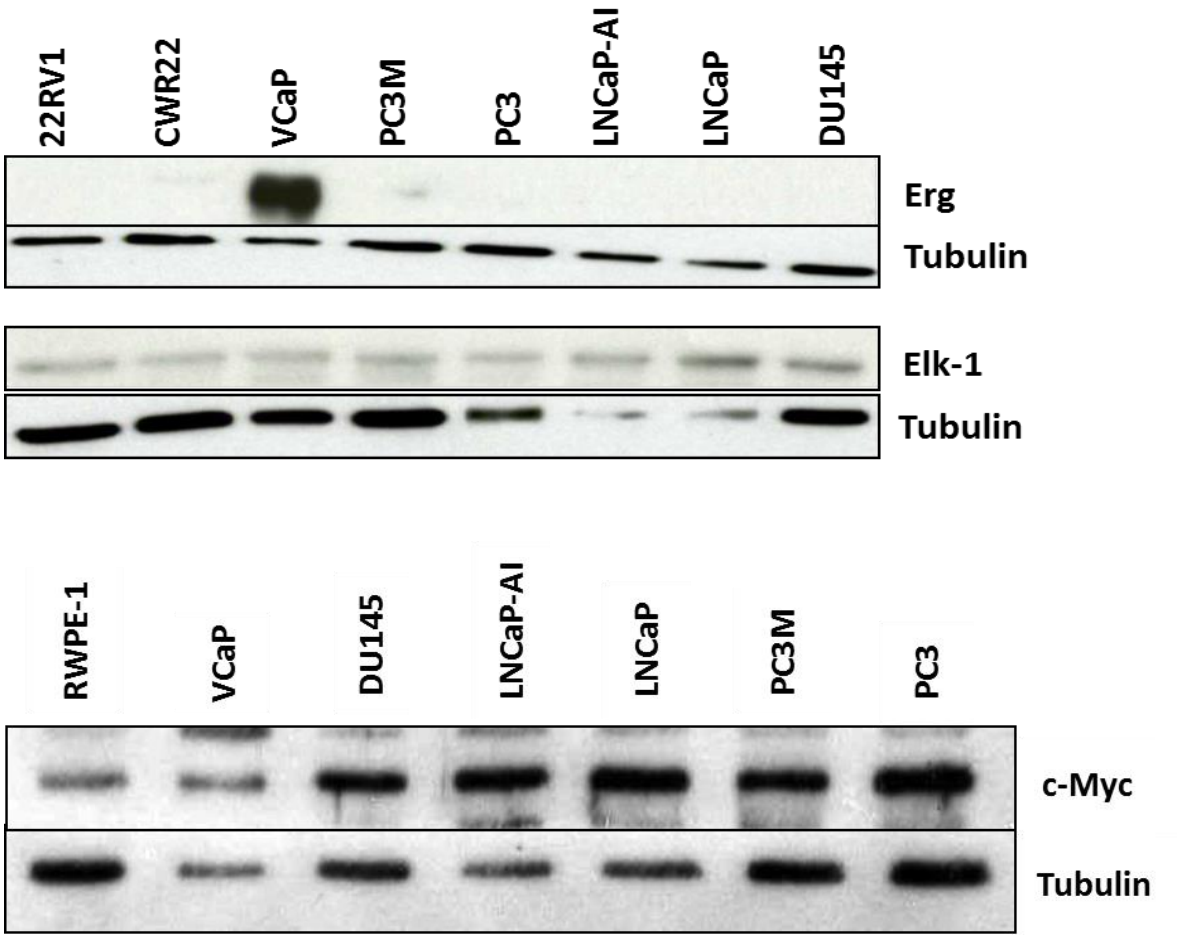

Figure 3-6 Western blot PC cell line panels showing protein expression of known oncogenes and potential BRF1 regulators.
The western blots show that VCaP is the only PC cell line that expresses ERG. All the PC cell line lines express ELK-1 and c-MYC. RWPE-1 expresses the least c-MYC with the other PC cell lines (except VCaP) expressing consistently high levels of c-MYC.

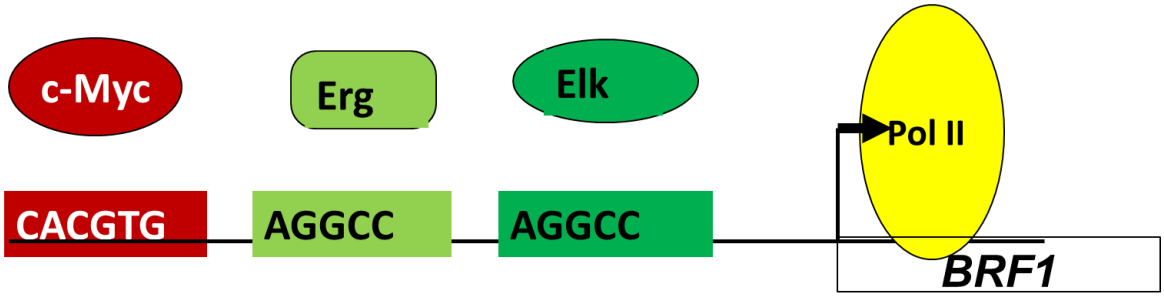

Figure 3-7 Model of *BRF1* upregulation by known PC oncogenes
BRF1 is transcribed by Pol II. It is known that the *BRF1* promoter has DNA binding sequences for c-MYC and ELK-1. ERG and ELK-1 have similar DNA binding specificity.

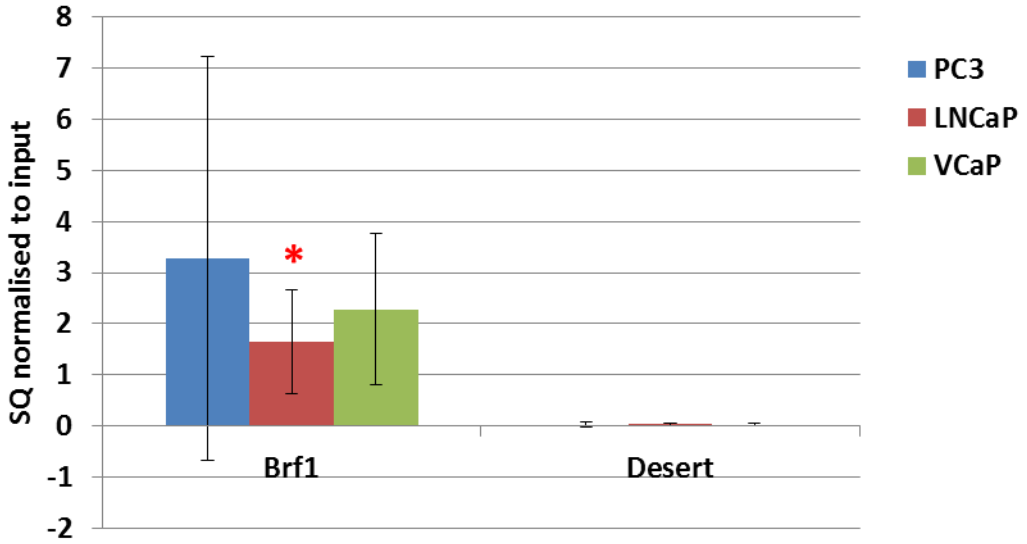

Figure 3-8 Pol II binding at the *BRF1* promoter in PC cells
Pol II binds to the *BRF1* promoter in all three PC cell lines tested. Gene Desert primer is a negative control and shows negligible ChIP binding. However, due to the high variability of PCR values, statistical significance with only the LNCaP cells was reached (student t test, p value < 0.05). PCR values (SQ) were normalised to inputs and subtracted from the negative control antibodyTaf1-48. Data is expressed as means of three independent experiments with error bars showing standard deviation.

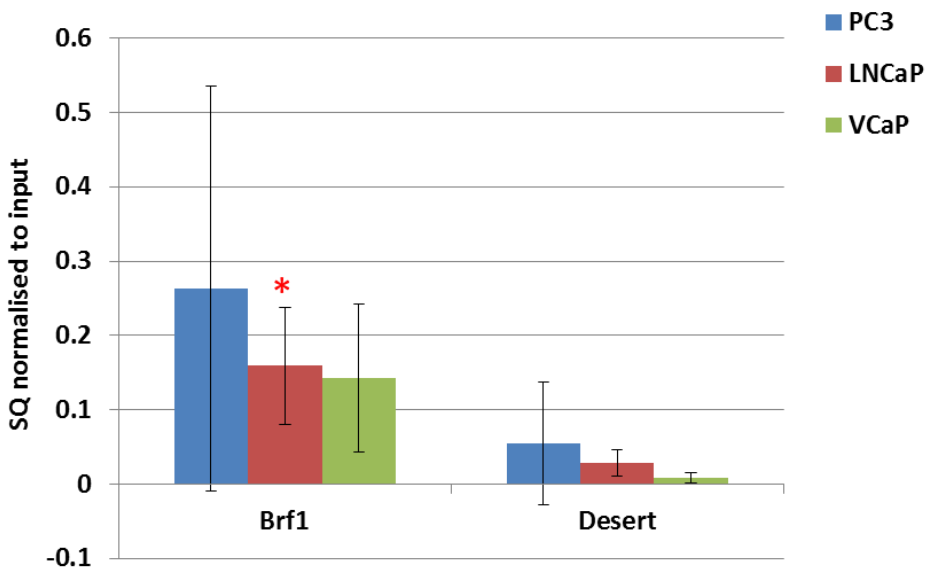

Figure 3-9 c-MYC binds to *BRF1* promoter in PC cells
c-MYC seems to bind to *BRF1* promoter in all three PC lines. Gene Desert primer is a negative control primer and shows negligible ChIP binding. However, due to the high variability and low PCR values only LNCaP reached statistical significance (t-test, p value <0.05). PCR values (SQ) were normalised to inputs and subtracted from negative control antibody Taf 1-48. Data is expressed as means of three independent experiments with error bars showing standard deviation.

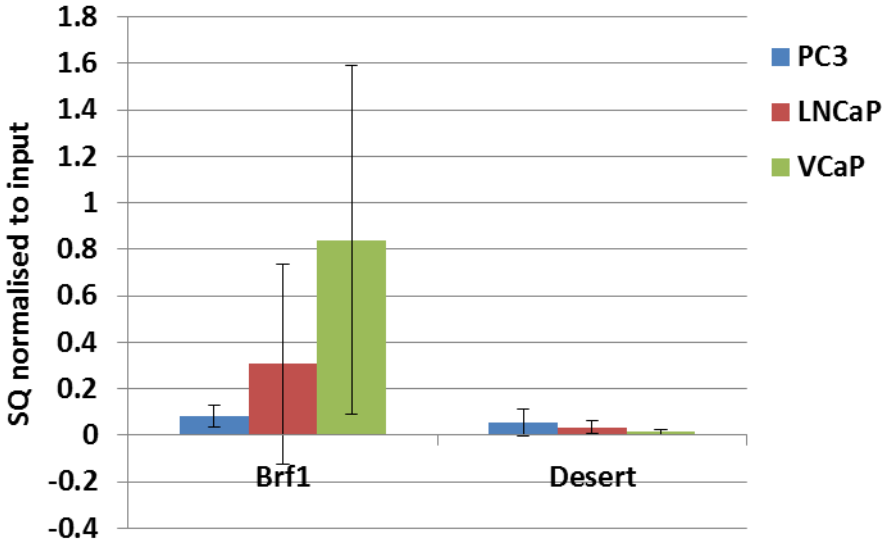

Figure 3-10 ERG binds to the *BRF1* promoter in VCaP cells
ERG seems to bind to the *BRF1* promoter in VCaP cells but not LNCaP and PC3 cells. Gene Desert primer is a negative control and shows negligible ChIP binding. PCR values (SQ) were normalised to inputs and subtracted from negative control antibody Taf 1-48. Data is expressed as means of three independent experiments with error bars showing standard deviation.

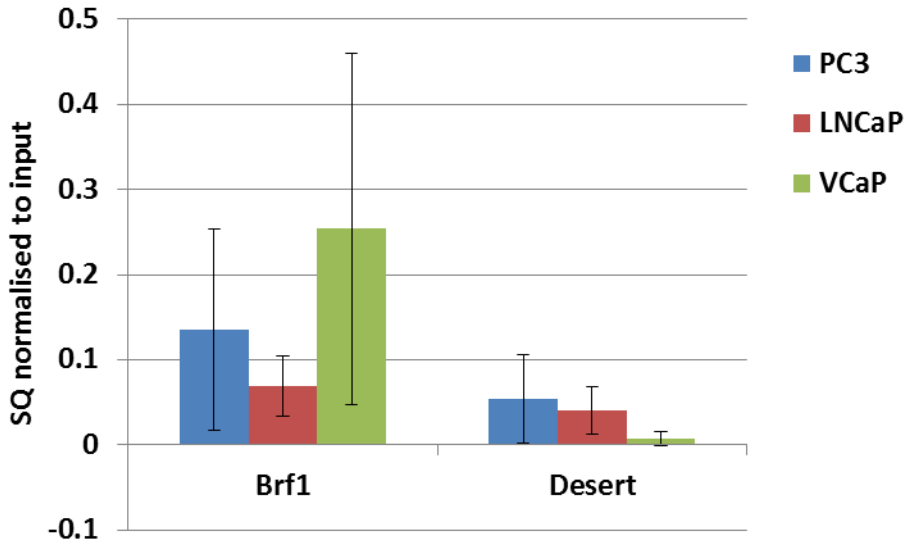

Figure 3-11 ELK-1 does not seem to bind to *BRF1* promoter in PC cell lines.
ELK-1 does not seem to bind to *BRF1* promoter in this ChIP experiment. Gene Desert primer is a negative control and shows negligible and similar results to *BRF1* ChIP binding. PCR values (SQ) were normalised to inputs and subtracted from the negative control antibody Taf1-48. Data is expressed as means of three independent experiments with error bars showing standard deviation.

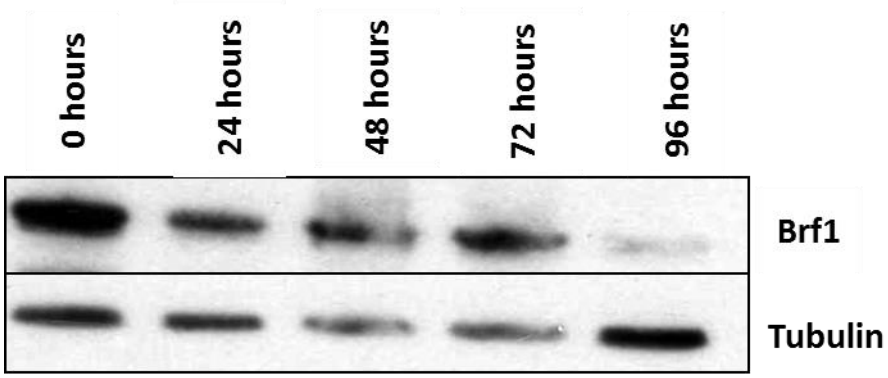

Figure 3-12 BRF1 expression in PC3M after serum starvation
The Western blot shows that at 96 hours of serum starvation the BRF1 expression is markedly reduced. Tubulin was used as the loading control.

3.2 Transient manipulation of BRF1 in human PC cells

3.2.1 Introduction

Complete inhibition of BRF1 or tRNA transcription is incompatible with life. A *Brf1* knock out mouse model was developed at the Beatson Institute which showed complete early embryonic lethality (White et al, Unpublished data). In yeast, deletion of *Brf1* is lethal (Colbert and Hahn, 1992). Homozygous *Brf* deletion ($brf^{EY02964}$ and brf^{c07161}) in flies is lethal and can be rescued by *GAL4*-dependent expression of a *UAS-brf* transgene (Marshall et al, 2012). Partial reduction in Brf1 is well tolerated and using murine primary bone marrow-derived macrophages to study lipopolysaccharides (LPS)-induction of Pol III activation, Brf1 knockdown (KD) pheno-copied the effects of chemical inhibition of Pol III by ML-60218, resulting in suppression of the expression of target tRNAs (Graczyk et al, 2015). This indicates that a KD approach can be used to investigate the cellular role of BRF1 *in vitro.*

Borck et al (2015) manipulated *Brf1* in developing zebrafish embryos and showed suppression of Brf1 expression in zebrafish embryos caused similar neuro-developmental phenotypes to patients with the cerebellar-facial-dental syndrome, an autosomal recessive disorder. Intriguingly, through whole-exome squencing, bi-allelic mis-sense alterations of the *BRF1* gene were identified in three affected families. In Drosophila, the status of Brf1 has also been demonstrated to critically control growth. Using the ubiquitous *daughterless (da)-GAL4* driver and *UAS-brf RNAi* to suppress Brf1 expression and associated Pol III-dependent transcription in Drosophila, the developing larvae were shown to have significantly reduced growth rates (Marshall et al, 2012). In addition, more targeted suppression of Brf1 expression in the salivary glands or the eye marginal discs of flies also led to reduced tissue growth (Marshall et al, 2012). Importantly, *UAS-brf* mediated rescue of Brf1 expression was able to reverse the growth inhibition associated with the *brf RNAi* transgene. Interestingly, they found that overexpression of Brf1 alone was not sufficient to stimulate Pol III activity or affect organismal growth (Marshall et al, 2012).

As high levels of BRF1 expression was associated with poor prognosis in patients with PC (Figures 1.4 and 1.5) and was detected in the more aggressive derived PC3M cells relative to the parental PC3 cells (Figure 3.3), I decided to manipulate BRF1 levels in PC cell lines *in vitro* to determine whether this would affect cellular activity.

3.2.2 Results

To enhance the level of BRF1 expression, I employed two mammalian expression systems containing the human *BRF1* coding sequence, namely EGFP-Brf1 and HA-Brf1 along with the respective vector alone controls (EGFP- empty and HA-empty). Following transient transfection of BRF1 encoding plasmids mediated by lipofectamine, BRF1 expression was significantly increased in PC3, PC3M and DU145 cells relative to controls (Figures 3.13 – 3.15). With the exception of the HA-Brf1 transfection experiments in PC3M and DU145 cells, both BRF1 expressing constructs significantly promoted proliferation in PC3, PC3M and DU145 cells as determined by WST1 assay (Figures 3.13 – 3.15). Therefore, transiently increasing BRF1 levels appears to be mitogenic in PC cell lines, consistent with expression studies shown earlier in this chapter. This suggests that modulation of BRF1 may be a potential new target in PC treatment.

I was interested to further test if suppression of BRF1 expression may have the opposite effect to inhibit cell proliferation. A siRNA-mediated gene silencing approach using three independent siRNAs targeting distinct regions of the *BRF1* coding sequence was employed to transiently knockdown (KD) BRF1 expression. Two transfection protocols were evaluated lipofectamine (RNAimax) and electroporation (Amaxa). Both were effective at reducing BRF1 expression on Western blot analysis but RNAimax was less toxic to the cells generally and was therefore used for all further experiments. In addition to *BRF1*-targeting siRNAs, two *Pol III*-targeting siRNAs were also included as technical positive controls. BRF1 expression was significantly suppressed by all three *BRF1*-targeting siRNAs, while cells transfected with the non-targeting (NT) control siRNAs (namely NT siRNA2, 3) continued to express BRF1 (Figure 3.16). BRF1 siRNA2 appeared to be most consistent and reproducible in the three PC cell lines tested. It is reassuring to note that upon Pol III KD, Pol III expression was drastically reduced without significant impact on BRF1 expression (Figure 3.16).

In all five PC cell lines, namely PC3, PC3M, DU145, LNCaP and LNCaP-AI cells, transient BRF1 KD reduced cell proliferation as determined by WST1 assay (Figures 3.17 - 3.21). I further investigated this BRF1-mediated effect on proliferation using BrdU/FACS cell cycle profile analysis. I found that transient KD of BRF1 in PC3, PC3M and DU145 consistently resulted in a decrease in G1 phase and an accumulation of the G2/M population (Figure 3.22 – 3.24). This was statistically significant in PC3 and PC3M for both BRF1 siRNA2 and BRF1 siRNA3 when compared to NT siRNA2. The sub-G1

cell population was not found to be affected by BRF1 KD, suggesting that apoptosis or cell death did not play a key part in the observed changes in proliferation and instead that decreased BRF1 reduces proliferation by impacting on the cell cycle (Figures 3.23-3.24).

A final WST1 assay experiment was set up to pose the question whether transient BRF1 KD could have a synergistic anti-proliferative effect with chemotherapy agent docetaxel (Figure 3.25). PC3M cells were transfected with BRF1 siRNAs by RNAimax reverse transcription protocol overnight and then docetaxel (Doc.) at a concentration to achieve growth inhibition of 20% (GI20) was added. DMSO was used as the control. Interestingly, BRF1 siRNA2 had the greatest reduction in cell proliferation and adding in docetaxel did not add to this effect. However when the BRF1 KD was less effective such as with BRF1 siRNA3 it initially appears adding in docetaxel does have a potentially synergistic effect of lowering the cell proliferation. However, this also happens with the NT siRNA controls and therefore, most likely signifies that adding in docetaxel is just more toxic to the cells and not acting synergistically with BRF1 KD.

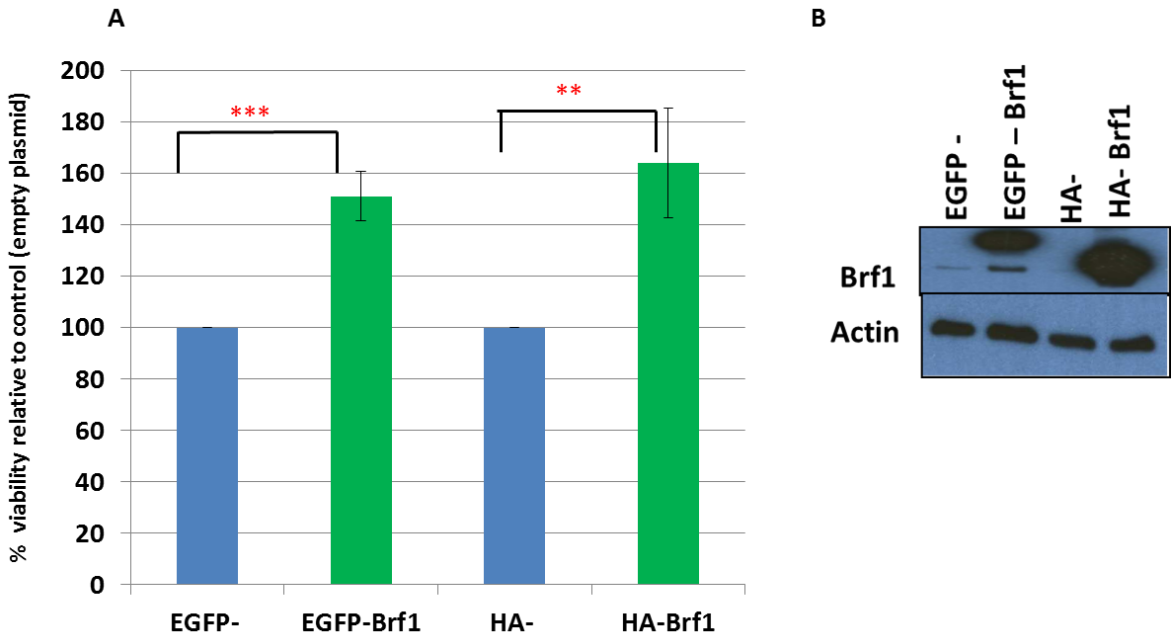

Figure 3-13 Transient BRF1 upregulation in PC3 cells increases cell proliferation.
BRF1 was transiently upregulated by lipofectamine plasmid transfection (EGFP-Brf1 and HA-Brf1) in PC3 cells. EGFP-empty (EGFP-) and HA-empty (HA-) were used as controls.

A) WST1 assay was performed 72 hours later, as a marker of cell proliferation. WST1 assay measures cell viability via changes in wavelength absorbance ($OD_{450-650}$) and the results are expressed as a percentage of their empty vector OD values. For both EGFP-Brf1 (t-test, p= 0.0008) and HA-Brf1 (t-test, p = 0.006) the increase in cell viability in relation to their controls were statistically significant. Data is expressed as means of three independent experiments with error bars showing standard deviation.

B) Western blot analysis confirmed transient overexpression of BRF1 with actin as a loading control. The top Brf1 band is ectopic BRF1 as EGFP adds 27 kDA of weight to endogenous BRF1 (90kDa, the lower Brf1 band). HA only adds 1kDa of weight to endogenous BRF1 and therefore, there is no obvious separation between the endogenous and ectopic BRF1 bands for HA- Brf1 cells.

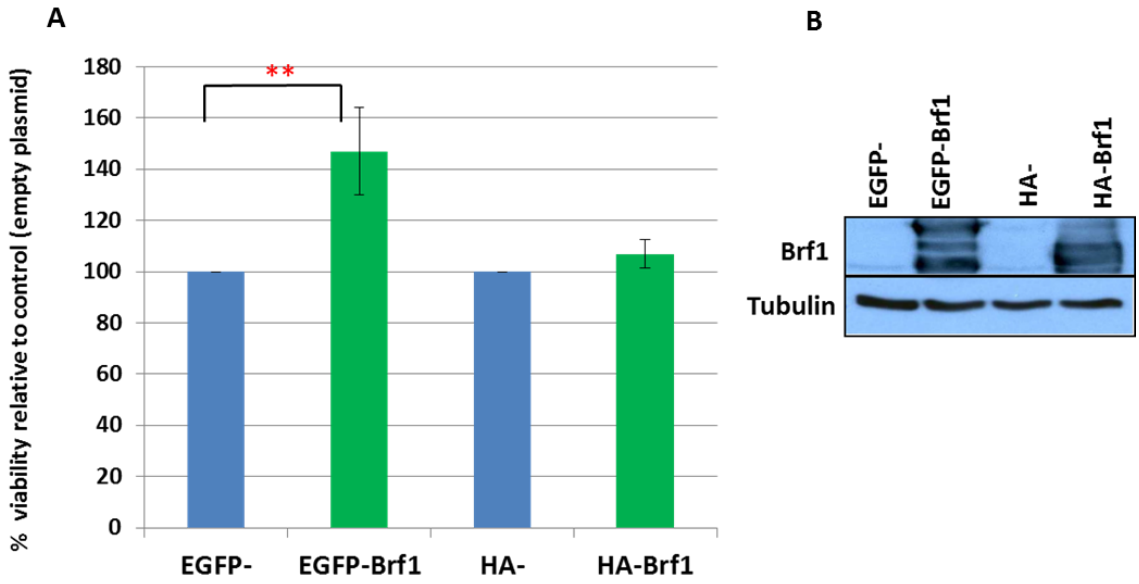

Figure 3-14 Transient BRF1 upregulation in PC3M cells increases cell proliferation.
BRF1 was transiently upregulated by lipofectamine plasmid transfection (EGFP-Brf1 and HA-Brf1) in PC3M cells.

A) WST1 assay was performed 72 hours later, as a marker of cell proliferation. WST1 assay measures cell viability via changes in wavelength absorbance ($OD_{450-650}$) and the results are expressed as a percentage of their control empty vector OD values. EGFP-Brf1 shows an increase in cell viability relative to its control ($p = 0.009$) as analysed by t-test. Data is expressed as means of three independent experiments with error bars showing standard deviation.

B) Western blot analysis confirmed transient overexpression of BRF1 with tubulin as a loading control. The top Brf1 band is ectopic BRF1 as EGFP adds 27 kDA of weight to endogenous BRF1 (the lower Brf1 band). HA only adds 1kDa of weight to endogenous BRF1 and therefore, there is no obvious separation between the endogenous and ectopic BRF1 bands for HA- Brf1 cells.

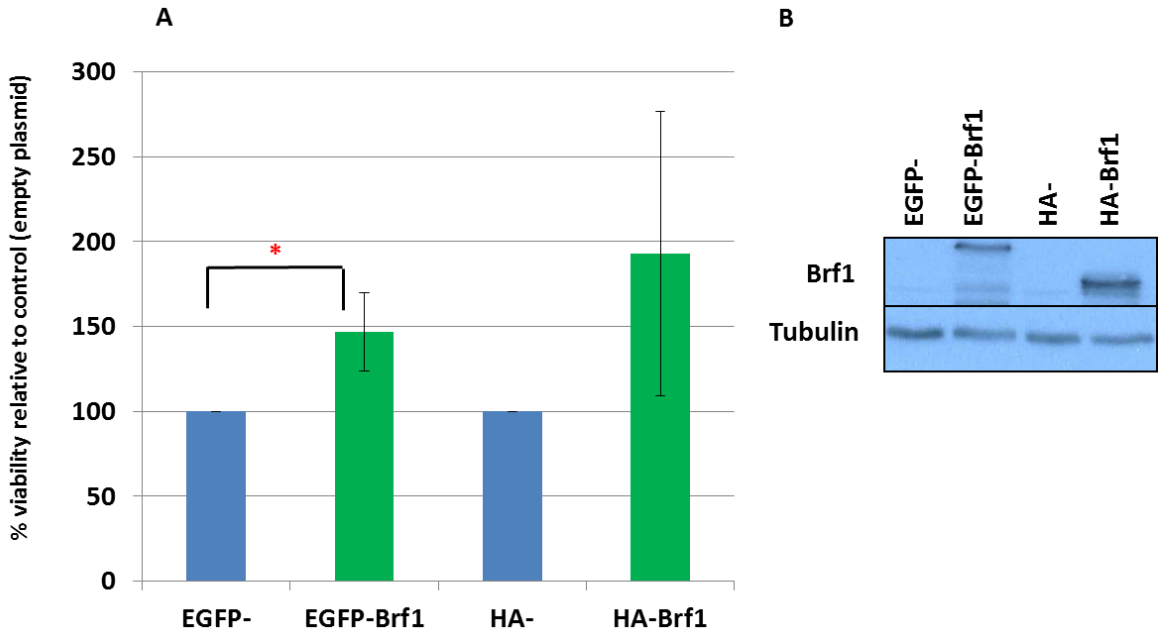

Figure 3-15 Transient BRF1 upregulation in DU145 cells increases cell proliferation.
BRF1 was transiently upregulated by lipofectamine plasmid transfection (EGFP-Brf1 and HA-Brf1) in DU145 cells.
A) WST1 assay was performed 72 hours later, as a marker of cell proliferation. WST1 assay measures cell viability via changes in wavelength absorbance ($OD_{450-650}$) and the results are expressed as a percentage of their empty vector OD values. EGFP-Brf1 showed significantly increased cell viability relative to its EGFP- control (t test, $p = 0.02$). HA-Brf1 showed a trend of increased cell viability relative to its HA-control but due to large variability this was not significant. Data is expressed as means of three independent experiments with error bars showing standard deviation.
B) Western blot analysis confirmed transient overexpression of BRF1 with tubulin as a loading control. The top Brf1 band is ectopic BRF1 as EGFP adds 27 kDA of weight to endogenous BRF1 (the lower Brf1 band). HA only adds 1kDa of weight to endogenous BRF1 and therefore, there is no obvious separation between the endogenous and ectopic BRF1 bands for HA- Brf1 cells.

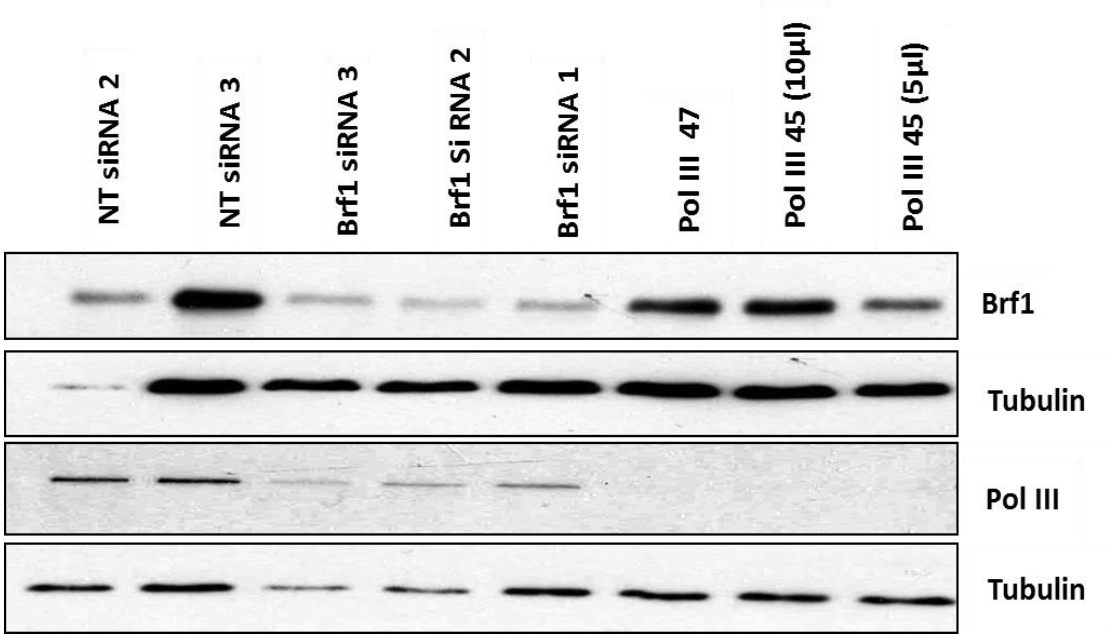

Figure 3-16 Transient knock down (KD) of Pol III and BRF1 in PC3M cells.
This shows a Western blot confirming BRF1 siRNA knockdown with Amaxa using 3 different BRF1 siRNAs and 2 different Pol III siRNAs. BRF1 siRNA2 seems to be the most effective and reliable of the siRNAs.

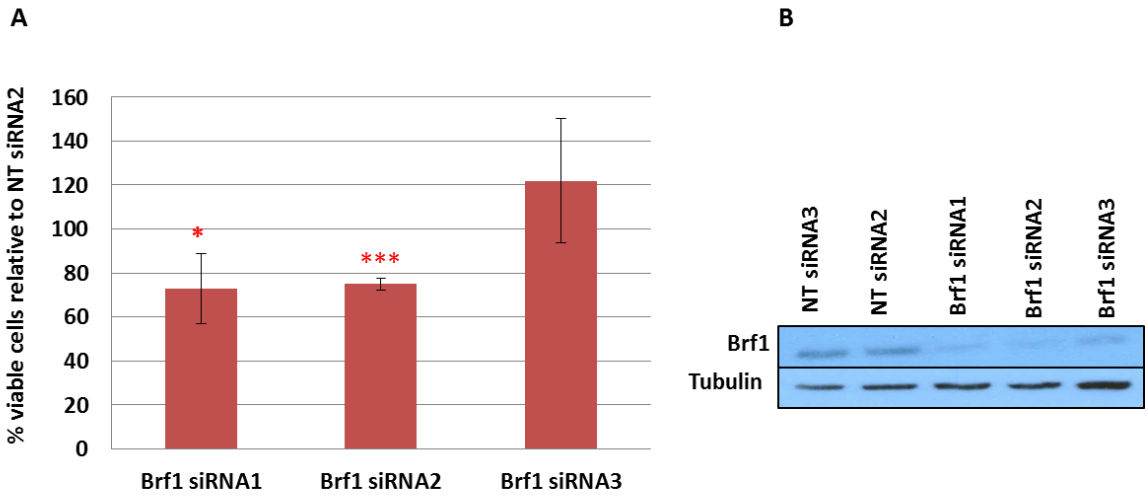

Figure 3-17 Transient BRF1 KD decreases cell proliferation in PC3 cells.
BRF1 was transiently knocked down by siRNA transfection using RNAimax in PC3 cells. A) WST1 assay was performed 72 hours later as a marker of cell proliferation ($OD_{450-650}$). Results are expressed as percentages relative to NT siRNA2 (purchased from Dharmacon). Cells treated with BRF1 siRNA1 ($p = 0.024$) and BRF1 siRNA2 ($p= 0.000003$) show reduced cell viability relative to NT siRNA2 as calculated by t-test. BRF1 siRNA3 did not reduce cell proliferation. Data is expressed as means of four independent experiments with error bars showing standard deviation.
B) Western blot analysis confirms KD of BRF1 by BRF1 siRNA1, siRNA2 and siRNA3 at 72 hours.

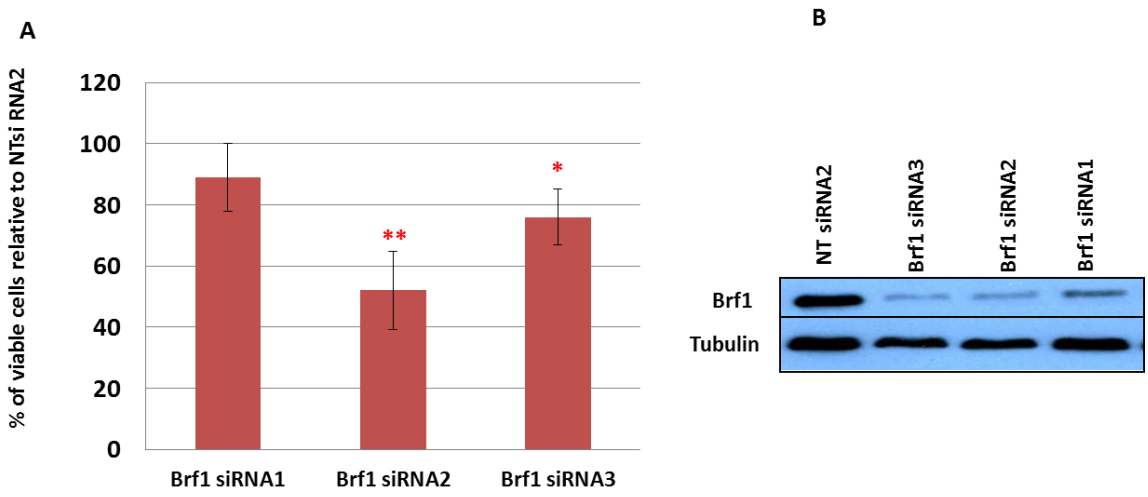

Figure 3-18 Transient BRF1 KD reduces cell proliferation in PC3M cells.
BRF1 was transiently knocked down by siRNA transfection with RNAimax in PC3M cells. A) WST1 cell viability assay was performed at 72 hours (as a marker of cell proliferation) ($OD_{450\text{-}650}$). WST1 assay results are expressed as percentages relative to NT siRNA2 (purchased from Dharmacon). BRF1 siRNA2 ($p = 0.006$) and BRF1 siRNA3 ($p= 0.021$) show decreased cell viability relative to NT siRNA2 as calculated by t-test. Data is expressed as means of three independent experiments with error bars showing standard deviation.
B) The western blot of BRF1 and tubulin (loading control) shows the BRF1 KD was successful at 72 hours.

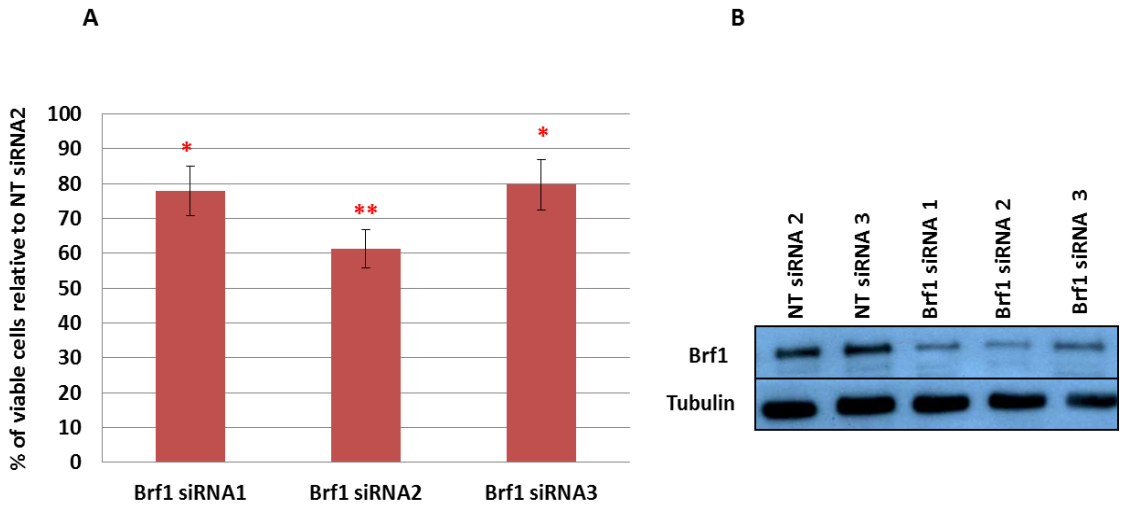

Figure 3-19 Transient BRF1 KD reduces cell proliferation in DU145 cells.
BRF1 was transiently knocked down by siRNA transfection with RNAimax in DU145 cells. WST1 cell viability assay was performed at 72 hours (as a marker of cell proliferation) ($OD_{450-650}$).
A) WST1 assay results are expressed as percentages relative to NT siRNA2 (Dharmacon). BRF1 siRNA1 ($p = 0.012$), BRF1 siRNA2 ($p= 0.001$) and BRF1 siRNA3 ($p=0.018$) all show reduced cell viability relative to NTsiRNA2 as calculated by t-test. Data is expressed as means of three independent experiments with error bars showing standard deviation.
B) Western blot analysis confirms BRF1 KD at 72 hours.

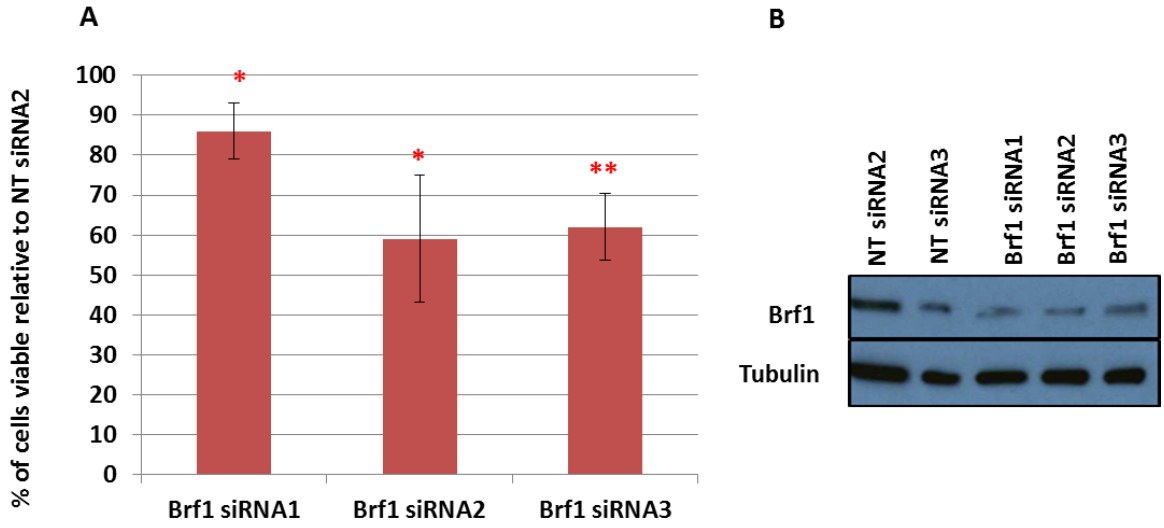

Figure 3-20 Transient BRF1 KD reduces cell proliferation in LNCaP cells.
BRF1 was transiently knocked down by siRNA transfection with RNAimax in LNCaP cells. WST1 cell viability assay was performed at 72 hours (as a marker of cell proliferation) ($OD_{450\text{-}650}$).
A) WST1 assay results are expressed as percentages relative to NT siRNA2 (purchased by Dharmacon). BRF1 siRNA1 ($p = 0.043$), BRF1 siRNA2 ($p= 0.022$) and BRF1 siRNA3 ($p=0.003$) all show decreased cell viability relative to NT siRNA2 as calculated by t-test. Data is expressed as means of three independent experiments with error bars showing standard deviation.
B) Western blot analysis confirms BRF1 KD at 72 hours.

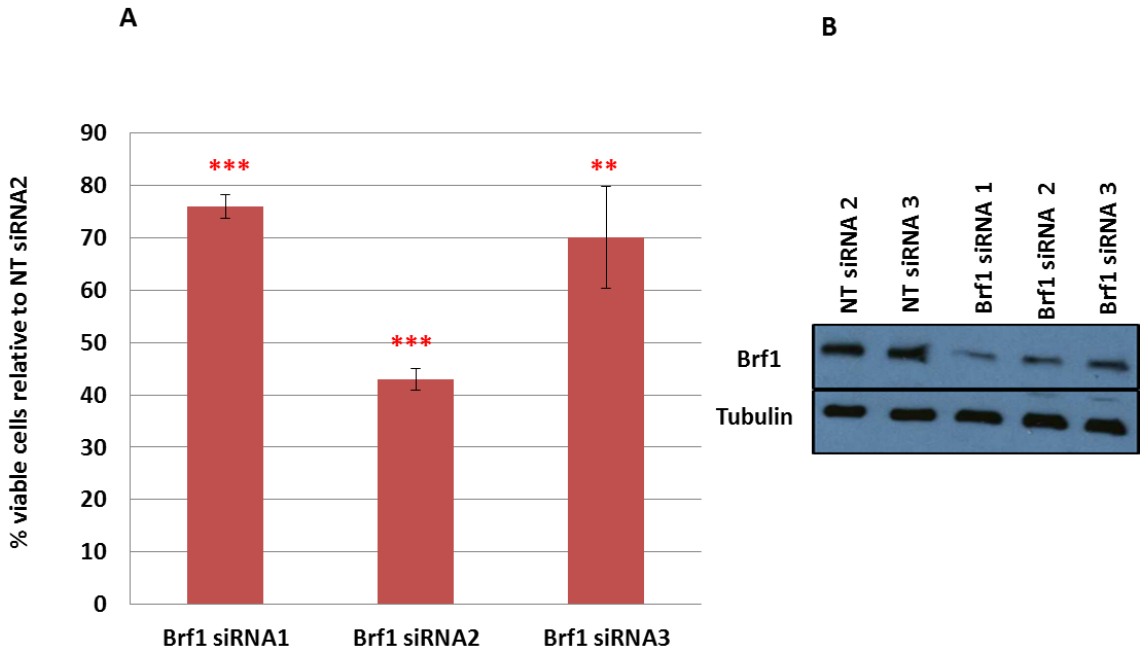

Figure 3-21 Transient BRF1 KD reduces cell proliferation in LNCaP-AI cells.
BRF1 was transiently knocked down by siRNA transfection with RNAimax in LNCaP-AI cells. WST1 cell viability assay was performed at 72 hours (as a marker of cell proliferation) ($OD_{450-650}$).

A) WST1 assay results are expressed as percentages relative to NT siRNA2 (purchased by Dharmacon). BRF1 siRNA1 ($p = 0.0005$), BRF1 siRNA2 ($p= 0.000001$) and BRF1siRNA3 ($p=0.0061$) all show reduced cell viability relative to NT siRNA2 as calculated by t-test. Data is expressed as means of three independent experiments with error bars showing standard deviation.

B) Western blot analysis confirms BRF1 KD was successful at 72 hours.

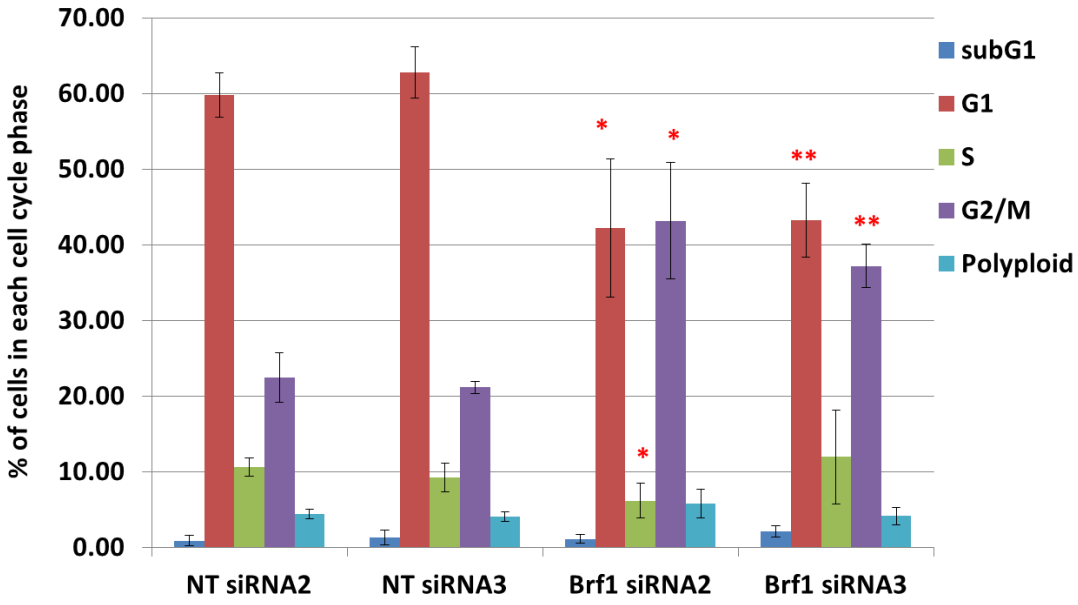

Figure 3-22 Transient BRF1 KD causes G2/M arrest in PC3 cells.
BRF1 was transiently KD by siRNA transfection with RNAimax in PC3 cells. FACS (BrdU/PI) analysis of PC3 cells following siRNA mediated KD of BRF1 shows a change in the cell cycle profile in comparison NT siRNA2 (Dharmacon) at 72 hours. In PC3 cells KD by BRF1 siRNA2 shows a significant decrease in G1 phase ($p = 0.034$) and S phase ($p = 0.042$) and increase in G2/M phase ($p = 0.013$) in comparison to NTsiRNA2 as calculated by t-test. With BRF1 siRNA3 KD there is a significant decrease in G1 phase ($p = 0.007$) and increase in G2/M phase ($p = 0.004$) when compared to NT siRNA2 by t-test analysis. Data is expressed as means of four independent experiments with error bars showing standard deviation.

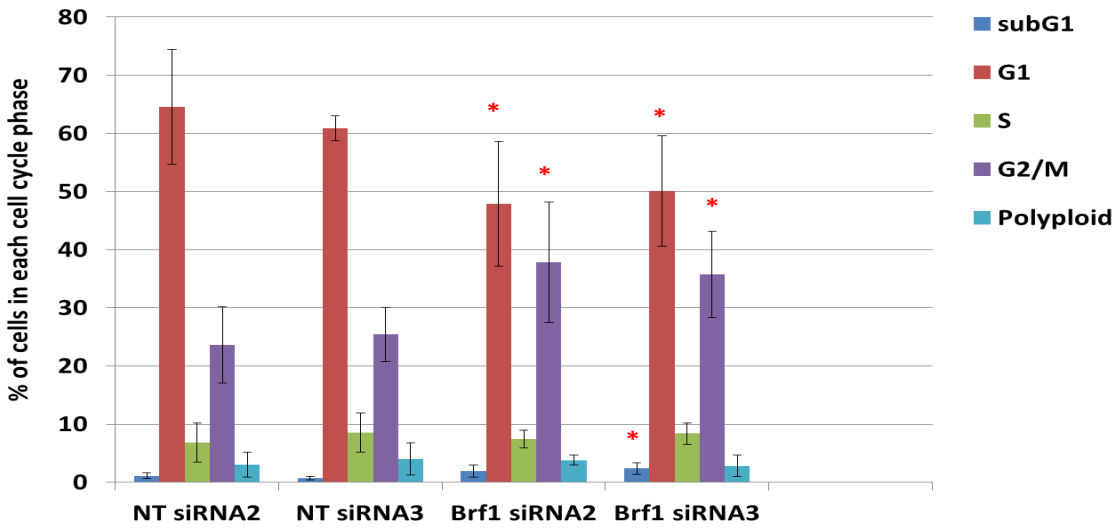

Figure 3-23 Transient BRF1 KD causes G2/M arrest in PC3M cells.
BRF1 was transiently knocked down by siRNA transfection with RNAimax in PC3M cells. FACS (BrdU/PI) analysis of PC3M cells following siRNA mediated KD of BRF1 shows a change in the cell cycle profile in comparison to NT siRNA2 (Dharmacon) at 72 hours. In PC3M cells KD by BRF1 siRNA2 shows a significant decrease in G1 phase ($p = 0.034$) and increase in G2/M phase (p 0.032) in comparison to NT siRNA2. BRF1 siRNA3 KD results in significant subG1 increase ($p = 0.030$), G1 phase decrease ($p = 0.046$) and G2/M phase increase ($p = 0.025$) in comparison to NT siRNA2, by t-test analysis. Data is expressed as means of four independent experiments with error bars showing standard deviation.

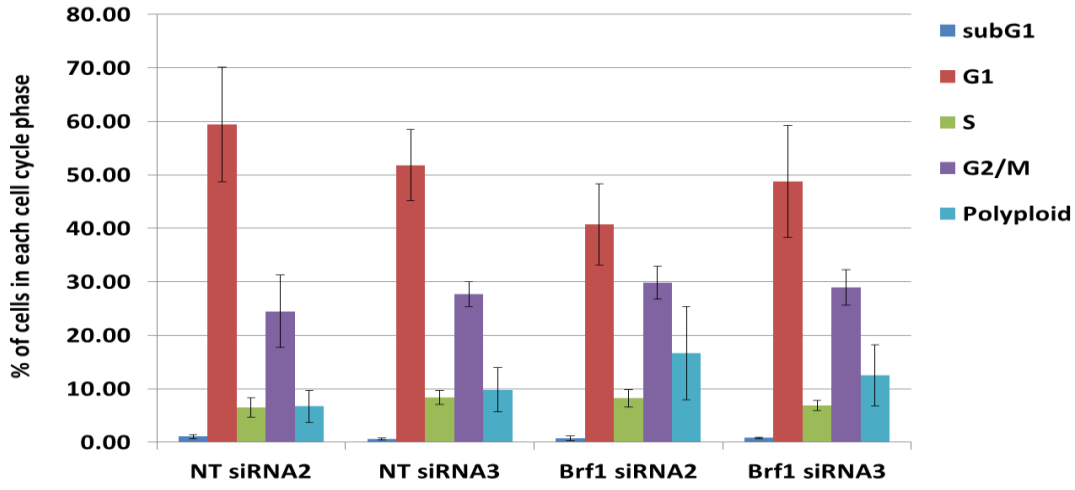

Figure 3-24 Transient BRF1 KD causes trend of G2/M arrest in DU145 cells.
BRF1 was transiently knocked down by siRNA transfection with RNAimax in DU145 cells. FACS (BrdU/PI) analysis of DU145 cells following siRNA mediated KD of BRF1 shows a change in the cell cycle profile in comparison to NT siRNA2 (Dharmacon) at 72 hours. However, in DU145 cells none of the observed changes of G1 decrease and G2/M increase reach statistical significance by t- test analysis. Data is expressed as means of three independent experiments with error bars showing standard deviation.

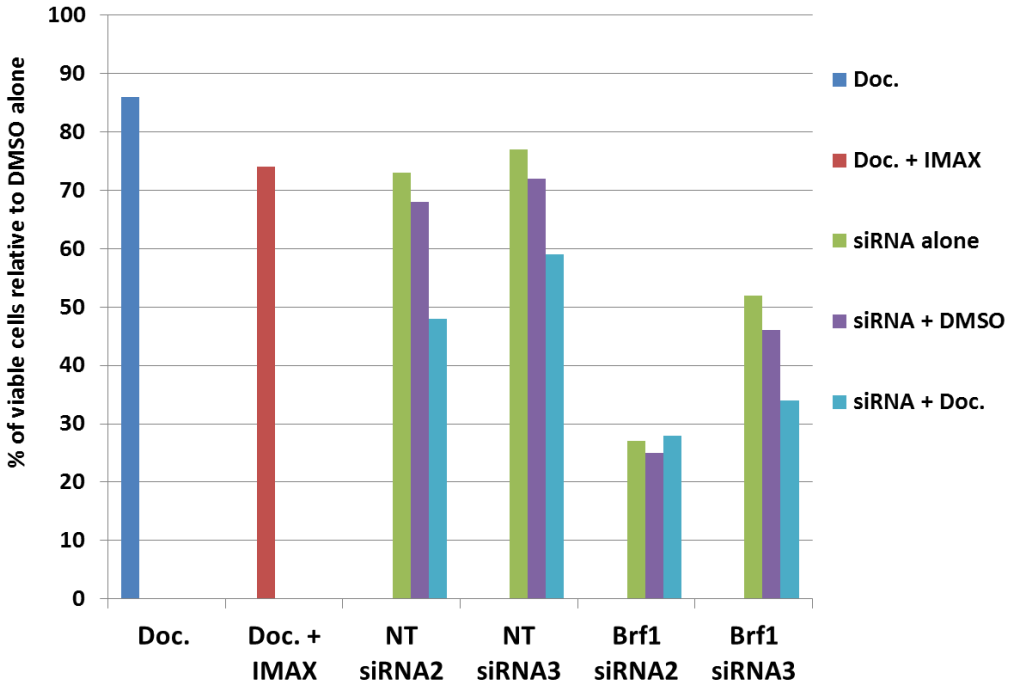

Figure 3-25 WST1 assay of transient BRF1 KD with docetaxel (GI20) treatment in PC3M cells.

PC3M cells were transfected with BRF1 siRNAs by RNAimax reverse transcription protocol overnight and then docetaxel (Doc.) at a concentration to achieve growth inhibition of 20% (GI20) was added. DMSO was used as the control. In this experiment it is clear to see that BRF1 siRNA2 has the greatest reduction in cell proliferation and adding in docetaxel does not add to this effect. However when the BRF1 KD is less effective such as with BRF1 siRNA3 it seems adding in docetaxel does have a potentially synergistic effect of lowering the cell proliferation. However, adding in docetaxel to the NTsiRNAs also shows a reduction in cell proliferation. Therefore, this may simple be showing the additional toxicity of docetaxel to the cells. This experiment was a pilot study and only repeated twice and therefore, no meaningful statistical analysis is possible. (Means of n=2 are shown).

3.2.3 Discussion

There has been limited published data on BRF1 protein expression in PC cell lines. Cabarcas et al, 2008 analysed BRF1 protein expression level in DU145 cells and found that it was similar to cervical cancer HeLa cells and breast cancer MCF-7 cells. However, they found that tRNA transcription levels varied considerably between the three cancer cell lines. tRNA transcription was approximately five fold higher in HeLa cells as compared to DU145 and MCF-7 cells. They suggested a possible explanation for the observed tRNA transcription levels not correlating with BRF1 protein levels is that cancer cells may already express BRF1 levels far above limiting concentrations for RNA Pol III transcription.

All the PC cancer cell lines tested in this study showed easily reproducible BRF1 protein expression on Western blot. The variation in BRF1 expression between the PC cell lines is interesting because it suggests that the AR dependent cell lines have higher BRF1 protein expression than the AR independent cell lines. There is some emerging evidence that Pol III activity may be hormone driven. For example, estrogen receptor positive (ER+) human breast cancer biopsies had higher BRF1 expression than estrogen receptor negative (ER-) breast cancer cases (Julka et al, 2008). Also, AR dependent LNCaP-FGC cells expressed more SHOT-RNAs than AR independent PC3 and DU145. Zhong et al, 2014 have shown Alcohol induced increases in c-Jun activity increases estrogen receptor (ER)α expression and ERα occupancy in the *BRF1* promoter to enhance BRF1 expression, resulting in elevating Pol III gene transcription. In contrast, tamoxifen was shown to inhibit BRF1 expression and Pol III gene transcription via the c-Jun and ERα pathway to repress cell proliferation (Zhong et al, 2014).

The other interesting finding from the PC cell line panel is that BRF1 protein expression is lower in PC3 cells levels than its more aggressive metastatic counterpart, PC3M. This suggests Pol III activity may be a marker of a more aggressive phenotype in PC cell lines. This is in keeping with the cBioportal data that shows BRF1 mRNA expression is greater in the metastatic samples than the all PC sample data. Also, Nam's unpublished TMA data also supports that the patient tumour samples with higher BRF1 IHC staining had poorer survival outcomes than those with lower BRF1 staining scores. It would certainly be useful to examine further PC patient clinical samples with a wider variety of Gleason grades and metastatic samples with clinical follow up data to see whether BRF1 IHC scoring is a potential prognostic marker.

Interestingly, the mRNA levels of BRF1 in PC3M were lower than in PC3 cells, in contrast to BRF1 protein expression. It would be interesting to do further qRT- PCR analysis of the other cell lines to see whether there is a common theme that the mRNA and protein levels do not correlate. This may give further evidence that BRF1 protein expression is dominantly under post-transcriptional control.

It is likely that the regulation of BRF1 protein expression is extremely complicated and variable depending on the cell line and patient. BRF1 expression is probably controlled at the transcription and translational level by multiple transcription factors and epigenetic factors. It should also be remembered that *in vitro* cell line studies are essentially looking at one patient's molecular biology and therefore to get a good overall understanding of mechanisms regulating BRF1 transcription many different *in vitro* and *in vivo* models should be analysed. From our ChIP data, the three cell lines tested seem to have different drivers regulating BRF1 expression and Pol III activity generally. For example, ERG seems to only bind to the *BRF1* promoter in VCaP cells in appreciable levels in keeping with ERG protein expression only being evident in VCaP cells. However, it is difficult to draw firm conclusions due to wide result variation. Frustratingly, the ChIP protocol is a multistep process with numerous technical variables that could be potentially optimised. For example, if time had allowed, additional antibodies and primers could have been tried. Positive control primer sets for genes known to be regulated by these transcription factors could have been tested, for example, cyclin D2 for MYC. However, as the regulation of the *BRF1* promoter was not the central focus of this study further optimisation of ChIP protocol can be addressed in future studies.

Transient manipulation of BRF1 in this study was effective and reproducible in all the PC cell lines tested. These experiments have shown that increasing BRF1 increases cell proliferation, whereas reducing BRF1 expression decreases cell proliferation. Some may argue that WST1 assay is not a definitive marker of cell proliferation but instead cell viability. However, in the context of short-lived transient experiments other measurements of cell proliferation are difficult to achieve. Reassuringly, the FACS analysis of the BRF1 KD experiments did not show a significant change in sub-G1 phase which would signify apoptosis and cell death. Instead BRF1 KD impacts the cell cycle of the cell causing the cells to arrest in G2/M phase with a reduction in G1 phase. Interestingly, it is known that the Pol III activity is at its highest in late G1, S and G2 phases and lowest levels during early G1 and M phases (Johnson et al, 1974; Gottesfeld et al, 1994; White et al, 1995; Hu et al, 2004).

To determine the mechanism for the resulting increase in cell proliferation with transient manipulation of BRF1 it is important to assess whether BRF1 is actually incorporated into the pol III complex. This could be tested by co-immunoprecipitation experiments using antibodies to pull down pol III and western blot for BRF1 to see whether increased levels of BRF1 are incorporated into the transcription complex. Alternatively, one could use ChIP assays to show higher levels of BRF1 at promoters of genes where one could also see pol III binding. Furthermore, to see if the phenotypes seen from overexpression are due to altered pol III activity one could perform knock-down of pol III to see whether this reverses the phenotype.

Docetaxel is a semi-synthetic taxane and is the first line chemotherapy drug for CRPC. Docetaxel-induced microtubule stabilisation arrests cells in G2/M phase of cell cycle and induces bcl-2 phosphorylation which promotes a cascade of events leading to apoptotic cell death. Therefore, we were interested to see whether combining BRF1 KD and docetaxel treatment on PC cells would have a synergistic effect. It is clear that both docetaxel and BRF1 KD reduce cell proliferation of PC3M cells. However, when BRF1 KD is working at its maximal level at suppressing cell proliferation (Brf1 siRNA2) it seems adding in docetaxel does not enhance this antiproliferative effect. In contrast, when the BRF1 KD is less effective in supressing cell growth (Brf1 siRNA3), the addition of docetaxel caused a further reduction in cell proliferation. However, this was also evident in the NT siRNA controls and therefore, the addition of docetaxel is more likely just more toxic to all the PC3M cells and not acting synergistically with Brf1 KD. To take these experiments forward, different levels of BRF1 KD and growth inhibition of docetaxel could be tested. Also, FACS analysis to assess cell cycle effects of combination treatment of BRF1 KD and docetaxel. Furthermore, different cell lines should be tested especially androgen dependent cell lines. Interesingly, the pathways for docetaxel-induced apoptosis appear to be different in androgen-dependent and androgen-independent PC cells (Pienta, 2001).

4 Functional contribution of BRF1 upregulation in PC3 cells

4.1 Introduction

A number of studies have investigated the impact of altered BRF1 expression on cell growth and RNA Pol III activity. Drosophila harbouring functional-deficient Brf1 mutants showed reduced levels of expression for Pol III targets such as tRNAs and 5S RNA. These mutants progressed through embryogenesis and organogenesis normally, but failed to grow due to cell-autonomous decrease in growth as well as abnormal cell cycle progression to result in polyploidy and mitotic cells (Marshall et al, 2012). Cervical biopsies infected with oncogenic HPV16 expressed elevated levels of 5S rRNA, $tRNA^{Arg}$ and $tRNA^{Sec}$ when compared with HPV-negative biopsies. BRF1 expression was maximal in those samples displaying the highest levels of tRNA and 5S rRNA (Daly et al, 2005). Furthermore, increasing the level of BRF1 in cervical cells specifically increased the induction of tRNA and 5S rRNA genes (Daly et al, 2005). In mouse embryonic fibroblast (MEFs), changes in cellular TBP concentrations altered cellular proliferation rates (Zhong et al, 2007).

In Rat1a fibroblasts, increasing cellular TBP (TATA-binding protein) expression did not alter the proliferation rates, but promoted anchorage-independent growth and tumour formation in athymic mice (Johnson et al, 2003). Johnson et al, 2008, studied the effects of suppressing TBP function or expression, by stably expressing increased amounts of TBP containing a mismatch RNA or shRNA to target Brf1 expression (reducing BRF1 levels by two-fold), respectively. While these cells showed no changes in the proliferation rates, there was significant inhibition of TBP-mediated anchorage-independent growth upon reduction of Brf1 expression. Furthermore, decreasing Brf1 expression significantly decreased tumour volume of subcutaneous xenografts in an athymic mouse model, along with reduced Pol III transcription (Johnson et al, 2008).

Johnson et al, 2008, also generated stable cell lines (Rat1a fibroblasts) expressing HA-tagged Brf1 (HA-Brf1) as well as a mutant form of BRF1 (BRF1-T145D) that mimics phosphorylation at this position. Phosphorylation of BRF1 at threonine 145 by ERK enhances BRF1 interactions with Pol III and TFIIIC (Felton-Edkins et al, 2003a). HA-Brf1 was consistently expressed at levels approximately 30% higher than BRF1-T145D. Brf1 overexpression (HA-Brf1) resulted in modest enhancement of Pol III transcription of pre-$tRNA^{Leu}$ and 7SL RNA and more pronounced increase in $tRNA^{Met}_{i}$, whereas BRF1-T145D resulted in a more significant increase in all of these RNA pol III transcripts. However, neither Brf1 overexpression nor Brf1 activation had an effect on cell proliferation rates and anchorage independent growth. Therefore, they concluded that

while Brf1 overexpression or activation induces Pol III transcription, this is insufficient to promote transformation of Rat1a fibroblasts (Johnson et al, 2008).

Using the Rat1a fibroblast cell line, Johnson et al, 2008, manipulated *cMyc* and *Brf1* expression, with overexpression of *c-Myc* via lentiviral infection and *Brf1* knockdown via shRNA which repressed Brf1 expression by 50% without altering TBP expression. c-Myc expression resulted in increased Pol III transcription with increased precursor $tRNA^{Leu}$, $tRNA^{Met}_{i}$ and 7SL RNA expression, whereas reducing Brf1 expression inhibited the Myc-driven increase in these tRNAs. Interestingly, c-Myc mediated growth in soft agar and tumorigenesis were repressed by decreases in Brf1 and RNA pol III transcription. Therefore, it was concluded that Brf1 overexpression in Rat1a fibroblasts and subsequent enhanced Pol III transcription is necessary for c-Myc mediated transformation and tumorigenesis (Johnson et al, 2008).

There is currently no published data on manipulating BRF1 in prostate cancer cells. From my transient BRF1 manipulation experiments, I would hypothesise that stable up-regulation of BRF1 expression in PC cells would promote cellular proliferation and enhance soft agar cell colony growth. If this proves to be the case, I would plan to carry out *in vivo* experiments and inject these more aggressively behaving cells subcutaneously into nude mice and compare tumour size and presence of metastases with nude mice injected with cells containing the empty control plasmid.

4.2 Results

To fully assess the effects of BRF1 overexpression in PC cells, I wish to develop PC cell lines that show stable upregulation of BRF1 expression. PC3 and LNCaP were selected for transfection with a BRF1 containing expression plasmid construct. PC3 cells have fairly low levels of BRF1 expression, and are androgen independent. The androgen receptor (AR) positive LNCaP cells have relatively high levels of BRF1 expression and are androgen responsive. Unfortunately, in my hand, LNCaP cells did not tolerate the transfection process, and hence I focused subsequent investigations on PC3 cells over-expressing BRF1.

I used electroporation with Amaxa® to transfect EGFP- (EGFP-empty and EGFP-Brf1) and HA- (HA-empty and HA-Brf1) containing expression plasmids into PC3 cells. The EGFP-plasmid expressing PC3 cells grew very well, and three independent cell clones were derived, namely EGFP-Brf1 clone 4, clone 5 and clone 6 (referred as EGFP-Brf1 CL4, CL5, CL6 thereafter). The EGFP-Brf1 selected cells all demonstrated high levels of BRF1 expression, while the cell clones transfected with the EGFP-empty vector (EGFP- clones 1 and 2; EGFP –CL1 and CL2 thereafter) consistently showed lower BRF1 (Figure 4.1- 4.3, including data from a pooled cell line; see section below). Unfortunately, the HA-plasmid PC3 cells did not show consistently elevated BRF1 expression in comparison to their empty HA-plasmid cells so they were not studied in subsequent experiments (data not shown).

Stable overexpression of BRF1 was hypothesised to cause increased cell proliferation. However, our WST1 assay and Casey® counting cell proliferation studies suggest there is no effect on cell proliferation when BRF1 is overexpressed in PC3 cells (EGFP-Brf1 CL4 and CL5 versus EGFP-CL1). In fact, initially it appeared that BRF1 overexpression caused a reduction in cell proliferation as measured by WST1 assay (Figure 4.1), and this effect appeared to be lost in higher passaged cells, with higher passages of the EGFP-Brf1 clones showing similar proliferation rate to EGFP- control cells (Figure 4.2). This may be a result of a delayed recovery period in cell growth after BRF1 transfection or an adaptive response to changes caused by BRF1 overexpression. Western blots confirmed that the EGFP-Brf1 plasmid was still present in the cells, resulting in elevated BRF1 overexpression at later passages (Figure 4.2). Furthermore, BRF1 mRNA was confirmed to be highly elevated in EGFP-Brf1 cells (Figure 4.3. Data provided by Dr. C. Loveridge, Unpublished 2015).

To further characterise downstream effects of BRF1 overexpression on Pol III transcription, I carried out qPCR (quantitative polymerase chain reaction) to examine the expression levels of tRNAs. I expected BRF1 overexpression to drive RNA Pol III transcripts, such as tRNAs. However, due to the huge abundance of tRNAs in the control and BRF1 upregulated cells, any difference in tRNA levels between these cell populations could not be quantified meaningfully (data not shown).

To fully characterise the effects of BRF1 overexpression on cell proliferation, an additional EGFP-Brf1 clone (namely EGFP-Brf1 clone 6; EGFP-Brf1 CL6) was generated and analysed. In addition, a pooled population was obtained by Fluorescence- Activated Cell Sorting (FACS) on EGFP CL4, CL5 and CL6 cells; this pooled multi-clonal population is referred to as EGFP-Brf1 Pool thereafter. The corresponding control was derived from FACS sorting of EGFP-CL1 and EGFP-CL2 cells, referred to as EGFP-pool thereafter. BRF1 protein expression was increased in all the EGFP-Brf1 clones and EGFP-Brf1 Pool cells when compared to the EGFP- and EGFP-pooled cells (Figure 4.4). Of note, the EGFP-Brf1 pool has less BRF1 protein expression than the individual EGFP-Brf1 clones.

Cell proliferation is similar between all the EGFP- and EGFP-Brf1 cells on both Casey® counter and WST1 assay (Figures 4.5 and 4.6). Therefore, it seems BRF1 overexpression does not influence cell proliferation rates. Using soft agar colony assays, I next tested if BRF1 overexpression could influence cell colony forming ability. Initially, EGFP-Brf1 CL4 and CL5 versus EGFP-CL1 were tested with 100,000 cells seeded in triplicate in 6 ml dishes and this was repeated twice. EGFP-Brf1 CL5 and EGFP-CL1 behaved the same with very similar colony forming ability. EGFP-Brf1 CL4 had noticeably less colonies formed by 10 days (Figure 4.7). This was repeated with the EGFP-Brf1 CL6 and EGFP-Brf1Pool, with EGFP-CL1 and EGFP-Pool as controls, respectively. Seeding 30,000 cells and running experiment for 14 days, I obtained fewer but larger colonies, which could be counted easier and with more confidence (Figure 4.8). Interestingly, the EGFP-Brf1 CL6 and EGFP-CL1 behaved the same with low colony forming ability and the EFGP-Brf1Pool and EGFP-Pool were similar with high colony forming ability. Perhaps, the process of FACS sorting cells selected cells with certain degree of stickiness or polarity, such that FACS-selected pooled cells were more efficient in forming colonies. However, regardless of this peculiarity, overexpression of BRF1 does not seem to influence colony forming ability of PC3 cells.

To investigate whether increased BRF1 can influence migration, I carried out wound scratch tests using the IncuCyte® system. There was no marked difference between EGFP-Brf1CL5, EGFP-Brf1 CL4 and EGFP-CL1 cells (Figure 4.9). Statistical analysis of triplicate experiments did not show any significant difference in migration velocity between any of the cell clones (data not shown). EGFP-Brf1 CL6 and EGFP-CL1 also showed similar ability to close the wound introduced (data not shown). Therefore, at least in a migration assay, BRF1 overexpression did not influence the mobility of PC3 cells.

Immunofluorescence microscopy was performed to look for the impact of BRF1 overexpression on cellular morphology, as well as to characterise the sub-cellular localisation of BRF1 (Figure 4.10). EGFP-Brf1 cells looked distinctly different from EGFP- cells. Firstly, as expected from its transcriptional role, marked nuclear BRF1 staining was observed in EGFP-Brf1 cells. Second, EGFP-Brf1 cells also tend to have enlarged multi-lobulated nuclei which seemed to correlate with the cells that had the highest BRF1 immunofluorescence intensity.

To assess BRF1 overexpression effects on cell cycle progression, FACS analysis was performed using Propidium Iodide (PI) to profile the cell cycle (Figure 4.11). Interestingly, the EGFP-Brf1 cells showed a reduction in G1 phase and an increase in the following cell sub-populations: S phase, G2/M compartment and polyploid cells, in comparison to EGFP-cells. These differences were all statistically significant (Figure 4.11). The increase in polyploidy cells supports the morphological changes seen on immunofluorescence microscopy.

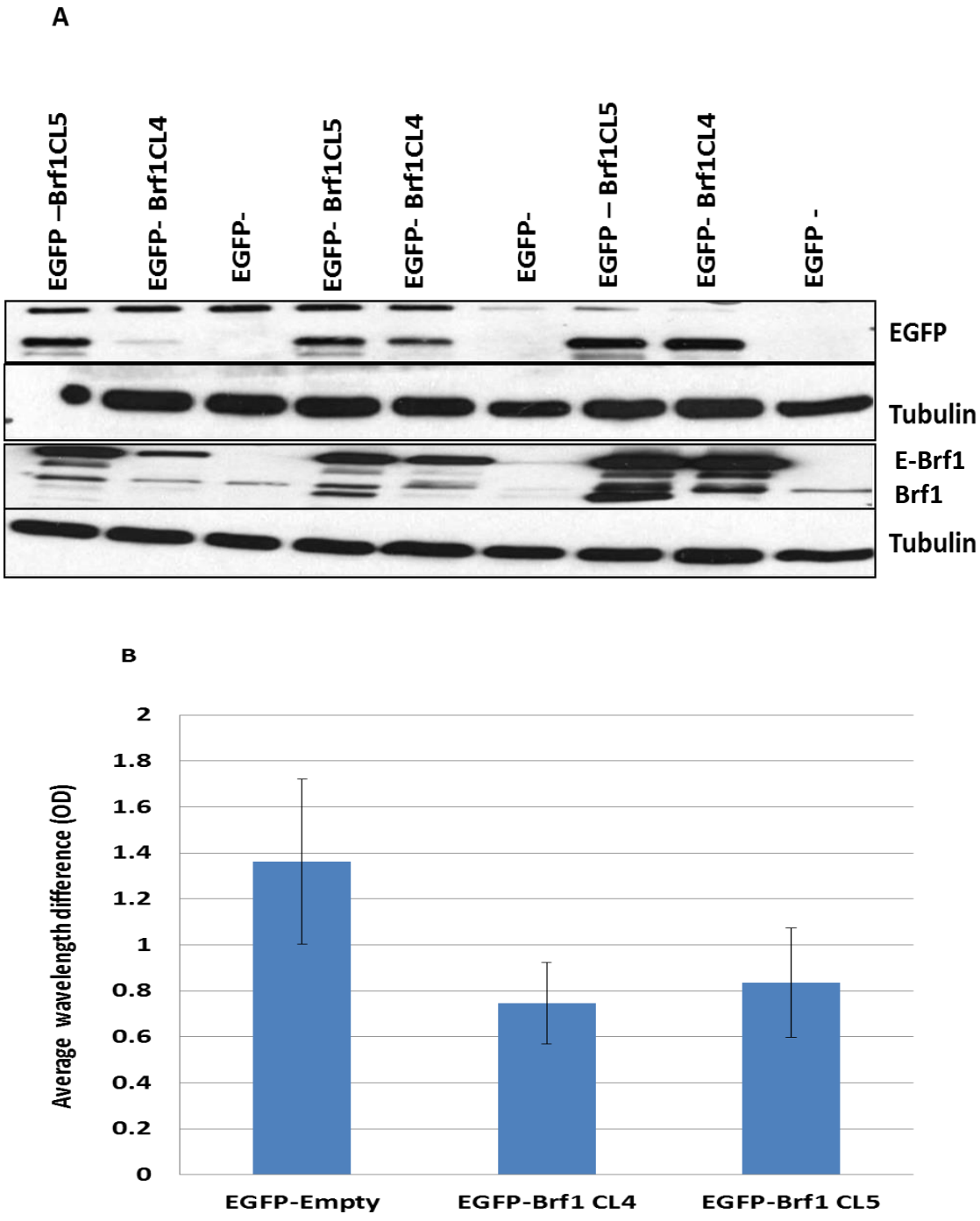

Figure 4-1 Stable overexpression of BRF1 in PC3 cells passage 7-9

A) Western blot of PC3 EGFP-clone 1 (EGFP-) and EGFP-Brf1 clones 4 and 5 passages 7-9 (right-left) showing high expression of BRF1 and EGFP in the EGFP-Brf1 CL4 and CL5 in comparison to EGFP-. The top BRF1 band is ectopic BRF1 (E-Brf1) as EGFP adds 27 kDA to weight of endogenous BRF1 (Brf1).

B) WST1 assay of PC3 EGFP-clone 1 (EGFP-) and EGFP-Brf1 CL4 and CL5. EGFP- appears to have slightly higher cell proliferation than EGFP-Brf1 CL4 at passages 7-9. Data is expressed as means of three independent experiments with error bars showing standard deviation.

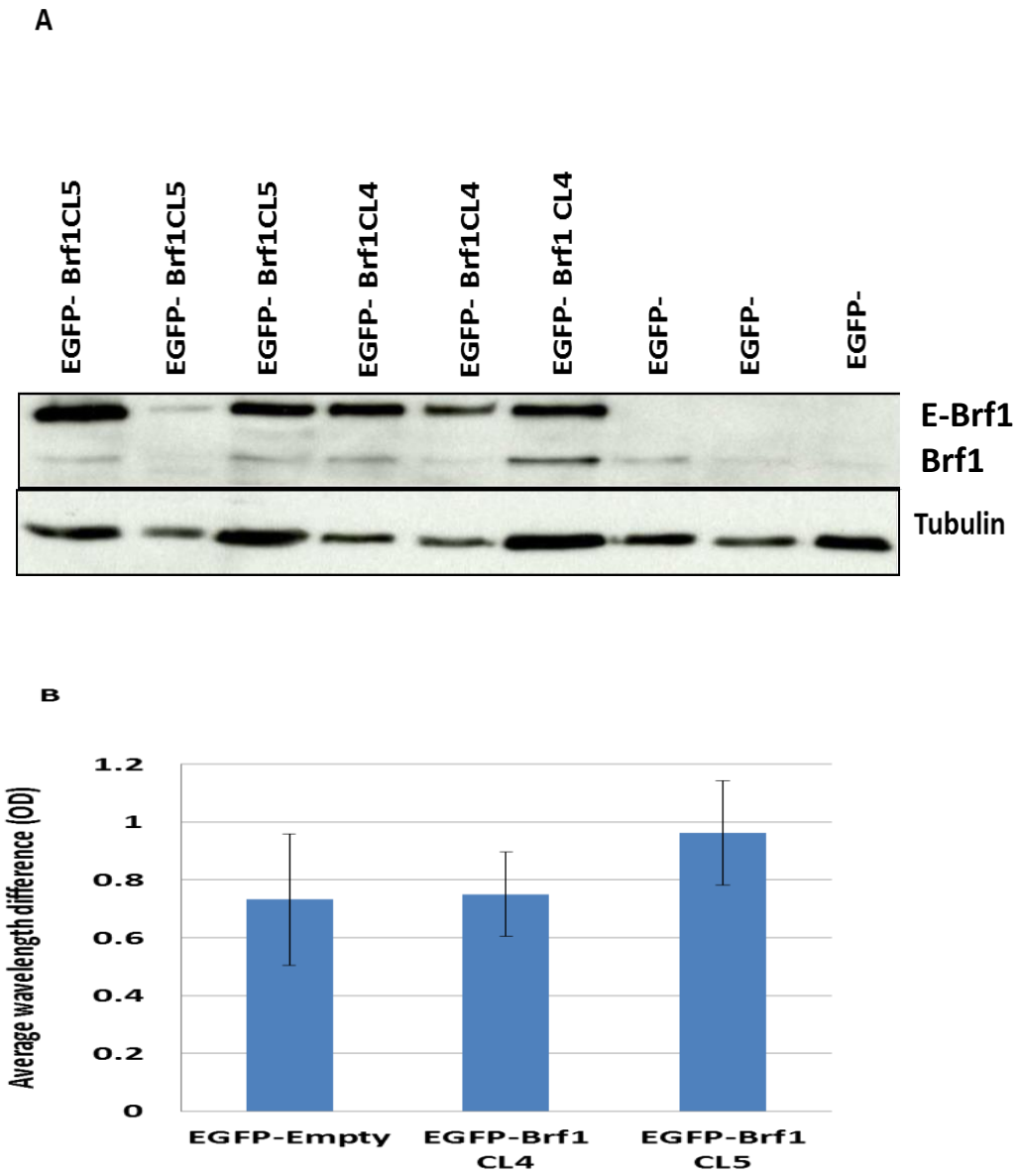

Figure 4-2 Stable overexpression of BRF1 in PC3 cells passages 18-20.

A) Western blot of PC3 EGFP- and EGFP-Brf1 clones 4 and 5 passages 18-20 (right – left) showing high BRF1 expression in EGFP-Brf1 clones 4 and 5 in comparison to EGFP-. The top BRF1 band is ectopic BRF1 (E-Brf1) as EGFP adds 27 kDA to weight of endogenous BRF1 (Brf1).

B) WST1 assay of PC3 EGFP- and EGFP-Brf1 CL4 and CL5 showing that cell proliferation is the same between all the clones at higher passage numbers. Data is expressed as means of three independent experiments with error bars showing standard deviation.

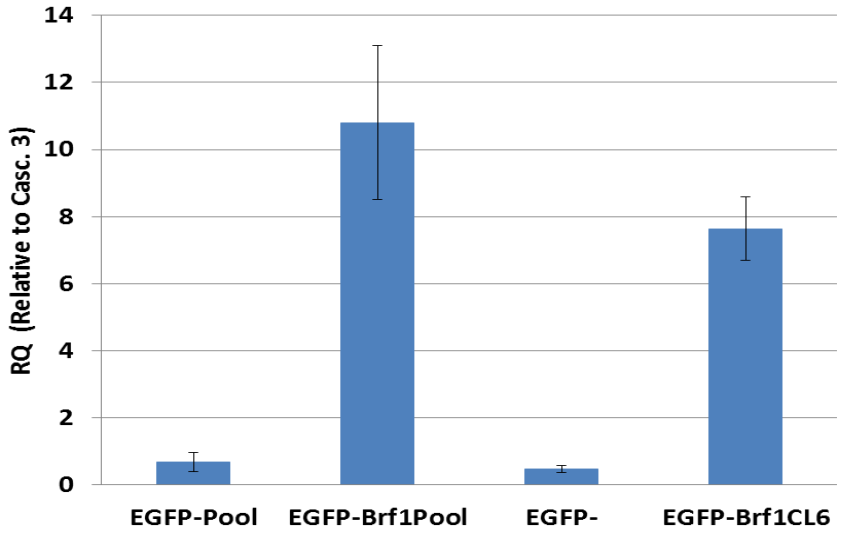

Figure 4-3 BRF1 mRNA levels are higher in the EGFP-Brf1 cells than the EGFP- cells
EGFP-Brf1Pool and EGFP-Brf1 CL6 have higher levels of BRF1 mRNA in comparison to EGFP- Pool and EGFP-CL1 respectively as measured by qPCR (Data provided by C. Loveridge, Unpublished, 2015). Data is expressed as means of three independent experiments with error bars showing standard deviation.

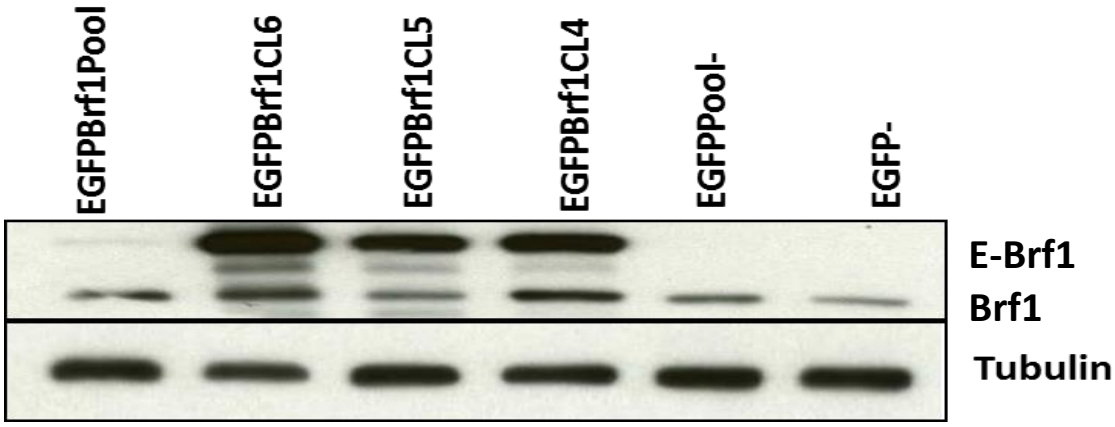

Figure 4-4 Stable overexpression of BRF1 in PC3 cells
This WB shows BRF1 expression in PC3 stably transfected cells with EGFP-Brf1 (clones 4, 5 and 6) and EGFP-empty (EGFP-clone 1) plasmids. EGFP-pool is EGFP FACS sorted pool of EGFP- clone 1 and 2. EGFP-Brf1 Pool is EGFP FACS sorted pool of clones 4, 5 and 6. EGFP-Brf1 Pool has lower levels of BRF1 expression than the individual EGFP-Brf1 clones. The top BRF1 band is ectopic BRF1 (E-Brf1) as EGFP adds 27 kDA to weight of endogenous BRF1 (Brf1). Tubulin was used as a loading control.

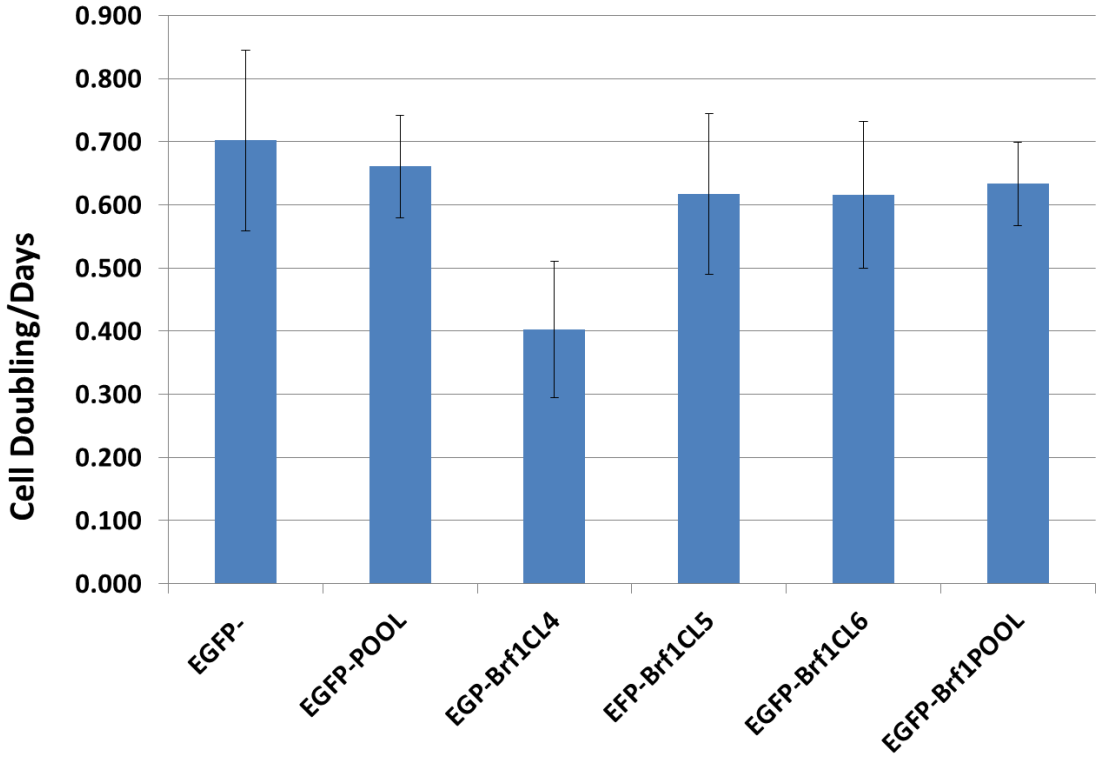

Figure 4-5 Casey® counter: BRF1 upregulation in PC3 cells does not affect cell proliferation.

Cell proliferation was calculated as cell doubling/days by Casey® Counting cells every 3 days after 1 million cells were seeded in flasks for all the different clones. EGFP-Brf1 CL4 has the slowest proliferation rate but all the other BRF1 upregulated clonal subsets are equal to the EGFP- clone and pool. This experiment lasted for 9 passages. (Passage 7-16) Data is expressed as means of nine cell doubling/day calculations with error bars showing standard deviation.

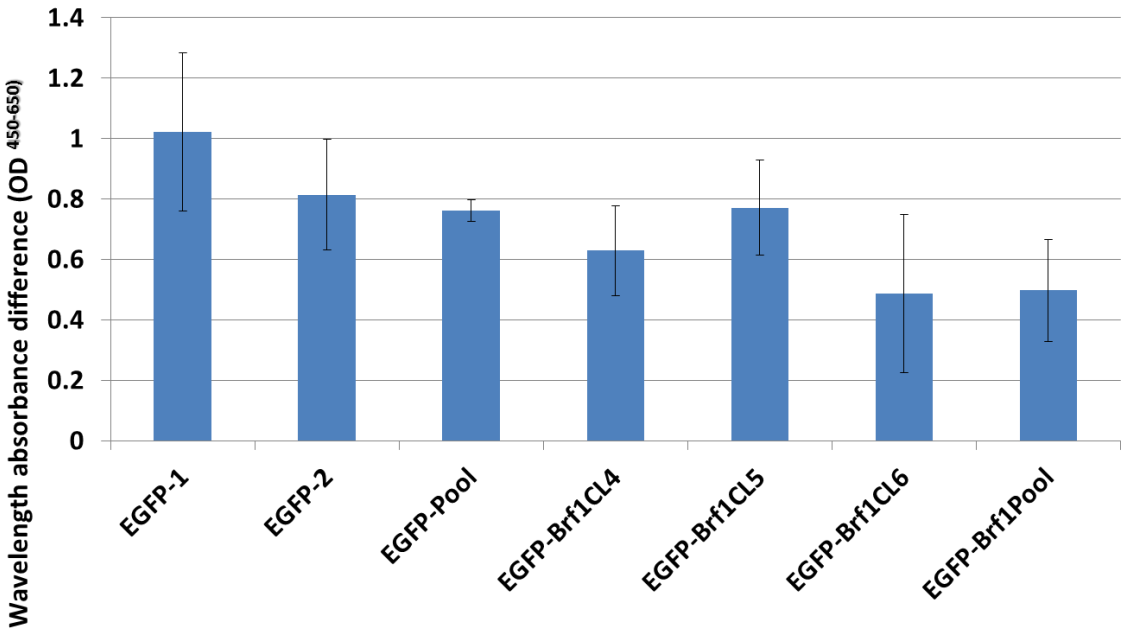

Figure 4-6 WST1 assay: BRF1 upregulation in PC3 cells does not affect cell proliferation. WST1 assay results show there is a high variability within each of the cell clonal subsets and therefore, there is no significant difference between the EGFP-Brf1 cells and the EGFP- cell. Data is expressed as means of three independent experiments with error bars showing standard deviation.

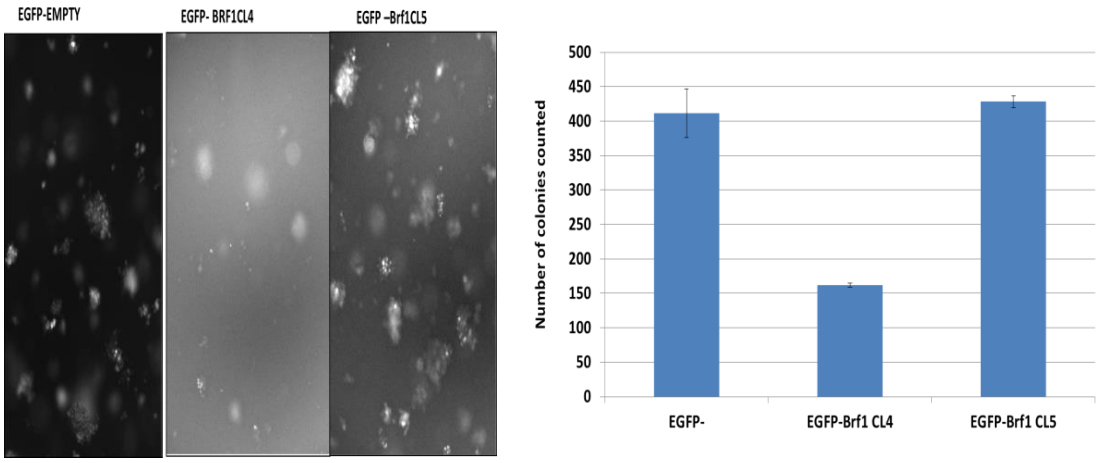

Figure 4-7 Soft agar colony assay of EGFP- versus EGFP-Brf1 CL4 and CL5.
100,000 cells were seeded and colonies above a predetermined size were counted 10 days later. EGFP-Brf1 CL5 and EGFP- were very similar in their colony forming abilities and caused colonies readily. EGFP-Brf1 CL4 formed markedly less colonies than both EGFP-Brf1 CL5 and EGFP- . Data is expressed as means of two independent experiments with error bars showing standard deviation.

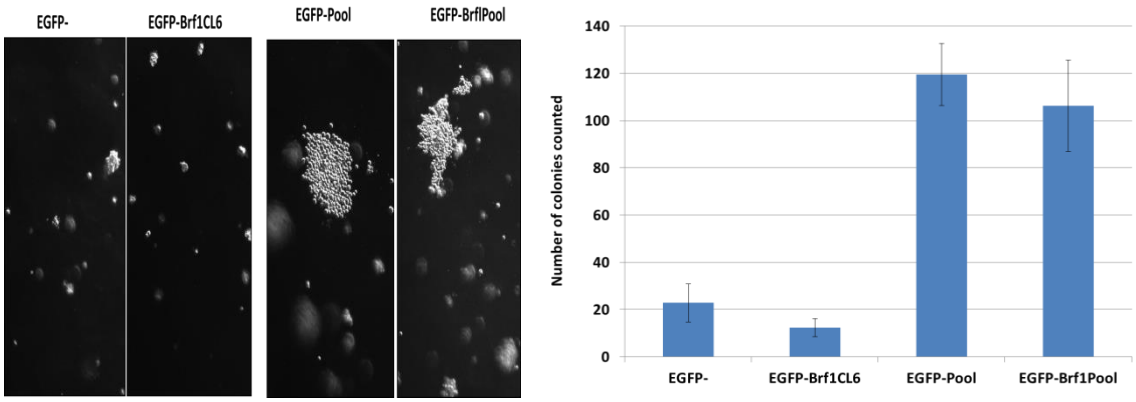

Figure 4-8 Soft agar colony assay of EGFP- versus EGFP-Brf1 CL6 and EGFP-Pool versus EGFP-Brf1 Pool.
30,000 cells were seeded and colonies above a predetermined size were counted 14 days later. EGFP-Brf1 CL6 and EGFP- (clone 1) had similar colony forming abilities and this was generally low. Interestingly, despite these experiments being set up at exactly the same time and same conditions the EGFP FACS sorted pools of EGFP- and EGFP-Brf1 had very high colony forming abilities and similar to each other. Data is expressed as means of two independent experiments with error bars showing standard deviation.

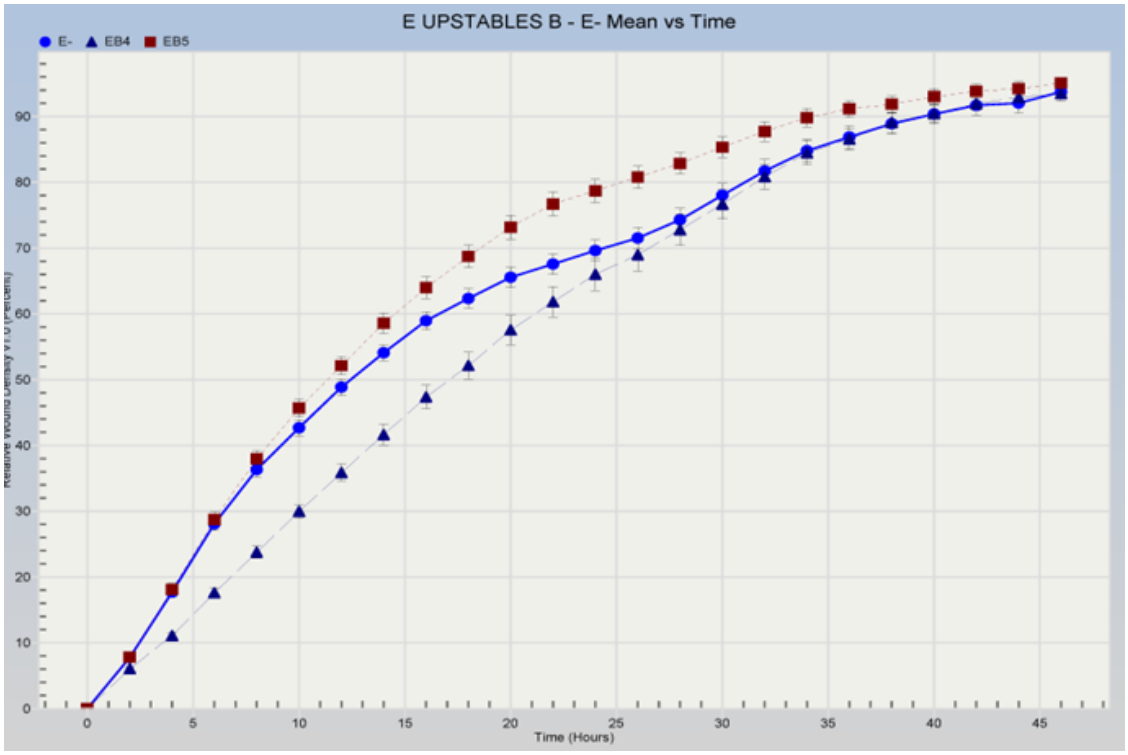

Figure 4-9 BRF1 upregulation in PC3 cells does not affect cell migration
Scratch wound test analysis using IncuCyte® showed that EGFP-Brf1 CL5 and EGFP- behaved in a similar way. EGFP-Brf1 CL4 cells were slightly slower at migrating together to close the wound gap but not significantly. This figure only shows one representative experiment. The experiment was repeated 3 times and showed no statistically significant difference in cell migration velocity between all the PC3 cell EGFP clones (Data not shown). E- (blue circle) = EGFP-CL1; EB4,5 = EGFP-Brf1 CL4, CL5 cells (black triangle and red square respectively).

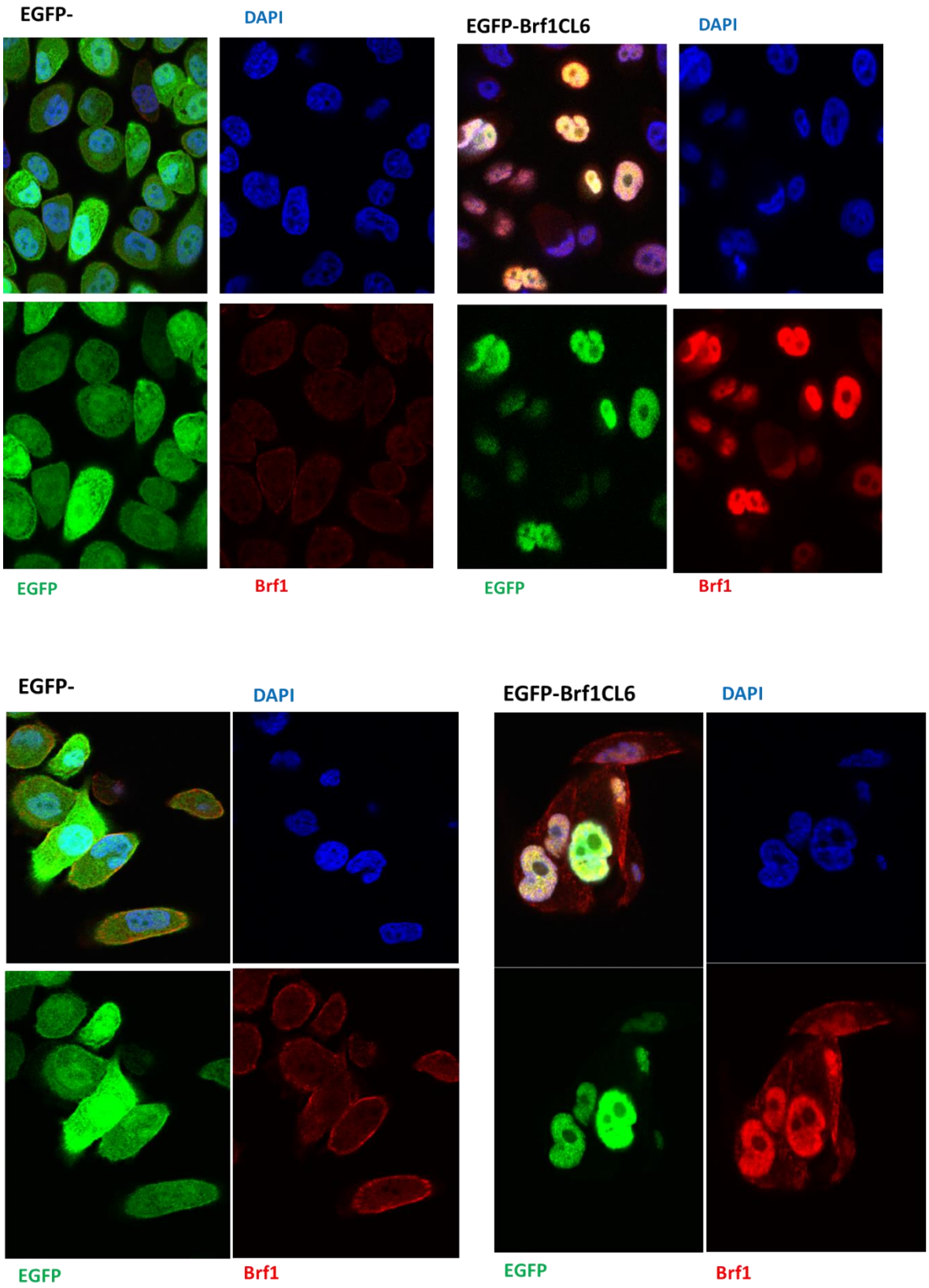

Figure 4-10 BRF1 upregulation causes cell morphology changes .
Immunofluorescence microscopy showing nuclear DAPI (blue), EGFP (green) and BRF1 (red Alexa 555) staining in EGFP- (clone1) and EGFP-Brf1 CL6. BRF1 is densely concentrated in the nucleus in the BRF1 upregulated cells as expected. Interestingly, some of the BRF1 upregulated cells appear polyploidy with multiple nuclear in the cells and look very different from the EGFP- cells.

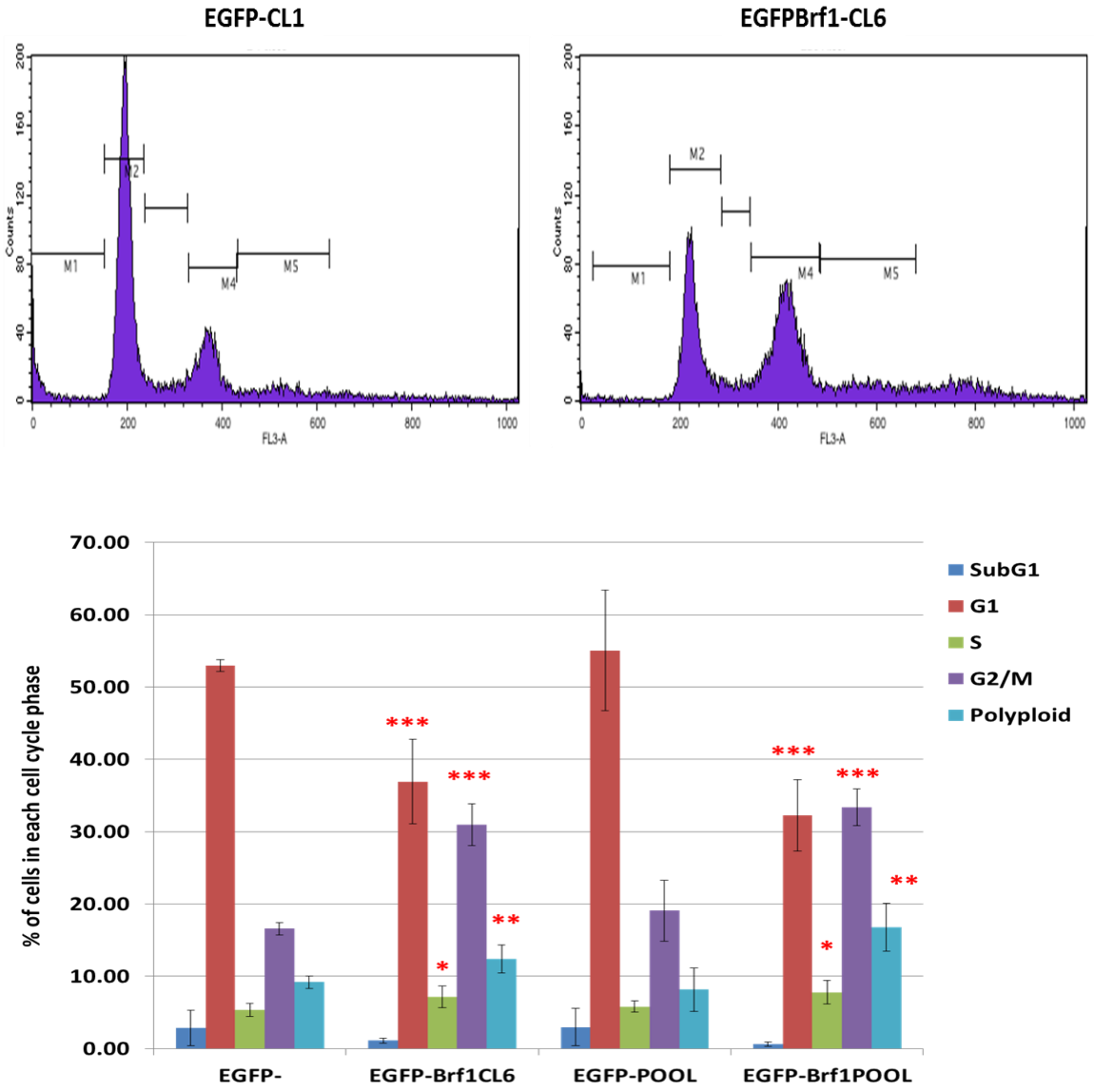

Figure 4-11 BRF1 upregulation in PC3 cells leads to cell cycle changes.
FACS/PI analysis shows EGFP-Brf1 CL6 cells cause a markedly significant reduction in G1 phase ($p < 0.00006$), increase in S phase ($p < 0.03$) and G2/M arrest ($p < 0.00001$) and polyploidy cells ($p < 0.005$) in comparison to EGFP- CL1. EGFP-Brf1 Pool in comparison to EGFP-Pool showed the same marked changes with decrease in G1 phase ($p < 0.0003$) with increase in S phase ($p < 0.04$), G2/M arrest ($p < 0.00007$) and polyploidy ($p < 0.002$). (*,**, *** = p values < 0.05, 0.01, 0.001 respectively). Data is expressed as means of three independent experiments with error bars showing standard deviation.

4.3 Discussion

In summary, BRF1 overexpression in PC3 cells did not display significant functional impact. Therefore, *in vivo* subcutaneous xenograft experiments in a nude mouse model were not performed. It was unfortunate that transfection experiments using LNCaP cells were not successful. It would be important to study additional cell lines stably over-expressing BRF1. PC cell lines with higher levels of endogenous BRF1, such as LNCaP or CWR22, may respond differently to increasing BRF1 expression and produce a more aggressive phenotype. It may be the case that BRF1 is not an important driver in PC3 cells and therefore, overexpressing BRF1 has minimal impact on PC3 phenotype.

Interestingly, stable upregulation of BRF1 in PC3 cells produces similar cell cycle profile changes as transient reduction of BRF1 in PC3 and PC3M, with G2/M arrest being the dominant feature (Figure 3.24 & 3.25). Therefore, perhaps there is a critical level of BRF1 and going above or below this affects cell cycle profile and progression. It would be interesting to see the downstream effects of BRF1 overexpression on other cell cycle dependent transcription factors as a means of explaining these cell cycle changes. If our stable overexpressing BRF1 PC3 cell line had produced a more significant functional phenotype, it would have been important to do RNA deep sequencing analysis as a means of assessing its downstream effectors. However, without a distinct difference in cell behaviour between the control cells (EGFP- cells) and the upregulated cells (EGFP-Brf1 cells) this would be an unnecessary cost.

Enhanced BRF1 expression in PC3 nevertheless clearly resulted in significant changes in their cellular morphology and cell cycle profile. Besides these observations on morphology and cell cycle profile, the evidence of enhanced BRF1 in clinical PC and its association with reduced patient survival would suggest a meaningful role of BRF1 expression in clinical PC. Hence, analysis of the role of BRF1 in an *in vivo* genetically modified mouse model (GEMM) was considered.

5 Manipulation of BRF1 in GEMM

5.1 Introduction

There is now abundant evidence that mouse prostate models can recapitulate different stages of prostate tumorigenesis, including the time taken for tumour to develop and the behaviour of the resulting malignancy, through manipulation of selected genes of interest. Prostate tumours that develop in GEMM often do not have the same complexity of copy number alterations as clinical human prostate tumours studied and therefore, they can provide an opportunity to conduct integrative mouse-human tumour genomic analysis to identify critical oncogenic drivers (Wanjala et al, 2015). They also allow assessment of tumour suppressors and oncogenic pathways, as potential targets for anticancer therapies and as preclinical models for development and validation of anticancer therapies.

Historically, there have been broadly two types of GEMM, transgenic (oncogene gain-of-function) or knockout (tumour suppressor loss-of-function). The knock out GEMM can be further divided into germline deletions, conditional deletion of a floxed allele and inducible deletion of an allele using a drug-induced system. In 1996, Gingrich et al described the first mouse transgenic prostate model, namely the Transgenic Adenocarcinoma of the Mouse Prostate (TRAMP) model, which used prostate specific promoters to express SV40 T antigens, leading to *Rb1* and *p53* inactivation solely in prostate epithelial cells. These mice developed;- at aged 6 weeks prostate intra-epithelial neoplasm (PIN), at 12 weeks high grade PIN (HGPIN) and at 24 weeks poorly differentiated prostate carcinomas with close to 100% penetrance and distant organ metastases (Gingrich et al, 1997). However, the TRAMP model had carcinomas with high neuroendocrine differentiation and rarely bone metastases, thus clinically dissimilar to human prostate adenocarcinomas (Chiaverotti et al, 2008; Masumori et al, 2001).

Germline inactivation of several classic tumour suppressor genes, such as *Rb1, p53* and *Cdkn1B* has not been informative for PC. For example, p53, *Cdkn1B (p27KIP1)* deletion has no effect on PC development and mice lacking *Rb1* are embryonic lethal (Powell et al, 2003). However, germline deletion of *Pten* in GEMM provided essential evidence that PTEN is an important tumour suppressor in human cancer. *Pten* null (*Pten* $^{-/-}$) mice result in embryonic lethality, whereas *Pten* heterozygote mice have dysplasia and/or carcinoma of multiple organs, such as the large and small intestines, lymphoid, breast, thyroid, endometrium and often later in life prostate (as reviewed by Di Cristofano et al, 2000). Heterozygote *Pten* knockout mice (*Pten*$^{+/-}$) have reported to develop PIN with a variable

penetrance from 40-50% (Podsypanina et al, 1999; Di Cristofano et al, 1998) to 90-100% but no progression to invasive carcinoma (Freeman et al, 2006; Wang et al, 2003b).

Second generation transgenic GEMM used variations of the *Probasin* promoter to investigate oncogenic pathways. For example, human c-MYC was expressed in the Lo-MYC mice under control of a weaker *Probasin* promoter, whereas, Hi-MYC mice under control of stronger promoter ARR_2PB, both developed PIN at 3-6 months and invasive adenocarcinoma at 10-12 months (Ellwood-Yen et al, 2003). To be able to investigate invasive PC, a GEMM with prostate specific *Pten* homozygote deletion (*PB-Cre4*: $Pten^{LoxP/LoxP}$) using *Probasin-Cre4* was developed (Wang et al, 2003b). PB-Cre4 has been engineered from prostate specific rat probasin (PB) promoter and incorporates two androgen-responsive regions required for AR mediated expression (Kasper et al, 1994). PB-Cre4 has been shown to be very effective and robust at driving prostate specific transgene expression (Wu et al, 2013). Heterozygote *Pten* loss in the prostate cells resulted in HGPIN whereas loss of two *Pten* alleles shortened the latency of PIN formation and led to invasive adenocarcinoma at 9-29 weeks, with evidence of metastases to lymph nodes and lung (Wang et al, 2003b). Furthermore, *Pten* null (*PB-Cre4*: $Pten^{LoxP/LoxP}$) mice developed androgen independent prostate tumours after castration (Wang et al, 2003b).

Wang et al, (2003b) were the first to show that prostate specific homozygous *Pten* loss alone is sufficient for PC initiation. Furthermore, *Pten* loss of heterozygosity (LOH) is a rate-limiting step for PC initiation and progression to metastatic PC (Wang et al, 2003b). However, other research groups using prostate specific homozygote *Pten* loss GEMM could not reproduce overt adenocarcinoma and metastatic spread (Backman et al, 2004; Trotman et al, 2003; Chen et al, 2005). In our lab, *PB-Cre4:*$Pten^{flox/flox}$ produced relatively slow progression to invasive cancer beyond 10 months of age without evidence of metastases at 18 months (Ahmad et al, 2013). Further analysis has shown that, in conditional *Pten* loss mice, prostate tumour cells develop senescence, thus explaining the long latency in tumour development and precludes their advancement to the invasive and metastatic phenotype (Chen et al, 2005).

A possible limitation of *Probasin-Cre* GEMM is that *Cre* activation and expression is post-natal, before the prostate gland has reached adult maturity (Wu et al, 2001). To address this, other promoters have been used to generate prostate specific *Cre*-mediated *Pten* conditional knockout GEMM leading to variable phenotypes based on timing of genetic event and therefore disease development and progression of prostate carcinogenesis. For

example, the *Osr1 (odd skipped related 1)- Cre* promoter activates at E11.5 (embryonic day 11.5) in urogenital sinus epithelium and remains switched on throughout prostatic epithelium development (Grieshammer et al, 2008). *Osr1-Cre:Pten*$^{LoxP/LoxP}$ mice can develop HGPIN at 4 weeks and locally invasive prostate tumours at 12-16 months of age (Kwak et al, 2013). Post-castration, there was no significant regression of prostate tumours but the signals for androgen receptor (AR) immunoreactivity shifted from nuclear to cytoplasm (Kwak et al, 2013). *Pten* knockout using human *PSA* promoter driven *Cre* expression showed that heterozygote *Pten* deletion at 10 months aged mice resulted in focal and low grade PIN, while homozygote *Pten* deletion at 4-5 months old resulted in hyperplasia and focal PIN, at 7-9 months PIN with focal micro-invasion and at 10-14 months invasive prostate carcinomas with rare metastases (Ma et al, 2005). *Pten* inactivation using MMTV (*mouse mammary tumour virus) -Cre* transgenic mice by 2 weeks old displayed HGPIN with complete penetrance and frequent progression to invasive adenocarcinomas at 7-14 weeks old (Backman et al, 2004). MPAKT *(murine prostate restricted Akt kinase activity)* model with constitutively activated Akt in mouse prostate epithelial cells developed PIN lesions in the ventral prostate with prominent bladder obstruction but no metastases (Majumder et al, 2003).

The prostate specific, *NKX3.1* is a homeobox gene encoding a transcriptional regulator expressed at early stage of prostate organogenesis and is crucial for structural development of the prostate gland and expression of its secretory proteins. *NKX3.1* maps to chromosome 8p21. In approximately 80% of human prostate cancer, *NKX3.1* undergoes allelic deletions and is strongly associated with prevalence of PIN lesions and thus, has been implicated in PC initiation (as reviewed by Dong, 2001). Mice harbouring homozygous and heterozygous *Nkx3.1* deletion at 1 year old develop PIN lesions (Bhatia-Gaur et al, 1999; Kim et al, 2002). Furthermore, Nkx3.1 protein loss is required for PIN development in both humans and mice (Kim et al, 2002), and, in human PC, while the remaining *NKX3.1* allele is not mutated (Voeller et al, 1997), it undergoes epigenetic inactivation (Bowen et al, 2000).

Carcinogenesis is a process involving an accumulation of multiple genetic aberrations and, therefore, mouse models that incorporate multiple genetic events are likely to be more relevant to human PC. For example, Kim et al 2002 found that combined loss of *Nkx3.1* and *Pten* (namely *Nkx3.1*$^{+/-}$ and *Pten*$^{+/-}$) cooperate in prostate carcinogenesis in that at 6 months HGPIN and carcinoma *in situ* were observed. Serially transplanting these HGPIN lesions into nude mice resulted in neoplastic progression, showing histopathological

changes in keeping with well differentiated adenocarcinoma in humans (Abate-Shen et al, 2012). By aging the *Nkx3.1*$^{+/-}$*Pten*$^{+/-}$ GEMM to over 1 year old, these mice developed invasive adenocarcinoma often with metastatic spread to lymph nodes (Abate-Shen et al, 2012). Further analysis of *Nkx3.1*$^{+/-}$*Pten*$^{+/-}$ GEMM shows loss LOH of *Pten* is required for progression to invasive carcinomas but not LOH of *Nkx3.1* (Kim et al, 2002).

Prostate tumours developing from the *Nkx3.1*$^{+/-}$*Pten*$^{+/-}$ GEMM are capable of developing androgen independence (Abate-Shen et al, 2012). Castrating *Nkx3.1*$^{+/-}$*Pten*$^{+/-}$ mice at 6 months of age followed by analysis of the prostate 3 months later, the HGPIN lesions lacked apoptotic cells and were highly proliferative. In addition, AR expression was localised to the cytoplasm (Abate-Shen et al, 2012). In this GEMM, prostate cells seemed to develop androgen independence before the occurrence of overt cancer, thus suggesting that androgen independence can emerge parallel with disease progression rather than as an end-point (Gao et al, 2006b). They also concluded that *Pten* loss-of-function, but not *Nkx3.1* loss-of-function, is sufficient to promote androgen independence (Gao et al, 2006b). *Nkx3.1*^{CreERT2}*Pten*$^{flox/flox}$ a tamoxifen inducible GEMM that mediates *Pten* loss in prostate epithelial cells, develop castration-resistant prostate tumours with virtually no evidence of senescence, in stark contrast to senescence rich non-castrated tumours (Floc'h et al, 2012). This is consistent with the notion that castration resistance promotes cancer progression by bypassing senescence (Irshad et al, 2013). Furthermore, *Pten* inactivation resulted in strong activation of the Akt and Erk mitogen-activated protein kinase (MAPK) pathway (Gao et al, 2006a), and further studies led them to conclude that the combined activation of these two pathways may enable PC cells to defeat androgen deprivation induced apoptosis *in vivo* (Shen et al, 2007).

Work in the Prostate Group at the Beatson Institute focused on identifying novel events that cooperate and/ or synergise with PTEN loss to drive prostate carcinogenesis. Using *PB-Cre4* promoter *Her2* knock in (KI) and *Pten* deletion (*PB-Cre4:Pten*$^{fl/fl}$*Her2*^{KI}*)* a more aggressive prostate cancer phenotype resulted in comparison to the controls *PB-Cre4:Pten*$^{fl/fl}$ with faster (median 355 days versus 465 days, P= 0.0014) and larger growing prostate tumours (5.2 g versus 2.9 g, $P < 0.0001$) but no metastases at autopsy (Ahmad et al, 2013). Treating *PB-Cre4:Pten*$^{fl/fl}$*Her2*^{KI} mice with a MEK inhibitor resulted in significant reduction in tumour bulk with increased apoptosis and cellular senescence (Ahmad et al, 2013). *Pten*$^{fl/+}$*Spry2*$^{+/-}$developed aggressive prostate tumours with lymph node metastases, with evidence of Her2 upregulation and Akt activation. PI3K inhibitor

treatment resulted in reduced proliferation of the prostate tumours and pAkt, EGFR and Her2 expression (Gao et al, 2012).

GEMM with combined deletion of *Pten* and incorporation of genetic manipulation of other tumour suppressor or oncogenes have been very informative at providing molecular insight into more aggressive PC phenotypes. GEMM with conditional inactivation of *p53* alone produced no prostate tumours, whereas combined *p53* and *Pten* loss (*PB-Cre:Pten* $^{lox/lox}$*p53*$^{lox/lox}$) GEMM mice rapidly developed invasive PC at 2 months with lethality by 6 months of age but no metastases (Chen et al, 2005). By disturbing telomerase function in *PB-Cre: Pten*$^{lox/lox}$*p53*$^{lox/lox}$ mice, the phenotype was accelerated resulting in fatal prostate tumours locally invasive to bone (Ding et al, 2012). Zhong et al 2006 showed GEMM with combined *Fgf8b* activation and *Pten* loss strongly cooperate in the induction of prostate adenocarcinoma including metastatic progression, whereas single models with individual genetic defects in isolation did not progress beyond PIN. GEMM with conditional loss of *Pten* and overexpression of *Erg* (*PB-Cre: Pten* $^{lox/lox}$*Rosa-26*$^{lox\text{-}stop\text{-}lox}$*Erg*) develop HGPIN by 2 months with progression to invasive adenocarcinoma by 6 months of age (Chen et al, 2013). Conditionally active *K-Ras* with inducible *Pten* deletion (*Nkx3.1-CreERT2*) resulting in fatal adenocarcinomas with distant metastases but no bone metastases (Tuveson et al, 2004).

None of the available GEMMs display all aspects of human prostate carcinogenesis. Wu et al, (2006) described the Gleason analogous grading system for their novel knock-in mouse prostate adenocarcinoma model, namely PSP-KIMAP. The PSP-KIMAP model developed a spectrum of Gleason grades and scores comparable to human PC. However, transgenic GEMM produce rapid growing tumours which may lack sufficient tumour heterogeneity without the full range of Gleason grade (and therefore score) distribution. As such, GEMM-derived PC can only be classified by crude histological descriptions. Moreover, in contrast to advanced human PC that has a propensity to develop bone metastases, currently no PC GEMM consistently lead to bone metastases (Irshad et al, 2013). They also do not precisely mimic the molecular events of human PC. For example, a significant proportion of clinical PCs do not harbour *PTEN* loss, yet *Pten*^{null} is one of the most frequently used GEMM.

There is also no optimal promoter to drive *Cre* expression. Among the promoters typically used to target the murine prostate, there are significant variations in the timing of their expression pattern, heterogeneity in their expression in the epithelium, their dependency on

androgens or tamoxifen induction (Irshad et al, 2013). *Probasin (Pb)* and *Nkx3.1* promoters are both androgen sensitive and therefore the development of androgen independence may be by different mechanisms than in human PC (Abate-Shen et al, 2012). Furthermore, basal epithelial cells express *Pb* whilst luminal epithelial cells express *Nkx3.1* and it is thought luminal epithelial cells are more responsive to hormone manipulation than basal cells (Roy-Burman et al, 2004).

5.1.1 BRF1- manipulated GEMM

Elevated Pol III transcription has been seen in a variety of human cancers and altered levels of Pol III specific transcription factors are a common feature of mouse and human tumours (reviewed by White, 2004; White et al, 2005). BRF1 is an essential transcription factor for Pol III activity and is a molecular target of regulation by a wide variety of tumour suppressors and oncogene activation (reviewed by White et al, 2004 and 2005). BRF1 expression is higher in patient tumour samples with prostate cancer in comparison to benign prostate. Patients with PC exhibiting high BRF1 IHC scores have poorer survival outcomes, when compared to those with low BRF1 IHC scores (Nam et al, 2013 Unpublished). I have shown that BRF1 is expressed at high levels in PC cell lines, especially in the androgen dependent cell lines, and that transient manipulation of BRF1 expression significantly affected *in vitro* proliferation and cell cycle profile of human PC cell lines. To fully investigate the functional *in vivo* effects of BRF1 in prostate cancer, two transgenic mouse models were developed.

***PbCre*-BRF1hTg$^{het/WT}$**

Transgenic mice utilising the human *BRF1* cDNA is constructed within the *Hprt* gene locus to be under the control of the constitutive CAAGS (*CMV β-actin β-globin*) promoter. A loxP-stop-loxP (LSL) sequence was placed upstream of *BRF1* to drive its conditional overexpression (Figure 5.1). These *LSL-BRF1* mice were crossed with lines with *PB-Cre4* (called PbCre in this study) to induce human BRF1 expression specifically in the prostate epithelium. Mice were born at expected Mendelian ratios. Cohorts were monitored to determine whether BRF1 overexpression in the prostate epithelium was sufficient to drive changes associated with prostate carcinogenesis. Eleven *PbCre-BRF1* mice were aged to 12-14 months and their littermates, including 9 *WT* and 9 *PbCre-*, were their controls. In

addition, a younger cohort of 4-6 months aged mice were studied (8 *PbCre-BRF1* mice, 4 *WT* and 4 *PbCre*-) to confirm that BRF1 was overexpressed, and that there were no microscopic evidence of dysplastic lesions or pre-malignant morphological changes.

***PbCre-Pten$^{fl/fl}$-BRF1*hTg$^{het/WT}$**

LSL-BRF1 transgenic lines were crossed with the *PbCre-Pten$^{fl/fl}$* to generate the *PbCre-Pten$^{fl/fl}$-BRF1*hTg$^{het/WT}$ *(or Pten-Brf1)* mice to see whether elevated BRF1 expression can synergise with Pten loss in the development of prostate cancer. The main control cohort of this GEMM is *PbCre-Pten$^{fl/fl}$* (referred to as *Pten*- thereafter), which has been well characterised by Wang et al 2003 and also by our laboratory, as previously discussed.

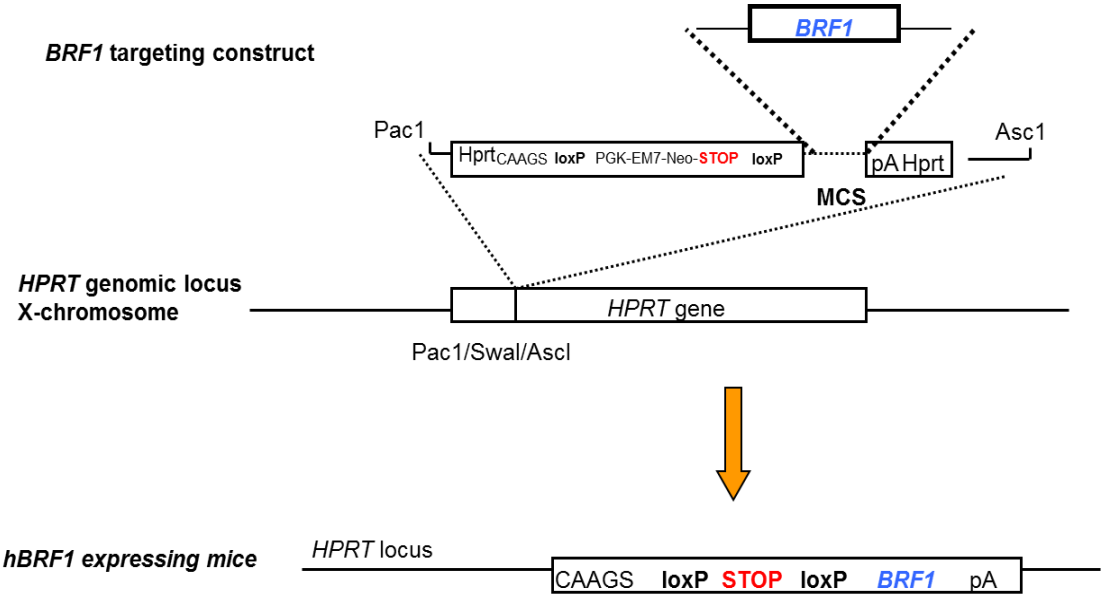

Figure 5-1 Constructing *BRF1* transgenic GEMM (*PbCre-hBRF1Tg* and *PbCrePtenhom-hBRF1Tg*).
Human *BRF1* cDNA is transcribed from constitutive CAAGS promoter after targeting HPRT locus. This construct carries upstream stop codon flanked by loxP sites, allowing us to control where transgenic *BRF1* mRNA is translated. These mice were crossed with *Probasin (Pb) Cre* mice and then expression of *cre recombinase* gene will mediate the excision of this sequence under the control of prostate –specific promoter (Brzezinska et al, 2015) so as to induce *BRF1* specifically in prostate epithelia.

5.2. Results

There is no published data of *BRF1* in a prostate GEMM; this study is therefore the first characterisation of such a GEMM. The following mouse colonies were generated: 14 *PbCre-Brf1*, 12 *PbCre* and 8 *wildtype* (WT) mice were aged to 12-14 months to see whether they developed any signs of prostatic dysplasia or neoplasia. It was thought unlikely that upregulation of *BRF1* alone would be sufficient to drive PC due to the complexity of multiple oncogenic drivers required for prostate carcinogenesis. Consistent with this notion, the *PbCre-Brf1* mice did not develop PIN nor adenocarcinoma, when mice were aged up to 14 months. Neither did the *WT* or *PbCre* control mice develop any early dysplastic lesions or PC phenotypes. However, IHC staining for BRF1 confirmed increased staining in *PbCre-Brf1* mice with strong nuclear staining consistent with the role of BRF1 as a transcription factor (Figure 5.2).

PbCre-Pten $^{fl/fl}$ (called *Pten-* thereafter*)* mice develop invasive adenocarcinoma, and in our lab this GEMM develops prostate tumours after 10 months and does not tend to metastasise. Therefore, we hypothesised that by adding in the human *BRF1*Tg to these mice, *Pten-Brf1,* a more aggressive phenotype may result with earlier invasive prostate tumours and metastases. Two cohorts of mice were set up to investigate this hypothesis. The first cohort of *Pten-* and *Pten-Brf1* mice were monitored for clinical end point and care was taken not to identify the mice genotypes until after they were culled to avoid selective bias. Clinical endpoint was determined when the mice had significantly swollen abdomens that made their mobility compromised. As the tumours were soft and cystic, it was not always clear on palpation whether the mice had tumours or subcutaneous fat. An objective test was therefore performed; if the mouse could no longer squeeze through a cardboard tube due to lower abdomen swelling, it was considered a suitable time to cull the particular mouse.

The second cohort of mice was an age-matched comparison of *Pten-Brf1* with *Pten-* litter mates, mice were aged until tumours became evident and then litter mates were culled to fully characterise the prostate tumours of *Pten-Brf1* mice, and identify any differences with *Pten-* GEMM and to see whether any metastases developed.

Pten-Brf1 GEMM is clinically or phenotypically similar to *Pten-* GEMM, in that, they present with swollen abdomens that grow rapidly within two weeks of first being observed. On post mortem, the tumours were large, usually bilateral, but occasionally unilateral,

cystic tumours filled with serous-like fluid (Figure 5.3). The fluid ranged from watery clear to straw coloured to thick brown paste consistency, and this happened equally in each of the genotypes. The prostate cystic fluid seemed to become darker and more viscous with increasing tumour sizes. On three occasions, enlarged retroperitoneal lymph nodes were noted (twice from *Pten-Brf1* and once from *Pten-* mice), but histology confirmed these were inflammatory and not metastatic in nature, being negative for androgen receptor (AR) IHC and showed no histological features of prostate tissue (data not shown). No other signs of metastasis were noted.

Pten-Brf1 mice grew larger tumours earlier than their *Pten-* litter mates and therefore, reached clinical endpoint earlier. *Pten-Brf1* mice reached clinical endpoint at 256.4 days versus 313.9 days for *Pten-* mice which is statistically significant (t test, $p = 0.000002$). Kaplan-Meier (KM) survival curve analysis was also significantly different between *Pten-Brf1* and *Pten-* mice (log rank test, p value <0.0001; Figures 5.4 and 5.5). The rest of their clinical measurements such as body weight, wet weight and dry weight of tumour at clinical endpoint were all similar, which is reassuring, indicating that the mice were culled at the same clinical end points without any obvious selection bias (Table 5.1). Therefore, increased BRF1 expression appeared to be associated with accelerated *Pten*-driven prostate cancer.

In primary clinical end point analysis on the first mouse cohort, there were 14 *Pten-Brf1* and 12 *Pten-* mice. *Pten-Brf1* mice body weights ranged from 31.5 g- 57.5 g and their tumour wet weights ranged from 1.3 g-7.6 g. *Pten-* mice body weights ranged from 36.9 g- 62.7 g, and their tumour wet weights ranged from 1.0 g- 6.3 g. Three mice from each of *Pten-* and *Pten-Brf1* cohorts that were culled who appeared to have cystic prostate masses, but, on post-mortem, were observed to have small tumours and excessive subcutaneous fat. Therefore, a secondary analysis of clinical endpoint was performed excluding these six mice with small prostate tumours. Three of each genotype were excluded and therefore, secondary analysis of wet weight tumours >3.5g as a new retrospective clinical endpoint including 11 *Pten-Brf1* and 9 *Pten-*. In the *Pten-Brf1* cohort, body weight ranged from 31.5 g- 57.5 g with wet weight tumours of 3.7 g- 7.6 g and *Pten-* mice body weight ranged from 37.6 g- 62.7 g with wet weight tumours of 4.1-6.3g (Table 5.2). The secondary analysis of retrospective clinical analysis also confirmed a statistically significant difference between *Pten-Brf1* and 9 *Pten-* mice, with short time point to observe tumour wet weight reaching 3.5 g in the *Pten-Brf1* group at 267 days versus 307 days (t test, $p = 0.0014$) and KM survival curve log rank $p = 0.0009$ (Figure 5.6).

In the age matched analysis on the second cohort, there were 17 *Pten*- and 14 *Pten-Brf1* mice. They were culled between 7.6 months and 10 months of age. When individual mice were culled for pre-determined signs indicative of prostate tumour, their cage mates were also culled as age matched controls, even when no obvious tumour was palpable. In the *Pten*- mice body weights ranged from 34.40 g- 63.80 g, with tumour wet weights ranging 0.66 g- 4.9 g and tumour dry weights ranging 0.3 g- 1.4 g. In the *Pten-Brf1* mice, the body weights ranged 31.80 g- 58.50 g, with tumour wet weights ranging 1.3 g- 6.6 g and tumour dry weights ranging 0.5 g- 2.3 g. There was a tendency for the *Pten-Brf1* mice to have larger prostate tumours, but the differences in wet and dry weights of tumour did not reach statistical significance (Figures 5.7 and 5.8). None of the mice showed signs of metastases.

Histologically, *Pten-Brf1* and *Pten*- were similar in that they showed signs of HGPIN and invasive carcinoma at 8-11 months (Figure 5.9). There were no obvious differences in histological phenotype. However, this GEMM produces rapidly growing cystic tumours, which are not typically captured in recognised prostate tumour histological scoring systems (Shappell et al, 2004). Further analysis was performed to identify any differences other than speed of tumour growth between *Pten-Brf1* and *Pten*-mice. Firstly, we assessed BRF1 expression protein levels in the mouse tumours by Western blot to ensure that the human transgene expression had remained switched on in the prostate tumours. In *Pten-Brf1* mice, the prostate had relatively higher levels of BRF1 expression (Figure 5.10). IHC analysis confirmed increased BRF1 expression in the epithelium of *Pten-Brf1* mice and further IHC analysis was performed to investigate potential differences between *Pten*- and *Pten-Brf1* tumours (Figures 5.11 and 5.12).

Using an automated scoring system, (Leica®), nuclear immunoreactivity for Ki67, AR, HNF4A and BRF1 were also studied and quantified. This was optimised by manual scoring of three slides, followed by "teaching or priming" of the automated system to register immunoreactivity intensities into relevant cut-offs for negative, weak, moderate and strong staining. Ten random areas of epithelium from 6-7 mice prostate slides of each genotype along with their age-matched controls were analysed (except for HNF4A, when only 3 slides from each mouse genotype were analysed). IHC staining for Ki67 (a marker of cell proliferation) and p63 (a marker of basal cells in the basement membrane – higher levels are found in benign normal prostate tissue and lower levels in adenocarcinoma) were performed as an assessment of the aggressiveness of the prostate tumours (Figure 5.12). Ki67 automated Leica® scoring showed *Pten*- mice had virtually identical intensity of staining to *Pten-Brf1* mice (Figure 5.13).

Manual scoring was carried out for p63, F4/80, NIMP, p21 and GH2AX for 13 *Pten-Brf1* and 14 *Pten-* tumour samples. The genotypes of the slides were not known at the time of scoring to avoid bias. The whole slide was examined and an overall score of high, medium, low and negative intensity was given to the prostate epithelium of each slide (examples of high and low staining shown in Figure 5.18). p63 staining seems to be higher in the *Pten-* mice in that there are slightly more scores of high and medium intensity than the *Pten-Brf1* prostates (Figure 5.14). However, with such low numbers of mice and small differences between the two genotypes, this result is not conclusive and requires further investigation.

Ki67 IHC staining was essentially identical in the two genotypes, there is no evidence to support increased cell proliferation as judged by IHC scoring. However, *Pten-Brf1* mice did reach clinical endpoint significantly earlier than the *Pten-* mice and did tend to have slightly larger tumours in the age-matched cohort. Perhaps at an earlier time point, for example 3-4 months, the prostate from *Pten-Brf1* mice might have higher Ki67 scoring than the prostate from *Pten-Brf1* mice if cell proliferation was switched on earlier, and this difference may be lost as mice from the two groups approaches clinical end point when the cell proliferation becomes less different with the final tumour sizes being essentially the same.

Due to the cystic nature of the prostate tumours and the increasing evidence that inflammation is an important driving force in prostate carcinogenesis (reviewed by De Marzo et al, 2007), a number of inflammatory markers were investigated by IHC. F4/80 is a marker of macrophages and NIMP (Anti-Neutrophil antibody) is a marker of neutrophils and interestingly both tend to have slightly higher IHC staining in the *Pten-* mice rather than the *Pten-Brf1* (Figures 5.15, 5.16 and 5.17). This suggests the *Pten*-mediated tumorigenesis may be associated with inflammatory processes relatively more than in *Pten-Brf1* mice, but due to the low numbers of mice and prostate slides, it is difficult to be conclusive about these results. Further investigation examining the cystic fluid would have been useful, but unfortunately at the time of collection of post-mortem prostate samples, the cystic prostate fluid was not analysed and it was merely noted what colour and consistency the fluid was which seemed to vary more with the size of the tumour rather than mouse genotype. In future, the prostate cystic fluid should be collected and tested by FACS analysis for presence of inflammatory cells and ELISA or proteomic analysis for abundance of cytokines and inflammatory mediators.

Phospho-γH2AX (GH2AX) is a marker of DNA damage and also seemed to have higher IHC staining in the *Pten*- mice than the *Pten-Brf1* (Figures 5.18 and 5.19). p21 a marker of G1 arrest and senescence and had low IHC scoring in both genotypes (Figures 5.18 and 5.20). The potential heightened inflammatory response in the prostate of *Pten*- mice may explain the increase in DNA damage. An altered balance between *Pten-Brf1* GEMM growth signalling pathways versus inflammatory signalling pathways of *Pten*- may result in less DNA damage, with accelerated tumour growth in *Pten-Brf1* mice. To investigate potential effects on apoptosis, IHC for cleaved caspase 3 was also performed however there were very low levels of apoptotic cells detected in either genotype (Figure 5.21).

To further understand the differences between the *Pten*- and *Pten-Brf1* GEMM, RNA sequencing analysis was performed to examine the underlying molecular basis of enhanced prostate tumorigenesis in *Pten-Brf1* mice by comparing the transcriptome of prostate tumours from *Pten-Brf1* mice to age-matched *Pten*- mice. It was hoped that this would provide insight into the molecular events driving prostate tumorigenesis in these two distinct GEMM. RNA extracted from 3 *Pten-Brf1* and 2 age-matched *Pten*- prostate tumours were analysed. The RNA sequencing data generated heat map and GeneGo analysis clearly shows these two GEMMs have distinct RNA expression profiles (Figures 5.22 and 5.23). From this data analysis, a number of interesting genes were shown to be upregulated specifically in the *Pten-Brf1* prostate tumours. This data set was compared with published *BRF1* ChIP sequencing data (Canella et al, 2010) to see whether there were any mutually upregulated genes. Hepatocyte nuclear factor 4 alpha (HNF4α) was upregulated in both our RNA microarray *Pten-Brf1* prostate tumours and *BRF1* ChIP sequence data, and therefore was considered a BRF1-target gene in prostate tumourigenesis and further investigated using Western blot analysis and IHC staining of mouse prostate tumours (Figures 5.24 and 5.25).

HNF4α is located on chromosome 20q13.12. It is a member of the steroid hormone nuclear receptor family of transcription factors (Odom et al, 2004). It regulates genes with functional roles in hepatic gluconeogenesis and lipid metabolism (summary by Chandra et al, 2013). Mutations of *HNF4α* have been implicated in the pathogenesis of non-insulin dependent diabetes mellitus (NIDDM) and maturity onset diabetes of young (MODY type 1) (Furuta et al, 1997). HNF4α with transcription factors Foxa1, Foxa2 or Foxa3 were able to transform mouse embryonic and adult fibroblasts into cells morphologically similar to hepatocytes *in vitro* (Sekiya and Suzuki, 2011). There are currently no known functions for HNF4α in prostate glands, but FOXA1 expression has been shown to be increased in

PC, especially in advanced disease (Feng et al, 2015). FOXA1 is a pioneering transcription factor involved in chromatin remodelling which allows AR to have genomic access at specific loci in prostate epithelial cells (Ya et al, 2015). Recently, HNF4α has been shown to have a similar function to FOXA1, in that HNF4α is constitutively bound to chromatin and guides AR to specific genomic loci upon hormone exposure in mouse kidney (Pihlajamaa et al, 2014).

We therefore hypothesised that BRF1 driven HNF4α expression could play a role in regulation of prostate tumorigenesis. Western blot analysis of prostate mouse tumours showed BRF1 was overexpressed in *Pten-Brf1* as expected. AR also appeared to have higher expression in the *Pten-Brf1* mice in comparison to the *Pten-*, whereas HNF4α expression seemed to be lower in *Pten-Brf1*. However, the HSP-70 loading control was variable between the prostate samples and therefore, conclusions are difficult to make (Figure 5.24).

Automated *Leica*® IHC scoring for AR immunoreactivity of 6 mouse prostates per genotype showed that AR had higher intensity scoring in *Pten-Brf1* mice versus *Pten-* whereas HNF4α had slightly higher intensity scoring in the *Pten-* mice (Figures 5.25, 5.26 and 5.27). This indicates that HNF4α mRNA levels may be uncoupled from protein levels and that increased BRF1 does not increase HNF4α in this model of prostate cancer. We also analysed the protein expression of AR, HNF4α and c-MYC in our stable PC3 cells with BRF1 overexpression. BRF1 overexpression does not correlate with increases in HNF4α nor c-MYC expression. Surprisingly, AR expression appeared to be elevated in presence of BRF1 overexpression. This is most interesting because PC3 cells do not normally express AR and requires further urgent investigation (Figure 5.28).

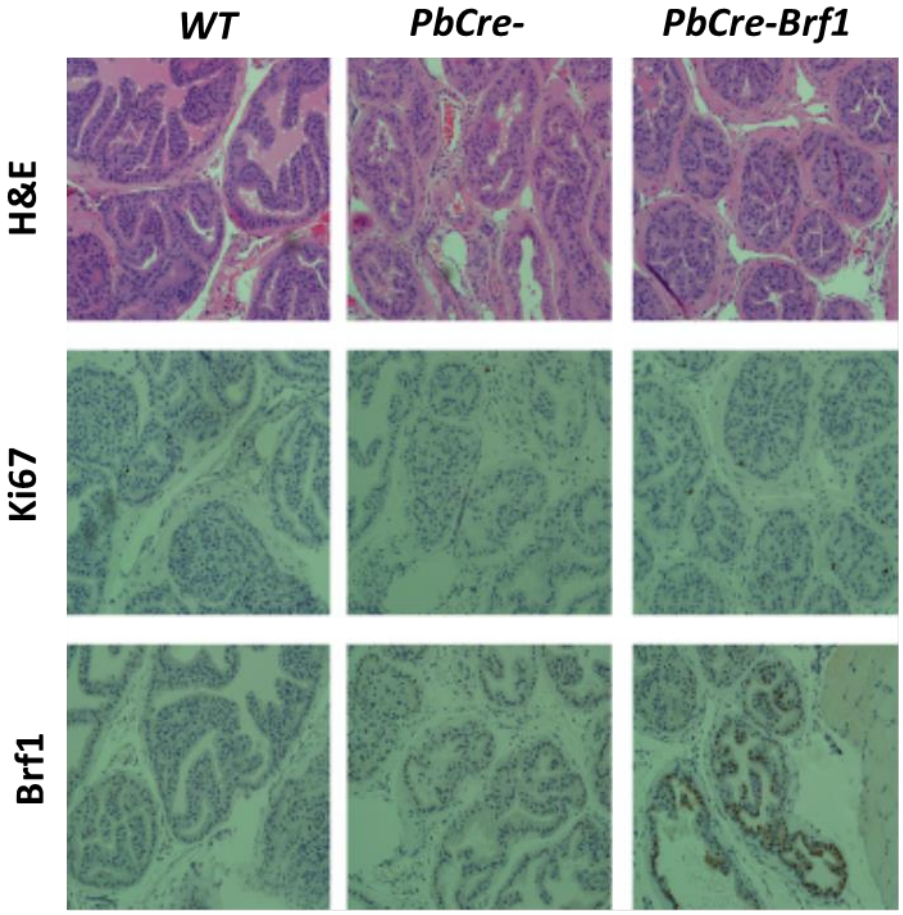

Figure 5-2 IHC of *WT*, *PbCre* and *PbCre-Brf1 GEMM.*
Mice were aged up to 14 months and no mice developed clinical signs of prostate tumours and histologically no evidence of any dysplastic or neoplastic changes in the control mice (*WT* and *PbCre*-) and the BRF1 over-expressing mice (*PbCre-Brf1*). BRF1 IHC staining is higher in the *PbCre-Brf1* mice and therefore this GEMM is valid. (20x magnification).

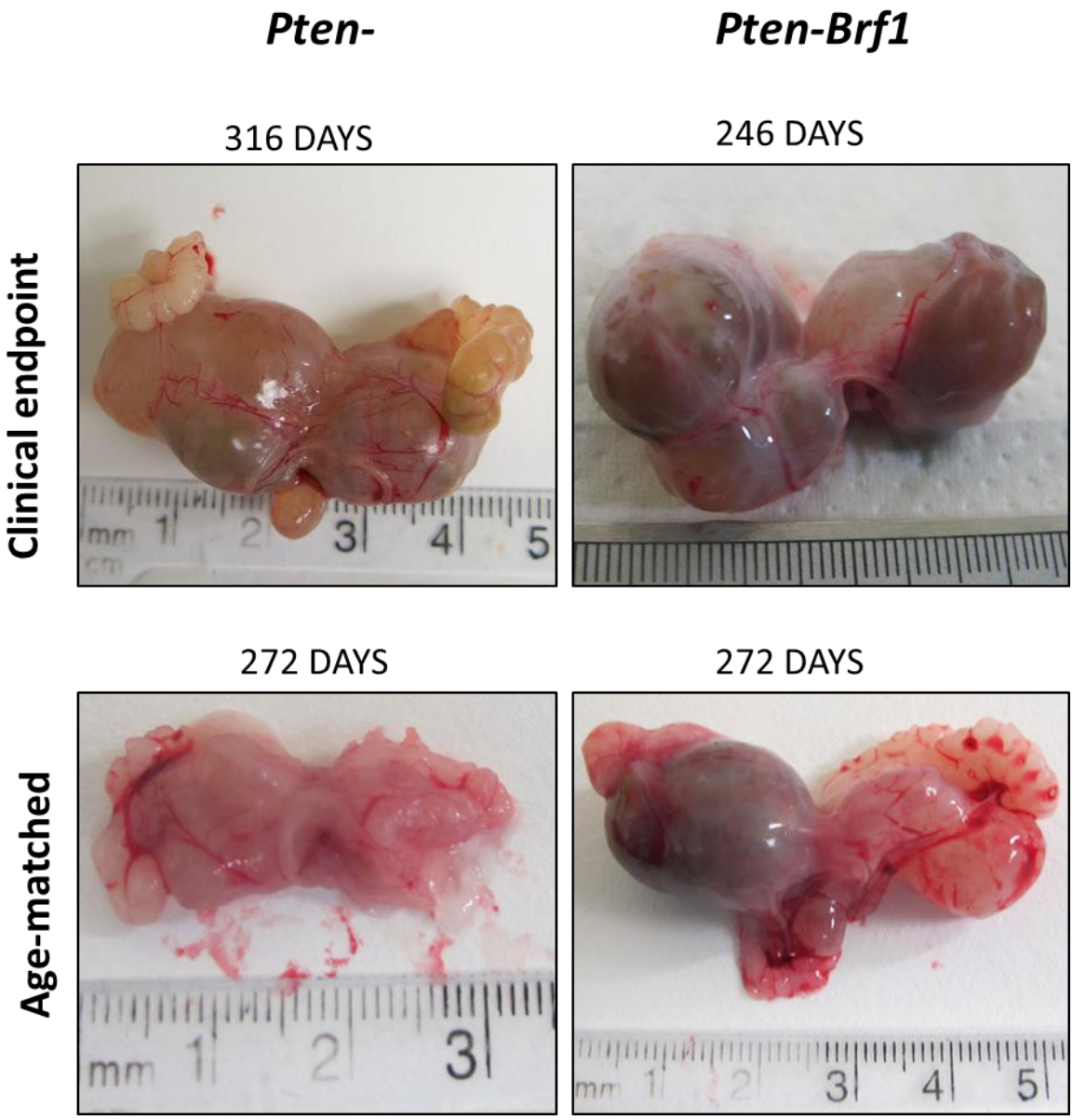

Figure 5-3 *Pten* and *Pten-Brf1* are phenotypically similar.
Pten- and *Pten-Brf1* both develop large cystic tumours. *Pten-Brf1* prostate tumours grow more rapidly. *Pten-Brf1* mice tend to develop larger tumours than their age-matched *Pten*- litter mates but this did not reach statistical significance. Images are of representative prostates along with the age of the individual mice at the time of sacrifice.

	Pten- (n = 12)		*Pten-Brf1* (n=14)	
Days alive	**313.9**	(255- 342)	**256.4**	(227- 275)
Bodywt (g)	**47.4**	(36.9- 62.7)	**45.6**	(31.5- 57.5)
Tumour (WW) (g)	**3.8**	(1.0- 6.3)	**3.8**	(1.3- 7.6)
Tumour (DW) (g)	**1.1**	(0.4- 1.9)	**1.1**	(0.5- 2.2)
WW/ Bodywt	**0.08**	(0.02- 0.15)	**0.09**	(0.03- 0.21)
DW / Bodywt	**0.02**	(0.01- 0.04)	**0.02**	(0.01- 0.06)

Table 5-1 Table of primary end point cohort mice clinical measurements
Pten-Brf1 and *Pten-* mice were culled when they developed clinically significant swollen abdomens in keeping with significant prostate tumour formation. On clinical examination if they could no longer squeeze through a cardboard tube and had an abdominal mass on palpation they were culled. The *Pten-Brf1* mice were culled significantly earlier than the *Pten-* mice ($p = 0.000002$). The post-mortem measurements of bodyweight and the prostate tumour's wet weight (WW) and dry weight (DW) were similar between the *Pten-Brf1* and *Pten-* mice.
(Means are in bold. Values in brackets are range of measurements within each cohort).

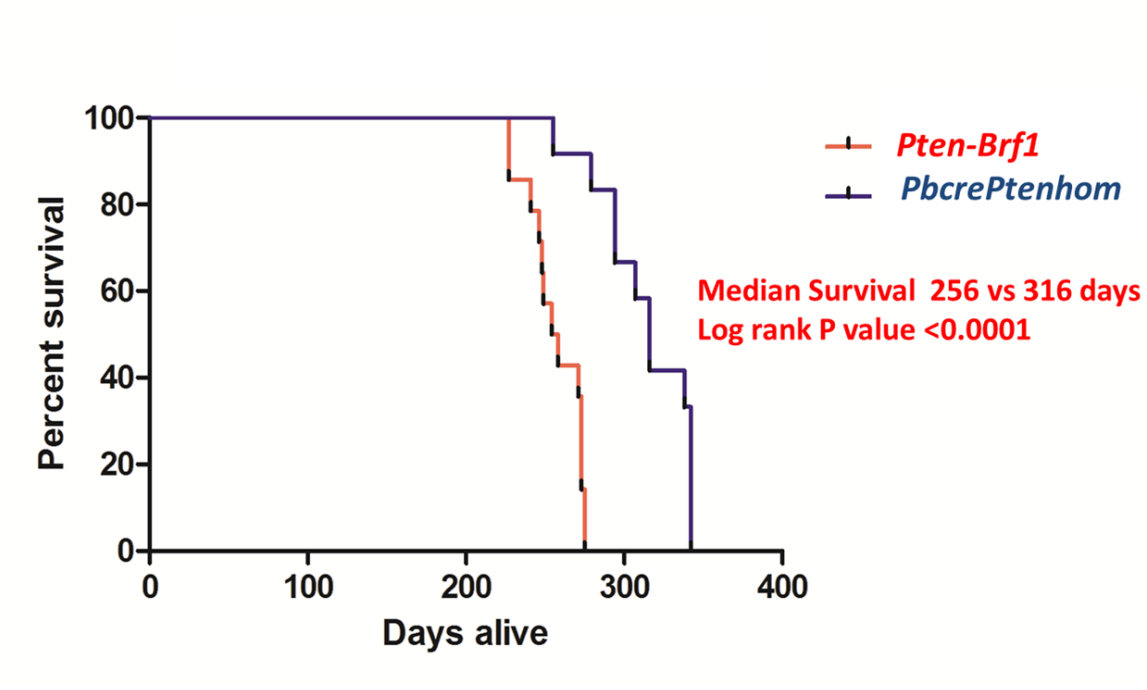

Figure 5-4 Kaplan-Meier (KM) curve of primary end point cohort mice
Pten-Brf1 mice had significantly shorter survival than the *Pten*- mice, 256 days versus 316 days respectively. Log rank, p <0.0001.

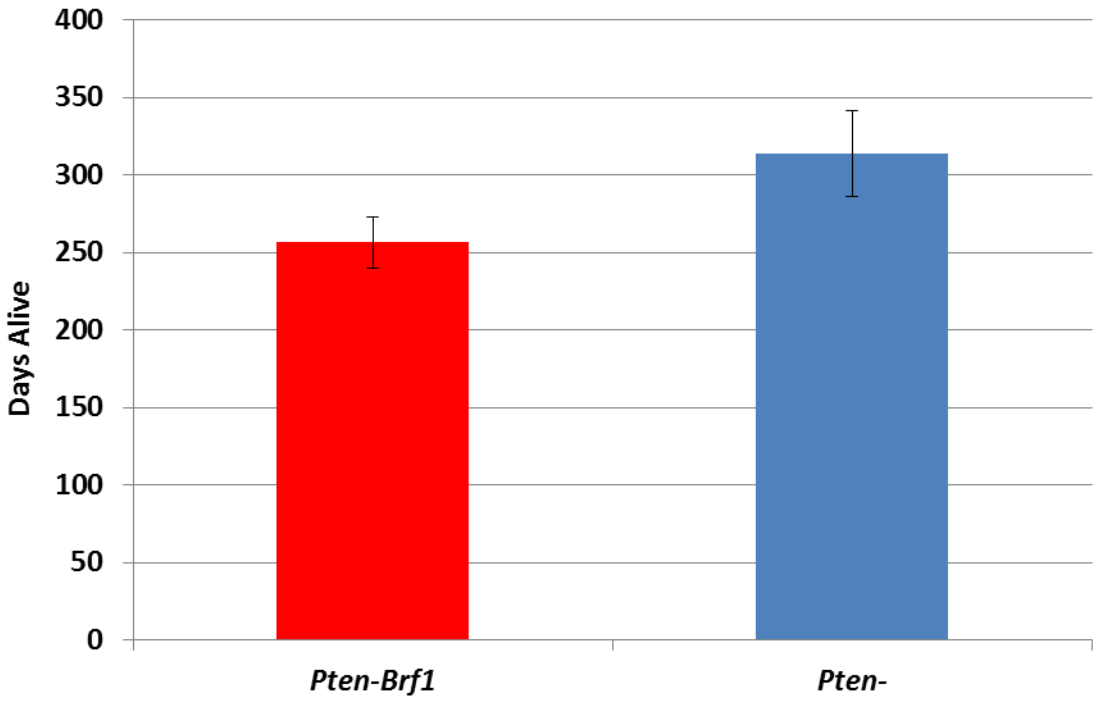

Figure 5-5 *Pten-Brf1* mice reach primary clinical endpoint sooner than *Pten*- mice.
Pten-Brf1 mice were culled at 256.4 days on average versus 313.9 days for *Pten*- mice (2-tailed 2-sample equal variance student t test, p = 0.000002). Primary clinical end point was swollen abdomens reducing mice agility. Means and SD error bars shown.

	Pten- (n = 9)		*Pten-Brf1* (n=11)	
Days alive	**307**	(255- 342)	**267**	(246- 275)
Bodywt (g)	**46.7**	(37.6- 62.7)	**45.6**	(31.5- 57.5)
Tumour (WW) (g)	**5.0**	(4.1- 6.3)	**5.4**	(3.7- 7.6)
Tumour (DW) (g)	**1.46**	(0.8- 1.9)	**1.53**	(0.9- 2.2)
WW/ Bodywt	**0.11**	(0.08- 0.15)	**0.123**	(0.08- 0.21)
DW / Bodywt	**0.032**	(0.02- 0.04)	**0.035**	(0.02- 0.06)

Table 5-2 Table of secondary analysis of clinical end point (prostate tumours > 3.5g wet weight on post mortem).
Pten-Brf1 mice reached retrospective clinical endpoint >3.5 g wet weight of tumours before the *Pten*- mice (t test, p = 0.0014). Three mice from each genotype were excluded in the secondary end point analysis as they were culled prematurely with small prostate tumours but large fat abdomens. (Means shown in bold. In brackets are the range of measurements within each cohort).

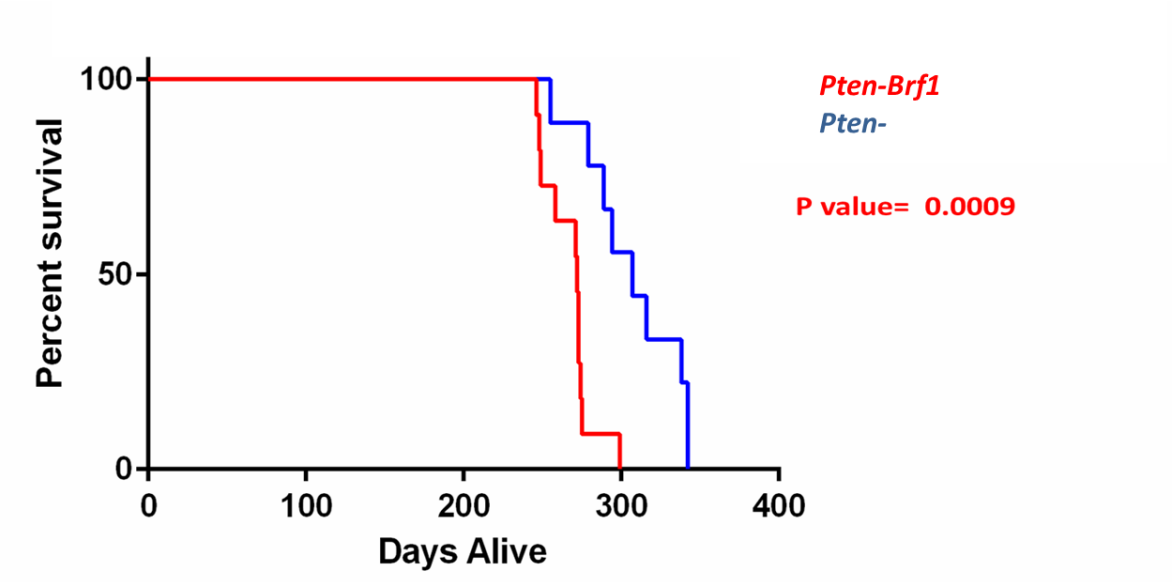

Figure 5-6 KM survival curve of secondary clinical end point cohort mice (prostate tumours > 3.5g wet weight on post mortem).
Pten-Brf1 mice had significantly shorter survival than the *Pten*- control mice, 267 days versus 307 days, Log rank p = 0.0009).

	Pten- (n=17)		Pten-Brf1 (n=14)		T test (p =)
Days alive	**270.9**	(227- 299)	**271.1**	(227- 299)	
Bodywt (g)	**43.7**	(34.4- 63.8)	**45.7**	(36.0- 58.5)	
Tumour (WW) (g)	**1.83**	(0.66- 4.9)	**2.75**	(1.3- 6.6)	**0.096**
Tumour (DW) (g)	**0.65**	(0.3- 1.4)	**1.0**	(0.5- 2.3)	**0.054**
WW/ Bodywt	**0.04**	(0.01- 0.1)	**0.06**	(0.03- 0.131)	**0.120**
DW / Bodywt	**0.02**	(0.01- 0.034)	**0.02**	(0.01- 0.054)	**0.084**

Table 5-3 Table of age-matched cohort of *Pten-Brf1* and *Pten-* mice clinical measurements
Pten-Brf1 mice have a tendency to have larger prostate tumours in both wet weight (WW) and dry weight (DW) measurements but this difference did not reach statistical significance. (Means are in bold and range of measurements are in brackets).

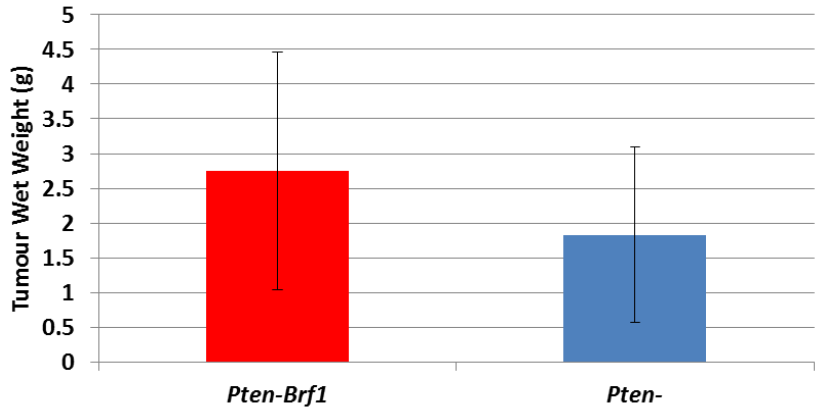

Figure 5-7 Wet weight of prostate tumours of *Pten-Brf1* and *Pten-* mice are not significantly different in age-matched cohort.
Means and SDs are shown.

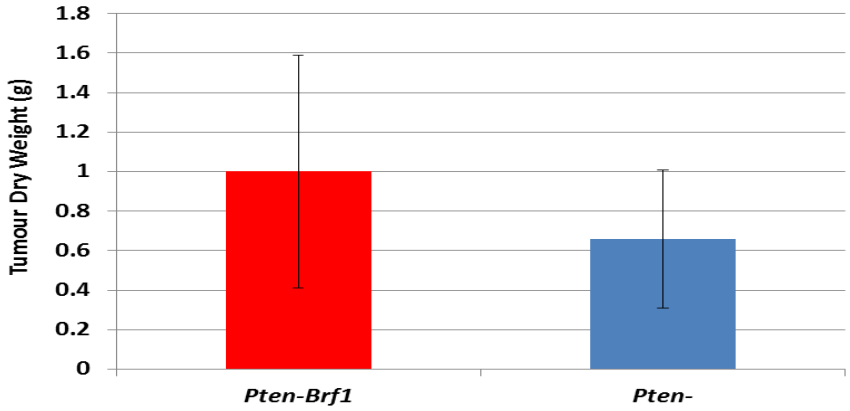

Figure 5-8 Dry weight of prostate tumours of *Pten-Brf1* and *Pten-* mice are not significantly different in the age-matched cohort.
Means and SDs are shown.

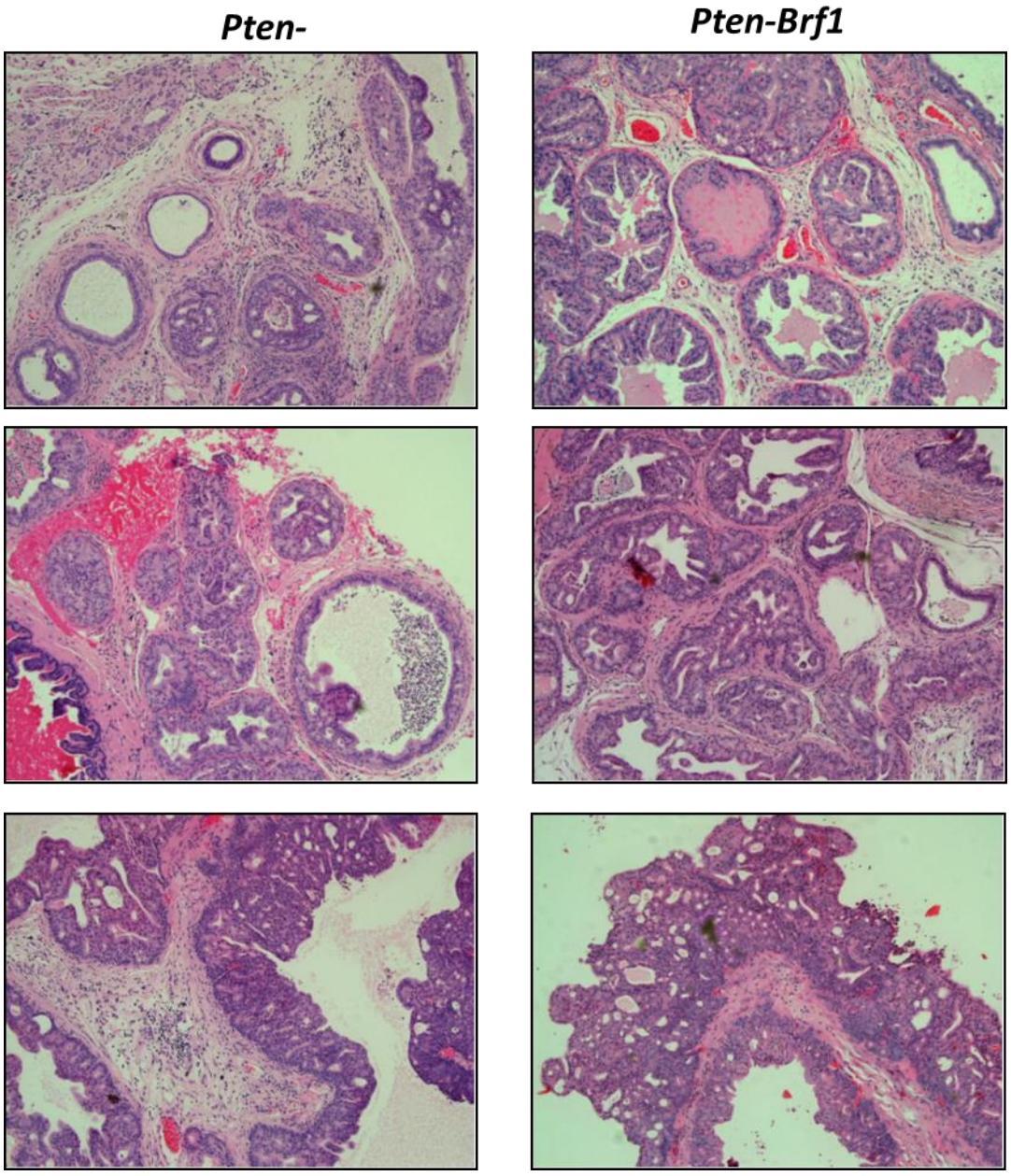

Figure 5-9 Histology of *Pten-* and *Pten-Brf1* mice appear similar.
The above images (20x magnification) are examples of images demonstrating similar histology found in prostates from the genotypes of *Pten- and Pten-Brf1*, and within the same mouse prostate. All the mice with prostate tumours had evidence of HGPIN and invasive carcinoma. There were no distinct differences in their histology
Top images: Areas of well differentiated single separate uniform glands closely packed but with definite boundaries and HGPIN where the lumen is filled in with cellular growth.
Middle images: Ducts have merged together which is a sign of basement membrane disruption and therefore invasive carcinoma.
Bottom images: Invasive carcinoma with non-glandular poorly differentiated cribriform masses with ragged invading edges.

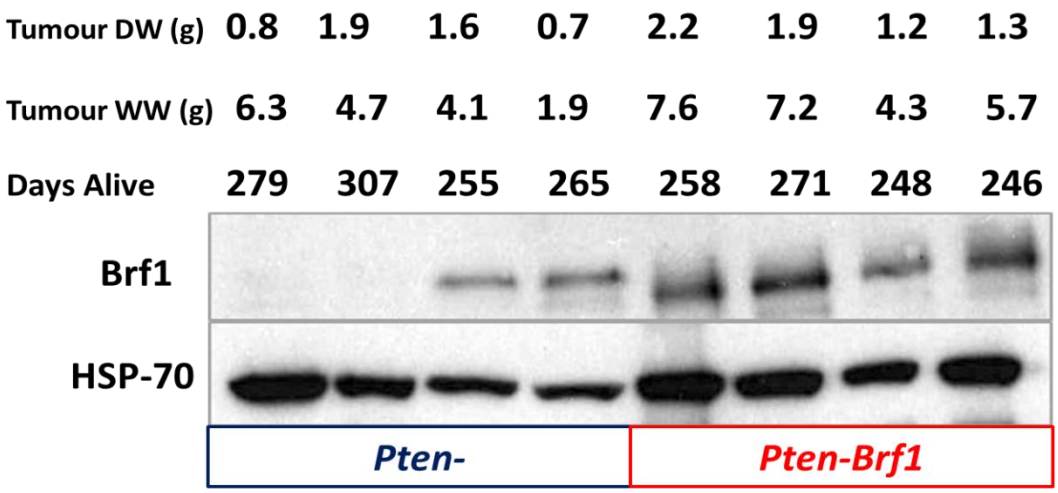

Figure 5-10 *Pten-Brf1* mice have higher expression of BRF1 protein than *Pten-* mice.
BRF1 expression does not appear to be influenced by tumour wet weight, dry weight nor age of mice. HSP-70 was used as a loading control. Four prostate tumours from each mouse genotype were analysed, with each mouse's individual clinical/tumour data shown.

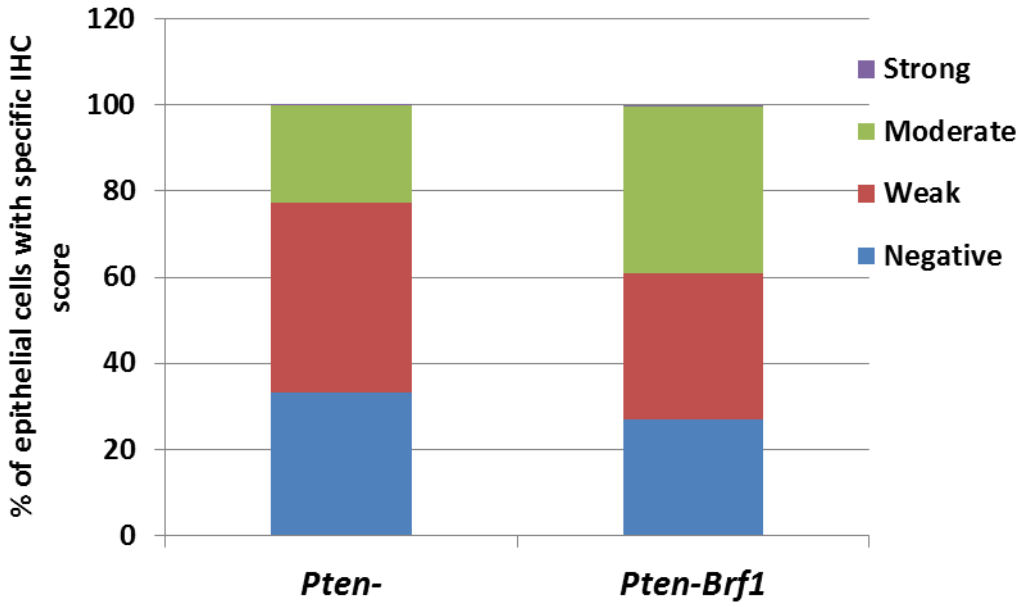

Figure 5-11 IHC BRF1 scoring appears higher in *Pten-Brf1* mice than *Pten-* mice.
Leica® automated scoring program was used. N=7 mice prostate tumour samples from each genotype.

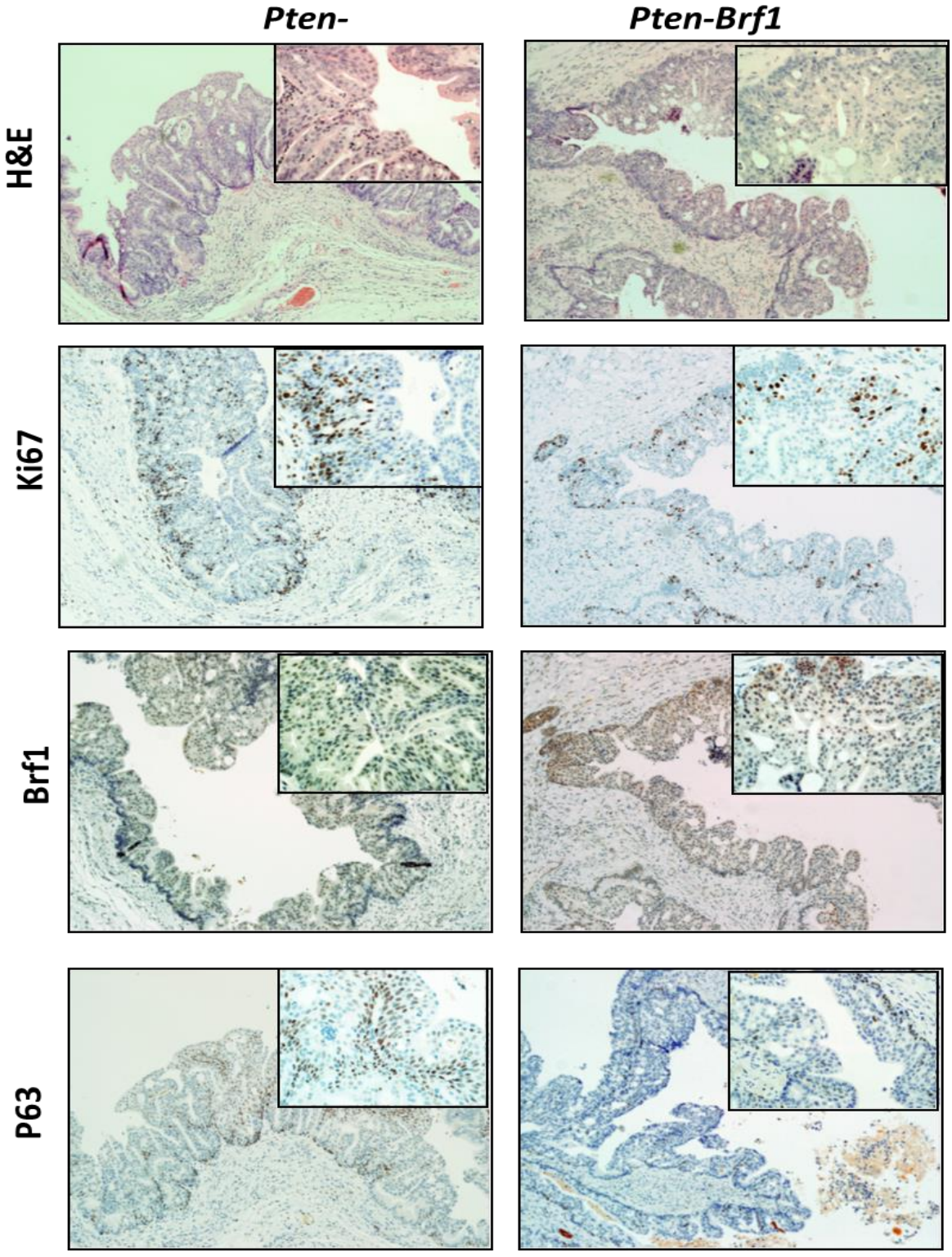

Figure 5-12 IHC staining of Ki67, BRF1 and p63 in *Pten-* and *Pten-Brf1* mice.
The *Pten-* and *Pten-Brf1* prostate slides shown are representative of their respective genotypes and age matched (Large image = 10x magnification, small image/insert = 40x magnification).

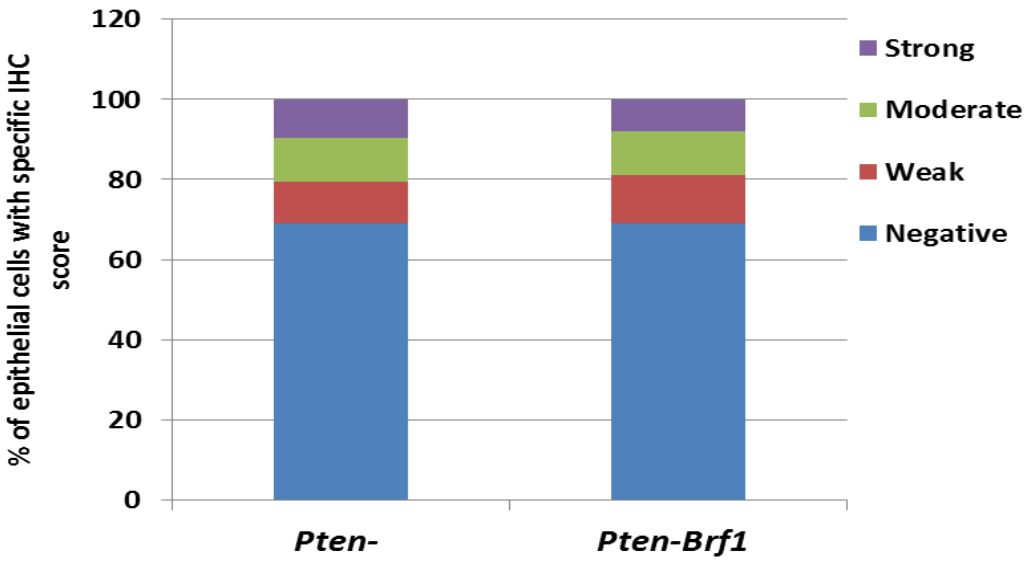

Figure 5-13 Ki67 IHC automated scoring is very similar in *Pten-* and *Pten-Brf1* mice.
Ki67 is marker of cell proliferation. (N=7 of each mouse genotype).

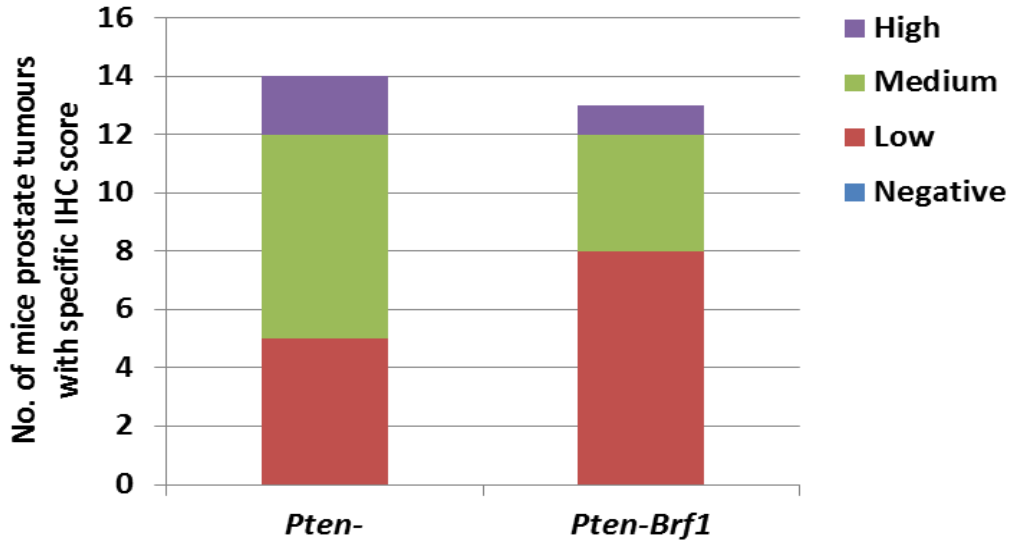

Figure 5-14 p63 IHC manual scoring appears higher in *Pten-* than in *Pten-Brf1* tumour samples.
p63 staining is a basal cell marker. There are more *Pten* slides scored as high or medium than the *Pten-Brf1* mice. However, due to low number of mice and slides scored these results are not conclusive.

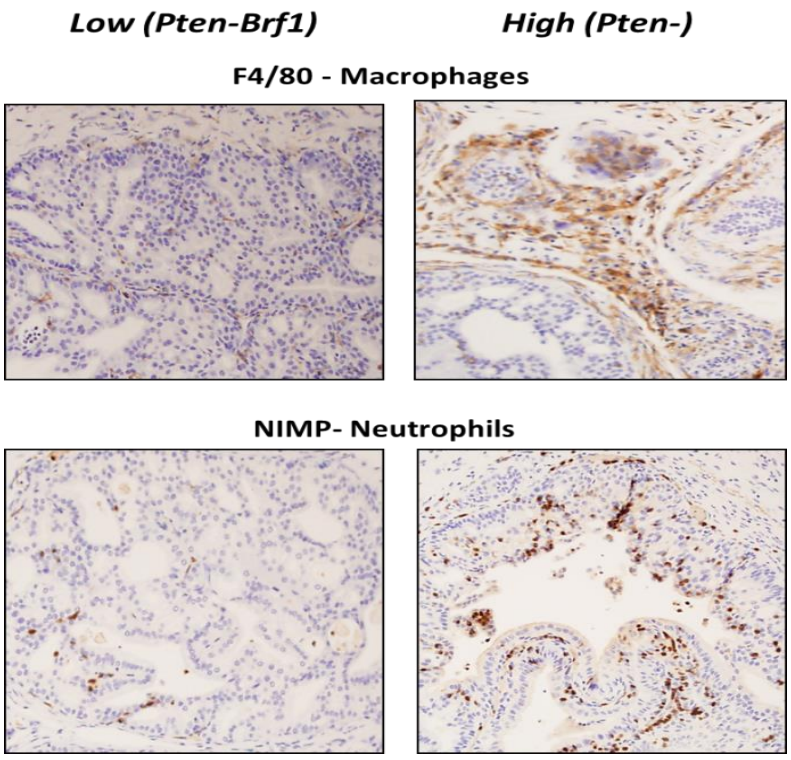

Figure 5-15 F4/80 and NIMP IHC staining is higher in *Pten*- than *Pten-Brf1* tumour samples. F4/80 is a marker of macrophages. NIMP is a marker of neutrophils. Here are examples of high and low IHC scoring. In the slides shown the low scoring slide is from a *Pten-Brf1* mouse prostate and the high IHC scoring slide is from a *Pten*- mouse. However, both genotypes had mice with low and high IHC scoring but more of the *Pten*- mice had high IHC scoring than the *Pten-Brf1* for F4/80 and NIMP IHC staining. (20x magnification).

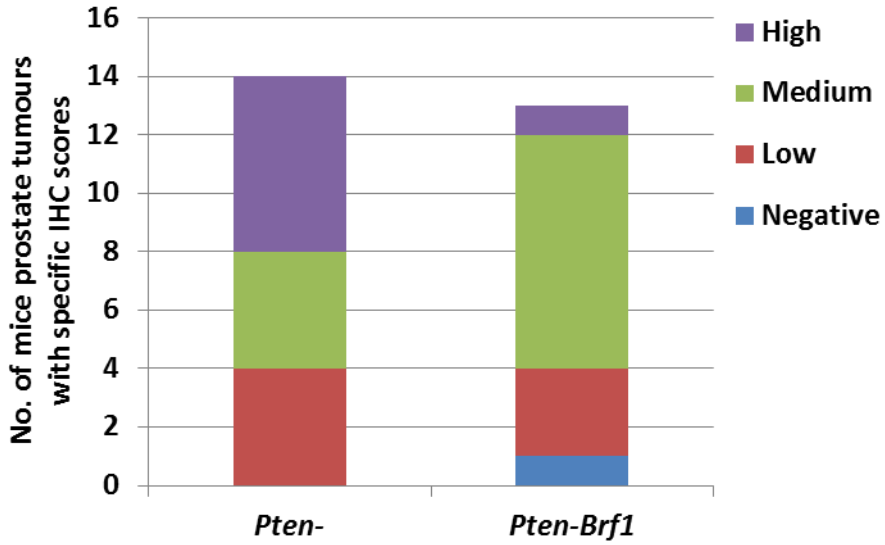

Figure 5-16 F4/80 IHC scoring appears higher in the *Pten*- than the *Pten-Brf1* tumour samples.

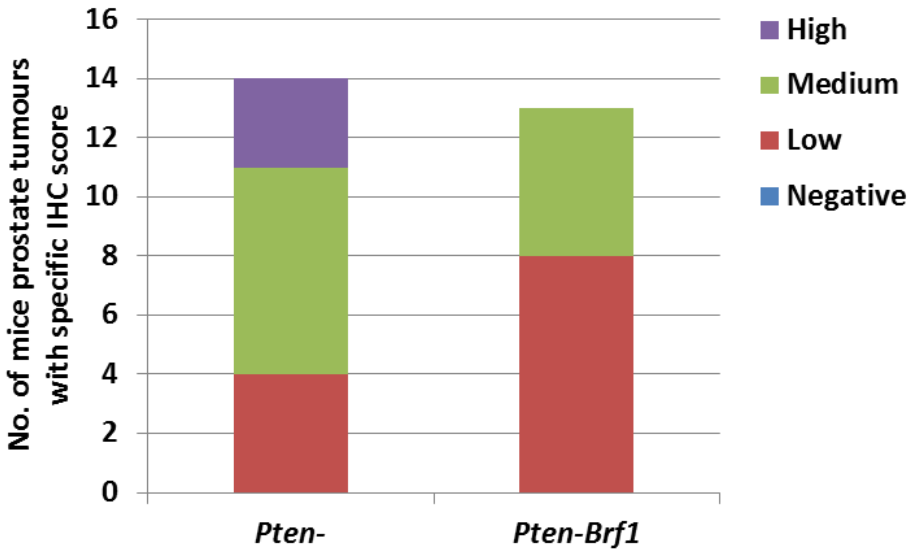

Figure 5-17 NIMP IHC scoring appears higher in the *Pten-* tumour samples than the *Pten-Brf1* tumours.

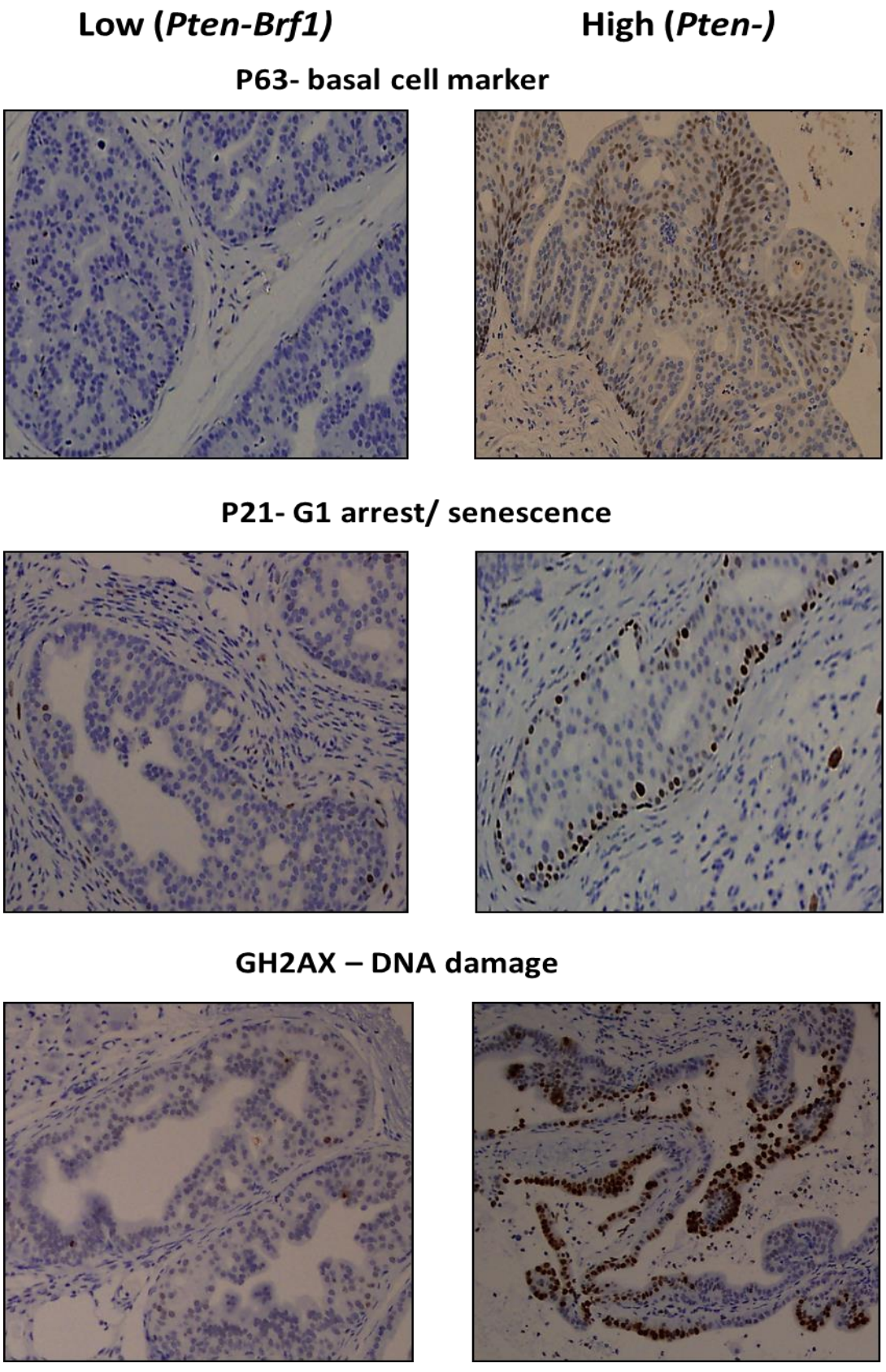

Figure 5-18 Manual scoring guide to IHC staining of p63, p21 and GH2AX
These images show examples of high and low scoring for the IHC staining of p63, p21 and GH2AX. A medium score would have had staining intensity in the middle of a low and high score. The images shown are from one *Pten-Brf1* mouse prostate tumour sample that had low IHC scoring and one *Pten*- tumour that had high scoring. Both genotypes had tumour samples with varied IHC scoring. (20X magnification).

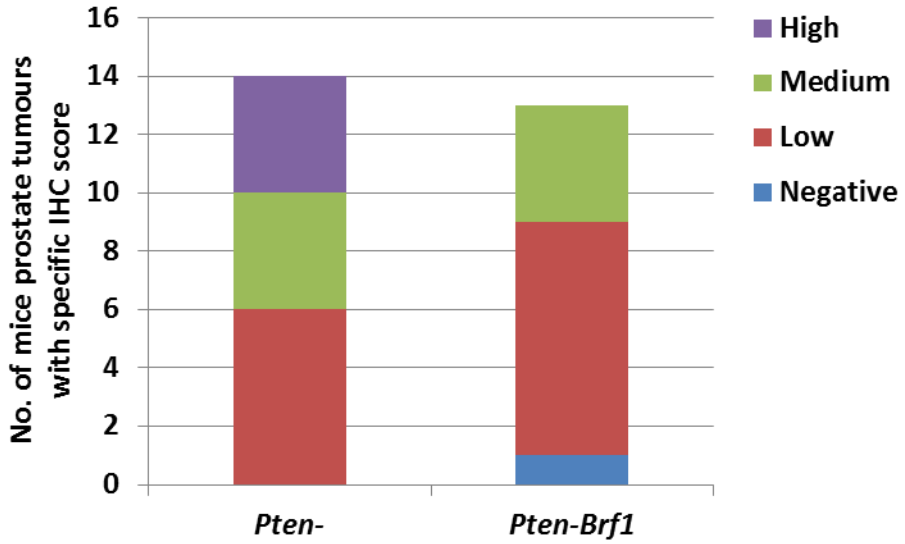

Figure 5-19 GH2AX appears to have higher IHC scoring in *Pten-* than *Pten-Brf1* mice.
GH2AX is a marker of DNA damage.

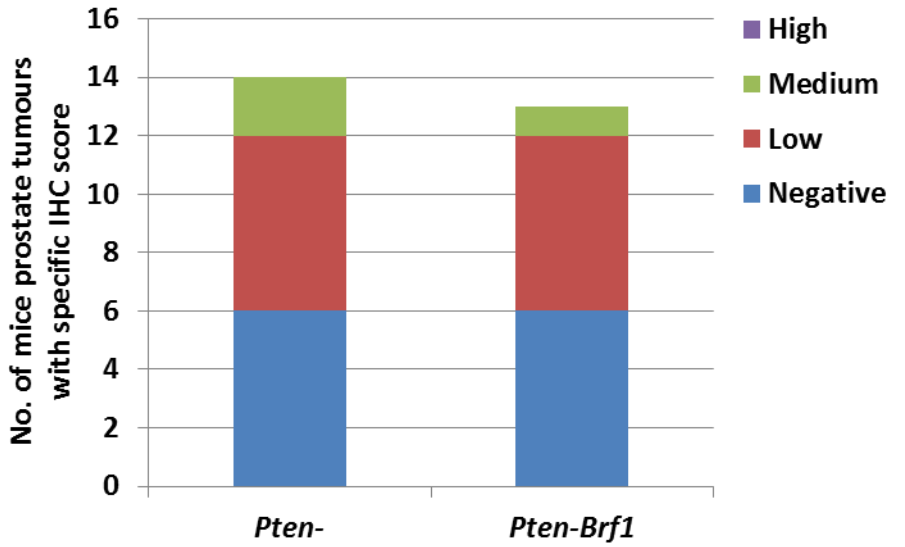

Figure 5-20 p21 IHC manual scoring is low in both *Pten-* and *Pten-Brf1* mice.
p21 is a marker of cell cycle G1 arrest and senescence. Both the *Pten-* and *Pten-Brf1* have very low levels of p21 IHC staining.

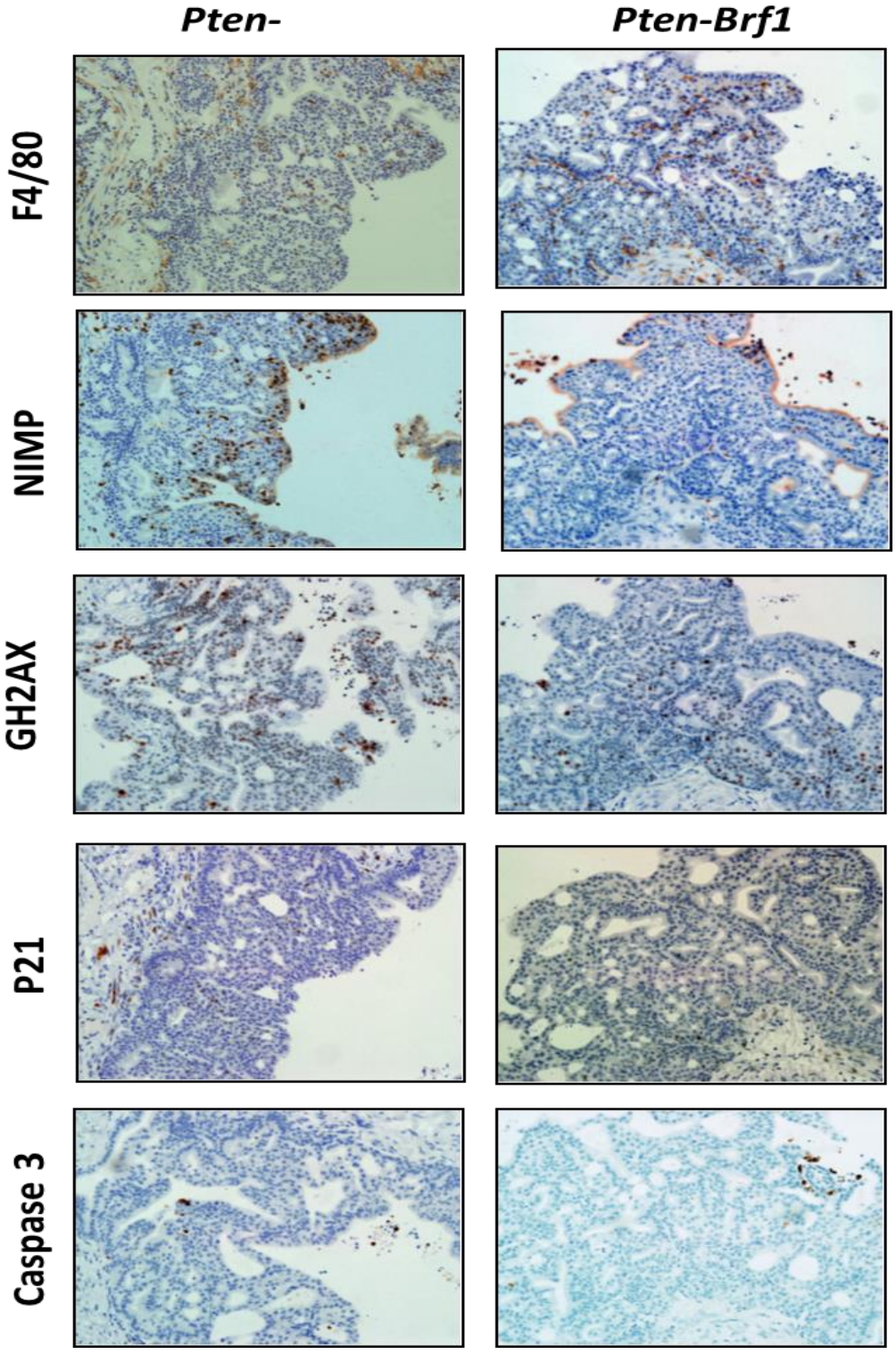

Figure 5-21 Age matched *Pten- and Pten-Brf1* mouse IHC staining.
Caspase 3 was also used for IHC staining for 5 slides for each genotype but this had either low or negative IHC scoring for all 10 slides so was not formally scored (20x magnification).

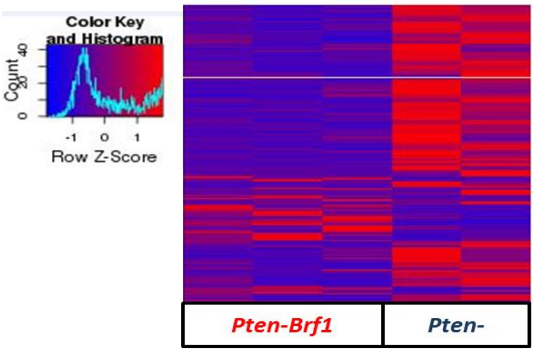

Figure 5-22 RNA sequencing heat map of prostate mouse tumours
Pten-Brf1 (n=3) and *Pten-* (n=2). Red means overexpressed and blue means low expression. It is clear from this heat map that RNA expression is very different between the two mice genotypes despite their prostate tumours looking phenotypically similar.

MOLECULAR PROCESSES	No. of genes differentially expressed in my data set / Total no. of genes known to be associated with these processes as characterised by Gene Ontology Consortium	FDR (False Discovery Rate)
response to wounding	124 / 1450	2.53×10^{40}
cell adhesion	97 / 1015	1.97×10^{34}
biological adhesion	97 / 1026	3.26×10^{34}
immune system process	151 / 2697	3.74×10^{29}
extracellular matrix organisation	61 / 471	7.94×10^{28}
extracellular structure organisation	61 / 472	7.94×10^{28}
response to external stimulus	143 / 2559	2.50×10^{27}
inflammatory response	68 / 621	5.15×10^{27}
wound healing	77 / 857	2.82×10^{25}
cell chemotaxis	40 / 199	3.85×10^{25}

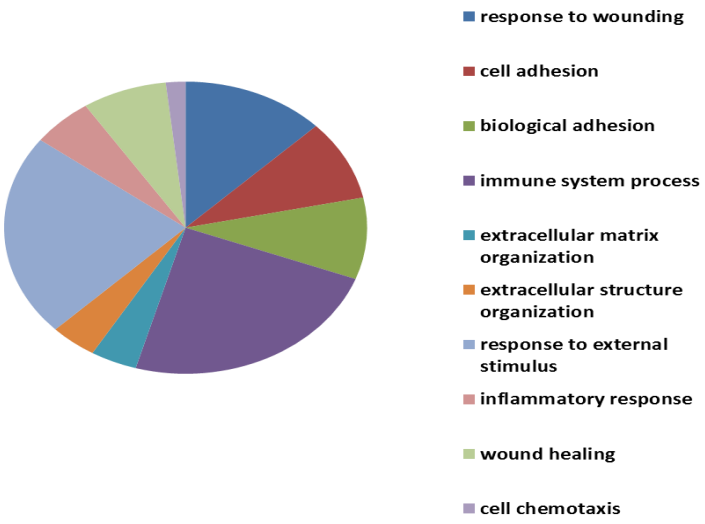

Figure 5-23 RNA sequencing pathway enrichment analysis
Using GeneGo data analysis the RNA expression profile of *Pten-Brf1* can be divided into pathway drivers for a variety of cell functions and physiological processes. FDR (false discovery rate) gives a P value that adjusts for multiple testing and shows that the differences in *Pten-Brf1* prostate tumours for genes expressed in these molecular pathways is significantly different from *Pten-* tumours. From here we were able to pick individual genes for further investigation that were expressed significantly different between the two GEMMs.

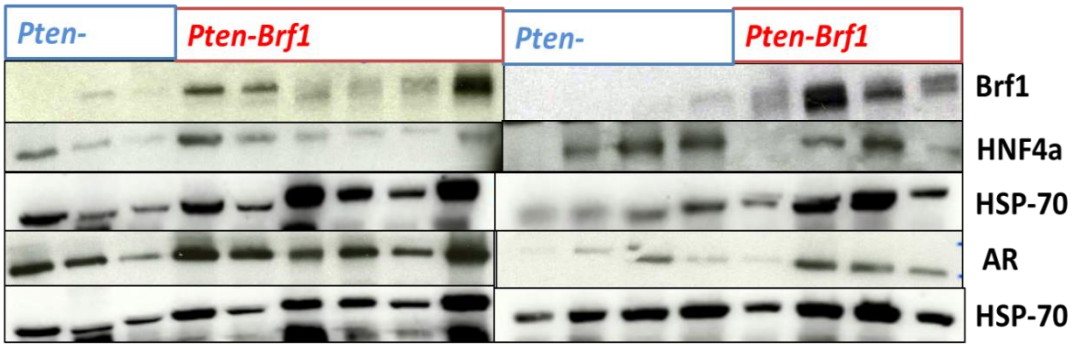

Figure 5-24 Western blot analysis of prostate mouse tumours showing BRF1, AR and HNF4α expression

AR expression appears to have slightly higher levels in the *Pten-Brf1* mice versus the *Pten-mice.* HNF4a seems to have higher expression in the *Pten-* mice versus the *Pten-Brf1*. However, as HSP-70 loading control is not equal between all the samples these results are not conclusive. Brf1 and HNF4a were analysed on the same blot and therefore share the same HSP-70 loading control.

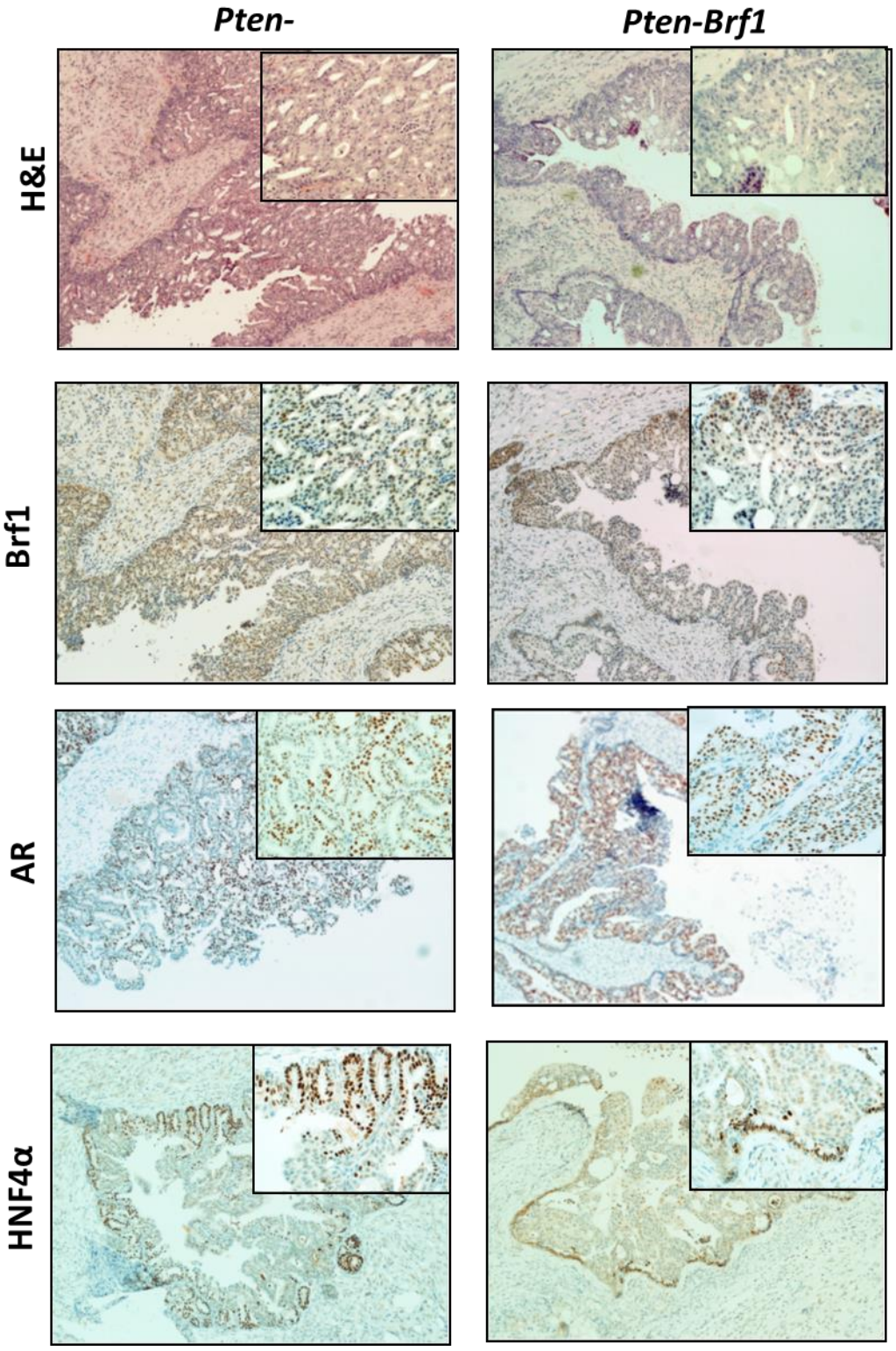

Figure 5-25 H&E and IHC of BRF1, AR and HNF4α in *Pten-* and *Pten-Brf1*
AR IHC staining appears to be of higher intensity in *Pten-Brf1* than *Pten-*, whereas, HNF4α appears to be slightly higher in *Pten-* mice. (H&E and Brf1 images are the same as shown in figure 5-12).
(Large image 10x magnification. Small image 40x magnification).

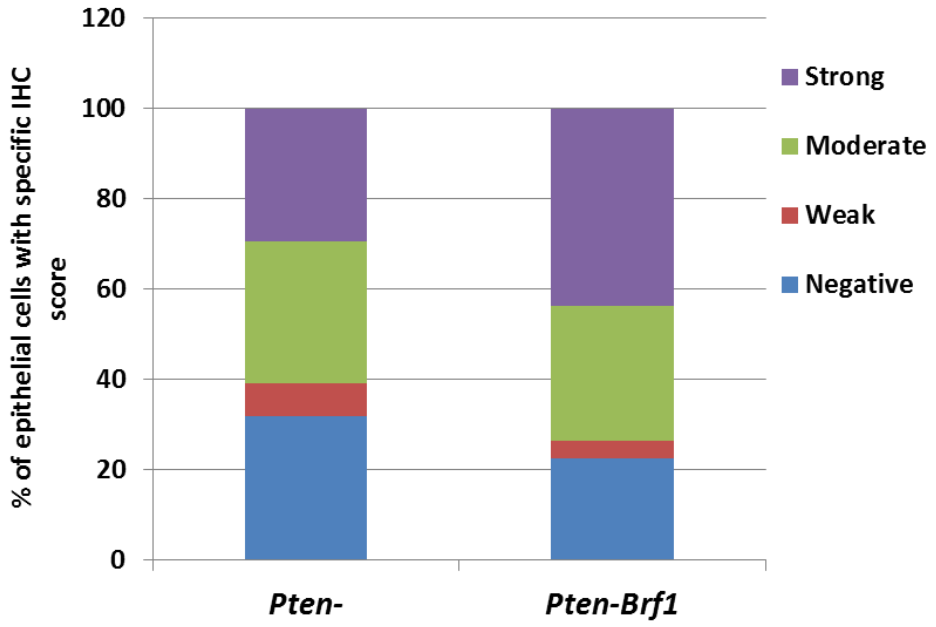

Figure 5-26 AR IHC automated scoring appears higher in *Pten-Brf1* than *Pten-* mice.
Leica® IHC scoring program was used. N= 6 mice prostate tumours per genotype.

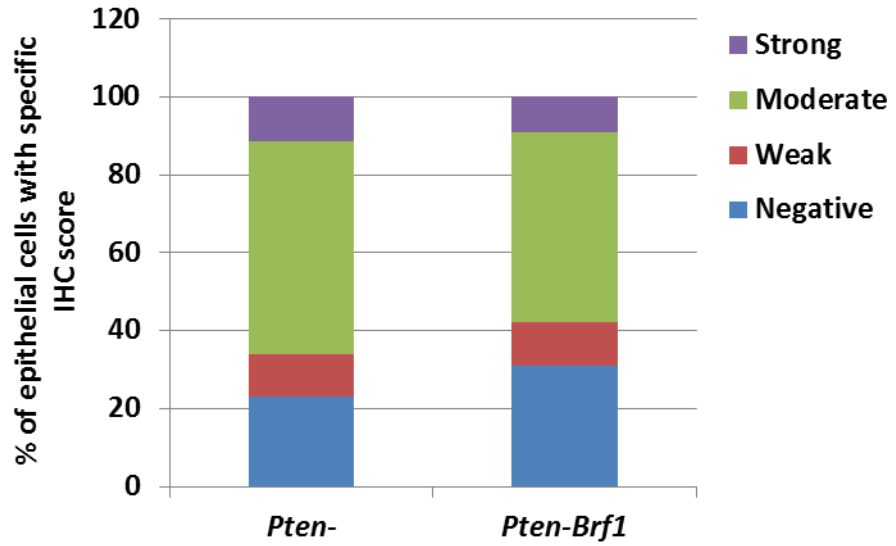

Figure 5-27 HNF4α IHC automated scoring is similar in *Pten-* and *Pten-Brf1* mice.
Leica® IHC scoring program was used. There is a slight increase in the positive scoring of *Pten-* over *Pten-Brf1* samples but no conclusions can be made due to only 3 prostate samples from each genotype being stained and scored for HNF4α.

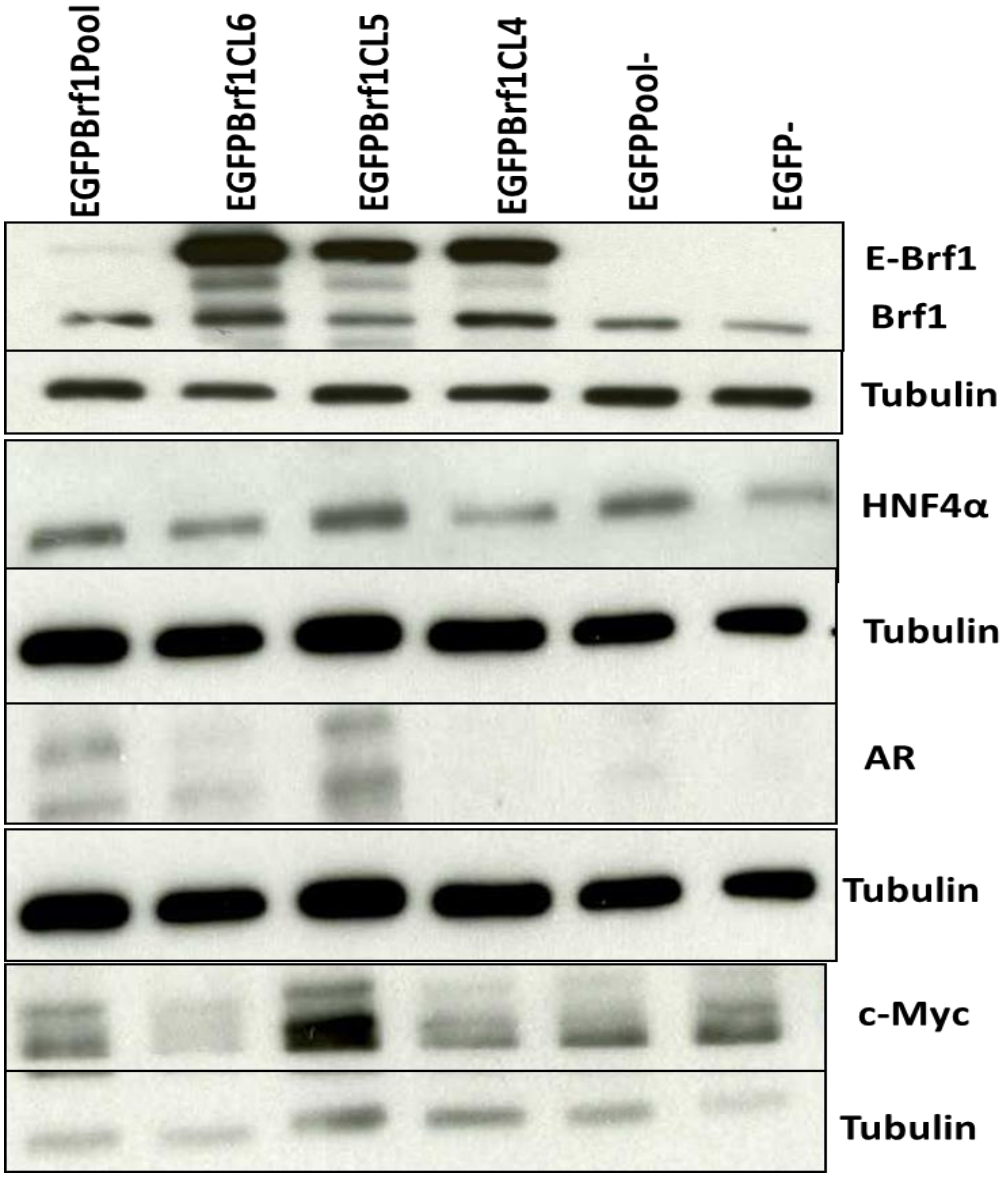

Figure 5-28 Western blot analysis of PC3 stable BRF1 overexpressed cells.
A cell line panel of the stable PC3 EGFP- and EGFP-Brf1 clonal subsets were analysed by Western blot for c-MYC and HNF4α expression. BRF1 overexpression does not seem to affect HNF4α and c-MYC expression in any clear pattern. Interestingly, PC3 is AR independent and normally has no AR protein expression, but, in EGFP-Brf1 CL5, CL6 and EGFP-Brf1 Pool cells, AR expression is present but not in EGFP- cells. (E-Brf1 band represents ectopic BRF1 which is higher than the Brf1 band because EGFP adds 27 kDA to weight of endogenous BRF1).

5.3 Inducible GEMM

In designing GEMM the other important factor to consider is not only the genes you are manipulating but also when you want them to be switched on or off. In contrast to constitutively active GEMM, inducible GEMM in PC allow the genetic event to be switched on when a promoter is activated at a specified time. For example, *Nkx3.1-Cre*-ER knock in allele inactivates 1 allele of *Nkx3.1* and drives tamoxifen-dependent Cre-mediated recombination specifically in prostate epithelial cells. Floc'h et al 2012 used this inducible system to cross *Nkx3.1*^{CreERT2} with a *Pten* conditional allele to produce *Nkx3.1*$^{CreERT2/+}$*; Pten*$^{flox/flox}$, so that the *Pten* inactivation occurred via tamoxifen induction at mice aged 2 months old adult mice, instead of in its germline or immature prostate epithelial. Their method for tamoxifen induction was intra-peritoneal (i.p.) injection (225mg/kg) or oral gavage (100mg/kg) for 4 consecutive days to mice aged 2 - 3 months. In control experiments, tamoxifen induction was shown to have negligible effect on the prostate phenotype of control or mutant mice (Wang et al, 2009).

Nkx3.1-Cre^{ERT2} has a Cre-ERT2 cassette knocked in to the *Nkx3.1* gene which allows deletion of gene in adult prostate epithelium after tamoxifen induction (Wang et al, 2009). In the inducible *Nkx3.1-Cre*$^{ER-T2}$ system, tamoxifen activates *Cre* gene because a mutated ligand binding domain of human ER is fused to the *Cre* gene. This allows excision of floxed genes at selected time points by induction of *Cre-ER*.

The resulting phenotype of *Nkx3.1*$^{CreERT2/+}$*; Pten*$^{flox/flox}$ post-tamoxifen induction was the development of PIN lesions at 6-7 months and HGPIN at 9-12 months and extensive HGPIN with invasive cancer by 16 months (Floc'h et al, 2012). Mice were surgically castrated at 4 months after tamoxifen resulting in tumour regression at 2 weeks post-surgery with castration resistant lesions evident by 6-7 months progressing to poorly differentiated adenocarcinoma by 16 months post-tamoxifen induction (Floc'h et al, 2012). Further analysis of these castration resistant prostate tumours showed virtually no evidence of senescence in comparison to the non-castrated mice which harboured less aggressive prostate tumours (Floc'h et al, 2012).

Aytes et al (2013) reported that *Nkx3.1*^{CreERT2} allele is prostate epithelial cell specific, and they saw no evidence of leaky expression in absence of tamoxifen. For tamoxifen induction of their mice they dissolved tamoxifen in corn oil (100 mg/kg) and used oral gavage once daily for 4 consecutive days at 2 months of age. They generated an inducible

metastatic GEMM with combined *Pten* loss and *Kras* activation (*Nkx3.*$^{1CreERT2/+}$; *Pten*$^{flox/flox}$; *Kras*$^{LSL-G12D/+}$). Following tamoxifen induction, this GEMM developed aggressive PC with 100% penetrance of metastases predominantly to liver and lung, and lesser extent diaphragm, pancreas, kidney and proximal lymph nodes but notably not bone metastases (Aytes et al, 2013).

Mouse model 3 *(Nkx-CreER Brf1* $^{flox/+}$*)*

Our third *Brf1* manipulated GEMM was an inducible model using Nkx3.1-CreER with heterozygote *Brf1* loss switched off by tamoxifen at 3- 4 months of age (Figure 5.29). We predicted that homozygote loss of *Brf*1 in mouse prostate epithelial would lead to cell death. I wish to test whether heterozygote loss of *Brf*1 would affect the normal morphology and homeostasis of the adult prostate gland. If this mouse model had been successful, the plan was to cross it with an aggressive mouse model, such as prostate specific homozygote loss of *Pten* and *p53* to see whether loss of *Brf*1 could slow down prostate tumorigenesis.

Tamoxifen induction was performed with 225 mg/kg i.p. injections for 4 consecutve days. Unfortunately, we found there was no obvious reduction in Brf1 on Western blots and IHC staining on the prostate from post-mortem carried out two to four weeks after tamoxifen induction. This suggests that tamoxifen induction was not successful in inducing the *Cre* recombination expression or that Brf1 expression is upregulated in a compensatory manner as a consequence of a floxed *Brf1* allele (see figures 5.30- 5.32). To see whether prostate specific homozygote deletion of *Brf*1 could be tolerated by the mice, we set up matings between *Brf1* $^{flox/flox}$ mice and *NkxCreER-Brf1*$^{flox/+}$ mice. Of 114 male offspring genotyped, none were confirmed to have a *NkxCreER-Brf1*$^{flox/flox}$ genotype. Predicted offspring genotypes from those matings would be one-quarter (28 mice) for each of the following genotypes (in brackets is how many mice actually had each genotype): (36) *Brf1*$^{flox/+}$; (39) *Brf1*$^{flox/flox}$; (40) *NkxCreER-Brf1*$^{flox/+}$; (0) *NkxCreER-Brf1*$^{flox/flox}$. An explanation for this may be that the *NkxCreER* is leaky and therefore the NkxCreER is being activated in utero and the *NkxCreER-Brf1*$^{flox/flox}$ genotype is being expressed outside the prostate in the mice foetuses resulting in embryonic lethality. The way to test for this would be to look for embryonic death in pregnant mice and test the foetus genotypes. However, since this mouse model was not the primary focus of this study we decided not to spend time investigating this.

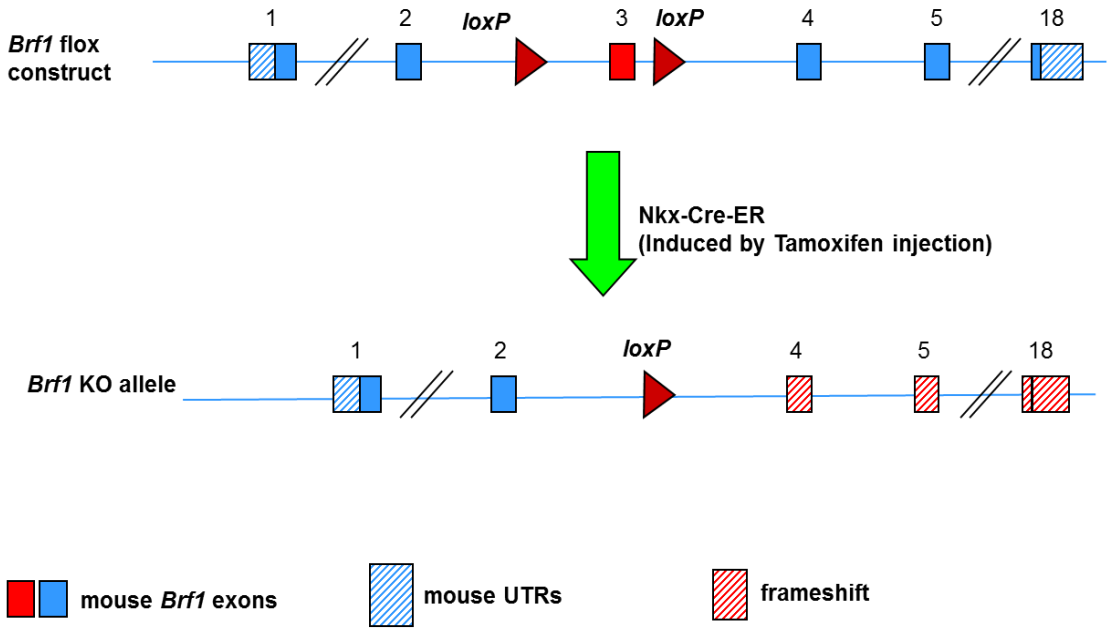

Figure 5-29 Constructing *Nkx-CreER-Brf1*$^{flox/+}$ GEMM
This GEMM was designed to assess whether heterozygote loss of *Brf1* in the mouse prostate is detrimental to prostate gland homeostasis.

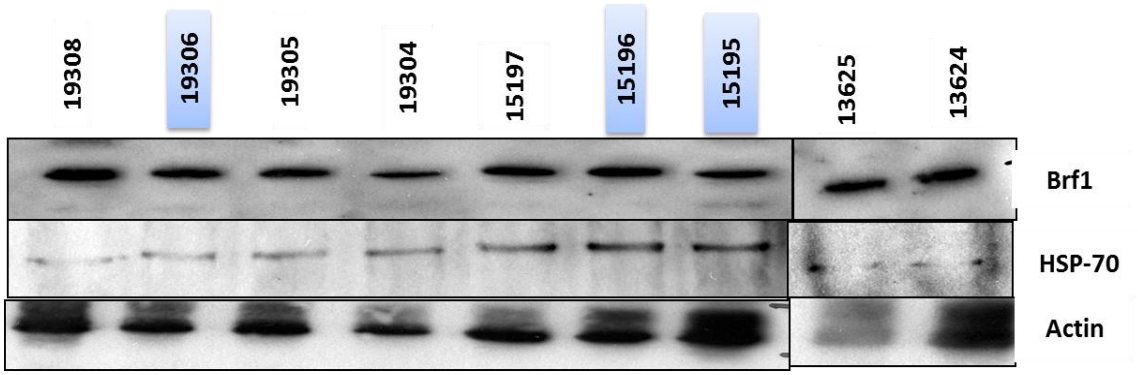

Figure 5-30 Western blot of Brf1 expression in *NkxCreER-Brf1*$^{flox/+}$ and *NkxCreER*- mice prostates
Blue prostate lysate identity numbers are derived from *NkxCre-Brf1*$^{flox/+}$ mice and the remaining are control mice (*WT* and *NkxCreER-).* There is no difference in Brf1 expression between the different genotypes. HSP-70 and actin are loading controls.

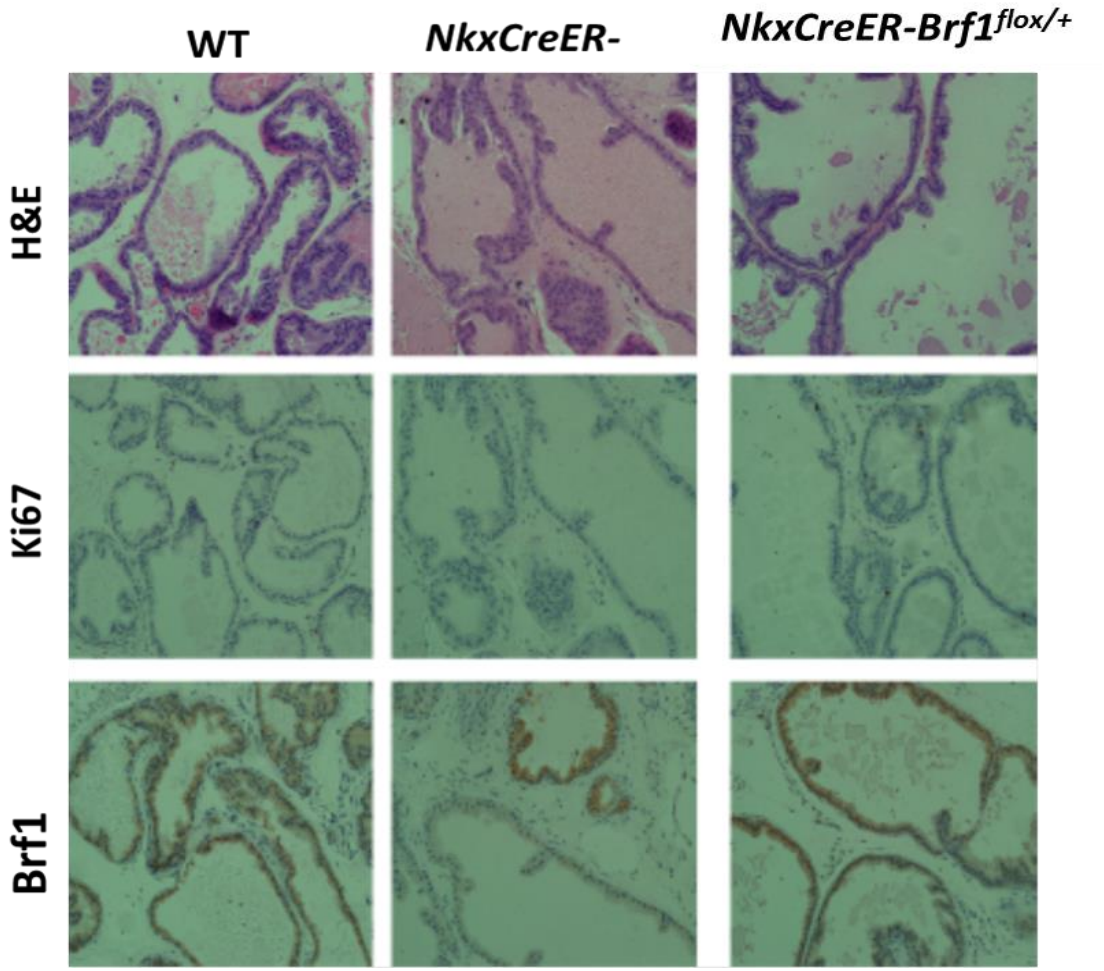

Figure 5-31 IHC staining of *WT*, *NkxCreER* and *NkxCreER-Brf1$^{flox/+}$* of ventral prostates
Histologically all the prostates were similar with no signs of dysplasia or abnormal morphology. Ki67 and caspase 3 (not shown) were both negative. Brf1 IHC staining tended to be similar in all three genotypes. Tamoxifen induction should have reduced Brf1 expression and consequently Brf1 IHC staining in *NkxCreER-Brf1$^{flox/+}$* but this was not successful (20X magnification).

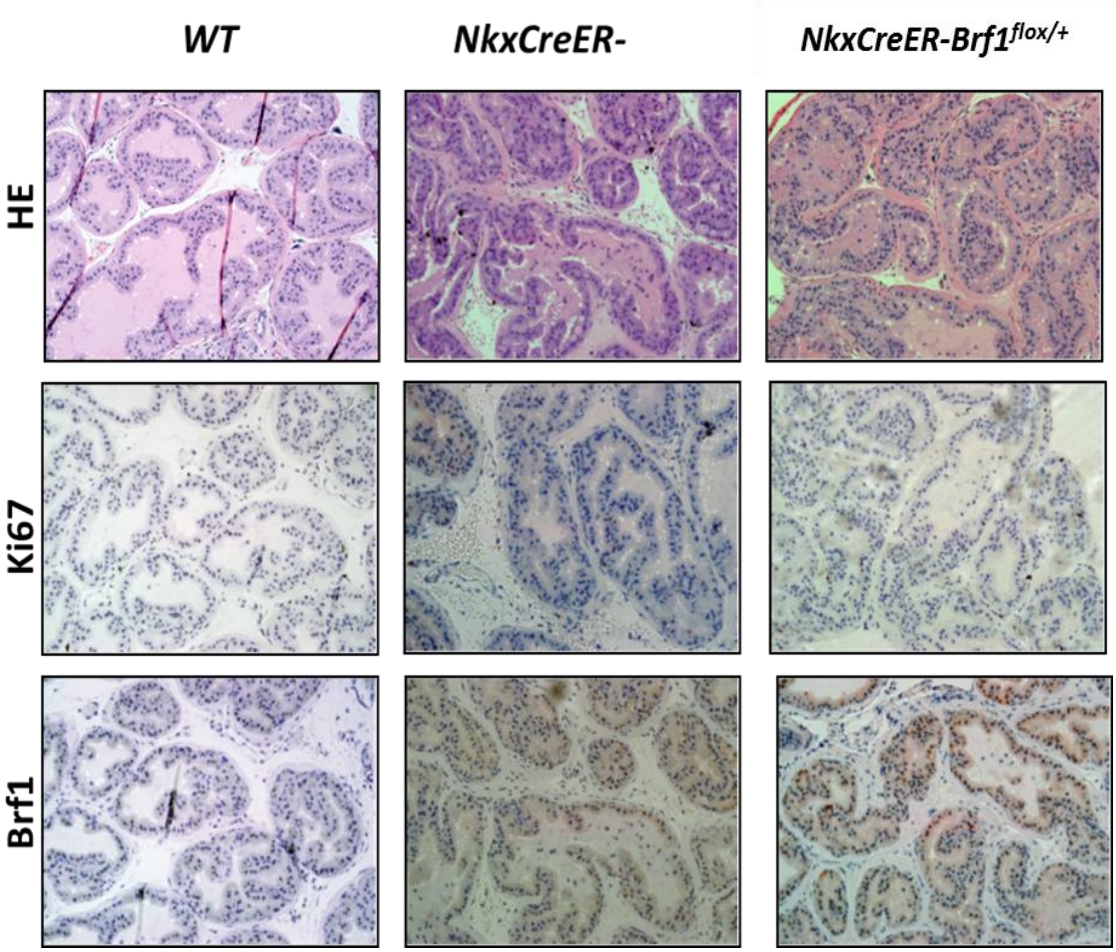

Figure 5-32 IHC staining of *WT*, *NkxCreER-* and *NkxCreER-Brf1$^{flox/+}$* of dorsolateral prostate
All three genotypes were histologically similar with no signs of dysplasia or abnormal morphology. Ki67 and caspase 3 (not shown) were both negative for staining. Brf1 staining tended to be similar between the genotypes generally. Tamoxifen induction should have reduced the BRF1 expression in *NkxCreER-Brf1$^{flox/+}$* but this was unsuccessful (20x magnification).

5.4 Discussion

Within the time and financial constraints of this study, it has not been possible to fully characterise this novel BRF1 overexpressing *Pten-Brf1* GEMM. Unfortunately, an earlier time point of 3-5 months was not achieved due to the low fertility of the *PbCre-Pten*$^{fl/fl}$ male mice and thus long time delays in developing the clinical end point cohorts. *PbCre-Pten*$^{fl/fl}$ male mice are only fertile for the first few months of life and PbCre-Pten$^{fl/fl}$ female mice are not fertile. It would have been useful to investigate whether PIN lesions and early tumour growth developed earlier in the *Pten-Brf1* mice versus the *Pten-* mice. Furthermore, imaging the mice with detailed sequential ultrasound (US) scans may have allowed for growth velocity measurements to be made. This would have answered the question whether BRF1 is an early initiator of tumour growth.

The protein analysis and IHC scoring confirms that Brf1 is overexpressed in the mouse prostate tumours of the *Pten-Brf1* in comparison to the *Pten-* mice and therefore the GEMM is a success in a technical sense. However, the addition of human BRF1 to *PbCrePten*$^{fl/fl}$ mice only produced a fairly subtle change in phenotype. BRF1 overexpression to a known PC GEMM does cause the prostate tumours to grow quicker and reach clinical end point significantly sooner. However, it does not appear to result in a metastatic phenotype. Perhaps, this is not surprising as other studies have shown that BRF1 overexpression can act as a driver of tumorigenesis in the presence of oncogenes, such as c-MYC (Johnson et al, 2008). In hindsight a more useful GEMM would have been an aggressive GEMM with *Brf1* KD, for example, *Pten* and *p53* loss in prostate epithelium or *Pten* loss and *MYC* activation in prostate epithelium with *Brf1* KD. This would have shown whether suppression of Brf1 status can put the brakes on an aggressive model by slowing down proliferation.

Further analysis of the RNA sequencing data may provide important downstream molecular drivers and regulators that *Brf1* overexpression harnesses to stimulate tumour growth. Due to time constraints we focused on HNF4α as this was also upregulated in published ChIP data but unfortunately, western blot analysis did not confirm that HNF4α was upregulated at the protein level in *Pten-Brf1* mice. However, only one HNF4α antibody was tested and therefore, it is difficult to confirm this is a true result. To strengthen the RNA sequencing data ideally five age-matched prostate tumours from each mouse cohort, *Pten-* and *Pten-Brf1* should have been analysed. However, even with only three *Pten-Brf1* and two *Pten-* tumours tested it is clear from the heat map and GeneGo

analysis there are a number of genes significantly upregulated in the *Pten-Brf1* prostate tumours that require further investigation.

The most interesting finding from this novel GEMM is that BRF1 overexpression is associated with higher AR expression in comparison to the control mice *Pten*- tumours. It is well known AR signalling is essential for the development and progression of PC. It would have been interesting to see whether BRF1 function is influenced by AR signalling. In the hypothetical *Brf1* KD GEMM discussed above, castration experiments could be used to investigate whether removal of androgens enhances the inhibitory growth effects of *Brf1* KD.

PC3 cells are thought to express little or no androgen receptor (Kaighn et al, 1979). However, with our PC3 stably upregulated BRF1 cells there is a definite band on the western blot analysis at the molecular weight size of AR. This urgently requires further investigation. In the first instance qPCR of mRNA AR levels should be quantified in the stable PC3 EGFP- and EGFP-Brf1 clones. There has been a recent surge of interest in researching the steroid hormone-regulated transcriptome and it seems estrogen receptor signalling drives Pol III activity in breast cancer cells (Hah et al, 2014). *c-JUN* oncogene activity increases estrogen receptor (ER)α expression and ERα occupancy at the *BRF1* promoter ultimately leading to elevated Pol III transcription (Zhong et al, 2014).

Pten- prostate tumours showed a trend of higher IHC scoring for the inflammation markers, such as NIMP and F4/80 and DNA damage, γH2AX. This suggests that *Pten*-mediated tumorigenesis may have more active inflammatory pathways than the *Pten-Brf1*. It may be that there is an altered balance between growth signalling pathways versus inflammatory signalling pathways in *Pten-Brf1* and *Pten*- prostates. Disappointingly, Ki67 (a marker of cell proliferation) was virtually identical between the two genotypes. A reason for this may be that as most of the prostate tumours had reached clinical end point, they had reached their maximum proliferation capacity. Ki67 IHC scoring at an earlier time point may have revealed a higher proliferative capacity in *Pten-Brf1* prostates. However, due to low numbers of mouse tumours analysed in the age matched cohort, it is difficult to make firm conclusions. However, obvious differences should be detected at n> 5, and the fact that the differences are subtle suggests phenotypically the tumours of *Pten-Brf1* and *Pten*- are fairly similar.

It is important that limitations of GEMM are recognised and evaluated so that future GEMM and other models become the most precise replicas for human cancer. Firstly, mice and other rodents do not develop PC spontaneously (Wu et al, 2012). Human prostate glands are structurally different to mouse prostate glands, in that mouse prostates are composed of multiple lobes, whereas the human prostate has a zonal architecture. There is some evidence that the mouse dorso-lateral lobe is most similar to the human peripheral zone in reference to carcinogenesis (Berquin et al, 2005). It is also well documented that the phenotype can be affected by mouse genetic background. For example, in *Trp53* knockout mice, tumour type and onset is highly variable between BALB/c versus C57BL/6 genetic backgrounds (Kuperwasser et al, 2000). Background mice strains have been shown to modify the latency and spectrum of tumours that develop in $Pten^{+/-}$ mice (Freeman et al, 2006).

An effective GEMM replicating human PC should have the following characteristics: prevalence increasing with age; slow growth rate; histological progression from PIN, HGPIN, invasive adenocarcinoma, androgen dependence to androgen independence; high propensity for bone metastases. Our GEMM with BRF1 overexpression clearly does not meet this criteria but it does highlight the complexity of developing GEMM and does suggest that addition of BRF1 can change the growth dynamics of prostate tumours in a known PC GEMM.

6 Discussion

6.1 Is BRF1 a driver of prostate carcinogensis?

The overarching aim of this thesis was to provide evidence to support or refute whether BRF1 has an important role in prostate carcinogenesis. I will now go through all the evidence with that sole question in mind. A former PhD student, Noor Nam reported that in human clinical samples PC has higher BRF1 expression than benign prostate pathology. Furthermore, the patients with higher BRF1 IHC scoring of their prostate tumours also had higher Ki67 IHC scoring, a marker of proliferation and more importantly, poorer survival outcomes. Oncomine and cBioportal data also supports that human clinical PC tumours have higher BRF1 levels than benign prostate pathology, and metastatic disease has even higher levels of BRF1 expression than primary PC tumours (Figures 3.1 and 3.2).

Western blot analysis of BRF1 protein expression in a human PC cell line panel showed BRF1 was easily detectable in all studied PC cell lines (Figure 3.3). BRF1 protein expression was higher in PC3M cells relative to its less aggressive primary cell line PC3. Interestingly, BRF1 mRNA was higher in PC3 than PC3M as measured by RT-qPCR (Figure 3.4). This suggests that BRF1 expression is, at least in part, controlled at the post-transcriptional level.

The *in vitro* transient BRF1 manipulation experiments clearly showed that upregulating BRF1 increased cell proliferation in PC cell lines, whereas knocking down *BRF1* expression with siRNAs to lower BRF1 protein expression reduced cell proliferation (Section 3.2). This is in keeping with elevated Pol III activity resulting in increased tRNAs production and, therefore, protein synthesis for cell proliferation. However, stable *BRF1* overexpression in PC3 cells produced less impressive results despite high levels of BRF1 expression at protein and mRNA levels in comparison to their EGFP- control cells (Figures 4.1- 4.4). They failed to show an increased proliferative or colony forming capability when compared to their EGFP- controls (Figures 4.5- 4.8). However, interestingly they displayed altered cell morphology with polyploidy nuclear and G2/M arrest on cell cycle analysis by FACS (Figure 4.11).

As only one PC cell line was successfully developed with stable transfection of *BRF1* overexpression, it is difficult to draw too many conclusions from those experiments. Furthermore, from western blot analysis, PC3 was not one of the PC cell lines that had the highest BRF1 expression; it may be that BRF1 is not an important driver in PC3 cells. PC cell lines with higher levels of endogenous BRF1, such as LNCaP or CWR22, may

respond differently to increasing BRF1 expression and produce a more aggressive phenotype. Once a functional upregulated stable PC cell line is developed, it will be invaluable to assess its Pol III transcription activity, including tRNA production.

We developed two novel GEMM with hBRF1 added to a prostate specific *Cre* (*PbCr*e-Brf1) and the PC GEMM *PbCrePten*$^{fl/f}$ model (*PbCrePten*$^{fl/fl}$-hBRF1 or *Pten-Brf1*). These were both successful models in that BRF1 was confirmed to be overexpressed on western blot and IHC (Figures 5.2, 5.10 and 5.11). However, BRF1 overexpression alone did not result in a PC phenotype, or any distinctive histological differences from the control mice *PbCre*. *Pten-Brf1* reached clinical end point of a sizeable prostate tumour that affected the mouse's agility sooner than the *Pten-* control mice (Figures 5.4 and 5.5. However, the histology of *Pten-Brf1* GEMM looks very similar to the control mice and disappointingly there is no increase in Ki67 IHC scoring (Figures 5.9, 5.12 and 5.13). This GEMM produces large cystic prostate tumours and therefore, it is difficult to let the mice age longer to develop metastatic lesions. Furthermore, an early time point to assess whether BRF1 overexpression was causing early dysplastic changes or tumour growth was not possible.

The most interesting result from the GEMM is that BRF1 overexpression appears to be associated with AR overexpression on IHC and western blot (Figures 5.24, 5.25 and 5.26). Therefore, future studies in BRF1 manipulated GEMM should include castration experiments to further explore this relationship. Furthermore, it takes considerable time and finance to develop and characterise new GEMM and therefore, a more rapid alternative for further analysis of BRF1's functional role in PC is to develop subcutaneous or orthotopic (prostate) xenografts. Future studies should explore the functional significance of BRF1 manipulation in androgen responsive human PC cells in both *in vitro* and *in vivo* studies. This will provide insight into how BRF1 overexpression behaves *in vivo* with its host extracellular signalling interactions. Further analysis of the GEMM prostate tumour RNA sequencing data is required to see whether any further molecular drivers can be identified that may be responsible for the increased tumour growth in the *Pten-Brf1* mice.

In summary the hypothesis that BRF1 has an important functional role in prostate carcinogenesis is partially supported by my data. Further research questions have been raised, which should facilitate identifying BRF1's role in PC. Primarily, the relationship

between BRF1 regulation, Pol III activity and AR would be an interesting focus of future research studies.

6.2 Is Pol III a potential target for anticancer therapy?

In cancer cells, acquired oncogenic drivers (for example overexpression of *MYC*) or loss of tumour suppressors such as *TP53* result in consistent Pol I and III activity. Therefore, Pol I and III transcription machinery are potential anticancer therapeutic targets. However, this has proved controversial due to their essential housekeeping role in sustaining the proliferation of normal cells. Yee et al, 2007 showed in zebrafish *slj* mutants Pol III transcription reduction inhibits development and growth in highly proliferative larval tissues, such as digestive system and retinae. Furthermore, the effects of Pol III reduction was more evident in actively proliferating cells than on quiescent post-mitotic cells, for example heart, skeletal muscle and pancreatic islet cells. Their research illustrates developmental defects are tissue-specific because Pol III-dependent demands of these cells are not met and thus, the threshold of Pol III activity required to sustain proliferation is variable between cells (Yee et al, 2007). It may be that cells control Pol III transcription partly by regulating the expression of its subunit. Yee et al, 2007 found that *polr3b* (second largest subunit of Pol III subunit, the zebrafish ortholog of yeast Pol III subunit *rpc2)* expression was consistently higher in the cells of the more proliferative tissue.

As a pilot study, we looked at whether *BRF1* KD by siRNA could behave synergistically with docetaxel. The initial results do seem to suggest that at less effective levels of *BRF1* KD they may act synergistically but as they both cause G2/M arrest, at higher effective levels of *BRF1* KD, there is no obvious synergistic anti-proliferative effect. Interestingly, other researchers have started exploring Pol I, II and III inhibitors as potential anti-cancer drugs.

Inhibiting protein synthesis and therefore halting cancer cell proliferation and tumour growth is an attractive anti-cancer strategy. Conceptually, targeting Pol III activity is similar to how cytotoxic drugs work, that is, they attack cells with rapid growth and cell cycle turnover. Cancer specific hyper-activation of Pol III suggests that cancer cells may be more sensitive to the effect of Pol III inhibition than normal cells. Partial inhibition of Pol III transcription potentially could have less toxic effects than inhibiting an oncogene

upstream that has multiple effects. For example, inhibition of PI3K signalling has focused on inhibiting PI3K, AKT and mTOR signalling complex but this has proved relatively toxic, and the presence of complex feedback loops also limits its efficacy.

The tumour suppressor p53 is a transcription factor that is induced by cell stress to switch on genes involved in DNA damage repair, apoptosis, senescence, cell cycle arrest and autophagy. *TP53* is mutated in approximately half of all human cancers (Petitjean et al, 2007). In healthy unstressed cells, p53 levels are low due to activity of p53 antagonist, E3 ubiquitin-protein ligase MDM2. Many cytotoxic agents work by damaging DNA and rely on the subsequent activation of p53 for their therapeutic activity. However, this can induce genetic instability and lead to secondary malignancies and other serious side effects, such as myelosuppression (Hijiya et al, 2009). Therefore, there has been considerable effort to develop novel drugs to activate p53 in a more specific and therefore less damaging way. For example, MDM2 antagonists, mutant p53 re-activators and immunotherapy have been developed and evaluated in clinical trials. However, success has been limited by low potency and a suboptimal therapeutic window (as reviewed by Drygin et al, 2014).

Induction of nucleolar stress is not a current anti-cancer therapeutic strategy, but it has been found coincidentally to be a major component of some current chemotherapy drugs (Drygin et al, 2014). Inhibiting Pol I transcription can result in nucleolar stress leading to stabilisation of p53 and induction of p53-dependent apoptosis (Kalita et al, 2008). This is mediated by the sequestration of mdm2 by ribosomal proteins, thus allowing the liberation and activation of p53 (Deisenroth et al, 2010). A recent screen of common chemotherapeutic drugs by Burger et al, (2010) demonstrated that 21 out of 36 drugs tested affected ribosome biogenesis. For example, the commonly used platinum agent cisplatin inhibits Pol I transcription with a high degree of specificity through its ability to cross-link DNA thus preventing transcription factor UBF associating with rDNA gene promoter (Treiber et al, 1994). Also, the anti-metabolite 5'fluorouracil (5'FU) disrupts rRNA processing by preventing the cross-linking of rRNA binding proteins at key processing sites of the precursor rRNA transcript (Ghosal et al, 1997).

The metabolites of pyrimidines such as 5'FU were analysed so that novel compounds could be developed by molecular design. The novel nucleoside 1-(3-C-ethyl-β-*ribo*-pentofuranosyl/cytosine (ECyd or TAS-106 in human clinical trials) was designed to inhibit RNA and DNA synthesis by blocking RNA polymerases I, II and III (Tabata et al, 1996; Fukushima et al, 1998; Kazuno et al, 2007). ECyd has demonstrated potent *in vitro*

cytotoxicity against a number of human cancer cell lines (Hattori et al, 1996; Tabata et al, 1996). When ECyd was administered intravenously in a nude mouse xenograft model, strong anti-tumour activity was demonstrated without evidence of severe toxicities (Shimamoto et al, 2001; Takatori et al, 1999).

ECyd is phosphorylated by uridine/cytidine kinase 2 (UCK2) into the active metabolite ECyd-triphosphate (ECTP) (Azuma et al, 2001; Murata et al, 2004). UCK2 is expressed higher in tumour cells versus normal cells and TAS-106 sensitivity has been correlated with UCK2 activity in tumour cell lines (Murata et al, 2004; Shimamoto et al, 2002). Expression of UCK2 seemed to correlate with cellular sensitivity to ECyd *in vitro* (Shimamoto et al, 2002). However, in a subsequent clinical trial no significant correlation was observed between tumour UCK2 protein expression and TAS-106 mediated anti-tumour effects (Tsao et al, 2013).

There is increasing evidence that ECyd could be more effective in combination with other anticancer therapies. Radiotherapy kills cancer cells by generating double strand breaks (DSBs) in DNA within tumour cells, leading to apoptosis and cell death (Kaina et al, 2003). The efficacy of radiotherapy seems to be closely associated with cellular DNA repair capacity (Mirzayans et al, 2006). TAS-106 enhances radiosensitivity in various cell lines, and xenografts by suppressing the repair of radiation-induced DSBs (Meike et al, 2011; Yasui et al, 2007). It seems TAS-106 achieves this by downregulating the mRNA and protein levels of homologous recombination (HR) -related proteins, especially BRCA2 (Meike et al, 2011).

Preclinical studies of ECyd and cisplatin have shown enhanced growth inhibition in tumour cell lines and murine xenograft models (Kazuno et al, 2009). Further analysis showed that ECyd potently reduced cell cycle checkpoint- associated proteins expression and Chk1 and Chk2 phosphorylation status. ECyd also abrogated cisplatin-induced S and G2-M checkpoints, and apoptosis was induced in A549 cells (Kazuno et al, 2009). Interestingly, ECyd has been shown to inhibit the synthesis of vault RNAs (vRNAs, a Pol III product), while inducing the major vault protein (MVP, a Pol II product), both of which are essential components of Vaults as a drug transporter (Fukushima et al, 2014). This is thought to explain how ECyd ‘overcomes’ resistance to cisplatin of KB cells (cisplatin-resistant head and neck cancer cells) in *in vtiro* as well as *in vivo* xenograft tumours (Fukushima et al, 2014).

Patients who have progressed through conventional anti-cancer treatments with good performance status should be considered for clinical trials. Several Phase I clinical trials have shown the dose limiting toxicities (DLTs) of TAS-106 are cumulative sensory peripheral neuropathy, tremor, fatigue and myelosuppression (Takimoto et al, 2007; Hammond-Thelin et al, 2010; Friday et al, 2012). There has been no anti-tumour efficacy seen in TAS-106 monotherapy clinical trials to date (Abdelrahim et al, 2013; Tsao et al, 2013). A Phase I dose escalation study with TAS-106 and carboplatin also did not show any clinical response. Nonetheless, TAS-106 was shown to be well tolerated, with dose limiting toxicity (DLT) being neutropenia (Naing et al, 2014).

Cylene Pharmaceuticals developed the first selective Pol I transcription inhibitor called CX-3543. CX-3543 specifically inhibits the elongation stage of Pol I transcription by preventing the stabilising interactions between nucleolar protein nucleolin (NCL) and G-quadruplexes in the rDNA gene (Drygin et al, 2009). In pre-clinical studies, CX-3543 demonstrated anti-proliferative effects in broad panel of cancer cell lines and xenograft models of breast and pancreatic cancer (Drygin et al, 2009). CX-3543 progressed through to a first in human study, Phase I dose-escalation study (ClinicalTrials.gov NCT00955786) and Phase II trial in low to intermediate grade neuroendocrine carcinoma (ClinicalTrials.gov NCT00780663) but due to low bioavailability was withdrawn from further clinical trials (Balasubramanian et al, 2011).

Using a functional assay, Cylene Pharmaceuticals screened a small molecule library and identified CX-5461, a Pol I inhibitor that blocks the binding of SL1 transcription factor to its rDNA promoter, thus inhibiting initiation of rRNA synthesis by the Pol I multiprotein complex (Drygin et al, 2011). It has been shown to be highly selective inhibitor of Pol I activity, 300-400 folds more selective than for Pol II or III transcription (Quin et al, 2014). CX-5461 has high potent anti-proliferative effects over a broad panel of human cancer cell lines (NCI-60 panel) in a p53 independent manner with resistance in non-cancer cell lines (Drygin et al, 2011). Negi et al, 2015 studied the effects of a 2-days treatment with CX-5461 in bone marrow derived cells from 6 patients with acute lymphoblastic leukaemia (ALL) as well as 3 healthy individuals as controls. A therapeutic window for CX-5461 treatment was proposed comparing cancer and healthy cells, with the leukaemic cells dying and the healthy cells surviving the treatment. In A375 (melanoma) and Mia Paca-2 (pancreatic) carcinoma cells, it was shown that CX-5461 induces cellular senescence and autophagy (Drygin et al, 2011). This response is not driven by reductions in ribosomes or protein synthesis, as the cancer cell death pathway is induced long before these reductions

can occur (Drygin et al, 2011). Furthermore, in murine xenograft models of human cancers, melanoma A375 and pancreatic carcinoma Mia Paca-2, CX-5461 displayed anti-tumour activity (Drygin et al, 2011).

Cancers with high levels of ribosome biogenesis, such as tumours with c-MYC gene amplification or overexpression are likely to respond well to nucleolar-targeting therapies. MYC modulates transcriptional activity of Pol I, Pol II and Pol III and thus acts as a global regulator of ribosome biogenesis (Gomez-Roman et al, 2006; van Riggelen et al, 2010). CX-5461 induced rapid p53-dependent apoptosis in Eμ-*MYC* lymphoma cells, whereas normal B cells were resistant to Pol I transcription inhibition (Bywater et al, 2012). Furthermore, p53 wildtype B-lymphomas are more sensitive to CX-5461 than p53 mutant B-lymphoma cells, and apoptosis in these cells is p53-dependent (Bywater et al, 2012). CX-5461 selectively activated p53-dependent apoptosis to reduce tumour size in mouse models of B-lymphoma and acute myeloid leukaemia (AML) (Bywater et al, 2012). Interestingly, p53 mediated apoptosis induction was rapid and independent of changes in protein translation or total ribosome levels (Bywater et al, 2012). Transgenic Eμ-*MYC* mice lymphomas are very sensitive to CX-5461 (Quin et al, 2014). Importantly, the apoptotic activity of CX-5461 *in vivo* was specific for *MYC* overexpressing lymphoma cells with no deleterious effect on normal B-lymphocyte population (Bywater et al, 2012).

A transgenic mouse model that develops MLL-ENL (mixed lineage leukaemia- eleven nineteen leukaemia protein) fusion oncogene driven AML (acute myeloid leukaemia) is resistant to cytarabine and doxorubicin due to a lack of p53 activation (Zuber et al, 2009). CX-5461 was able to induce p53 and doubled the lifespan of these mice in comparison to vehicle alone or combination of cytarabine and doxorubicin (Hein et al, 2011). However, this appears to be cell specific as p53-independent pathways were more dominant in CX-5461 mediated apoptosis in ALL cells (Negi et al, 2015). Furthermore, in ALL cells ATM (ataxia telangiectasia-mutated)/ATR (ATM-rad3-related) pathway is activated by CX-5461 resulting in G2 phase arrest. ATM and ATR are responsible for checkpoint kinases CHK1 and CHK2 activation in response to cellular stress and lead to G2 arrest (Jackson et al, 2009). Negi et al, (2015) demonstrated treating ALL cells with a combination of CX-5461 and ATR inhibitor (VE-822) resulted in marked increase in apoptosis compared to CX-5461 alone, as the cells are no longer allowed to go into G2 arrest to recover from the drug induced stress.

CX-5461 activity is variable depending on the cancer cell type. In solid tumour cell lines, CX-5461 produces cell senescence and autophagy in a p53 independent manner, whereas in haematological cancer cells it produces p53-dependent apoptosis. This highlights different cancer types may have different signalling mechanisms that mediate nucleolar stress and cell death.

There is increasing evidence that regression of cell transformation can be achieved by decreasing expression of BRF1 and Pol III genes (Johnson et al, 2008; Zhang et al, 2013; Zhang et al, 2011). Deregulation of Pol III transcription and particularly, targeting of BRF1 by tumour suppressors and oncogenes in cancer cells suggests that Pol III transcription has an important role in tumorigenesis and potentially could be a novel anticancer target. Targeting Pol III transcription machinery may represent novel strategy for controlling tumorigenesis and cancer progression.

7 List of References

Aaronson SA (1991). Growth factors and cancer. *Science* **254:** 1146-52.

Abate-Shen C, Banach-Petrosky WA, Sun X, Economides KD, Desai N, Gregg JP, Borowsky AD, Cardiff RD & Shen MM (2003). *Nkx3.1; Pten* mutant mice develop invasive prostate adenocarcinoma and lymph node metastases. *Cancer Research* **63:** 3886-90.

Abate-Shen C, Shen MM, Gelmann E (2008). Integrating differentiation and cancer: The Nkx3.1 homeobox gene in prostate organogenesis and carcinogenesis. *Differentiation* **76(6):** 717-27.

Abdelrahim M, Matsuda A & Naing A (2013). TAS-106: Preclinical, Clinical and Beyond. *Oncology* **85:** 356-363.

Adamson ED & Mercola D (2002). Egr1 transcription factor: multiple roles in prostate tumor cell growth and survival. *Tumour Biol.* **23(2):** 93-102.

Ahmad I, Gao M, Patel R & Leung HY (2013). Modelling synergistic interactions between HER2, Sprouty2 and PTEN in driving prostate carcinogenesis. *Asian Jo. Of Andrology* **15(3):** 323-7.

Ahmad Y, Boisvert FM, Gregor P, Cobley A, Lamond AI (2009). NOPdb: Nucleolar Proteome Database 2008 update. *Nucleic Acids Res* **37:** D181-84.

Andersen JS, Lyon CE, Fox AH, Leung AKL, Lam YW, Steen H, Mann M, Lamond AI (2002). Directed proteomic analysis of the human nucleolus. *Curr. Biol.* **12 (1):** 1-11.

Askew EB, Gampe RT, Stanley TB, Faggart JL, Wilson EM (2007). Modulation of androgen receptor activation function 2 by testosterone and dihydrotestosterone. *J. Biol. Chem.* **282:** 25801-16.

Aytes A, Mitrofanova A, Waugh Kinkade C, Lefebvre C, Lei M, Phelan V, LeKaye CH, Koutcher JA, Cardiff RD, Caifano A, Shen MM & Abate-Shen C (2013). *ETV4* promotes metastasis in response to activation of PI3-kinase and Ras signalling in a mouse model of advanced prostate cancer. *PNAS* **110 (37)*:*** E3506-E3515.

Azuma A, Matsuda A, Sasaki T (2001), 1-(3-C-ethynyl-beta-D-ribo-pentofuranosyl) cytosine (ECyD, TAS-106)1: antitumor effect and mechanism of action. *Nucleosides Nucleotides Nucleic Acids* **20:** 609-19.

Baca SC, Prandi D, Lawrence MS, Mosquera JM, Romanel A, Drier Y, Park K, Kitabayashi N, MacDonald TY, Ghandi M, Van Allen E, Kryukov GV, Sboner A, Theurillat JP, Soong TD, Nickerson E, Auclair D, Tewari A, Beltran H, Onofrio RC, Boysen G, Guiducci C, Barbieri CE, Cibulskis K, Sivachenko A, Carter SL, Saksena G, Voet D, Ramos AH, Winckler W et al (2013). Punctuated evolution of prostate cancer genomes. *Cell* **153 (3):** 666-77.

Backman SA, Ghazarian D, So K, Sanchez O, Wagner KU et al (2004). Early onset of neoplasia in the prostate and skin of mice with tissue specific deletion of Pten. *Proc Natl Acad Sci USA* **101:** 1725-30.

Balasubramanian S, Hurley LH, Neidle S (2011). Targeting G-quadruplexes in gene promoters: a novel anticancer strategy? *Nat Rev Drug Discov.* **10:** 261-75.

Balbas MD, Evans MJ, Hosfield DJ, Wongvipat J, Arora VK, Watson PA et al (2013). Overcoming mutation-based resistance to antiandrogens with rational drug design. eLife 2013; 2:e00499.

Barbieri CE, Baca SC, Lawrence MS, Demichelis F, Blattner M, Theurillat JP, White TA, Stojanov P, Van Allen E, Stransky N, Nickerson E, Chae SS, Boysen G, Auclair D, Onofrio RC, Park K, Kitabayashi N, MacDonald TY, Shiekh K, Vuong T, Guiducci C, Cibulskis K, Sivachenko A, Carter SL, Saksena G, Voet D, Hussain WM, Ramos AH, Winckler W, Redman MC et al (2012). Exome sequencing identifies recurrent SPOP, FOXA1 and MED12 mutations in prostate cancer. *Nat Genet* **44:** 685-9.

Barski A, Chepelev I, Liko D, Cuddapah S, Fleming AB, Birch J, Cui K, White RJ & Zhao K (2010). Pol II and its associated epigenetic marks are present at Pol III-transcribed noncoding RNA genes. *Nature Struct. Mol. Biol.* **17:** 629-34.

Baumann M, Pontiller J, Ernst W (2010). Structure and basal transcription complex of RNA polymerase II core promoters in the mammalian genome: an overview. *Mol. Biotechnol.* **45(3):** 241-7.

Bensaad K, Tsuruta A, Selak MA, Vidal MN, Nakano K & Bartrons R (2006). TIGAR, a p53-inducible regulator of glycolysis and apoptosis. *Cell* **126**: 107-120.

Berger MF, Lawrence MS, Demichelis F, Drier Y, Cibulskis K, Sivachenko A, Sboner A, Esgueva R, Pflueger D, Sougnez C, Onofrio R, Carter SL, Park K, Habegger L, Ambrogio L, Fennell T, Parkin M, Saksena G, Voet D, Ramos AH, Pugh TJ, Wilkinson J, Fisher S, Winckler W, Mahan S, Ardlie K, Baldwin J, Simons JW, Kitabayashi N, MacDonald TY, Kantoff PW, Chin L, Gabriel SB, Gerstein MB, Golub TR, Meyerson M, Tewari A, Lander ES, Getz G, Rubin MA & Garraway LA (2011). The genomic complexity of primary human prostate cancer. *Nature* **470 (7333):** 214-20.

Beroukhim R, Mermel CH, Porter D, Wei G, Raychaudhuri S, Donovan J (2010). The landscape of somatic copy-number alteration across human cancers. *Nature* **463:** 899-905.

Berquin IM, Min Y, Wu R, Wu H & Chen YQ (2005). Expression signature of the mouse prostate. *J. Biol Chem* **280 (43):** 36442-51.

Berthold DR, Pond GR, Soban F, de Wit R, Eisenberger M, Tannock IF (2008). Docetaxel plus prednisolone or mitoxantrone plus prednisolone for advanced prostate cancer: updated survival in the TAX 327 study. *J. Clin. Oncol.* **26:** 242-5.

Bhatia-Gaur R, Donjacour AA, Sciavolina PJ, Kim M, Desai N, Young P, Norton CR, Gridley T, Cardiff RD, Cunha GR, Abate-Shen C & Shen MM (1999). Roles for Nkx3.1 in prostate development and cancer. *Genes Dev* **13***:* 966-77.

Billack B, Monteiro AN (2005). BRCA1 in breast and ovarian cancer predisposition. *Cancer Lett* **227(1):** 1-7.

Bill-Axelson A, Holmberg L, Ruutu M, Garmo H, Stark JR, Busch C, Nordling S, Haagman M, Andersson SO, Bratell S, Spangberg A, Palmgren J, Steineck G, Adami HO, Johansson JE (SPCG-4 Investigators) (2011). Radical prostatectomy versus watchful waiting in early prostate cancer. *N. Engl. J. Med* **364:** 1708-17.

Bjornsti MA & Houghton PJ (2004). Lost in translation: dysregulation of cap-dependent translation and cancer. *Cancer Cell* **5:** 519-23.

Blando J, Portis M, Benavides F, Alexander A, Mills G, Dave B, Conti CJ, Kim J & Walker CL (2009). Pten deficiency is fully penetrant for prostate adenocarcinoma in C57BL/6 mice via mTOR- dependent growth. *Am. J of Pathol.* **174 (5):** 1869-79.

Boon K, Caron HN, van Asperen R, Valentijn L, Hermus MC, van Sluis P, Roobeek I, Weis I, Voute PA, Schwab M & Versteeg R (2001). N-MYC enhances the expression of a large set of genes functioning in ribosome biogenesis and protein synthesis. *EMBO J.* **20:** 1383-93.

Borck G, Hog F, Dentici ML, Tan PL, Sowada N, Medeira A, Gueneau L, Thiele H, Kousi M, Lepri F, Wenzeck L, Blumenthal I, Radicioni A, Schwarzenberg TL, Mandriani B, Fischetto R, Morris-Rosendahl DJ, Altmuller J, Reymond A, Nurnberg P, Merla G, Dallapiccola B, Katsanis N, Cramer P & Kubisch C (2015). BRF1 mutations alter RNA polymerase III-dependent transcription and cause neurodevelopmental anomalies. *Genome Res* **25(2):** 155-66.

Bowen C, Bubendorf L, Voeller HJ, Slack R, Willi N, Sauter G, Gasser TC, Koivisto P, Lack EE, Konenen J, Kallioniemi OP & Gelmann EP (2000). Loss of NKX3.1 expression in human prostate cancers correlates with tumor progression. *Cancer Res* **60:** 6111-15.

Boyer LA, Latek RR & Peterson CL (2004). The SANT domain: a unique histome-tail-binding module? *Nature Rev. Mol. Cell Biol.* **5:** 158-163.

Brooks RF (1977). Continuous protein synthesis is required to maintain the probability of entry into S phase. *Cell* **12:** 311-7.

Brown CJ, Lain S, Verma CS, Fersht AR & Lane DP (2009). Awakening guardian angels: drugging the p53 pathway. *Nat Rev Cancer* **9:** 862-73.

Brzezinska EA, Nixon C, Patel R & Leung H (2015). Genetically engineered mouse models to study prostate cancer. *Methods in Molecular Biology* **1267**: 73-91.

Buchkovich K, Duffy LA, Harlow E (1989). The retinoblastoma protein is phosphorylated during specific phases of the cell cycle. *Cell* **58:** 1097-105.

Budde A & Grummt I (1999). P53 represses ribosomal gene transcription. *Oncogene* **18 (4):** 1119-24.

Burger K, Muhl B, Harasim T, Rohrmoser M, Malamoussi A, Orban M, Kellner M, Gruber-Eber A, Kremmer E, Holzel M & Eick D (2010). Chemotherapeutic drugs inhibit ribosome biogenesis at various levels. *J. Biol. Chem* **285(16):** 12416-425.

Burkhart DL & Sage J (2008). Cellular mechanisms of tumour suppression by the retinoblastoma gene. *Nat. Rev. Cancer* **8(9):** 671-82.

Bywater MJ, Poortinga G, Sanji E, Hein N, Peck A, Cullinane C, Wall M, Cluse L, Drygin D, Anderes K, Huser N, Proffitt C, Bliesath J, Haddach M, Schwaebe MK, Ryckman D, Rice WG, Schmitt C, Lowe SW, Johnstone RW, Pearson RB, McArthur G & Hananan RD (2012). Inhibition of RNA polymerase I as a therapeutic strategy to promote cancer-specific activation of p53. *Cancer Cell* **22:** 51-65.

Bywater MJ, Pearson RB, McArthur GA, Hannan RD (2013). Dysregulation of the basal RNA polymerase transcription apparatus in cancer. Nat Rev Cancer 13: 299-314.

Cabarcas S, Jacob J, Veras I & Schramm L (2008). Differential expression of the TFIIIB subunits BRF1 and BRF2 in cancer cells. *BMC Molecular Biology* **9:** 74.

Cabarcas S & Schramm L (2011). RNA polymerase III transcription in cancer: the BRF2 connection. *Molecular Cancer* **10:** 47-57.

Cairns CA & White RJ (1998). P53 is a general repressor of RNA polymerase III transcription. *EMBO J.* **17:** 3112-23.

Canavese M, Santo L, Raje N (2012). Cyclin dependent kinases in cancer: potential for therapeutic intervention. *Cancer Biol Ther.* **13:** 451-7.

Canella D, Praz V, Reina JH, Cousin P & Hernandez N (2010). Defining the RNA polymerase III transcriptome: Genome-wide localisation of the RNA polymerase III transcription machinery in human cells. *Genome Res.* **20**: 710-21.

Carter BS, Epstein JI, Isaacs WB (1990). Ras gene mutations in human prostate cancer. *Cancer Res* **50 (21):** 6830-2.

Carver BS, Trans J, Gopolan A, Chen Z, Shaikh (2009). Aberrant ERG expression cooperates with loss of PTEN to promote cancer progression in the prostate. *Nat Genet* **41:** 619 -24.

Castro E, Goh C, Leongamornlert D, Saunders E, Tymrakiewicz M, Dadaev T, Govindasami K, Guy M, Ellis S, Frost D, Bancroft E, Cole T, Tischkowitz M, Kennedy MJ, Eason J, Brewer C, Evans DG, Davidson R, Eccles D, Porteous ME, Douglas F, Adlard J, Donaldson A, Antoniou AC, Kote-Jarai Z, Easton DF, Olmos D, Eeles R (2015). Effect of BRCA mutations on metastatic relapse and cause specific survival after radical treatment for localised prostate cancer. *Eur Urol* **68 (2):** 186-93.

Chan JC, Hannan KM, Riddell K, Ng PY, Peck A, Lee RS, Hung S, Astle MV, Bywater M, Wall M, Poortinga G, Jastrzebski K, Sheppard KE, Hemmings BA, Hall MN, Johnstone RW, McArthur GA, Hannan RD, Pearson RB (2011). AKT promotes rRNA synthesis and cooperates with c-MYC to stimulate ribosome biogenesis in cancer. *Sci Signal* **4,** 56.

Chaux A, Albadine R, Toubaji A, Hicks J, Meeker A, Platz E, De Marzo A & Netto G (2011). Immunohistochemistry for ERG expression as a surrogate for TMPRSS2-ERG fusion detection in prostatic adenocarcinomas. *Am J Surg Pathol* **35:** 1014-20.

Chaveroux C, Eichner LJ, Dufour CR, Shatnawi A, Khoutorsky A, Bourque G, Sonenberg N, Giguere V (2013). Molecular and genetic crosstalks between mTOR and ERRalpha are key determinants of rapaMYCin-induced non-alcoholic fatty liver. *Cell Metab* **17:** 586-98.

Chedin S, Laferte A, Hoang T, Lafontaine DL, Riva M & Carles C (2007). Is ribosome synthesis controlled by Pol I transcription? *Cell Cycle* **6:** 11-15.

Chen CD, Welsbie DS, Tran C (2004). Molecular determinants of resistance to antiandrogen therapy. *Nat Med* **10:** 33-9.

Chen PL, Scully P, Shew JY, Wang JY, Lee WH (1989). Phosphorylation of the retinoblastoma gene product is modulated during the cell cycle and cellular differentiation. *Cell* **58:** 1193-8.

Chen W, Bocker W, Brosius J & Tiedge H (1997). Expression of neural BC200 RNA in human tumours. *J. Pathol.* **183(3):** 345-51.

Chen W, Heierhorst J, Brosius J & Tiedge H (1997). Expression of neural BC1 RNA: induction in murine tumours. *Eur J. Cancer* **33:** 288-92.

Chen Y, Chi P, Rockowitz S, Iaquinta PJ, Shamu T, Shukla S (2013). ETS factors reprogram the AR cistrome and prime prostate tumorigenesis in response to PTEN loss. *Nat. Med* **19:** 1023-9.

Chen Z, Trotman L, Shaffer D, Lin H-K, Dotan Z, Niki M, Koutcher J, Scher H, Ludwig T, Gerald W, Cordon-Cardo C & Pandolfi P (2005). Crucial role of p53-dependent cellular senescence in suppression of Pten-deficient tumorigenesis. *Nature* 2005 **436:** 725-730.

Chiaverotti T, Couto SS, Donjaccour A, Mao JH, Nagese H, Cardiff RD, Cunha GR, Balmain A (2008). Dissociation of epithelial and neuroendocrine carcinoma lineages in the transgenic adenocarcinoma of mouse prostate model of PC. *Am J of Pathol* **172 (1):** 236-46.

Chicas A, Wang X, Zhang C, McCurrach M, Zhao Z, Mert O, Dickins RA, Narita M, Zhang M, Lowe SW (2010). Dissecting the unique role of the retinoblastoma tumour suppressor during cellular senescence. *Cancer Cell* **17:** 376-87.

Christofk HR, Vander Heiden MG, Wu N, Asara JM & Cantley LC (2008). Pyruvate kinase M2 is a phosphotyrosine-binding protein. *Nature* **452 (7184):** 181-6.

Chu WM, Wang Z, Roeder RG, Schmid CW (1997). RNA polymerase III transcription repressed by Rb through its interactions with TFIIIB and TFIIIC2. *J. Biol. Chem* **272:** 14755-61.

Clark JP, Cooper CS (2009). ETS gene fusions in prostate cancer. *Nat Rev Urol* 2009 **6:** 429-39.

Cleary AS, Leonard TL, Gestl SA & Gunther EJ (2014). Tumour cell heterogeneity maintained by cooperating subclones in Wnt-driven mammary cancers. *Nature* **508:** 113-7.

Colbert T & Hahn S (1992). A yeast TFIIB-related factor involved in RNA polymerase III transcription. *Genes & Dev.* **6:** 1940-9.

Coller HA, Grandori C, Tamayo P, Colbert T, Lander ES, Eisenman RN & Golub TR (2000). Expression analysis with oligonucleotide microarrays reveals that MYC regulates genes involved in growth, cell cycle, signalling and adhesion. *Procl Natl Acad Sci USA* **97:** 3260-5.

Conesa C, Ruotolo R, Soularue P, Simms TA, Donze D et al (2005). Modulation of yeast genome expression in response to defective RNA polymerase III-dependent transcription. *Mol Cell Biol* **25:** 8631-42.

Cooperberg MR, Moul JW & Carroll PR (2005). The changing face of prostate cancer. *J. Clin. Oncol* **10;23(32):** 8146-51.

Craft N, Chhor C, Tran C (1999). Evidence for clonal outgrowth of androgen-independent prostate cancer cells from androgen-dependent tumors through a two-step process. *Cancer Res* **59:** 5030-6.

Crick F (1968). The origin of the genetic code. *J. Mol. Biol.* **38:** 367-79.

Crick F (1970). Central dogma of molecular biology. *Nature* **227:** 561-3.

Crighton D, Woiwode A, Zhang C, Mandavia N, Morton J, Warnock L, Milner J, White R.J. & Johnson D (2003). P53 represses RNA polymerase III transcription by targeting TBP and inhibiting promoter occupancy by TFIIIB. *EMBO J.* **22**: 2810-20.

Dahia PL (2000). PTEN, a unique tumour suppressor gene. *Endocr. Relat. Cancer* **7:** 115-129.

Dakubo GD (2010) Chapter 2: The Warburg Phenomenon and Other Metabolic Alterations of Cancer Cells. In *Mitochondrial Genetics and Cancer.* 39- 66. © Springer-Verlag Berlin Heidelberg 2010.

Dall'Era MA, Albertsen PC, Bangma C, Carroll PR, Carter HB, Cooperberg MR, Freedland SJ, Klotz LH, Parker C & Soloway MS (2012). Active surveillance for Prostate Cancer: A systematic review of the literature. *Eur. Urol.* **62(6):** 976-83.

Daly NL, Arvanitis DA, Fairley JA, Gomez-Roman N, Morton JP, Graham SV, Spandidos DA & White RJ (2005). Deregulation of RNA polymerase III transcription in cervical epithelium in response to high-risk human papillomavirus. *Oncogene* **24**: 880-8.

D'Amico AV, Whittington R, Malkowicz SB, Fondurulia J, Chen MH, Tomaszewski JE & Wein A (1998). The combination of preoperative prostate specific antigen and postoperative pathological findings to predict prostate specific antigen outcome in clinically localised prostate cancer. *J. Urol* **160(6):** 2096-101.

Dang CV, Kim JW, Gao P, Yustein J (2008). The interplay between MYC and HIF in cancer. *Nat Rev Cancer* **8:** 51-6.

Dang CV (2012). MYC on the path to cancer. *Cell* **149:** 22-35.

Dawson SJ, Tsui DW, Murtaza M, Biggs H, Rueda OM, Chin SF(2013). Analysis of circulating tumour DNA to monitor metastatic breast cancer. *N. Engl. J. Med* **368:** 1199-209.

de Bono JS, Oudard S, Ozguroglu M, Hansen S, Malchiels JP, Kocak I, Gravis G, Bodrogi I, Mackenzie MJ, Shen L et al; TROPIC investigators (2010). Prednisolone plus cabazitaxel or mitoxantrone for metastatic castration-resistant prostate cancer progressing after docetaxel treatment: a randomised open-label trial. *Lancet* **376:** 1147-54.

de Bono JS, Logothetis C, Molina A, Fizazi K, North S, Chu L, Chi K, Jones R, Goodman O, Saad Fred, Staffurth J, Mainwaring P, Harland S, Flaig T, Hutson T, Pharm D, Cheung T, Patterson H, Hainsworth J, Ryan C, Sternberg C, Ellard S, Flechon A, Saleh M, Scholz M, Efstathiou E, Zivi A, Bianchini D, Loriot Y, Chieffo N, Kheoh T, Haqq C and Scher H (COU-AA-301 Investigators) (2011). Abiraterone and increased survival in Metastatic Prostate Cancer. *NEJM* **364:** 1995-2005.

DeCaprio JA, Ludlow JW, Lynch D, Furukawa Y, Griffin J, Piwnica-Worms H, Huang CM, Livingston DM (1989). The product of the retinoblastoma susceptibility gene has properties of a cell cycle regulatory element. *Cell* **58:** 1085-95.

Deisenroth C, Zhang Y (2010). Ribosome biogenesis surveillance: probing the ribosomal protein-Mdm2-p53 pathway. *Oncogene* **29**: 4253-60.

De Marzo AM, Platz EA, Sutcliffe S, Xu J, Gronberg H, Drake CG, Nakai Y, Isaacs WB & Nelson WG (2007). Inflammation in prostate carcinogenesis. *Nature Reviews Cancer* **7:** 256-69.

Demir A, Cecen K, Karadag MA, Kocaaslan R & Turkeri L (2014). The course of metastatic prostate cancer under treatment. *SpringerPlus* **3:** 725.

Deng CX (2006). BRCA1: cell cycle checkpoint, genetic instability, DNA damage response and cancer evolution. *Nucleic Acids Res* **34 (5):** 1416-26.

Derenzini M, Betts CM, Ceccarelli C, Eusebi V (1986). Ultrasound organization of nucleoli in benign nevi and malignant melanomas. *Virchows Arch B-cell Pathol. Incl. Mol Pathol* **52:** 343-52.

Dhahbi JM, Spindler SR, Atamna H, Yamakawa A, Boffelli D, Mote P & Martin DI (2013). 5' tRNA halves are present as abundant complexes in serum, concentrated in blood cells and modulated by aging and calorie restriction. *BMC Genomics* **14:** 298.

Dhahbi JM, Spindler SR, Atamna H, Boffelli D & Martin DI (2014). Deep sequencing of serum small RNAs identifies patterns of 5' tRNA half and YRNA fragment expression associated with breast cancer. *Biomark Cancer* **6:** 37-47.

Di Cristofano A, Pesce B, Cordon-Cardo C & Pandolfi PP (1998). Pten is essential for embryonic development and tumour suppression. *Nature Genetics* **19(4):** 348-55.

Di Cristofano A and Pandolfi PP (2000). The multiple roles of PTEN in tumor suppression. *Cell* **100:** 387-90.

Dieci G, Fiorino G, Castelnuovo M, Teichmann M & Pagano A (2007). The expanding RNA polymerase III transcriptome. *Trends Genet.* **23:** 614-22.

Ding Z, Wu CJ, Jaskelioff M, Ivanova E, Kost-Alimova M, Protopopov A, Chu GC, Wang G, Lu X, Labrot ES, Hu J, Wang W, Xiao Y, Zhang H, Zhang J, Gan B, Perry SR, Jiang S, Li L, Horner JW, Wang YA, Chin L, DePinho RA (2012). Telomerase reactivation following telomere dysfunction yields murine prostate tumours with bone metastases. *Cell* **148 (5):** 896-907.

Dittmar KA, Goodenbour JM & Pan T (2006). Tissue-specific differences in human transfer RNA expression. *PLoS Genet.* **2:** 2107-15.

Donati G, Bertoni S, Brighenti E, Vici M, Trere D, Volarevic S, Montanaro L & Derenzini M (2011). The balance between rRNA and ribosomal protein synthesis up- and downregulates the tumour suppressor p53 in mammalian cells. *Oncogene* **30:** 3274-88.

Dong JT (2001). Chromosomal deletions and tumor suppressor genes in prostate cancer. *Cancer Metastasis Rev* **20:** 173-93.

Dong XY, Chen C, Sun X, Guo P, Vessella RL, Wang RX et al (2006). FOXO1A is a candidate for the 13q14 tumour suppressor gene inhibiting androgen receptor signalling in prostate cancer. *Cancer Res* **66:** 6998-7006.

Doyen J, Alix-Panabieres C, Hofman P, Parks SK, Chamorey E, Naman H (2012). Circulating tumour cells in prostate cancer: a potential surrogate marker of survival. *Crit. Rev. Oncol. Hematol.* **81**: 241-56.

Drygin D, Siddiqui-Jain A, O'Brien S, Schwaebe M, Lin A, Bliesath J, Ho CB, Proffitt C, Trent K, Whitten JP, Lim JK, Von Hoff D, Anderes K & Rice WG (2009). Anticancer activity of CX-3543: a direct inhibitor of rRNA biogenesis. *Cancer Res* **69**: 7653-61.

Drygin D, Rice WG & Grummt I (2010). The RNA polymerase I transcription machinery: an emerging target for the treatment of cancer. *Annu. Rev. Pharmacol. Toxicol.* **50**: 131-156.

Drygin D, Lin A, Bliesath J, Ho CB, O'Brien SE, Proffitt C, Omori M, Haddach M, Schwaebe MK, Siddiqui-Jain A, Streiner N, Quin JE, Sanij E, Bywater MJ, Hannan RD, Ryckman D, Anderes K, Rice WG (2011). Targeting RNA Polymerase I with an oral small molecule CX-5461 inhibits ribosomal RNA synthesis and solid tumour growth. *Cancer Res* **71:** 1418-30.

Drygin D, O'Brien SE, Hannan RD, McArthur GA & Von Hoff DD (2014). Targeting the nucleolus for cancer specific activation of p53. *Drug Discovery Today* **19 (3):** 259-65.

Dundr M, Misteli T, Olson MO (2000). The dynamics of post-mitotic reassembly of the nucleolus. *J. Cell Biol.* **150:** 433-46.

Duttke SH (2014). RNA polymerase III accurately initiates transcription from RNA polymerase II promoters *in vitro*. *J. Biol. Chem.* **289(29):** 20396-404.

Dyson N (1998). The regulation of E2F by pRB-family proteins. *Genes Dev* **12:** 2245-62.

Edwards J, Krishna NS, Witton CJ, Bartlett JM (2003). Gene amplifications associated with the development of hormone-resistant prostate cancer. *Clin Cancer Res* **9:** 5271-81.

Ellwood-Yen K, Graeber TG, Wongvipat J, Iruela-Arispe ML, Zhang J, Matusik R (2003). MYC-driven murine PC shares molecular features with human prostate tumours. Cancer Cell **4:** 223-38.

Elstrom RL, Bauer DE, Buzzai M, Karnauskas R, Harris MH, Plas DR, Zhuang H, Cinalli RM, Alavi A, Rudin CM & Thompson CB (2004). Akt stimulates aerobic glycolysis in cancer cells. *Cancer Res* **64:** 3892-9.

Emara MM, Ivanov P, Hickman T, Dawra N, Tisdale S, Kedersha N, Hu GF & Anderson P (2010). Angiogenin-induced tRNA-derived stress-induced RNAs promote stress-induced stress granule assembly. *J. Biol Chem* **285 (**14): 10959-68.

Fairley JA, Scott PH & White RJ (2003). TFIIIB is phosphorylated, disrupted and selectively released from tRNA promoters during mitosis *in vivo*. *EMBO J.* **22:** 5841-50.

Fedoriw AM, Starmer J, Yee D, Magnuson T (2013). Nucleolar association and transcriptional inhibition through 5S rDNA in mammals. *PLoS Genet*. **8:** 11.

Feldman BJ, Feldman D (2001). The development of androgen-independent prostate cancer. *Nat Rev Cancer* **1:** 34-45.

Felton-Edkins ZA & White RJ (2002). Multiple mechanisms contribute to the activation of RNA polymerase III transcription in cells transformed by papovaviruses. *J. Biol. Chem* **277(50):** 48182-91

Felton-Edkins ZA, Fairley JA, Graham EL, Johnston IM, White RJ. & Scott PH (2003a). The mitogen –activated protein kinase ERK induces tRNA synthesis by phosphorylating TFIIIB. *Embo J* **22:** 2422-32.

Felton-Edkins ZA, Kenneth NS, Brown TR, Daly NL, Gomez-Roman N (2003b). Direct regulation of RNA polymerase III transcription by RB, p53 and c-MYC. *Cell Cycle* **2:** 181-4.

Feng W, Zhang HB, Wang YM, Hu L (2015). Correlation of FOXA1 with the malignancy and progression of prostate cancer. *Zhonghua Nan Ke Xue* **21(5):** 414-9.

Fidler IJ (2003). The pathogenesis of cancer metastases: the seed and soil hypothesis revisited. *Nature Rev Cancer* **3:** 453-8.

Fine SW & Epstein JIA (2008). A contemporary study correlating prostate needle biopsy and radical prostatectomy Gleason score. *J. Urol.* **179:** 1335-9.

Fizazi K, Carducci M, Smith M, Damiao R, Brown J, Karsh L, Milecki P, Shore N, Rader M, Wang H, Jiang Q, Tadros S, Dansey R, Goessl C (2011). Denosumab versus zoledronic acid for treatment of bone metastases in men with castration-resistant prostate cancer: a randomised, double blind study. *Lancet* **377(9768):** 813-22.

Floc'h N, Kinkade CW, Kobayashi T, Aytes A, Lefebvre C, Mitrofanova A, Cardiff RD, Califano A, Shen MM & Abate-Shen C (2012). Dual targeting of the Akt/mTOR signalling pathway inhibits castration-resistant prostate cancer in a genetically engineered mouse model. *Cancer Res* **72 (17):** 4483-93

Freeman D, Lesche R, Kertesz N, Wang S, Li G, Gao J, Groszer M, Martinez-Diaz H, Rozengurt N, Thomas G, Liu X, Wu H (2006). Genetic background controls tumor development in PTEN-deficient mice. *Cancer Res* **66:** 6492-6.

Friday B, Lassere Y, Meyers CA, Mita A, Abbruzzese JL, Thomas MB (2012). A phase I study to determine the safety and pharmacokinetics of intravenous administration of TAS-106 once per week for three consecutive weeks every 28 days in patients with solid tumours. *Anticancer Res* **32**: 1689-96.

Furuta H, Iwasaki N, Oda N, Hinokio Y, Horikawa Y, Yamagata K, Yano N, Sugahiro J, Ogata M, Ohgawara H, Omori Y, Iwamoto Y & Bell GI (1997). Organisation and partial sequence of hepatocyte nuclear factor-4-alpha/MODY1 gene and identification of a missense mutation, R127W, in a Japanese family with MODY. *Diabetes* **46:** 1652-57.

Fukushima H, Abe T, Sakamoto K, Tsujimoto H, Mizuarai S & Oie S (2014). 3'-Ethynylcytidine, an RNA polymerase inhibitor, combined with cisplatin exhibits a potent synergistic growth-inhibitory effect via Vaults dysfunction. *BMC Cancer* **14:** 562.

Gao H, Ouyang X, Banach-Petrosky WA, Gerald WL, Shen MM, Abate-Shen C (2006a). Combinatorial activities of Akt and B-Raf/Erk signalling in a mouse model of androgen independent prostate cancer. *Proc Natl Acad Sci USA* **103:** 14477-82.

Gao H, Ouyang X, Banach-Petrosky WA, Shen MM & Abate-Shen C (2006b). Emergence of androgen independence at early stages of prostate cancer progression in *Nkx3.1; Pten* mice. *Cancer Res* **66 (16):** 7929-33.

Gao M, Patel R, Ahmad I, Fleming J, Edwards J, McCracken S, Sahadevan K, Seywright M, Norman J, Sansom O & Leung HY (2012). SPRY2 loss enhances ErbB trafficking and PI3K/AKT signalling to drive human and mouse prostate carcinogenesis. *EMBO Mol.Med* **4 (8):** 776-90.

Garcia MJ, Pole JC, Chin SF, Teschendorff A, Naderi A, Ozdag H, Vias M, Kranjac T, Subkhankulova T, Paish C, Ellis I, Brenton JD, Edwards PA, Caldas C (2005). A 1 Mb minimal amplicon at 8p11-12 in breast cancer identifies new candidate oncogenes. *Oncogene* **24(33):** 5235-45.

Geiduschek EP & Kassavetis GA (2001). The RNA polymerase III transcription apparatus. *J. Mol. Biol* **310(1):** 1-26.

Gelmann EP (2002). Molecular biology of the androgen receptor. *J. Clin Oncol* **20**: 3001-15.

Ghosal K, Jacob ST (1997). An alternative molecular mechanism of action of 5-fluorouracil, a potent anti-cancer drug. *Biochem Pharmacol.* **53:** 1569-75.

Gingold H, Tehler D, Christoffersen NR, Nielsen MM, Asmar F, Kooistra SM, Christophersen NS, Christensen LL, Borre M, Sorensen KD, Andersen LD, Andersen CL, Hulleman E, Wurdinger T, Ralfkiaer E, Helin K, Gronbaek K, Orntoft T, Waszak SM, Dahan O, Pedersen JS, Lund AH, Pilpel Y (2014). A dual program for translation regulation in cellular proliferation and differentiation. *Cell* **158:** 1281-92.

Gingrich JR, Barrios RJ, Kattan MW, Nahm HS, Finegold MJ & Greenberg NM (1997). Androgen independent prostate cancer progression in TRAMP model. *Cancer Res.* **57 (21):** 4687-91.

Gingrich JR et al (1996). Metastatic prostate cancer in a transgenic mouse. *Cancer Res* **56 (18):** 4096-102.

Gjidoda A & Henry RW (2013). RNA polymerase III repression by the retinoblastoma tumor suppressor protein. *Biochim. Biophys. Acta* **1829:** 385-92.

Goeze A, Schluns K, Wolf G, Thasler Z, Petersen S & Petersen I (2002). Chromosomal imbalances of primary and metastatic lung adenocarcinomas. *J. Pathol* **196:** 8-16.

Goldstein A, Huang J, Guo C, Garraway I & Witte O (2010). Identification of a cell of origin for human prostate cancer. *Science* **329** (5991): 568-71.

Gomez-Roman N, Grandori C, Eisenman N & White R.J (2003). Direct activation of RNA polymerase III transcription by c-MYC. *Nature* **421**: 290-4.

Gomez-Roman N, Felton-Edkins ZA, Kenneth NS, Goodfellow SJ, Athineos D, Zhang JX, Ramsbottom BA, Innes F, Kantidakis T, Kerr ER, Brodie J, Grandori C & White RJ (2006). Activation by c-MYC of transcription by RNA Pol I, II and III. *Biochem Soc Symp.* **73:** 141-54.

Goodfellow SJ, Innes F, Derblay LE, MacLellan WR, Scott PH & White RJ (2006). Regulation of RNA polymerase III transcription during hypertrophic growth. *EMBO J.* **25:** 1522-33.

Goodfellow SJ & Zomerdijk (2012). Basic mechanisms in RNA polymerase I transcription of the ribosomal RNA genes. *Subcell. Biochem.* **61:** 211-36.

Gosselaar C, Roobol MJ, Roemeling S & Schroder FH (2008). The role of the digital rectal examination in subsequent screening visits in the European randomised study of screening for prostate cancer (ERSPC), Rotterdam. *Eur. Urol.* **54:** 581-8.

Gottesfeld JM, Wolf VJ, Dang T, Forbes DJ & Hartl P (1994). Mitotic repression of RNA polymerase III transcription in vitro mediated by phosphorylation of a TFIIIB component. *Science* **263:** 81-4.

Gottesfeld JM, Johnson DL & Nyborg JK (1996). Transcriptional activation of RNA polymerase III-dependent genes by the human T-cell leukemia virus type 1 tax protein. *Mol Cell Biol* **16(4):** 1777-85.

Graczyk D, White RJ & Ryan KM (2015). Involvement of RNA polymerase III in immune responses. *Mol. Cell Biol.* **35:** 1848-59.

Grandori C, Cowley SM, James LP, Eisenman RN (2000). The MYC/Max/Mad network and the transcriptional control of cell behaviour. *Annu Rev Cell Dev Biol* **16:** 653-99.

Grasso CS, Wu YM, Robinson DR, Cao X, Dhanasekaran SM, Khan AP, Quist MJ, Jing X, Lonigro RJ, Brenner JC, Asangani IA, Ateeq B, Chun SY, Siddiqui J, Sam L, Anstett M, Mehra R, Prensner JR, Palanisamy N, Ryslik GA, Vandin F, Raphael BJ, Kunju LP, Rhodes DR, Pienta KJ, Chinnaiyan AM, Tomlins SA (2012). The mutational landscape of lethal castration-resistant prostate cancer. *Nature* **487 (7406):** 239-43.

Greaves M & Maley CC (2012). Clonal evolution in cancer. *Nature* **481:** 306-13.

Grewal SS, Li L, Orian A, Eisenman RN, Edgar BA (2005). MYC-dependent regulation of ribosomal RNA synthesis during *Drosophila* development. *Nat Cell Biol.* **7:** *295*-302.

Grewal SS (2015). Why should cancer biologists care about tRNAs? tRNA synthesis, mRNA translation and the control of growth. *Biochimica Biophys Acta* **1849 (7):** 898-907.

Grieshammer U, Agarwal P, Martin GR (2008). A Cre transgene active in developing endodermal organs, heart, limb and extra-ocular muscle. *Genesis* **46:** 69-73

Grummt I (2010). Wisely chosen paths – regulation of rRNA synthesis. *FEBS J.* **277:** 4626-39.

Gundem G, Van Loo P, Kremeyer B, Alexandrov L, Tubio J, Papaemmanuil E, Brewer D, Kallio H, Hognas G, Annala M, Kivinummi K, Goody V, Latimer C, O'Meara S, Dawson K, Isaacs W, Emmert-Buck M, Nykter M, Foster C, Kote-Jarai Z, Easton D, Whitaker H. ICGC Prostate UK Group, Neal D, Cooper C, Eeles R, Visakorpi T, Campbell P, McDermott U, Wedge D & Bova S (2015). The evolutionary history of lethal metastatic prostate cancer. *Nature* **520:** 353-57.

Gupta GP & Massague J (2006). Cancer metastasis: building a framework. *Cell* **127**: 679-95.

Haddach M, Schwaebe MK, Michaux J, Nagasawa J, O'Brien SE, Whitten JP, Pierre F, Kerdoncuff P, Darjania L, Stansfield R, Drygin D, Anderes K, Proffitt C, Bliesath J, Siddiqui-Jain A, Omori M, Huser N, Rice WG & Ryckman DM (2012). Discovery of CX-5461, the first direct and selective inhibitor of RNA polymerase I for cancer therapeutics. *ACS Med. Chem. Lett***. 3:** 602-6.

Hah N, Danko CG, Core L, Waterfall JJ, Siepel A, Lis JT, Kraus WL (2011). A rapid, extensive and transient transcriptional response to estrogen signalling in breast cancer cells. *Cell* **145:** 622-34.

Hah N & Kraus WL (2014). Hormone-regulated transcriptomes: Lessons learned from estrogen signalling pathways in breast cancer cells. *Molecular and Cellular Endocrinology* **382:** 652-64.

Hammond-Thelin LA, Thomas MB, Iwasaki M, Abbruzzese JL, Lassere Y, Meyers CA, Hoff P, de Bono J, Norris J, Matsushita H, Mita A, Rowinsky EK (2012). Phase I and pharmacokinetic study of 3'-C-ethynylcytidine TAS-106, an inhibitor of RNA polymerase I, II and III, in patients with advanced solid malignancies. *Invest New Drugs* **30:** 316-26.

Hanahan D & Weinberg RA (2000). The hallmarks of cancer. *Cell* **100:** 57-70.

Hanahan D & Weinberg RA (2011). Hallmarks of cancer: the next generation. *Cell* **144**: 646-74.

Hannan KM, Brandenburger Y, Jenkins A, Sharkey K, Cavanaugh A, Rothblum L, Moss T, Poortinga G, McArthur GA, Pearson RB, Hannan RD (2003). mTOR-dependent regulation of ribosomal gene transcription requires S6K1 and is mediated by phosphorylation of the carboxy- terminal activation domain of the nucleolar transcription factor UBF. *Mol. Cell Biol.* **23**: 8862-77.

Hannan KM, Hannan RD, Smith SD, Jefferson LS, Lun M & Rothblum LI (2000). Rb and p130 regulate polymerase I transcription: Rb disrupts the interaction between UBF and SL-1. *Oncogene* **19(43):** 4988-99.

Hattori H, Tanaka M, Fukushima M, Sasaki T, Matsuda A (1996). Nucleosides and nucleotides. 158. 1-(3-C-ethynyl-beta-D-ribo-pentofuranosyl)uracil, and their nucleobase analogues as new potential multifunctional anti-tumour nucleosides with a broad spectrum of activity. *J. Med Chem* **39:** 5005-11.

Hein N (2011). Inhibition of RNA Pol I transcription by CX-5461 as a therapeutic strategy for the cancer specific activation of p53 in MLL-rearranged AML. ASH abstract. (https://ash.confex.com/ash/2011/webprogram/Paper42896.html)

Hirsch H, Jawdekar G, Lee K, Gu L & Henry R (2004). Distinct mechanisms for repression of RNA polymerase III transcription by the retinoblastoma tumour suppressor protein. *Mol. Cell Biol.* **24 (13):** 5989-99.

Hijiya N, Ness KK, Ribeiro RC & Hudson MM (2009). Acute leukaemia as a secondary malignancy in children and adolescents: current findings and issues. *Cancer* **115:** 23-35.

Holcomb IN, Grove DI, Kinnunen M, Friedman CL, Gallaher IS, Morgan TM et al (2008). Genomic alterations indicate tumour origin and varied metastatic potential of disseminated cells from prostate cancer patients. *Cancer Res* **68:** 5599-608.

Hollenhorst PC, Paul L, Ferris MW & Graves B (2011). The ETS gene ETV4 is required for anchorage-independent growth and a cell proliferation gene expression program in PC3 prostate cells. *Genes & Cancer* 1 (10): 1044-52.

Honda S, Loher P, Shigematsu M, Palazzo JP, Suzuki R, Imoto I, Rigoutsos I & Kirino Y (2015). Sex hormone-dependent tRNA halves enhance cell proliferation in breast and prostate cancers. *PNAS* **112 (29):** E3816- 25.

Horwich A, Parker C, de Reijke T & Kataja V (2013). Prostate cancer: ESMO clinical practice guidelines for diagnosis, treatment and follow up. *Annals of Oncology* **24 (6):** 1-9.

Hsieh AC, Costa M, Zollo O, Davis C, Feldman ME, Testa JR, Meyuhas O, Shokat KM, Ruggero D (2010). Genetic dissection of the oncogenic mTOR pathway reveals druggable addiction to translational control via 4EBP-eIF4E. *Cancer Cell* **17:** 249-61.

Huggins C, Stephens R & Hodges CV (1941). Studies on prostate cancer: 2. The effects of castration on advanced carcinoma of the prostate gland. *Arch Surg* **43:** 209.

Hu P, Samudre K, Wu S, Sun Y, Hernandez N (2004). CK2 phosphorylation of BDP1 executes cell cycle-specific RNA polymerase III transcription repression. *Mol Cell* **16:** 81-92.

Huo L & Scarpulla RC (2001). Mitochondrial DNA instability and peri-implantation lethality associated with targeted disruption of NRF1 in mice. *Mol. Cell Biol.* **21(2):** 644-54.

Imamura Y, Sakamoto S, Endo T, Utsumi T, Fuse M, Suyama T (2012). FOXA1 promotes tumor progression in prostate cancer via the insulin-like growth factor binding protein 3 pathway. *PLoS One* **7:** e42456.

Irshad S & Abate-Shen C (2013). Modelling prostate cancer in mice: Something old, something new, something premalignant, something metastatic. *Cancer Metastasis Rev* **32(1-2):** 109-122.

Ishiguro A & Aruga J (2008). Functional role of Zic2 phosphorylation in transcriptional regulation. *FEBS Lett.* **582(2):** 154-8.

Ivanov P, Emara MM, Villen J, Gygi SP, Anderson P (2011). Angiogenin-induced tRNA fragments inhibit translation initiation. *Mol Cell* **43(4)**: 613-623.

Jackson SP, Bartek J (2009). The DNA damage response in human biology and disease. *Nature* **461:** 1071-8.

Jeronimo C, Bastian PJ, Bjartell A, Carbone GM, Catto JW, Clark SJ, Henrique R, Nelson WG, Shariat SF (2011). Epigenetics in prostate cancer: biologic and clinical relevance. *Eur Urol* **60(4):** 753-66.

Johnson LF, Abelson HT, Green H, Penman S (1974). Changes in RNA in relation to growth of the fibroblast. 1. Amounts of mRNA, rRNA and tRNA in resting and growing cells. *Cell* **1**: 95-100.

Johnson SA, Dubeau L, Kawalek M, Dervan A, Schonthal AH, Dang CV and Johnson DL (2003). Increased expression of TATA-binding protein, the central transcription factor, can contribute to oncogenesis. *Mol Cell Biol* **23(9):** 3043-51.

Johnson SA, Dubeau, L. & Johnson D (2008). Enhanced RNA polymerase III-dependent transcription is required for oncogenic transformation. *J Biol Chem* **283**: 19184-91.

Johnson SS, Zhang C, Fromm J, Willis IM, Johnson DL (2007). Mammalian MAF1 is a negative regulator of transcription by all three nuclear RNA polymerases. *Mol Cell* **26:** 367-79.

Julka PK, Chacko RT, Nag S, Parshad R, Nair A, Oh DS, Hu Z, Koppiker CB, Nair S, Dawar R, Dhindsa N, Miller ID, Ma D, Lin B, Awasthy B, Perou CM (2008). A phase II study of sequential neoadjuvant gemcitabine plus doxorubicin followed by gemcitabine plus cisplatin in patients with operable breast cancer: prediction of response using molecular profiling. *Br J Cancer* **98:** 1327-35.

Kaighn ME, Narayan KS, Ohnuki Y, Lechner JF & Jones LW (1979). Establishment and characterisation of a human carcinoma cell line (PC3). *Invest Urol* **17:** 16-23.

Kaina B (2003). DNA damage-triggered apoptosis: critical role of DNA repair, double-strand breaks, cell proliferation and signalling. *Biochem Pharmacol* **66:** 1547-54.

Kalita K, Makonchuk D, Gomes C, Zheng JJ, Hetman M (2008). Inhibition of nucleolar transcription as a trigger for neuronal apoptosis. *J. Neuro-chem* **105:** 2286-99.

Kantidakis T, Ramsbottom BA, Birch JL, Dowding SN & White RJ (2010). Mtor associates with TFIIIC, is found at tRNA and 5S rRNA genes, and targets their repressor MAF1. *PNAS* **107** (26): 11823-8.

Kasper S, Rennie PS, Bruchovsky N, Sheppard PC, Cheng H (1994). Cooperative binding of androgen receptors to two DNA sequences is required for androgen induction of the probasin gene. *J. Biol. Chem.* **269:** 31763-9.

Kassavetis GA & Geiduschek EP (2006). Transcription factor TFIIIB and transcription by RNA polymerase III. *Biochem. Soc. Trans*. **34**: 1082-7.

Kazuno H, Fujioka A, Fukushima M, Wataya Y, Matsuda A, Sasaki T (2009). ECyd, TAS-106, a novel potent inhibitor of RNA polymerase, potentiates the cytotoxicity of CDDP in human cancer cells both in vitro and in vivo. *Int J Oncol* **34:** 1373-80.

Kenneth NS, Marshall L & White RJ (2008). Recruitment of RNA polymerase III in vivo. *Nucleic Acids Research* **36** (11): 3757-64.

Kim MJ, Cardiff RD, Desai N, Banach-Petrosky WA, Parsons R, Shen MM & Abate-Shen C (2002). Cooperativity of Nkx3.1 and Pten loss of function in a mouse model of prostate carcinogenesis. *Proc Natl Acad Sci* **99:** 2884-9.

Kuperwasser C, Hurlbut GD, Kittrell FS, Dickinson ES, Laucirica R, Medina D, Naber SP, Jerry DJ (2000). Development of spontaneous mammary tumors in BALB/c p53 heterozygous mice. A model for Li-Fraumeni syndrome. *Am J Pathol* **157:** 2151-9.

Kurzrock R, Sherman SI, Ball DW, Forastiere AA, Cohen RB, Mehra R (2011). Activity of XL 184 (Cabozantinib) an oral tyrosine kinase inhibitor, in patients with medullary thyroid cancer. J Clin Oncol 29: 2660-6.

Kwak MK, Johnson DT, Zhu C, Lee SH, Ye DW, Luong R & Sun Z (2013). Conditional deletion of the *Pten* gene in the mouse prostate induces prostatic intraepithelial neoplasms at early ages but a slow progression to prostate tumors. *PLOS ONE* **8 (1):** 53476-88.

Larminie CG, Cairns CA, Mital R, Martin K, Kouzarides T, Jackson SP & White RJ (1997). Mechanistic analysis of RNA polymerase III regulation by the retinoblastoma protein. *EMBO J.* **16**: 2061-7.

Larminie CG, Sutcliffe JE, Tosh K, Winter AG, Felton-Edkins ZA, White RJ (1999). Activation of RNA polymerase III transcription in cells transformed by simian virus 40. *Mol Cell Biol* **19(7):** 4927-34.

Leary DJ & Huang S (2001). Regulation of ribosome biogenesis within the nucleolus. *FEBS Lett* **509:** 145-50.

Lee YS, Shibata Y, Malhotra A & Dutta A (2009). A novel class of small RNAs: tRNA-derived RNA fragments (tRFs). *Genes and Development* **23:** 2639-49.

Levy DS, Kahana JA, Kumar R (2009). AKT inhibitor, GSK690693, induces growth inhibition and apoptosis in acute lymphoblastic leukemia cell lines. *Blood* **113:** 1723-9.

Leung AKL, Trinkle-Mulcahy L, Lam YW, Andersen JS, Mann M, Lamond AI, NOPdb: Nucleolar Proteome Database, *Nucleic Acids Res* **34:** D218-20.

Li LY, Chen H, Hsieh YH, Wang YN, Chen YH, Chen HY, Chien PJ, Ma HT, Tsai HC, Lai CC, Sher YP, Lien HC, Tsai CH, Hung MC (2011). Nuclear ErbB2 enhances translation and cell growth by activating transcription of ribosomal RNA genes. *Cancer Res* **71:** 4269-79.

Lin C, Yang L, Tanasa B, Hutt K, Ju B, Ohgi K, Zhang J, Rose DW, Fu XD, Glass CK, Rosenfeld MG (2009). Nuclear receptor-induced chromosomal proximity and DNA breaks underlie specific translocations in cancer. *Cell* **139(6):** 1069-83.

Lin H & Yin H (2008). A novel epigenetic mechanism in *Drosophila* somatic cells mediated by Piwi and piRNAs. *Cold Spring Harb. Sym. Quant. Biol.* **73:** 273-81.

Linn DE, Bronson RT & Li Z (2015). Genetic interaction between Tmprss2-ERG gene fusion and Nkx3.1 loss does not enhance prostate tumorigenesis in mouse models. *PLoS ONE* 10 (3): e0120628.

Liu P, Li S, Gan L, Kao TP, Huang H (2008). A transcription-independent function of FOXO1 in inhibition of androgen-independent activation of the androgen receptor in prostate cancer cells. *Cancer Res* **68:** 10290-9.

Lockwood WW, Chari R, Coe BP, Thu KL, Garnis C, Malloff CA, Campbell J, Williams AC, Hwang D, Zhu CQ, Buys TPH, Yee J, English JC, MacAuley C, Tsao MS, Gazdar AF, Minna JD, Lam S & Lam WL (2010). Integrative genomic analyses identify BRF2 as a novel lineage-specific oncogene in lung squamous cell carcinoma. *PLOS Medicine* **7 (7):** e1000315.

Lomberk G & Urrutia R (2005). The family feud: turning off Sp1 by Sp1-like KLF proteins. *Biochem. J.* **392(1):** 1-11.

Long R, Morrissey C, Fitzpatrick J & Watson W (2005). Prostate epithelial cell differentiation and its relevance to the understanding of prostate cancer therapies. *Clinical Science* **108:** 1-11.

Lopez-Lazaro M (2008). The Warburg Effect: Why and how do cancer cells activate glycolysis in the presence of oxygen? *Anticancer Agents Med Chem* **8 (3):** 305-12.

Ludlow JW, Shon J, Pipas JM, Livingston DM, DeCaprio JA (1990). The retinoblastoma susceptibility gene product undergoes cell cycle-dependent dephosphorylation and binding to and release from SV40 large T cell. *Cell* **60:** 387-96.

Lui AY, True LD & LaTray L (1999). Analysis and sorting of prostate cancer cell types by flow cytometry. *Prostate* **40:** 192-9.

Lunenfeld B (2002). The ageing male: demographics and challenges. *World J. Urol* **20:** 11-16.

Luo JH, Yu YP, Cieply K, Lin F, Deflavia P, Dhir R, Finkelstein S, Michalopoulos G, Becich M (2002). Gene expression analysis of prostate cancers. *Mol. Carcinog.* **33(1):** 25-35.

Ma X, Ziel-van der Mde AC, Autar B, van der Korput HA, Vermeji M, van Duijn P, Cleutjens KB, de Krijger R, Krimpenfort P, Berns A, van der Kwast TH, Trapman J (2005). Targeted biallelic inactivation of Pten in mouse prostate leads to prostate cancer accompanied by increased epithelial cell proliferation but not by reduced apoptosis. *Cancer Res* **65(13):** 5730-9.

Muhlbauer KR, Grone HJ, Ernst T, Grone E, Tschada R, Hergenhahn M & Hollstein M (2003). Analysis of human prostate cancers and cell lines for mutations in the TP53 and KLF6 tumour suppressor genes. *Br. J. Cancer* **89(4):** 687-90.

MacCarty WC (1936). The value of the macronucleolus in the cancer problem. *Am J Cancer* **26:** 529-32.

Magee JA, Araki T, Patil S, Ehrig T, True L, Humphrey PA, Catalona WJ, WatsonMA & Milbrandt J (2001). Expression profiling reveals hepsin overexpression in prostate cancer. *Cancer Res* **61** (15): 5692-6.

Majumder PK, Yeh JJ, George DJ, Febbo PG, Kum J, Xue Q, Bikoff R, Ma H, Kantoff PW, Golub TR, Loda M, Sellers WR (2003). Prostate intraepithelial neoplasia induced by prostate restricted Akt activation: the MPAKT model. PNAS USA **100(13):** 7841-6.

Mamane Y, Petroulakis E, Rong L, Yoshida K, Wee Ler L & Sonenberg N (2004). eIF4E-from translation to transformation. *Oncogene* **23:** 3172-9.

Manning BD & Cantley LC (2007). AKT/PKB signalling: navigating downstream. *Cell* **129(7):** 1261-74.

Marshall L, Rideout EJ & Grewal SS (2012). Nutrient/TOR dependent regulation of RNA polymerase III controls tissue and organismal growth in *Drosophila.* *EMBO J.* **31:** 1916-30.

Marshall L. & White RJ (2008). Non-coding RNA production by RNA Pol III is implicated in cancer. *Nature Reviews Cancer* **8:** 911-14.

Martens-Uzunova ES, Olvedy M & Jengster G (2013). Beyond microRNA – Novel RNAs derived from small noncoding RNA and their implications in cancer. *Cancer Lett* **340:** 201-211.

Martens-Uzunova ES, Hoogstrate Y, Kalsbeek A, Pigmans B, Vredenbregt-van den Berg M, Dits N, Nielsen SJ, Baker A, Visakorpi T, Bangma C & Jenster G (2015). C/D-box snoRNA-derived RNA production is associated with malignant transformation and metastatic progression in prostate cancer. *Oncotarget* **6 (19):** 17430-44.

Masumori N, Thomas TZ, Chaurand P, Case T, Paul M, Kasper S, Caprioli RM, Tsukamoto T, Shappell SB & Matusik RJ (2001). A probasin-large T antigen transgenic mouse line develops prostate adenocarcinoma and neuroendocrine carcinoma with metastatic potential. *Cancer Res* **61:** 2239-49.

Matoba S, Kang JG, Patino WD, Wragg A, Boehm M, Gavrilova O, Hurley PJ, Bunz F & Hwang PM (2006). P53 regulates mitochondrial respiration. *Science* **312:** 1650-3.

McFadden DG, Papagiannakopoulos T, Taylor-Weiner A, Stewart C, Carter SL, Cibulskis K, Bhutkar A, McKenna A, Dooley A, Vernon A, Sougnez C, Malstrom S, Heimann M, Park J, Chen F, Farago AF, Dayton T, Shefler E, Gabriel S, Getz G, Jacks T (2014). Genetic and clonal dissection of murine small cell lung carcinoma progression by genome sequencing. *Cell* **156(6):** 1298-1311

McMenamin ME, Soung P, Perera S, Kaplan I, Loda M, Sellers WR (1999). Loss of PTEN expression in paraffin-embedded primary prostate cancer correlates with high Gleason score and advanced stage. *Cancer Res* **59(17):** 4291-6.

McStay B & Grummt I (2008). The epigenetics of rRNA genes: from molecular to chromosome biology. *Annu. Rev. Cell Dev. Biol.* **24:** 131-57.

Mei YP, Liao JP, Shen J, Yu L, Liu BL, Liu L, Li RY, Ji L, Dorsey SG, Jiang ZR, Katz RL, Wang JY & Jiang F (2012). Small nucleolar RNA 42 acts as an oncogene in lung tumorigenesis. *Oncogene* **31:** 2794-804.

Meike S, Yamamori T, Yasui H, Eitaki M, Matsuda A, Morimatsu M, Fukushima M, Yamasaki Y, Inanami O (2011). A nucleoside anticancer drug, 1-(3-C-ethynyl-beta-D-ribo-pentofuranosyl)cytosine (TAS-106) sensitises cells to radiation by suppressing BRCA2 expression. *Mol Cancer* **10**: 92.

Melchor L, Garcia MJ, Honrado E, Pole JC, Alvarez S, Edwards PA, Caldas C, Brenton JD, Benitez J (2007). Genomic analysis of the 8p11-12 amplicon in familial breast cancer. *Int J Cancer* **120 (3):** 714-7.

Mirzayans R, Severin D, Murray D (2006). Relationship between DNA double-strand break rejoining and cell survival after exposure to ionizing radiation in human fibroblast strains with differing ATM/p53 status: implications for evaluation of clinical radiosensitivity. *Int J Radiat Oncol Biol Phys* **66:** 1498-1505.

Mohler JL, Gregory CW, Ford OH 3rd, Kim D, Weaver CM, Petrusz P, Wilson EM, French FS (2004). The androgen axis in recurrent prostate cancer. *Clin. Cancer Res* **10(2):** 440-8.

Morton JP, Kantidakis T, White RJ (2007). RNA polymerase III transcription is repressed in response to the tumour suppressor ARF. *Nucleic Acids Res* **35(9):** 3046-52.

Moss T, Langlois F, Gagnon-Kugler T, Stefanovsky V (2007). A housekeeper with power of attorney: the rRNA genes in ribosome biogenesis. *Cell Mol Life Sci* **64(1):** 29-49.

Murata D, Endo Y, Obata T (2004). A crucial role of uridine/cytidine kinase 2 in antitumor activity of 3'-ethynyl nucleosides. *Drug Metab. Dispos.* **32:** 1178-82.

Murayama A (2008). Epigenetic control of rDNA loci in response to intracellular energy status. *Cell* **133:** 627-39.

Naing A, Fu S, Zinner RG, Wheeler JJ, Hong DS, Arakawa K, Falchook GS, Kurzrock R (2014). Phase I dose-escalating study of TAS-106 in combination with carboplatin in patients with solid tumors. *Invest New Drugs* **32:** 154-9.

Nam NA (2013). RNA Polymerase III transcription deregulation: a study on Brf1 overexpression in prostate cancer. PhD thesis, University of Glasgow.

Nanni S, Priolo C, Grasselli A, D'Eletto M, Merola R, Moretti F, Gallucci M, De Carli P, Sentinelli S, Cianciulli AM, Mottolese M, Carlini P, Arcelli D, Helmer-Citterich M, Gaetano C, Loda M, Pontecorvi A, Bacchetti S, Sacchi A & Farsetti A (2006). Epithelial-restricted gene profile of primary cultures from human prostate tumors: a molecular approach to predict clinical behaviour of prostate cancer. *Mol Cancer Res.* **4(2):** 79-92.

Negi S & Brown P (2015). rRNA synthesis inhibitor, CX-5461, activates ATM/ATR pathway in acute lymphoblastic leukaemia arrests cells in G2 phase and induce apoptosis. *Oncotarget* **6 (20):** 18094-104.

Nesbit CE, Tersak JM, Prochownik EV (1999). MYC oncogenes and human neoplastic disease. *Oncogene* **18:** 3004-16.

Nguyen le XT, Mitchell BS (2013). Akt activation enhances ribosomal RNA synthesis through casein kinase II and TIF-IA. *Procl Natl Acad Sci USA* **110:** 20681-6.

Nikitina TV, Tischenko LI & Schulz WA (2011). Recent insights into regulation of transcription by RNA polymerase III and the cellular functions of its transcripts. *Bio chem* **392:** 395-404.

Norton JT, Pollock CB, Wang C, Schink JC, Kim JJ, Huang S (2008). Perinucleolar compartment prevalence is a phenotypic pancancer marker of malignancy. *Cancer* **113:** 861-869.

Nouri M, Ratther E, Stylianou N, Nelson CC, Hollier BG & Williams ED (2014). Androgen-targeted therapy-induced epithelial mesenchymal plasticity and neuroendocrine transdifferentiation in prostate cancer: an opportunity for intervention. *Front. Oncol.* **4:** 370-6.

Nowell PC (1976). The clonal evolution of tumour cell populations. *Science* **194:** 23-28.

Numoto M, Yokoro K, Yanagihara K, Kamiya K & Niwa O (1995). Over-expressed ZF5 gene product, a c-MYC binding protein related to GL 1-Kruppel protein, has a growth suppressive activity in mouse cell lines. *Jpn J. Cancer Res.* **86(3):** 277-83.

Odom DT, Zizlsperger N, Gordon DB, Bell GW, Rinaldi NJ, Murray HL, Volkert TL, Schreiber J, Rolfe PA, Gifford DK, Fraenkel E, Bell GI, Young RA (2004). Control of pancreas and liver gene expression by HNF transcription factors. *Science* **303:** 1378-81.

Oler AJ, Alla RK, Roberts DN, Wong A, Hollenhorst PC, Chandler KJ, Cassiday PA, Nelson CA, Hagedorn CH, Graves BJ & Cairns BR (2010). Human RNA polymerase III transcriptomes and relationships to Pol II promoter chromatin and enhancer-binding factors. *Nature Struct Mol Biol* **17:** 620-8.

Olson MOJ (2011). The Nucleolus. New York: Springer.

Olson MOJ & Dundr M (2005). The moving parts of the nucleolus. *Histochem. Cell Biol.* **123:** 203-16.

Osthus RC, Shim H, Kim S, Li Q, Reddy R, Mukherjee M, Xu Y, Wonsey D, Lee LA, Dang CV (2000). Deregulation of glucose transporter 1 and glycolytic gene expression by c-Myc. *J. Biol Chem.* **275(29):** 21797-800.

Palian BM, Rohira AD, Johnson SA, He L, Zheng N, Dubeau L, Stiles BL & Johnson DL (2014). MAF1 is a novel target of PTEN and PI3K signalling that negatively regulates oncogenesis and lipid metabolism. *PLOS Genetics* **10 (12):** 1-13.

Pandolfi PP (2004). Aberrant mRNA translation in cancer pathogenesis: an old concept revisited comes finally of age. *Oncogene* **23:** 3134-7.

Panteleakou Z, Lembessis P, Sourla A, Pissimissis N, Polyzos A, Deliveliotis C, Koutsilieris M (2009). Detection of circulating tumour cells in prostate cancer patients: methodological pitfalls and clinical relevance. *Mol. Med.* **15:** 101-14.

Parker C, Nilsson S, Heinrich D, Helle SI, O'Sullivan JM, Fossa SD, Chodacki A, Wiechno P, Logue J, Seke M, Widmark A, Johannessen DC et al (ALSYMPCA Investigators) (2013). Alpha emitter radium-223 and survival in metastatic prostate cancer. *N. Eng. J.Med.* **369:** 213-223.

Parsons JK, Gage WR, Nelson WG, De Marzo AM (2001). P63 protein expression is rare in prostate adenocarcinoma; implications for cancer diagnosis and carcinogenesis. *Urology* **58:** 619.

Pavon-Eternod M, Gomes S, Geslain R, Dai Q, Rosner MR & Pan T (2009). tRNA over-expression in breast cancer and functional consequences. *Nucleic Acids Res* **37:** 7268-80.

Pavon-Eternod M, Gomes S, Rosner MR, Pan T (2013). Overexpression of initiator methionine tRNA leads to global reprogramming of tRNA expression and increased proliferation in human epithelial cells. *RNA* **19:** 461-6.

Pedersen PL (2007). Warburg, me and Hexokinase 2: Multiple discoveries of key molecular events underlying one of cancers' most common phenotypes , the "Warburg Effect", i.e. elevated glycolysis in the presence of oxygen. *J. Bioenerg. Biomembr.* **39 (3):** 211-22.

Petitjean A, Mathe E, Kato S, Ishioka C, Tavtigian SV, Hainaut P, Olivier M (2007). Impact of mutant p53 functional properties on TP53 mutation patterns and tumour phenotype: lessons from recent developments in the IARC TP53 database. *Hum. Mutat.* **28**: 622-29.

Pianese G (1896). Beitrag zur Histologie und Aetiologie der Carcinoma. Hisologische und experimentelle. Untersuchungen. *Beitr. Pathol. Anat. Allg. Pathol.* **142:** 1-193.

Pienta KJ (2001). Preclinical mechanisms of action of docetaxel and docetaxel combinations in prostate cancer. *Seminars in Oncology* **(28):** 3-7

Pihlajamaa P, Sahu B, Lyly L, Aittomaki V, Hautaniemi S & Janne OA (2014). Tissue-specific pioneer factors associate with androgen receptor cistromes and transcription programs. *The EMBO Journal* **33 (4):** 312- 26

Podsypanina K, Lee RT, Politis C, Hennessey I, Crane A, Puc J, Neshat M, Wang H , Yang L, Gibbons J, Frost P, Dreisbach V, Blenis J, Gaciong Z, Fisher P, Sawyers C, Hedrik-Ellenson L, Parsons R (2001). An inhibitor of mTOR reduces neoplasia and normalises p70/S6 kinase activity in Pten$^{+/-}$ mice. *Proc. Natl. Acad. Sci. USA* **98:** 10320-5.

Poortinga G, Wall M, Sanij E, Siwicki K, Ellul J, Brown D, Holloway TP, Hannan RD & McArthur GA (2011). C-MYC coordinately regulates ribosomal gene chromatin remodelling and Pol I availability during granulocyte differentiation. *Nucleic Acids Res* **39:** 3267-81.

Poste G & Fidler IJ (1980). The pathogenesis of cancer metastasis. *Nature* **283:** 139-46.

Powell WC, Cardiff RD, Cohen MB, Miller GJ & Roy-Burman P (2003). Mouse strains for prostate tumorigenesis based on genes altered in human prostate cancer. *Curr. Drug Targets* **4:** 263-79.

Prat A, Ellis MJ & Perou CM (2012). Practical implications of gene-expression-based assays for breast oncologists. *Nat. Rev. Clin. Oncol.* **9:** 48-57.

Prior IA, Lewis PD & Mattos C (2012). A comprehensive survey of Ras mutations in cancer. *Cancer Res* **72 (10):** 2457-67.

Pylayeva-Gupta Y, Grabocka E, Bar-Sagi D (2011). RAS oncogenes: weaving a tumorigenic web. *Nat Rev Cancer* **11:** 761-74.

Quin JE, Devlin JR, Cameron D, Hannan K, Pearson R and Hannan R (2014). Targeting the nucleolus for cancer intervention. *Biochimica et Biophysica Acta* **1842:** 802-16.

Raha D, Wang Z, Moqtaderi Z, Wu L, Zhong G, Gerstein M, Struhl K, Snyder M (2010). Close association of RNA polymerase II and many transcription factors with Pol III genes. *Proc Natl Acad Sci USA* **107(8):** 3639-44.

Ribeiro FR, Henrique R, Martens AT, Jeronimo C & Teixeira MR (2007). Relative copy number gain of MYC in diagnostic needle biopsies is an independent prognostic factor for prostate cancer patients. *Eur Urol* **52:** 116-25.

Rideout EJ, Marshall L & Grewal SS (2012). *Drosophila* RNA polymerase III repressor MAF1 controls body size and developmental timing by modulating tRNAiMet synthesis and systemic insulin signalling. *PNAS* **109:** 1139-44.

Risbridger GP, Taylor RA, Clouston D, Sliwinski A, Thorne H, Hunter S, Li J, Mitchell G, Murphy D, Frydenberg M, Pook D, Pedersen J, Toivanen R, Wang H, Papargiris M, Lawrence MG & Bolton DM (2015). Patient-derived xenografts reveal that intraductal carcinoma of the prostate is a prominent pathology in BRCA2 mutation carriers with prostate cancer and correlates with poor prognosis. *Eur Urol* **67 (3):** 496-503.

Robbins CM, Tembe WA, Baker A, Sinari S, Moses TY, Beckstrom-Sternberg S, Beckstrom-Sternberg J, Barrett M, Long J, Chinnaiyan A, Lowey J, Suh E, Pearson JV, Craig DW, Agus DB, Pienta KJ, Carpten JD (2011). Copy number and targeted mutational analysis reveals novel somatic events in metastatic prostate tumors. *Genome Res* **21:** 47-55.

Robey RB & Hay N (2009). Is Akt the Warburg kinase? Akt energy metabolism interactions and oncogenesis. *Semin Cancer Biol* **19:** 25-31.

Roeder RG, Rutter WJ (1969). Multiple forms of DNA-dependent RNA polymerase in eukaryotic organisms. *Nature* **224:** 234-7.

Roehl KA, Antenor JAV & Catalona WJ (2002). Serial biopsy results in prostate cancer screening study. *J. Urol* **167:** 2435-9.

Rosen EM, Fan S, Ma Y (2006). BRCA1 regulation of transcription. *Cancer Lett* **236(2):** 175-85.

Roux PP, Topisirovic I (2012). Regulation of mRNA translation by signalling pathways. Cold Spring Harb. *Perspect. Biol.* **1**, 4-11.

Roy-Burman P, Wu H, Powell WC, Hagenkord J & Cohen MB (2004). Genetically defined mouse models that mimic natural aspects of human prostate cancer development. *Endocrine Related Cancer* **11:** 225-54.

Ruggero D, Pandolfi PP (2003). Does the ribosome translate cancer? *Nat Rev Cancer* **3 (3):** 179-92.

Russell J & Zomerdijk J (2006). The RNA polymerase I transcription machinery, in: Roberts SGE, Weinzierl ROJ & White RJ (Eds) *Transcription* pp203-16.

Saad F, Gleason DM, Murray R, Tchekmedyian S, Venner P, Lacombe L, Chin JL, Vinholes JJ, Goas JA, Chen B (2002). A randomised placebo controlled trial of zoledronic acid in patients with hormone-refractory metastatic prostate carcinoma. *J. Natl. Cancer Inst.* **94:** 1458-68.

Saikia M, Jobava R, Parisien M, Putnam A, Krokowski D, Gao XH, Guan BJ, Yuan Y, Jankowsky E, Feng Z, Hu GF, Pusztai-Carey M, Gorla M, Sepuri NB, Pan T & Hatzoglou M (2014). Angiogenin-cleaved tRNA halves interact with cytochrome c, protecting cells from apoptosis during osmotic stress. *Mol Cell Biol* **34:** 2450-63.

Saikia M & Hatzoglou M (2015). The many virtues of tiRNAs: Discovering novel mechanisms of stress response and effect on human health. *J. Biol. Chem*. R115.694661

Sansom OJ, Meniel VS, Muncan V, Phesse TJ, Wilkins JA, Reed KR, Vass JK, Athineos D, Clevers H & Clarke AR (2007). *MYC* deletion rescues Apc deficiency in the small intestine. *Nature* **446:** 676-9.

Saxena A, Ma B, Schramm L, Hernandez N (2005). Structure-function analysis of the human TFIIB-related factor II protein reveals an essential role for the C-terminal domain in RNA polymerase III transcription. *Mol Cell Biol* **25(21):** 9406-18.

Schaefer A, Jung M, Mollenkopf HJ, Wagner I, Stephan C, Jentzmik F, Miller K, Lein M, Kristiansen G, Jung K (2010). Diagnostic and prognostic implications of microRNA profiling in prostate carcinoma. *Int J. Cancer* **126(5):** 1166-76.

Scher HI, Fizazi K, Saad F, Taplin M.E, Sternberg C, Miller K, deWit R, Mulders P, Chi K, Shore N, Armstrong A, Flaig T, Flechon A, Mainwaring P, Fleming M, Hainsworth J, Hirmand M, Selby B, Seely L & de Bono J (2012). Increased survival with Enzalutamide in prostate cancer after chemotherapy. *NEJM* **367(13):** 1187-97.

Scherl A, Coute Y, Deon C, Calle A, Kindbeiter K, Sanchez JC, Greco A, Hochstrasser D, Diaz JJ (2002). Functional proteomic analysis of human nucleolus. *Mol Biol Cell* **13:** 4100-09

Schoenborn JR, Nelson P & Fang M (2013). Genomic profiling defines subtypes of prostate cancer with the potential for therapeutic stratification. *Clin Cancer Res* **19:** 4058-66.

Schramm L. & Hernandez N (2002). Recruitment of RNA polymerase III to its target promoters. *Genes Dev* **16(20)**: 2593-2620.

Scott MR, Westphal KH & Rigby PW (1983). Activation of mouse genes in transformed cells. *Cell* **34(2):** 557-67.

Sears R, Leone G, DeGregori J, Nevins JR (1999). Ras enhances MYC protein stability. *Mol Cell* **3:** 169-79.

Sekiya S & Suzuki A (2011). Direct conversion of mouse fibroblasts to hepatocyte-like cells by defined factors. *Nature* **475(7356):** 390-3.

Shah AA, Rosen A, Hummers L, Wigley F, Casciola-Rosen (2010). Close temporal relationship between onset of cancer and scleroderma in patients with RNA polymerase I/III antibodies. *Arthritis Rheum* **62:** 2787-95.

Sharma A, Yeow WS, Ertel A, Coleman I, Clegg N, Thangavel C, Morrissey C, Zhang X, Comstock CE, Witkiewicz AK, Gomella L, Knudsen ES, Nelson PS, Knudsen KE (2010). The retinoblastoma tumour suppressor controls androgen signalling and human prostate cancer progression. *J Clin Invest* **120(12):** 4478-92.

Shappell SB, Thomas GV, Roberts RL, Herbert R, Ittmann MM, Rubin MA, Humphrey PA, Sundberg JP, Rozengurt N, Barrios R, Ward JM, Cardiff RD (2004). Prostate pathology of genetically engineered mice: definitions and classification. The consensus report from the Bar Harbor meeting of mouse models of Human Cancer Consortium Prostate Pathology Committee. *Cancer Res* **64:** 2270-2305.

Shen MM & Abate-Shen C (2007). Pten inactivation and the emergence of androgen independent prostate cancer. *Cancer Research* **67**: (14) 6535 – 8.

Shen MM & Abate-Shen (2010). Molecular genetics of prostate cancer: New prospects for old challenges. *Genes Dev* **24 (18):** 1967-2000.

Shim H, Dolde C, Lewis BC, Wu CS, Dang G, Jungmann RA, Dalla-Favera R & Dang C (1997). C-Myc transactivation of LDH-A: implications for tumour metabolism and growth. *PNAS* **94(13):** 6658-63.

Shimamoto Y, Fujioka A, Kazuno H, Murakami Y, Ohshimo H, Kato T, Matsuda A, Sasaki T, Fukushima M (2001). Antitumour activity and pharmacokinetics of TAS-106. *Jpn J Cancer Res* **92:** 343-51.

Shimamoto Y, Koizumi K, Okabe H, Kazuno H, Murakami Y, Nakagawa F, Matsuda A, Sasaki T, Fukushima M (2002). Sensitivity of human cancer cells to the new anticancer ribo-nucleoside TAS-106 is correlated with expression of uridine-cytidine kinase 2. *Jpn J Cancer Res* **93:** 825-33.

Shor B, Wu J, Shakey Q, Toral-Barza L, Shi C, Follettie M, Yu K (2010). Requirement of the mTOR kinase for the regulation of MAF1 phosphorylation and control of RNA polymerase III-dependent transcription in cancer cells. *J. Biol. Chem* **285:** 15380-92.

Sobala A, Hutvagner G (2011). Transfer RNA-derived fragments: Origins, processing and functions. *Wiley Interdiscip Rev RNA* 2 (6): 853-62.

Stefanovsky V, Langlois F, Gagnon-Kugler T, Rothblum LI & Moss T (2006). Growth factor signalling regulates elongation of RNA polymerase I transcription in mammals via UBF phosphorylation and r-chromatin remodelling. *Mol Cell* **21**: 629-39.

Stein T, Crighton D, Warnock LJ, Milner J, White RJ (2002). Several regions of p53 are involved in repression of RNA Pol III transcription. *Oncogene* **21:** 5540-7.

Sun C, Dobi A, Mohamed A, Li H, Thangapazham R, Furusato B, Shaheduzzaman S, Tan S, Vaidyanathan G, Whitman E, Hawksworth D, Chen Y, Nau M, Patel V, Vahey M, Gutkind J, Sreenath T, Petrovics G, Sesterhenn I, McLeod D & Srivastava S (2008). TMPRSS2-ERG fusion, a common genomic alteration in prostate cancer activates c-MYC and abrogates prostate epithelial differentiation. *Oncogene* **27**: 5348-53.

Sun Y, Campisi J, Higano C, Beer TM, Porter P, Coleman I, True L & Nelson PS (2012). Treatment-induced damage to the tumour microenvironment promotes PC therapy resistance through WNT16B. *Nature Med.* **18(9):** 1359-68.

Sutcliffe JE, Brown TR, Allison SJ, Scott PH & White RJ (2000). Retinoblastoma protein disrupts interactions required for RNA polymerase III transcription. *Mol Cell Biol.* **20:** 9192-9202.

Suzuki H, Freije D, Nusskern DR, Okami K, Cairns P, Sidransky D, Isaacs WB & Bova GS (1998). Interfocal heterogeneity of PTEN/MMAC1 gene alterations in multiple metastatic prostate cancer tissues. *Cancer Res* **58:** 204-9.

Tabata S, Tanaka M, Matsuda A, Fukushima M, Sasaki T (1996). Anti-tumour effect of a novel multifunctional anti-tumour nucleoside, 3'ethynylcytidine on human cancers. *Oncol Rep* **3**: 1029-34.

Takatori S, Kanda H, Takenaka K, Wataya Y, Matsuda A, Fukushima M, Shimamoto Y, Tanaka M, Sasaki T (1999). Antitumour mechanisms and metabolism of the novel antitumour nucleoside analogues, 1-(3-C-ethynyl-beta-D-ribo-pentofuranosyl)cytosine and 1-(3-C-ethynyl-beta-D-ribo-pentofuranosyl)uracil. *Cancer Chemother Pharmacol* **44:** 97-104.

Takimoto CH, Hammond-Thelin LA, Latz JE, Forero L, Beeram M, Forouzesh B, de Bono J, Tolcher AW, Patnaik A, Monroe P, Wood L, Schneck KB, Clark R, Rowinsky EK (2007). Phase I and pharmokinetic study of pemetrexed with high-dose folic acid supplementation or multivitamin supplementation in patients with locally advanced or metastatic cancer. *Clin Cancer Res* **13**: 2675-83.

Talmadge JE & Fidler IJ (2010). AACR centennial series: the biology of cancer metastasis: historical perspective. *Cancer Res.* **70:** 5649-69.

Tannock IF, de Wit R, Berry WR, Horti J, Pluzanska A, Chi KN, Oudard S, Theodore C, James ND, Turesson I, Rosenthal MA, Eisenberger MA (TAX 327 Investigators) (2004). Docetaxel plus prednisolone or mitoxantrone plus prednisolone for advanced prostate cancer. *N. Eng. J. Med* **351(15):** 1502-12.

Taylor BS, Schultz N, Hieronymus H, Gopalan A, Xiao Y, Carver BS, Arora VK, Kaushik P, Cerami E, Reva B, Antipin Y, Mitsiades N, Landers T, Dolgalev I, Major JE, Wilson M, Socci ND, Lash AE, Heguy A, Eastham JA, Scher HI, Reuter VE, Scardino PT, Sander C, Sawyers CL & Gerald WL for the MSKCC Prostate Cancer Oncogenome Group (PCOG) (2010). Integrative genomic profiling of human prostate cancer. *Cancer Cell* **18 (1):** 11-22.

Teleman AA, Hietakangas V, Sayadian AC , Cohen SM (2008). Nutritional control of protein biosynthetic capacity by insulin via MYC in *Drosophila*. *Cell Metabol.* **7:** 21-32.

Telonis AG, Loher P, Kirino Y, Rigoutsos I (2014). Nuclear and mitochondrial tRNA-lookalikes in the human genome. *Front Genet* **5:** 344.

Terry S & Beltran H (2014). The many faces of neuroendocrine differentiation in prostate cancer progression. *Front. Oncol.* **4:** 60.

Thomas GV, Schrage MI, Rosenfelt L, Kim JH, Salur G, deKernion JB, Dorey F, Said J, Reiter RE (2000). Preoperative prostate needle biopsy p27 correlates with subsequent radical prostatectomy p27, Gleason grade and pathological stage. *J. Urol* **164:** 1987-91.

Thompson DM, Parker R (2009). Stressing out over tRNA cleavage. *Cell* **138 (2):** 215-9.

Thompson IM, Goodman PJ, Tangen CM, Lucia MS, Miller GJ, Ford LG, Lieber MM, Cespedes RD, Atkins JN, Lippman SM, Carlin SM, Ryan A, Szczepanek CM, Crowley JJ, Coltman CA Jr (2003). The influence of finasteride on the development of prostate cancer. *N. Engl. J. Med* **349(3):** 215-24.

Tinker AV, Boussioutas A & Bowtell DD (2006). The challenges of gene expression microarrays for the study of human cancer. *Cancer Cell* **9:** 333-9.

Tomlins SA, Rhodes DR, Perner S, Dhanasekaran SM, Mehra R (2005). Recurrent fusion of TMPRSS2 and ETS transcription factor genes in prostate cancer. *Science* **310 (5748):** 644-8.

Tomlins SA, Laxman B, Dhanasekaran SM, Helgeson BE, Cao X, Morris DS, Menon A, Jing X, Cao Q, Han B, Yu J, Wang L, Montie JE, Rubin MA, Pienta KJ, Roulston D, Shah RB, Varambally S, Mehra R & Chinnaiyan AM (2007). Distinct classes of chromosomal rearrangements create oncogenic ETS gene fusions in prostate cancer. *Nature* **448 (7153):** 595-9.

Tomlins SA (2014). Urine PCA3 and TMPRRS2:ERG using cancer-specific markers to detect cancer. *European Urology* **65**: 543-5.

Treiber K, Zhai X, Jantzen HM, Essigmann JM (1994). Cisplatin-DNAadducts are molecular decoys for the ribosomal RNA transcription hUBF (human upstream binding factor). *Proc Natl Acad. Sci. USA* **91**: 5672-76.

Trotman LC, Niki M, Dotan ZA, Koutcher JA, Di Cristofano A, Xiao A, Khoo AS, Roy-Burman P, Greenberg NM, Van Dyke T, Cordon-Cardo C & Pandolfi PP (2003). Pten dose dictates cancer progression in the prostate. *PLoS Biol* **1:** E59.

Tsao A, Hui EP, Juergens R, Marur S, Huat TE, Cher GB, Hong RL, Hong WK & Chan ATC (2013). Phase II study of TAS-106 in patients with platinum-failure recurrent or metastatic head and neck cancer and nasopharyngeal cancer. *Cancer Medicine:* 351-9.

Tsang CK, Liu H, Zheng XF (2010). mTOR binds to the promoters of RNA polymerase I- and III-transcribed genes. *Cell Cycle* **9:** 953-7.

Tuveson DA, Shaw AT, Willis NA, Silver DP, Jackson EL, Chang S, Mercer KL, Grochow R, Hock H, Crowley D, Hingorani SR, Zaks T, King C, Jacobetz MA, Wang L, Bronson RT, Orkin SH, DePinho RA, Jacks T (2004). Endogenous oncogenic K-ras (G12D) stimulates proliferation and widespread neoplastic and developmental defects. *Cancer Cell* **5 (4):** 375-87.

van Riggelen J, Yetil A, Felsher DW (2010). MYC as a regulator of ribosome biogenesis and protein synthesis. *Nat Rev Cancer* **10:** 301-9.

Varambally S, Yu J, Laxman B, Rhodes D, Mehra R, Tomlins S, Shah R, Chandran U, Monzon F, Becich M, Wei J, Pienta K, Ghosh D, Rubin M & Chinnaiyan A (2005). Integrative genomic and proteomic analysis of prostate cancer reveals signatures of metastatic progression. *Cancer Cell* **8**: 393- 406.

Veras I, Rosen EM, Schramm L (2009). Inhibition of RNA polymerase III transcription by BRCA1. *J. of Mol. Biol.* **387(3):** 523-31.

Vis AN, van Rhijn BWG, Noordzij MA, Schroder FH & van der Kwast TH (2002). Value of tissue markers p27(kip1), MIB-1 and CD44s for the pre-operative prediction of tumour features in screen detected prostate cancer. *J.Pathol* **197:** 148-54.

Voeller HJ, Augustus M, Madike V, Bova GS, Carter KC & Gelmann EP (1997). Coding region of NKX3.1, a prostate-specific homeobox gene on 8p21, is not mutated in human prostate cancers. *Cancer Res* **57:** 4455-9.

Vousden KH & Lane DP (2007). P53 in health and disease. *Nat Rev Mol. Cell Biol.* **8:** 275-83.

Vousden KH & Ryan KM (2009). P53 and metabolism. *Nat Rev Cancer* **9:** 691-700.

Walter BA, Valera VA, Pinto PA & Merino MJ (2013). Comprehensive microRNA profiling of prostate cancer. *J. Cancer* **4:** 350-7.

Wang C, Politz JC, Pederson T & Huang S (2003a). RNA polymerase III transcripts and the PTB protein are essential for the integrity of the perinucleolar compartment. *Mol Biol. Cell* **14:** 2425-35.

Wang HD, Yuh CH, Dang CV & Johnson DL (1995). The hepatitis B virus X protein increases the cellular level of TBP, which mediates transactivation of RNA polymerase III genes. *Mol Cell Biol.* **15(12):** 6720-8.

Wang HD, Trivedi A and Johnson D (1997). Hepatitis B virus X protein induces RNA polymerase III- dependent gene transcription and increases cellular TBP by activating the Ras signalling pathway. *Mol. Cell Biol* **17:** 6838-46

Wang JY, Huang TJ, Chen FM, Hsieh MC, Lin SR, Hou MF & Hsieh JS (2003b). Mutational analysis of the putative tumor suppressor gene PTEN/MMAC1 in advanced gastric carcinomas. *Virchows Arch* **442:** 437-43.

Wang Q, Li W, Zhang Y, Yuan X, Xu K, Yu J, Chen Z, Beroukhim R, Wang H, Lupien M (2009). Androgen receptor regulates a distinct transcription program in androgen-independent prostate cancer. *Cell* **138:** 245-56.

Wang S, Gao J, Lei Q, Rozengurt N, Pritchard C, Jiao J, Thomas G, Li G, Roy-Burman P, Nelson P, Liu X & Wu H (2003). Prostate-specific deletion of the murine Pten tumour suppressor gene leads to metastatic prostate cancer. *Cancer Cell* **4**: 209 -21.

Wang X, Li W, Williams M, Tereda N, Alessi DR & Proud CG (2001). Regulation of elongation factor 2 kinase by p90 (RSK1) and p70 S6 kinase. EMBO J. **20:** 4370-9.

Wang X & Proud CG (2009). Nutrient control of TORC1, a cell cycle regulator. *Trends Cell Biol* **19(6):** 260-7.

Wang Xi, Kruithof-de Julio M, Economides K, Walker D, Hailong Y, Halili MV, Hu YP, Price S, Abate-shen C & Shen M (2009). A luminal epithelial stem cell that is a cell of origin for prostate cancer. *Nature* **461**: 495-500.

Wanjala J, Taylor B, Chapinski C, Hieronymous H, Wongvipat J, Chen Yu, Nanjangud G, Schultz N, Xie Y, Liu S, Lu W, Yang Q, Sander C, Chen Z, Sawyers CL & Carver BS (2015). Identifying actionable targets through integrative analyses of GEMM model and human prostate cancer genomic profiling. *Mol Cancer Ther.* **14 (1):** 278-88.

Warburg O (1956). On the origin of cancer cells. *Science* **123 (3191):** 309-14.

Weckermann D, Polzer B, Ragg T, Blana A, Schlimok G, Arnholdt H, Bertz S, Harzmann R & Klein CA (2009). Perioperative activation of disseminated tumour cells in bone marrow of patients with prostate cancer. *J. Clin. Oncol.***27(10):** 1549-56.

Wei G-H, Badis G, Berger MF, Kivioja T, Palin K, Enge M, Bonke M, Jolma A, Varjosalo M, Gehrke A, Yan J, Talukder S, Turunen M, Taipale M, Stunnenberg H, Ukkonen E, Hughes T, Bulyk M & Taipale J (2010). Genome wide analysis of ETS-family DNA binding *in vitro* and *in vivo*. *The EMBO journal* **29:** 2147-60.

Wendel HG, Silva RL, Malina A, Mills JR, Zhu H, Ueda T, Watanabe-Fukunaga R, Fukunaga R, Teruya-Feldstein J, Pelletier J & Lowe SW (2007). Dissecting eIF4E action in tumorigenesis. *Genes Dev* **21:** 3232-7.

White RJ, Stott D & Rigby PW (1990). Regulation of RNA polymerase III transcription in response to Simian virus 40 transformation. *EMBO J.* **9(11):** 3713-21.

White RJ, Gottlieb TM, Downes CS, Jackson SP (1995). Cell cycle regulation of RNA Pol III transcription. *Mol Cell Biol* **15:** 6653-62.

White RJ, Trouche D, Martin K, Jackson SP & Kouzarides T (1996). Repression of RNA polymerase III transcription by the retinoblastoma protein. *Nature* **382**: 88-90.

White RJ (2002). RNA polymerase III transcription (Landes Bioscience, Austin, TX).

White RJ (2004). RNA polymerase III transcription and cancer. *Oncogene* **23**: 3208-16.

White RJ (2005). RNA polymerases I and III, growth control and cancer. *Nat Rev Mol Cell Biol* **6 (1):** 69-78.

White RJ (2011). Transcription by RNA polymerase III: more complex than we thought. *Nature Genetics* **12:** 459-63.

Widmark A, Klepp O, Solberg A, Damber JE, Angelsen A, Fransson P, Lund JA, Tasdemir I, Hoyer M, Wiklund F, Fossa SD (Scandinavian Prostate Cancer Group Study 7) (2009). Endocrine treatment, with or without radiotherapy, in locally advanced prostate cancer (SPCG-7/SFUO-3): an open randomised phase III trial. *Lancet* **373:** 301-8.

Williamson D. (2006). Nascent pre-rRNA overexpression correlates with an adverse prognosis in alveolar rhabdomyosarcoma. *Genes Chromosomes Cancer* **45:** 839-45.

Winter AG, Sourvinos G, Allison SJ, Tosh K, Scott PH, Spandidos DA & White R.J (2000). RNA polymerase III transcription factor TFIIIC2 is overexpressed in ovarian tumours. *Proc Natl. Acad. Sci. USA.* **97:** 12619-24.

Woiwode A., Johnson SA, Zhong S, Zhang C, Roeder RG, Teichmann M & Johnson DL (2008). PTEN represses RNA polymerase III- dependent transcription by targeting the TFIIIB complex. *Mol. Cell Biol.* **28**: 4204-14.

Wolters T, Vissers KJ, Bangma CH, Schroder FH & van Leenders GJ (2010). The value of EZH2, p27 (kip1), BMI-1 and MIB-1 on biopsy specimens with low risk prostate cancer in selecting men with significant prostate cancer at prostatectomy. *BJU Int.* **106:** 280-6.

Wu G, Yu L, Wang L, Wang H & Xuan JW (2006). Application of Gleason analogous grading system and flow cytometry DNA analysis in a novel knock-in mouse prostate cancer model. *Prostgrad Med J* **82:** 40-45.

Wu X, Wu J, Huang J, Powell WC, Zhang J et al (2001). Generation of a prostate epithelial cell-specific Cre transgenic mouse model for tissue-specific gene ablation. *Mech Dev* **101:** 61-9.

Wu X, Gong S, Roy-Burman P, Lee P, Culig Z (2013). Current mouse and cell models in prostate cancer research. *Endocr. Relat. Cancer* **20(4):** R155-70.

Wullschleger S, Loewith R, Hall MN (2006). TOR signalling in growth and metabolism. *Cell* **124:** 471-84.

Wyatt AW, Mo F, Wang K, McConeghy B, Brahmbhatt S, Jong L, Mitchell DM, Johnston RL, Haegert A, Li E, Liew J, Yeung J, Shrestha R, Lapuk AV, McPherson A, Shukin R, Bell RH, Anderson S, Bishop J, Hurtado-Coll A, Xiao H, Chinnaiyan AM, Mehra R, Lin D, Wang Y, Fazli L, Gleave ME, Volik SV & Collins CC (2014). Heterogeneity in the inter-tumor transcriptome of high risk prostate cancer. *Genome Biology* **15:** 426.

Yamasaki S, Ivanov P, Hu GF, Anderson P (2009). Angiogenin cleaves tRNA and promotes stress induced translational repression. *J Cell Biol* **185**(1): 35-42.

Yakes FM, Chen J, Tan J, Yamaguchi K, Shi Y, Yu P (2011). Cabozantinib (XL184), a novel MET and VEGFR2 inhibitor, simultaneously suppresses metastasis, angiogenesis and tumor growth. *Mol Cancer Ther* **10:** 2298-308.

Yasui H, Inanami O, Asanuma T, Lizuka D, Nakajima T, Kon Y, Matsuda A, Kuwabara M (2007). Treatment combining x-irradiation and a ribonucleoside anticancer drug, TAS106, effectively suppresses the growth of tumour cells transplanted in mice. *Int. J. Radiat. Oncol. Biol. Phys.* **68:** 218-28.

Yee NS, Gong W, Huang Y, Lorent K, Dolan AC, Maraia RJ & Pack M (2007). Mutation of RNA Pol III subunit *rpc2/polr3b* leads to deficiency of subunit Rpc11 and disrupts zebrafish digestive development. *PLoS Biology* **5 (11):** 2484-92.

Yoshimoto M, Joshua AM, Chilton-Macneill S, Bayani J, Selvarajah S, Evans AJ, Zielenska M, Squire JA (2006). Three-color FISH analysis of TMPRSS2/ERG fusions in prostate cancer indicates that genomic microdeletion of chromosome 21 is associated with rearrangement. *Ne*oplasia **8(6):** 8465-9.

Zafarana G, Ishkanian AS, Malloff CA, Locke JA, Sykes J, Thoms J, Lam WL, Squire JA, Yoshimoto M, Ramnarine VR, Meng A, Ahmed O, Jurisica I, Milosevic M, Pintilie M, van der Kwast T, Bristow RG (2012). Copy number alterations of c-MYC and PTEN are prognostic factors for relapse after prostate cancer radiotherapy. *Cancer* **118(16):** 4053-62.

Zetterberg A & Killander D (1965). Qantitative cyclophotometric and autoradiographic studies on the rate of protein synthesis during interphase in mouse fibroblasts *in vitro. Exp. Cell Res* **40:** 1-11.

Zhai W & Comai L (2000). Repression of RNA Polymerase I transcription by the tumour suppressor p53. *Mol Cell Biol.* **20 (16):** 5930-8.

Zhang YP, Lu H (2009). Signalling to p53: ribosomal proteins find their way. *Cancer Cell* **16:** 369-77.

Zhong C, Saribekyan G, Liao C-P, Cohen M & Roy-Burman P (2006). Cooperation between FGF8b overexpression and PTEN deficiency in prostate tumorigenesis. *Cancer Res* **66** (4): 2188-94.

Zhang Q, Zhong Q, Evans AG, Levy D & Zhong S (2011). Phosphorylation of histone H3 serine 28 modulates RNA polymerase III-dependent transcription. *Oncogene* **30:** 3943-52.

Zhang Q, Jin J, Zhong Q, Yu X, Levy D & Zhong S (2013). ERα mediates alcohol-induced deregulation of Pol III genes in breast cancer cells. *Carcinogenesis* **34 (1):** 28-37.

Zhong Q, Shi GG, Zhang QS, Zhang YM, Levy D & Zhong S (2013). Role of phosphorylation histone H3 serine 10 in DEN-induced deregulation of Pol III genes and cell proliferation and transformation. *Carcinogenesis* **34 (11):** 2460-9.

Zhong Q, Shi G, Zhang Y, Lu L, Levy D & Zhong S (2015). Alteration of BRCA1 expression affects alcohol-induced transcription of RNA Pol III dependent genes. *Gene* **556:** 74-9.

Zhong S, Zheng C & Johnson DL (2004). Epidermal growth factor enhances cellular TBP levels and induces RNA Polymerase I and III-dependent gene activity. *Mol. Cell Biol.* **24:** 5119-29.

Zhong S & Johnson D (2009). The JNKs differentially regulate RNA polymerase III transcription by coordinately modulating the expression of all TFIIIB subunits. *PNAS* **106 (31):** 12682-7.

Zhong S, Fromm J & Johnson DL (2007). TBP is differentially regulated by c-Jun N-terminal kinase 1 (JNK1) and JNK2 through ELK-1, controlling c-Jun expression and cell proliferation. *Mol Cell Biol* **27(1):** 54-64.

Zhong S, Machida K, Tsukamoto H, Johnson DL (2011). Alcohol induces RNA polymerase III-dependent transcription through c-jun by co-regulating TBP and BRF1 expression. *J. Biol. Chem.* **286:** 2393-401.

Zhou Y, Goodenbour JM, Godley LA, Wickrema A & Pan T (2009). High levels of tRNA abundance and alteration of tRNA charging by bortezomib in multiple myeloma. *Biochem Biophys Res Commun* **385:** 160-4.

Zuber J, Radtke I, Pardee TS, Zhao Z, Rappaport AR, Luo W, McCurrach ME, Yang MM, Dolan ME, Kogan SC, Downing JR, Lowe SW (2009). Mouse models of human AML accurately predict chemotherapy response. *Genes Dev.* **23(7):** 877-89